PB81-107104

Oxidation of Water Supply Refractory Species by Ozone with Ultraviolet Radiation

North Texas State Univ.
Denton

Prepared for

Municipal Environmental Research Lab.
Cincinnati, OH

Aug 80

U.S. Department of Commerce
National Technical Information Service
NTIS

United States
Environmental Protection
Agency

Municipal Environmental Research
Laboratory
Cincinnati OH 45268

EPA-600/2-80-110
August 1980

PB81-107104

Research and Development

EPA

Oxidation of Water Supply Refractory Species by Ozone with Ultraviolet Radiation

REPRODUCED BY
NATIONAL TECHNICAL
INFORMATION SERVICE
U.S. DEPARTMENT OF COMMERCE
SPRINGFIELD, VA 22161

RESEARCH REPORTING SERIES

Research reports of the Office of Research and Development, U.S. Environmental Protection Agency, have been grouped into nine series. These nine broad categories were established to facilitate further development and application of environmental technology. Elimination of traditional grouping was consciously planned to foster technology transfer and a maximum interface in related fields. The nine series are:

1. Environmental Health Effects Research
2. Environmental Protection Technology
3. Ecological Research
4. Environmental Monitoring
5. Socioeconomic Environmental Studies
6. Scientific and Technical Assessment Reports (STAR)
7. Interagency Energy-Environment Research and Development
8. "Special" Reports
9. Miscellaneous Reports

This report has been assigned to the ENVIRONMENTAL PROTECTION TECHNOLOGY series. This series describes research performed to develop and demonstrate instrumentation, equipment, and methodology to repair or prevent environmental degradation from point and non-point sources of pollution. This work provides the new or improved technology required for the control and treatment of pollution sources to meet environmental quality standards.

This document is available to the public through the National Technical Information Service, Springfield, Virginia 22161.

TECHNICAL REPORT DATA
(Please read Instructions on the reverse before completing)

1. REPORT NO. EPA-600/2-80-110	2.	3. RECIPIENT'S ACCESSION NO. PB81 107104

4. TITLE AND SUBTITLE OXIDATION OF WATER SUPPLY REFRACTORY SPECIES BY OZONE WITH ULTRAVIOLET RADIATION	5. REPORT DATE August 1980 (Issuing Date) 6. PERFORMING ORGANIZATION CODE
7. AUTHOR(S) William H. Glaze; Gary R. Peyton; Francis Y. Huang; Jimmie L. Burleson; Priscilla C. Jones	8. PERFORMING ORGANIZATION REPORT NO.
9. PERFORMING ORGANIZATION NAME AND ADDRESS Institute of Applied Sciences North Texas State University N. T. Box 13078 Denton, Texas 76203	10. PROGRAM ELEMENT NO. 61C1C,C824A,SOS1,Task32 11. CONTRACT/GRANT NO. R-804640
12. SPONSORING AGENCY NAME AND ADDRESS Municipal Environmental Research Laboratory--Cin.,OH Office of Research and Development U.S. Environmental Protection Agency Cincinnati, Ohio 45268	13. TYPE OF REPORT AND PERIOD COVERED Final, 9/76 to 2/80 14. SPONSORING AGENCY CODE EPA/600/14

15. SUPPLEMENTARY NOTES

Project Officer: J. Keith Carswell (513) 684-7228

16. ABSTRACT

The use of ozone with ultraviolet radiation was studied as an advanced treatment process for the removal of micropollutants and trihalomethane precursors from drinking water. The model compounds chloroform, bromodichloromethane, tetrachloroethylene and 2,2",4,4",6,6"-hexachlorobiphenyl were treated with ozone/UV as well as UV and ozone individually in both highly purified water and lake water. Kinetic rate expressions which express the dependence of the reaction rate on ozone dose rate, UV intensity and substrate concentration were developed. The trihalomethane formation potential of a natural lake water was monitored as a function of ozone/UV treatment time. Products resulting from the ozone/UV treatment of some model compounds and lake water were studied. The kinetic data were submitted to a subcontracted consulting engineering firm for full-scale process design and a treatment cost estimate. Costs for a 1-50 Mgal/day plant to remove 90% of 100 ug/L of chloroform and bromodichloromethane and 20 ug/L of tetrachloroethylene were $0.063 - 0.16 per thousand gallons. Costs for removal of 90% of the trihalomethane formation potential from lake water were $0.099 - 0.20 per thousand gallons.

17. KEY WORDS AND DOCUMENT ANALYSIS

a. DESCRIPTORS	b. IDENTIFIERS/OPEN ENDED TERMS	c. COSATI Field/Group
Oxidation Ozone Ultraviolet radiation Water treatment Cost estimates	Precursors Trihalomethane Chemical kinetics Design scale-up	13B

18. DISTRIBUTION STATEMENT Release to Public	19. SECURITY CLASS *(This Report)* Unclassified	21. NO. OF PAGES
	20. SECURITY CLASS *(This page)* Unclassified	22. PRICE

☆ U.S. GOVERNMENT PRINTING OFFICE: 1980-657-165/0113

EPA-600/2-80-110
August 1980

OXIDATION OF WATER SUPPLY REFRACTORY SPECIES BY OZONE WITH ULTRAVIOLET RADIATION

by

William H. Glaze, Gary R. Peyton,
Francis Y. Huang, Jimmie L. Burleson,
Priscilla C. Jones
North Texas State University
Denton, Texas 76203

R-804640

Project Officer

J. Keith Carswell
Drinking Water Research Division
Municipal Environmental Research Laboratory
Cincinnati, Ohio 45268

MUNICIPAL ENVIRONMENTAL RESEARCH LABORATORY
OFFICE OF RESEARCH AND DEVELOPMENT
U.S. ENVIRONMENTAL PROTECTION AGENCY
CINCINNATI, OHIO 45268

i.a

DISCLAIMER

This report has been reviewed by the Municipal Environmental Research Laboratory, U.S. Environmental Protection Agency, and approved for publication. Approval does not signify that the contents necessarily reflect the views and policies of the U.S. Environmental Protection Agency, nor does mention of trade names or commercial products constitute endorsement or recommendation for use.

FOREWORD

The U.S. Environmental Protection Agency was created because of increasing public and government concern about the dangers of pollution to the health and welfare of the American people. Noxious air, foul water, and spoiled land are tragic testimonies to the deterioration of our natural environment. The complexity of that environment and the interplay of its components require a concentrated and integrated attack on the problem.

Research and development is that necessary first step in problem solution; it involves defining the problem, measuring its impact, and searching for solutions. The Municipal Environmental Research Laboratory develops new and improved technology and systems to prevent, treat, and manage wastewater and solid and hazardous waste pollutant discharges from municipal and community sources, to preserve and treat public drinking water supplies, and to minimize the adverse economic, social, health, and aesthetic effects of pollution. This publication is one of the products of that research and provides a most vital communications link between the researcher and the user community.

Reported here are results of a study of one treatment technique for the removal of potentially toxic organic substances from water: the ozone/ultraviolet radiation process. While still experimental, this process shows good promise as a tool to achieve the goal of providing pure water for the people of this country.

Francis T. Mayo, Director
Municipal Environmental Research
Laboratory

PREFACE

The purpose of the work described in this report was to investigate the efficacy of a new water treatment technology, the combination of ozone with ultraviolet light. Although the research itself was necessarily of a very technical nature, the results are of interest to people with a wide variety of backgrounds. For that reason, this report is arranged in such a way that the non-technical reader may read a simple description of the manner in which the experiments were performed, and a discussion of the results and conclusions, without being interrupted by chemical, mathematical and engineering details, which are collected in the respective Appendices. There are two exceptions to that format. The first is Section 4, Background. This section contains material essential to the understanding of the ozone/UV process and the details contained in the Appendices, and is necessarily technical in nature. This section may be skipped by the non-technical reader.

The second section which does not follow the above format is Section 7, Process Engineering Analysis and Sizing and Costing of Full-Scale Units, prepared as a final report to North Texas State University from Houston Research, Incorporated, the subcontractor who performed the engineering part of the final phase of this project. Their final report is included in its entirety as Section 7, and the non-technical reader may wish to skip certain sections of that report which deal with mathematical analysis of the data. The references, whether in Appendices or the main body of the report, refer to the main reference list.

ABSTRACT

The use of ozone in combination with ultraviolet radiation has been studied as an advanced treatment process for the removal of micropollutants and trihalomethane precursors from drinking water. The model compounds chloroform, bromodichloromethane, tetrachloroethylene, and 2,2',4,4',6,6'-hexachlorobiphenyl were treated with ozone/UV as well as ozone and UV individually in both highly purified water and lake water. The resulting data were analyzed in terms of kinetic rate expressions which express the dependence of the reaction rate on ozone dose rate, UV intensity, and substrate concentration. Similar studies were performed, monitoring the trihalomethane formation potential of a natural lake water as a function of ozone/UV treatment time. The data from the kinetic studies were submitted to a subcontracted consulting engineering firm, Houston Research, Inc., for design of a full-scale process and the estimation of treatment costs.

Products resulting from the ozone/UV treatment of hexachlorobiphenyl, chloroform, and the natural organics present in water from Caddo Lake, Texas, were studied. Complex products were identified by gas chromatography/mass spectroscopy and a hexachlorobiphenyl.

The ozone/UV process was found to be 4 to 50 times faster than either ozone or UV alone, depending on the compound and the matrix in which it was tested. Photolytic ozonation products of chloroform were found to be carbon dioxide, hydrogen ion, and chloride ion. Hexachlorobiphenyl degraded by a process where one ring appeared to degrade almost completely before the other ring was broken. Loss of organic halogen occurred very quickly after ring rupture.

The engineering subcontractor found that water treatment costs for a 1 to 50 MGD plant to remove 90% of 100 μg/L of chloroform and bromodichloromethane and 20 μg/L of tetrachloroethylene was \$0.063 to \$0.16 per thousand gallons. Treatment costs for removal of 90% of the trihalomethane formation potential was found to be \$0.099 to \$0.20 per thousand gallons.

This report was submitted in fulfillment of Grant Number R-804640 by North Texas State University under the sponsorship of the U. S. Environmental Protection Agency. This report covers the period from September 1, 1976, to February 29, 1980, and work was completed as of February 29, 1980.

CONTENTS

Foreword iii
Preface. iv
Abstract v
Figures. ix
Tables xv
Abbreviations and Symbols. xviii
Acknowledgement. xx

1. Introduction. 1
2. Conclusions 4
  - Kinetics of ozone/UV reactions 4
  - Products from ozone/UV treatment of model compounds 5
  - Details of the ozone/UV process. 6
  - Engineering analysis 6
3. Recommendations 8
4. Background. 9
  - Use of ozone in drinking water treatment . . 9
  - Chemistry of ozonation 11
  - Generation of active species in aqueous solution. 20
  - Applications of photolytic ozonation in aqueous solution. 27
  - UV photolysis of halogenated compounds in aqueous solution. 34
  - Kinetics of the decomposition of ozone and its reaction with organic compounds in water. 38
  - Models for ozone mass transfer and simultaneous chemical reaction. 42
  - Kinetic models for photolytic ozonation in aqueous solution. 45
  - Conclusions from literature survey 49
5. Chemical Kinetics of Ozone/Ultraviolet-Induced Reactions of Organic Compounds in Water. . . 52
  - Experimental Procedures. 52
  - Results and Discussion 54
6. Identification of Chemical By-products from Ozone/Ultraviolet-Induced Reactions of Organic Compounds in Water 108
  - Experimental procedures. 108
  - Results and discussion 108

7. Process Engineering Analysis and Sizing and Costing of Full Scale Units 121
Symbols & nomenclature. 123
Process engineering analysis basis. 125
Engineering analysis of the reaction data . . 126
Reaction rates for mixtures 142
Reactor dynamics -- mass and energy transfer. 149
Conclusions from the data analysis. 159
Sizing method and cases 160
Treating unit configuration 162
Capital and operating costs 162
Engineering conclusions and recommendations . 171

References. 176
Appendices

A. Destruction curves for first-order substrates. . . . 190
B. Chemical kinetics of ozone/ultraviolet-induced reactions of organic compounds in water -- experimental details 207
C. Chemical kinetics of ozone/ultraviolet-induced reactions of organic compounds in water - details of kinetic analysis for first-order substrates . . . 220
D. Results of kinetic analysis of ozone and ozone/UV destruction of hexachlorobiphenyl in water 238
E. Identification of chemical by-products from ozone/ultraviolet-induced reactions of organic compounds in water 256
F. Quality control during the kinetic runs. 289

FIGURES

Number Page

1 Direct and radical catalyzed reactions of ozone in aqueous solution 15

2 Proposed major reaction pathways in the ozonation of phenol 19

3 Proposed degradation mechanism for the ozonation of 4,4'-dichlorobiphenyl 21

4 The effect of UV light on ozone decomposition. . . . 23

5 Absorption spectrum of O_3 from Inn and Tanaka. . . . 24

6 Absorption coefficients of O_2 and O_3 32

7 Proposed mechanism of 2,4-D photodecomposition . . . 34

8 Photolysis of haloaromatics. 35

9 UV spectra of four isomeric tetrachlorobiphenyls . . 36

10 UV spectra of chlorobiphenyls. 37

11 NTSU photochemical reactor 53

12 Pseudo-first-order rate constants for ozone/UV destruction of tetrachloroethylene. 67

13 Pseudo-first-order rate constants for ozone/UV destruction of tetrachloroethylene, Detail. . . . 68

14 Pseudo-first-order rate constants for ozone/UV destruction of chloroform 69

15 Pseudo-first-order rate constants for ozone/UV destruction of bromodichloromethane 70

16 Tetrachloroethylene - effect of pH on treatment time (95% removal from 100 μg/L) ozone only (no UV) 72

Number Page

17 Effect of pH on ozonolysis of chloroform 74

18 Effect of pH on photolytic ozonolysis of chloroform . 75

19 Effect of pH on BDM destruction by ozone 76

20 Effect of pH on ozone/UV destruction of BDM. 77

21 Effects of dose rate on the direct ozonation of HCB in lake water 79

22 Effects of dose rate on the photolytic ozonation of HCB in lake water. 80

23 Ozone and ozone/UV destruction of THM precursors - Ohio River water (2/77) 82

24 Ozone and ozone/UV destruction of THM precursors - Ohio River water (2/76) 83

25 Ozone and ozone/UV destruction of THM precursors - humic acid (1ppm) 85

26 Normalized THM formation potential: Ozone destruction of THM precursors - Caddo Lake water 86

27 Analysis of THMFP destruction curves - Caddo Lake water 87

28 Normalized THM formation potential: Ozone destruction of THM precursors - Caddo Lake water. 88

29 Trihalomethane precursor destruction by ozone/UV: [UV] = 0.40 W/L 90

30 Trihalomethane precursor destruction by ozone/UV: [UV] = 0.196 W/L. 91

31 Trihalomethane precursor destruction by ozone/UV: [UV] = 0.096 W/L. 92

32 Mass transfer experiments showing "first run" and subsequent results. 103

33 Production of chloride from the photolysis of HCB in water. 112

Number		Page
34	Hexachlorobiphenyl photolysis pathway according to Ruzo	113
35	Proposed degradation scheme for photolytic ozonation of HCB in water	115
36	Formation of oxalic acid during photolytic ozonation of water.	116
37	Chlorine balance during ozone/UV treatment of HCB.	117
38	Oxyphotolysis^{TM} Process Unit for Drinking Water.	165
39	Correlation of Capital and Operating Costs (Assuming 50-60% O_3 Utilization).	172
A-1	Tetrachloroethylene in purified water. UV intensity = 0.375 W/L	191
A-2	Tetrachloroethylene in purified water. UV intensity = 0.189 W/L	192
A-3	Tetrachloroethylene in purified water. UV intensity = 0.091 W/L	193
A-4	Chloroform in purified water. UV intensity = 0.417 W/L	194
A-5	Chloroform in purified water. UV intensity = 0.184 W/L	195
A-6	Chloroform in purified water. UV intensity = 0.084 W/L	196
A-7	Bromodichloromethane in purified water. UV intensity = 0.375 W/L.	197
A-8	Bromodichloromethane in purified water. UV intensity = 0.189 W/L.	198
A-9	Bromodichloromethane in purified water. UV intensity = 0.084 W/L.	199
A-10	Tetrachloroethylene in Lake Lewisville water. UV intensity = 0.375 W/L.	200
A-11	Tetrachloroethylene in Lake Lewisville water. UV intensity = 0.189 W/L.	201

Number		Page
A-12	Tetrachloroethylene in Lake Lewisville water. UV intensity = 0.084 W/L.	202
A-13	Chloroform in Lake Lewisville water. UV intensity = 0.375 W/L.	203
A-14	Chloroform in Lake Lewisville water. UV intensity = 0.189 W/L.	204
A-15	Bromodichloromethane in Lake Lewisville water. UV intensity = 0.375 W/L.	205
A-16	Bromodichloromethane in Lake Lewisville water. UV intensity = 0.189 W/L.	206
B-1	Spectral distribution from ultraviolet lamp. . . .	208
B-2	Schematic diagram of the photolytic ozonation system.	209
B-3	Effect of water purity on photolytic ozonolysis of chloroform	217
C-1	Determination of order and rate constant of ozonolysis of tetrachloroethylene	223
C-2	Determination of substrate order in O_3/UV term (tetrachloroethylene)	225
C-3	Determination of UV intensity exponent and rate constant for O_3/UV term (tetrachloroethylene) .	226
C-4	Determination of photolysis rate constant for bromodichloromethane in purified water.	228
C-5	Pseudo-first-order rate constants for bromodichloromethane in purified water	229
C-6	Ozonolysis of tetrachloroethylene in lake water. .	232
D-1	Ozone concentration profile for ozonation of HCB in lake water	245
D-2	Ozone concentration profile for photolytic ozonation under 0.25 W/L UV radiation	246
D-3	Effects of dose rate on the direct ozonation of HCB in lake water	247

Number		Page
D-4	Initial rates of direct ozonation of HCB in lake water at various ozone dose rates	248
D-5	Effects of dose rate on the photolytic ozonation of HCB in lake water.	249
D-6	Effect of UV radiation transfer rates on the photolytic ozonation of HCB in lake water . . .	250
D-7	pH effects on the rate of ozonation of HCB in purified water.	251
D-8	Effect of pH on rates of photolytic ozonation of HCB in purified water	252
D-9	Photolytic ozonation of HCB in purified water. . .	253
D-10	Comparison of photolytic ozonation in lake water and purified water. UV intensity = 0.2 W/L. . .	254
D-11	Comparison of photolytic ozonation in lake water and purified water. UV intensity = 0.1 W/L. . .	255
E-1	Reactor for ozone and ozone/UV treatment of HCB. .	257
E-2	Extraction scheme.	259
E-3	GC/MS scan of HCB after photolysis under nitrogen.	262
E-4	GC/MS scan of HCB after photolysis under oxygen. .	263
E-5	Mass spectrum of spectrum no. 834.	264
E-6	Mass spectrum of spectrum no. 806.	265
E-7	Mass spectrum of spectrum no. 903.	266
E-8	GC/MS scan of acid fraction from the photolytic ozonation of HCB.	267
E-9	FID chromatogram of HCB/O_3/UV reaction mixture . .	268
E-10	HCB photolytic ozonation products at various time intervals	269
E-11	Mass spectrum of spectrum no. 590.	270
E-12	Mass spectrum of spectrum no. 640.	271
E-13	Mass spectrum of spectrum no. 690.	272

Number Page

E-14 Mass spectrum of spectrum no. 700. 273

E-15 Mass spectrum of spectrum no. 755. 274

E-16 Mass spectrum of spectrum no. 807. 275

E-17 Mass spectrum of spectrum no. 820. 276

E-18 Reconstructed gas chromatogram; Caddo Lake water, ozonated. neutral fraction 280

E-19 Reconstructed gas chromatogram; Caddo Lake water, ozone/UV. neutral fraction 281

E-20 Reconstructed gas chromatogram; Caddo Lake water, control. neutral fraction. 282

E-21 Reconstructed gas chromatogram; Caddo Lake water, ozonated. acidic fraction (diazomethane) 283

E-22 Reconstructed gas chromatogram; Caddo Lake water, ozone/UV. acidic fraction (diazomethane) 284

E-23 Reconstructed gas chromatogram; Caddo Lake water, control. acidic fraction (diazomethane). 285

F-1 Linearity of chloroform analysis. Broad Range (0-400 µg/L). 295

F-2 Linearity of chloroform analysis. Narrow Range (0-40 µg/L) 296

F-3 Linearity of bromodichloromethane analysis 297

F-4 Linearity of bromodichloromethane analysis upon serial dilution in water. 298

F-5 Linearity of hexachlorobiphenyl analysis upon serial dilution in water (error bars shown for solution A only). 299

TABLES

Number Page

1 Effect of pH on Half-life of Ozone in Water 13

2 Summary of Research on Ozone Decomposition in Water . 39

3 Kinetic Form of Pseudo-First-Order Rate Constants, K, for Tetrachloroethylene, Chloroform, and Bromodichloromethane 60

4 Reaction Rate Constants, k_i, for Individual Terms in Rate Expression of Tetrachloroethylene, Chloroform, and Bromodichloromethane 61

5 Contributions to Pseudo-First-Order Rate Constants by the Various Component Terms 62

6 Contributions to Pseudo-First-Order Rate Constants by the Various Component Terms - by Percent. . . . 63

7 Ratio of Rate Constants in Purified Water to Lake Lewisville Water 63

8 Elimination Times, $\tau(3)$, for Tetrachloroethylene by Ozone and Ozone/UV for Various pH Values 71

9 TOC Destruction in Cross Lake Water by Ozone and Ozone/UV 94

10 THMFP Destruction in Cross Lake Water by Ozone/UV . . 95

11 Mass Transfer Coefficients Determined for NTSU Reactor Compared with Literature Values. 105

12 Efficiency of Chloroform Destruction by Ozone/UV. . . 107

13 Products Resulting from Ozone/UV Treatment of Chloroform 109

14 Characteristics of the Lake Water 126

15 Analysis of Data Sets 127

Number Page

16 Summary Data Analysis, Tetrachloroethylene Destruction in Purified Water 130

17 Summary Data Analysis, TCE Destruction in Lake Water (A). 132

18 Summary Data Analysis, Chloroform Destruction in Purified Water 134

19 Summary Data Analysis, Chloroform in Lake Water. . . 136

20 Summary Data Analysis, Bromodichloromethane Destruction in Lake Water (A) 138

21 Composite Run, CF, BCM and TCE in Lake Water (A) . . 139

22 Summary of Data Analysis, THMP Destruction in Lake Water (B). 141

23 TOC Disappearance, Cross Lake Water. 143

24 TOC Disappearance, Lewisville Lake Water 144

25 Reaction Parameters, Micropollutants in Lake Water (A) 147

26 Reaction Parameters, THMP in Lake Water (B). 148

27 Comparison of Reactor Dimensions 149

28 Summary of O_3 Mass Transfer Coefficients and Transfer Numbers 154

29 Chloroform Mass Transfer Data. 156

30 Summary of Design Cases Sizings, Series A. 163

31 Summary of Design Case Sizings, B-Series 164

32 Summary of Capital Costs, A-Series 167

33 Summary of Operating Costs, A-Series 168

34 Summary of Capital Costs, B-Series 169

35 Summary of Operating Costs, B-Series 170

36 Operating Cost Estimate Sensitivity, A-Series. . . . 173

37 Operating Cost Estimate Sensitivity, B-Series. . . . 174

Number Page

D-1 Values of η, K_{La} and K_D for Ozone Profiles with and without UV in Lake Lewisville water 242

D-2 Initial Rate, R_o, and Initial Rate Constant, K_o, for Ozonation of HCB in Lake Lewisville water . . 243

D-3 Rate Constants, k_u, for Photolytic Ozonation of HCB in Lake Lewisville Water. 243

D-4 pH Effects on the Rate Constants, k_u, and k_o of HCB Destruction by Ozonation and Photolytic Ozonation in Purified Water 244

E-1 Major Acidic Products Identified in Photolytic Ozonation of HCB in Water 277

E-2 Products Identified from the Ozone and Ozone/UV Treatment of Water from Caddo Lake, Texas 286

LIST OF ABBREVIATIONS AND SYMBOLS

ABBREVIATIONS

BDM -- bromodichloromethane
CF -- chloroform
CTMA -- 2-chloro-3-trichlorophenylmaleic acid
FID -- flame ionization detector
GC/MS -- gas chromatography/mass spectrometry
HCB -- hexachlorobiphenyl
L -- liter
LLW -- Lewisville Lake water
NTSU -- North Texas State University
PFO -- pseudo-first-order
PW -- purified water
TCE -- tetrachloroethylene
THM -- trihalomethane
THMFP -- trihalomethane formation potential
TOC -- total organic carbon
UV -- ultraviolet
W -- watts

SYMBOLS

Upper Case

C_B -- concentration of ozone in liquid
D -- ozone dose rate, mg/L min
H -- Henry's Law constant
I -- UV intensity, W/L
K -- pseudo-first-order rate constant
P -- trihalomethane precursor; pressure
S -- substrate concentration (also C,A)
S_o -- initial substrate concentration
V -- volume

Lower Case

k -- rate constant
k_{La} -- mass transfer coefficient
k_o -- ozonolysis rate constant, autooxidation rate constant
k_p -- purging rate constant
k_{purge} -- purging rate constant

k_u -- ozone/UV rate constant
t -- time

Greek

α -- normalized concentration S/S_o
η -- yield factor; also ratio of equilibrium value to Henry's Law value of ozone concentration
λ -- wavelength
τ -- elimination time
Ω_M -- competition value

ACKNOWLEDGMENT

Section 7 of this report, Process Engineering Analysis and Sizing and Costing of Full Scale Units, was prepared by H. William Prengle, Jr., Arthur E. Nall and Dilip S. Joshi of Houston Research, Inc., Houston, Texas. Cooperation of the Houston Research, Inc. team in the initial phases of the experimental portion of this project is also acknowledged.

Support to the environmental chemistry program at North Texas State University by the NTSU Faculty Research Committee is also gratefully acknowledged.

SECTION 1

INTRODUCTION

Although ozone has been used in Europe to disinfect drinking water since the turn of the century, chlorination has traditionally been used in the United States. Within the last few years it has been shown that chlorination of natural water produces small amounts of compounds which are toxic or carcinogenic. Other substances undoubtedly are produced, the nature and toxicity of which are entirely unknown. Thus, alternatives to chlorine are the subject of many contemporary studies.

To date, applications of ozone in drinking water treatment have been made primarily in the area of disinfection, but with its great reactivity, ozone is of potential value in the removal of undesirable compounds which may be difficult to remove by other methods. Two major drawbacks to the use of ozone to remove organic compounds are the cost of the treatment and the tendency of most ozonation reactions to produce refractory compounds which are resistant to further degradation by ozone. The combination of ozonation with irradiation by ultraviolet light has been reported to overcome the latter difficulty by degrading even refractory organic compounds completely to carbon dioxide and water. In addition, the ozone/UV process has been reported to be considerably faster than ozone alone for the destruction of almost all organic substrates (103-105). This increased rate of reaction, coupled with the advances in the efficiency of ozone generation and contacting expected within the next few years, could make the ozone/UV process an attractive alternative for drinking water purification.

This project was conceived because of the need to investigate the possibility of using the ozone/UV process in drinking water treatment. In the original proposal, six model compounds of importance in drinking water treatment were chosen as substrates to be studied in purified water. In addition, destruction of trihalomethane precursors in a natural matrix (river or lake water) was to be studied. The six model compounds were chloroform, bromodichloromethane, tetrachloroethylene, a hexachlorobiphenyl, benzo-α-pyrene, and commercial grade "humic acid." Kinetic runs were to be performed in the twenty-liter stainless steel reactor located at Houston Research, Inc. (Houston, Texas), and samples shipped to North Texas State University to be analyzed. It soon became apparent that the original plan was not feasible, not only because of the volume of sample handling, breakage, etc., but also because of the number of runs which would be required to characterize the extremely complex ozone/UV system. For this reason, a quartz photochemical reactor, designed along the lines of the sparged, stirred-tank, semibatch reactor used at Houston Research, was built at North Texas State University, and was used for all of the kinetic results presented in this report.

Further modification to the original project plan was introduced when kinetic runs were attempted using benzo-α-pyrene. This compound is subject to adsorption onto many materials, photo-oxidation in room atmosphere and light, and has other properties which make it an unsuitable compound on which to perform precise kinetic studies. Furthermore, it was found to disappear after just a few seconds of ozonation, so that a treatment process as drastic as ozone/UV was not needed to remove it from solution. Benzo-α-pyrene was accordingly dropped from the model compound list.

"Humic acid" was dropped from the list of model compounds when it was learned from other investigators that the commercially available "humic acid" was not representative of aquatic humic material. Instead, greater efforts were concentrated on the study of a natural matrix, water from Cross Lake, Louisiana. It was realized during the course of the project that an important factor related to destruction of trihalomethane precursors (THMFP) in natural water was the rate of destruction of total organic carbon (TOC), because of the competition of the "TOC" matrix with substrate for the active ozone species. Accordingly the project plan was modified to include the study of TOC destruction in the same natural matrix for which THMFP was investigated.

It further became apparent as the project progressed that the effect of the TOC matrix would also be important in the destruction of model compounds. The project plan was then modified in the third and final year to include a complete rerun of all the purified water kinetics in a natural matrix, water from Lake Lewisville, Texas. This extensive addition to the work load necessitated the de-emphasis of product studies, and consequently only by-products from chloroform, hexachlorobiphenyl, and a natural matrix, Caddo Lake, Texas, were investigated.

The main purpose of this project was to investigate the efficacy of the ozone/UV process at a laboratory scale by obtaining kinetic data of sufficient quality that rate equations could be written which would predict how quickly a given impurity could be removed by the ozone/UV process, using a given ozone dose rate and UV intensity. This information could then be scaled up and optimized in an engineering calculation so that the total treatment cost of a proposed process could be projected. Another important goal of the project was to gain a better understanding of the ozone/UV process so that current technology could be improved to make this potentially powerful treatment technique more cost effective. This gain in understanding comes from careful analysis of the data collected from kinetic and product studies. Finally, as a potential drinking water treatment technique, it is important to investigate the products which are formed upon treatment of organic compounds with ozone/UV, in order to avoid problems of the type discovered with chlorination in the last few years.

SECTION 2

CONCLUSIONS

The conclusions presented in this report are divided into four sections:

A) Kinetics of Ozone/UV Reactions
B) Products from Ozone/UV Treatment of Model Compounds
C) Details of the Ozone/UV Process
D) Engineering Analysis

Section C is important since many general conclusions have been inferred from the kinetic and product work, and the characterization of the reactor. These general conclusions are important in the future consideration of the ozone/UV process as well as in shaping further developmental work.

KINETICS OF OZONE/UV REACTIONS

1) Ozone/UV treatment was found to be four to fifty times faster than ozone or UV alone, depending on compound and matrix.

2) Of the three contributing reactions considered to occur during an ozone/UV experiment (ozonolysis, photolysis, and ozone/UV), the ozone/UV term contributes 65-98% of the reaction rate. In other words, the ozone/UV reaction is 2-50 times faster than the other important reaction, photolysis, while ozone appears to contribute negligibly.

3) All reactions are much faster in purified water than in lake water, but the compound which photolyzes least (CF) shows a greater difference between the two matrices, probably because UV transmission is effected less than active specie propagation.

4) UV photolysis alone may prove to be an effective treatment tool, being somewhat specific for some compounds and not subject to serious interference in lake water.

5) All three compounds (chloroform, bromodichloromethane, and tetrachloroethylene) are destroyed more quickly by ozone alone at high pH than at neutral pH, but the ozone/UV reactions are all slower at high pH. The upper limit of the TCE reaction rate with ozone as pH increases approaches the lower limit of the ozone/UV reaction.

6) The ozone and ozone/UV reactions of 2,2',4,4',6,6'-hexachlorobiphenyl are kinetically complex and slow down significantly by the time substrate is half destroyed (high kinetic order in substrate).

7) THMFP (Trihalomethane Formation Potential) is seen to be destroyed more quickly than TOC.

8) Ozone/UV destroys THMFP and TOC faster than does ozone alone, for a given ozone dose.

9) Ozone/UV appears able to entirely destroy the THMFP of a natural water. Ozone does not.

10) Precursors in addition to those originally present may be produced during the ozone/UV process but are later destroyed as the treatment continues.

11) The rate at which the THMFP of a particular lake water is destroyed and formed by ozone/UV is very sensitive to changes in the matrix which may occur over a short time, either upon storage in the laboratory or in its natural source.

PRODUCTS FROM OZONE/UV TREATMENT OF MODEL COMPOUNDS

1) Ozone/UV treatment of chloroform results in the production of the innocuous products carbon dioxide, hydrogen ion, and chloride ion according to the ratio

$$CHCl_3 \xrightarrow{O_3/UV} CO_2 + 3H^+ + 3Cl^-$$

2) At the high substrate concentration (1.9 g/L) used in the chloroform product studies, 10.3 chloroform molecules were destroyed for every ozone molecule photolyzed. This is indicative of a chain reaction.

3) 2,2',4,4',6,6'-Hexachlorobiphenyl is degraded by ozone/UV according to a process where one of the two aromatic rings is ruptured and appears to degrade almost to completion before the other ring is attacked. One- and two-carbon fragments are successively split off,

presumably in the form of oxalic acid and carbon dioxide. One strength of the ozone/UV process over ozonolysis appears to be the ease of decarboxylation. Once a ring is attacked, chlorine is eliminated almost immediately so that the products are presumably more biodegradable than the parent compound.

4) Ozone treatment of lake water results in many more chromatographable products than does ozone/UV treatment of the same water, indicating greater destruction by ozone/UV.

DETAILS OF THE OZONE/UV PROCESS

1) The purity of the water used to perform ozone mass transfer experiments can be extremely important when an iodimetric method is used for ozone determination in the liquid. Water never before exposed to ozone or UV gave consistently higher values of the mass transfer coefficient than the same water in successive runs after ozone/UV treatment.

2) In the light of 1) above, the NTSU reactor compares reasonably well with engineering reactors reported in the literature.

3) Classical ozone mass transfer considerations appear to be inappropriate for the ozone/UV system, since efficiency calculations indicate that all photolyzed ozone contributes active species equally, whether photolyzed in the liquid or in the gas.

4) The autodecomposition of ozone was found to be higher in the quartz NTSU reactor than that reported by other investigators (103,145).

5) On a stoichiometric basis, ozone utilization in the NTSU reactor for substrate destruction at low concentrations (100 µg/L) is low. The reasons for this low efficiency are not known, but definitely warrant study, as a sizable increase in efficiency would yield a very powerful treatment tool.

ENGINEERING ANALYSIS

1) The ozone/UV photo-oxidation process can be used effectively to reduce micropollutants and trihalomethane precursors to the desired limits. Simultaneously, TOC will be reduced and disinfection will be accomplished.

2) The cost estimates indicate that daily operating costs, including amortization of capital equipment and interest on borrowed capital, are in the range of \$0.06 to \$0.15 per 1000 gals of water treated, for 10-50 MGD units using ozone generated from oxygen.

3) A treating cost of \$0.06 to \$0.15/1000 gals for combined micropollutant, trihalomethane and TOC removal, plus disinfection appears reasonable.

4) If higher ozone utilization values can be achieved, the capital and operating cost could be reduced significantly; the latter by as much as 30-40%.

5) For raw water streams containing TOC > 10 mg/L, the possibility of coupling the process with another pre-TOC removal process to minimize total treating cost may be desirable. For high TOC streams, each situation should be examined individually.

SECTION 3

RECOMMENDATIONS

The ozone/UV process shows promise as an advanced treatment process for the removal of micropollutants and trihalomethane precursors from water, and should be studied further. It is effective for removal of compounds such as halogenated organic compounds, for which other removal methods may be unsatisfactory, and would be of particular value in water re-use applications.

The mechanism and active species of the process should be studied in order to enhance the efficiency above that which was found in this report. Once the identities of the species present are known, information from the chemical literature may be of great help in optimizing the process. The conclusions should be checked at the pilot scale and various methods of contacting and reaction investigated in order to further optimize the ozone/UV process, as it appears that a sizable increase in efficiency may be possible.

SECTION 4

BACKGROUND

USE OF OZONE IN DRINKING WATER TREATMENT

Oxidants are applied in water treatment for several different purposes; namely, for the reduction of taste and odor, for disinfection of bacteria and viruses, for the reduction of the total organic content, and for the oxidation of micropollutants. It has been established that the use of oxidants does not completely remove many organics from treated water but merely changes their characteristics by partial oxidation or substitution mechanisms. Five chemical oxidants are commonly used in water treatment, chlorine, by far the most commonly used in the USA, ozone, chlorine dioxide, permanganate ion, and chloramines. Robeck and co-workers (1) reported the results of experiments with several oxidants and organic compounds. Studies of the overall impact of the use of chlorine as a disinfectant, and particularly the by-products of the chlorination process have increased in number since 1973. Glaze and co-workers (2,3) and Jolly and co-workers (4,5) showed that numerous chlorinated organic by-products are found as a result of the chlorination process, most of which are now recognized to have come from natural precursors. Early studies of Harlock and Dowlin (6), and Burtschell and co-workers (7) on the use of chlorine as an oxidant were generally confined to its effect on taste and odor-causing organics. Morris (8) has reviewed both theoretical and practical aspects of the chlorination of organic compounds.

Chlorination has been used extensively for water treatment primarily because chlorine is a powerful disinfecting agent, and has a relatively long lifetime in drinking water distribution systems. In 1974, however, Rook (9) and Bellar and Lichtenberg (10) linked the production of trihalomethanes with the chlorination of naturally occurring humic substances via the haloform reaction. The pioneering works by Jolly (4,5), Murphy and co-workers (11), Glaze and co-workers (2,3) have also indicated that a wide variety of halogenated organic compounds are produced as a result of the chlorination. Symons and co-workers (12) extensively discussed the use of this oxidant and the occurrence of trihalomethanes.

Because of the potential hazard associated with chlorination by-products, other methods of water and wastewater treatment are being examined as alternatives to chlorination. Among the alternatives, ozonation has received much attention recently. Ozonation has been used for water disinfection in Europe and at a few locations in North America. Guinvarch (13) and Lebout (14) described the experiences of ozonation in France. Rook (15) reviewed the practice for Europe as a whole. In general, the European emphasis is on ozone as the primary disinfection method with the use of a low level of chlorine to provide a residual disinfection capability in the distribution system.

Although ozonation has been used in treatment in Europe since the turn of the century, economics have usually favored other methods in North America. However, recent improvements in ozone generator technology (16) have lowered the cost considerably relative to chlorination, and many workers are looking with renewed interest at the advantages of ozonation.

Ozonation deserves consideration as an alternative to chlorination because it has many of the properties required for an oxidant used in water treatment for removal or organic compounds. It is known to be a more powerful disinfectant than chlorine. Katzenelson and co-workers (17) demonstrated that with the same concentration, 99% kill for poliovirus 1 is reached in less than 10 seconds with ozone. Chlorine requires about 100 seconds to achieve the same effect. Ozone is a powerful oxidizing agent with twice the chemical oxidation potential of hypochlorite ion. As a result, more complete oxidation can be expected from ozonation than from chlorination. It is effective at relatively low doses and short contact times. Ozone in water readily decomposes to oxygen leaving no by-products that need to be removed.

McNabney and Wynn (18) demonstrated at the Blue Plains Pilot Plant the reduction of chemical oxygen demand (COD) by ozonation. Numerous studies also revealed the ability of ozone to reduce total organic carbon (TOC) and biochemical oxygen demand (BOD) of wastewater. Jiejers (19) showed the reduction of color of ground and lake water by ozonation. A review by Rosen (20) gives an excellent overview of the application of ozonation for the removal of a variety of pollutants including potential carcinogens from drinking water.

Ozonation also is applied for tertiary treatment of municipal wastewater in combination with other treatment methods, such as mechanical filtration (21) or ultrasonics and catalysts (22). Elia and co-workers (23) used ozonation as a polishing process for the pre-treatment of reverse osmosis influents. Another study by Foulds (24) combines ozonation with froth flotation for disinfection and pollutant removal. An encouraging work by Guirguis and co-workers (25) demonstrated improved performance of activated carbon by pre-ozonation. In their pilot plant, ozone pre-treatment rendered certain organic species more sorbable and biodegradable. The ozonated effluent contains dissolved oxygen (DO) in sufficient concentrations to promote the growth of active micro-organisms in the filter unit and on the carbon surface in the sorption unit. A similar study is currently under extensive investigation by Glaze (26).

Several inorganic substances can essentially change the properties of water, such as smell, color and taste. These include compounds of iron, manganese, arsenic, sulfur, and several others. Removal of these substances can be effected significantly by ozonation. Shambaugh and Melnyk (27) found that ozonation with contact times on the order of 10 minutes will destroy metal-EDTA complexes. In the exhaustive ozonation of seawater, Williams and co-workers (28) observed a rapid oxidation of Br^- to BrO^-, with the evidence for the transitory formation of ClO^-. Removal of manganese and iron also has been demonstrated by Mignot (29). The treatment of wastewater containing lead has been developed by Collier (30). Lapidot (31) reported on the removal of silicones from a silicone manufacturing effluent. Ozone was the only treatment technique that was shown to clean up the silicone waste significantly.

Lawrence (32) found the pre-ozonation reduced the concentration of chloroform precursors so that less chloroform was detected after ozonation-chlorination than by chlorination alone. Glaze and co-workers (33) used the same procedures on river water and reported the reduction of trihalomethane formation potential (THMFP) by ozonation. In another study, Riley and co-workers (34) found that ozonation-post-chlorination may lead to higher levels of trihalomethanes than the conventional chlorination process. However, attention should be paid to the fact that pH played an important role in their study. The enhanced chloroform yields were found only if chlorination was done at high pH following ozonation. Other similar findings have been documented in the report of a pilot plant study (12). Although it was proposed that ozone oxidizes organic materials to form precursors which may, when subsequently chlorinated, produce chloroform, the complexity of humic material makes the chemistry of ozonation-post-chlorination difficult to investigate directly.

CHEMISTRY OF OZONATION

The chemical reactions between organic compounds and ozone have been studied extensively for many years, but the chemistry of ozone as an oxidizing agent of organic and inorganic solutes in water is relatively unknown. Studies of the nature of compounds formed during ozonation of wastewaters are currently underway to clarify the mechanism of its action.

At room temperature Ozone (O_3) is a highly unstable, colorless gas which is 1.5 times more dense than oxygen and which thermally decomposes to oxygen with critical decomposition temperature at 270°C (35,36). In water, ozone has an oxidation potential of 2.07 volts at 20°C, which makes it capable of oxidizing most organic and inorganic compounds. The microwave spectrum of ozone shows the molecule to be non-paramagnetic with an obtuse angle of 116° 49' and equal bond length of 1.278 A (37). On the basis of this structure, in nonaqueous solution or as a free molecule, ozone is expected to react as an electrophile or as a 1,3-dipole.

The aqueous solubility of ozone is ten times greater than that for oxygen. Kinman (38) reported 575 and 775 mg L^{-1} as the theoretical solubility at 20 and 10°C under one atmosphere of pressure and at normal pH. However, since ozone is generated in the form of a dilute mixture (1-5% W/W) in air or oxygen gas, solubilities in water in excess of 20 mg L^{-1} are seldom attained in water treatment practice.

The decomposition of ozone in aqueous solution is well known and is the subject of a number of studies. Ozone decomposes rapidly in water with a half life of a few minutes. The decomposition of ozone in water is favored at alkaline pH values. Table I shows the results obtained by Stumm (39) and Hoigne and Bader (40). Both the mechanism and kinetics of the dissociation of ozone in water are uncertain. Kilpatrick and co-workers (41) and Stumm (42) stated that ozone decomposes to yield oxygen and a small amount of hydrogen peroxide. Garbenko-Germanov and Kozolva (43) had investigated the decomposition of ozone in basic medium using the electron spin resonance technique and also absorption spectroscopy. They suggested the initial step of the decomposition probably is the reaction between ozone and hydroxide ion to form ozonide ion and hydroxyl radical (OH·):

$$O_3 + OH^- \longrightarrow O_3^- + OH\cdot$$

The hydroxyl radical then reacts further. This process would explain the increased dissociation of ozone with increasing alkalinity. Recently, Hoigne and Bader (40,44,45,46) have shown experimentally that as pH increases, the kinetics of ozonation of organic compounds changes. They found reaction rates for ozone oxidation reactions at high pH are similar to those obtained in studies in which the hydroxyl radical is generated by high energy radiation. Hydroxyl radical may be the important active species in ozonation as they concluded.

Peleg (47) reviewed the chemistry of ozone in the treatment of water and from several individual studies and findings, he suggested the following steps for ozone decomposition in aqueous solution:

TABLE 1. EFFECT OF pH ON HALF-LIFE OF OZONE IN WATER

pH	Half-Life (min.)	
	Stumm (39) 14.6°C	Hoigne and Bader (40) 25°C
4.0	. .	350
6.0	. .	50
7.6	41	. .
8.0	. .	33.3
8.5	11	. .
8.9	7	. .
9.2	4	. .
9.7	2	. .
10.0	. .	.33
10.4	0.5	. .

$$O_3 + H_2O \longrightarrow O_2 + 2OH\cdot \qquad [1]$$

$$O_3 + OH\cdot \longrightarrow O_2 + HO_2\cdot \qquad [2]$$

$$O_3 + HO_2\cdot \longrightarrow 2O_2 + OH\cdot \qquad [3]$$

$$OH\cdot + OH\cdot \longrightarrow H_2O_2 \qquad [4]$$

$$OH\cdot + HO_2\cdot \longrightarrow H_2O + O_2 \qquad [5]$$

$$OH\cdot + OH^- \longrightarrow O^- + H_2O \qquad [6]$$

$$O^- + O_2 \longrightarrow O_3^- \qquad [7]$$

$$HO_2\cdot + HO_2\cdot \longrightarrow H_2O_2 + O_2 \qquad [8]$$

In this mechanism, O^- has lower chemical reactivity which differs markedly from that of OH· in many reactions. The half-life of ozonide, O_3^-, at 25°C is only several milliseconds and the substance is reported to be unreactive to aromatic molecules as well as to methanol and ethanol (48). Barr and King (49) showed the hydroperoxyl radical ($HO_2\cdot$) to be almost inert towards organic substances. It would appear then that the hydroxyl radical is very likely the most important reactive intermediate in the decomposition of ozone. It is an even more powerful oxidizing agent than ozone with an oxidation potential of 2.80 volts at $[H^+] = 1.0$ M. (50). Consequently, one may speculate that the efficiency of the ozonation process might be enhanced if means were found to accelerate the decomposition of ozone so that hydroxyl radicals could be used effectively. Hewes and Davison (51) experimentally proved that the rate of organic oxidation increases as conditions are utilized which accelerate the decomposition of ozone.

Hoigne and Bader (40,44-46) stated that both molecular ozone and hydroxyl radical, which is generated from the decomposition of ozone, are involved in the ozonation process. The primary oxidation initiated by ozone in water can be described by the reaction sequences shown in Figure 1. The overall effect initiated by ozonation is a superposition of the "direct reaction" and the "radical-type reaction." Hoigne and Bader (147) later developed the kinetics formulation for the elimination of solute (M) in a batch or plug-type reactor:

$$-d[M]/dt = -\eta\, d[O_3]/dt = k[O_3][M]$$

and from integration:

$$-\ln([M]_e/[M]_o) = \eta \cdot k \cdot [\overline{O_3}] \cdot t$$

where,

η = yield factor; or the amount of M eliminated per mole of ozone used,

k = rate constant

$[M]_o, [M]_e$ = initial and final concentration of substrate assuming $[\overline{O_3}] >> [M]_o$.

$[\overline{O_3}]$ = mean ozone concentration, during reaction period t.

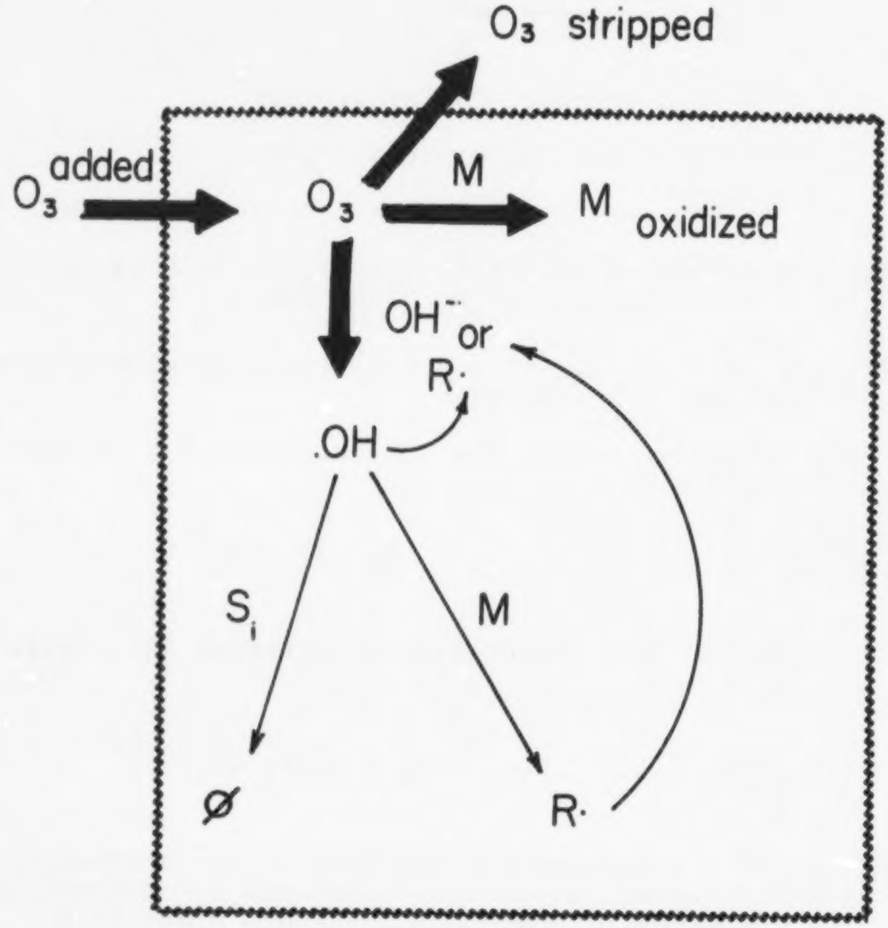
O₃ stripped
O₃ added
O₃
M
M oxidized
OH⁻ or R·
.OH
Sᵢ
M
Ø
R·

Figure 1. Direct and radical catalyzed reactions of ozone in aqueous solution (Hoigné, 1976-7).

Oxidation by molecular ozone is highly selective and is often rather slow (minutes). However, hydroxyl radicals are very reactive towards most organic solutes in water. The amount of OH radicals which are available for oxidation of a solute M depends on the amount of OH formed and the relative rate with which they react with M when compared with the rate by which hydroxyl radicals are consumed by all other solutes:

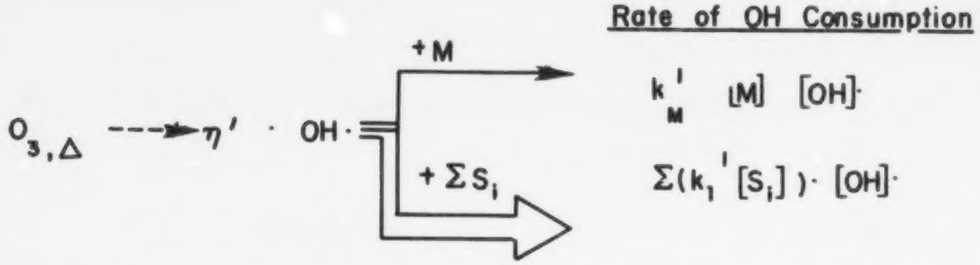
Rate of OH Consumption
+M
k'_M [M] [OH]·
$O_{3,\Delta}$ ---→ η' · OH·
$+\Sigma S_i$
$\Sigma(k_i'[S_i])\cdot[OH]\cdot$

where O_3,Δ = O_3 decomposed during process

η' = yield for OH formation from O_3,Δ

k' = 2nd order reaction rate constant for OH

$\Sigma(k_i[S_i])$ = rate of OH scavanging by all solutes, S_i, present including ozone and M

Only a fraction (η'') of the OH radicals reacting with solutes will result in a solute elimination.

The rate of solute oxidations in the presence of competing scavengers becomes:

$$-\frac{d[M]}{dt} = \eta'\,\eta''\,(d\,O_{3,\Delta/dt})\cdot k'_M\,[M]\,(\Sigma(k'_i\,[S_i]))^{-1} \qquad [9]$$

if $k'_M[M] \ll \Sigma(k'_i[S_i])$, then integration of equation [9] yields for a plug and batch type reactor:

$$-\ln\,[M]_e/[M]_o = \eta'\eta''\,O_{3,\Delta}\cdot k'_M\cdot(\Sigma(k'_i\,[S_i]))^{-1}$$

This equation and the assumptions involved in its derivation were successfully tested, since rate constants for OH radical reactions with hundreds of aqueous solutes are known from independent measurements in which the radicals are generated by high energy photolysis of water (40).

The direct reaction of ozone with organic substrates in nonaqueous systems has been well studied (52). Bailey (53) discussed the organic groupings which can be oxidized by ozone. Generally, carbon-carbon multiple bonds and aromatic molecules are very easily attacked by ozone. In aqueous ozonation, although the mechanism is not clear yet, one would expect molecular ozone, hydroxyl radicals, oxygen and even water molecules to be involved in the reaction. Consequently, one would expect final products to differ in aqueous ozonations as compared to those reported in nonaqueous solvents. For example, hydroxyl hydroperoxides or dihydroxy peroxides might be produced in the reaction of ozone with carbon-carbon double bonds as the well-recognized Criegee mechanism (54) shows:

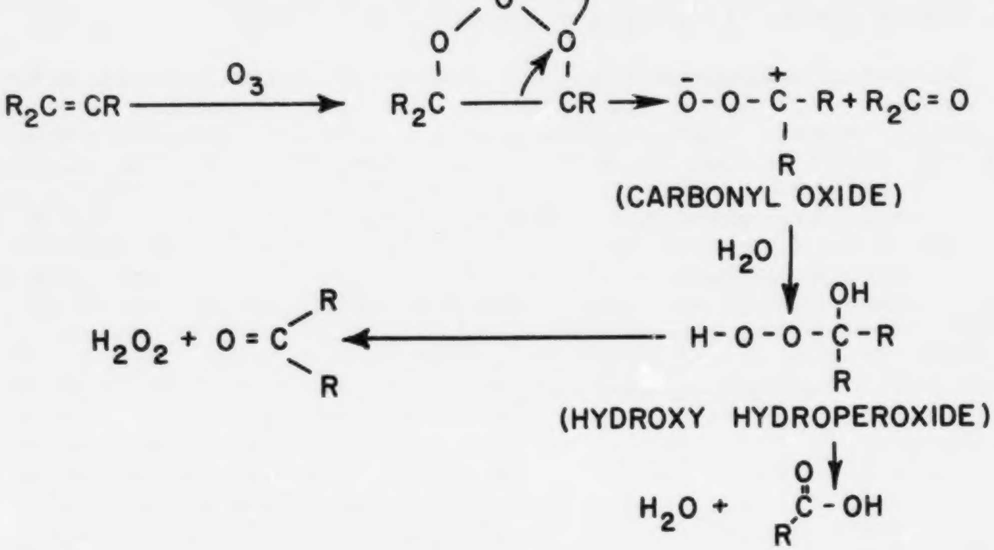

[10]

Aromatic compounds, amines, acetylene, and many other compounds have been subjected to ozonolysis in aqueous solution but few definitive mechanistic studies have been made. The results of these studies have been reviewed by Bailey (53), Oehlschaeger (55), Maggiolo (56) and Rice (57).

Ozonation of natural organic ("humic") material in water has been the subject of several investigations, but few of these report on the products of ozonation. Guirguis and co-workers (25) monitored the relative molecular weight distribution in wastewater before and after ozonation and found the concentration of UV-absorbing species of relative molecular weight between 500 and 180 increased as ozone dose rate increased.

Apparently, the larger humic molecules were cleaved at several points in the ozonation process. For identification of the possible small products, Kinney and co-workers (58,59) ozonized humic acids prepared from oxidized bituminous coal. They stated that both carbonic and oxalic acids appeared to be primary products and accounted for about 65% of the carbon. Sievers and co-workers (60) found unidentified aldehydes from the ozonation of biologically-treated secondary effluent from wastewater. Lawrence (61) ozonized the predominant classes of compounds found in natural waters: humic and fulvic acids, tannins and lignins and the products were identified by gas chromatography. He found humic and fulvic acids gave very similar oxidation products -- namely aliphatic and aromatic carboxylic acids of molecular weight less than 370. Tannic acid and lignosulfonic acids also yielded carboxylic acids, but mostly of low molecular weight. Shevchenko and Taran (62) identified aprocrenic, crenic and oxalic acids as ozonation products from peat humid acids.

Aromatic compounds are very common as pollutants in water and wastewater. Two types, phenols and chlorobenzenes, are of interest. Most aromatic compounds are reactive towards ozone although the reaction is said to be slower than that of olefins (63). Substituents which withdraw electrons from the ring, such as carbonyl, halogens, nitro and sulfonic acid groups, deactivate the ring towards attack by ozone. Electron-releasing substituents, such as hydroxyl, alkyl and alkoxyl groups, activate the ring towards attack by ozone. Phenols which are attacked very rapidly have been studied extensively because of the recent interest in the use of ozone to purify wastewater. Gould and Weber (64) ozonized aqueous phenol solutions and found catechol, hydroquinone, glyoxal, oxalic acid and glyoxylic acid. Yamamoto and co-workers (65) carried out the ozonation of a variety of compounds in water. The major products from the ozonation of phenol, they stated, were formic acid with minor amounts of hydroquinone, catechol, muconaldehyde, muconic acid, maleic aldehyde, glyoxal, glyoxlic acid, oxalic acid, carbon dioxide, and hydrogen peroxide. The proposed major reaction pathways are shown in Figure 2.

Shuval and Peleg (66) found about 80% of chlorine on o-chlorophenol was converted to chloride ion upon ozonation indicating that covalent carbon-chlorine bonds are broken with ozone. It was also suggested that the active oxidizing species attacks the ring at a site or sites other than the chlorine site, because an induction period was observed during which the concentration of o-chlorophenol decreased but no chloride ion was formed. After all of the o-chlorophenol had disappeared, chloride ion still was being produced upon continued ozonation. Gilbert (67) also observed the same phenomenon. Chloride ion was found only after 40% of the o-chlorophenol had been destroyed.

A. Hydroxylation (---) and Cleavage (——) of Aromatic Ring

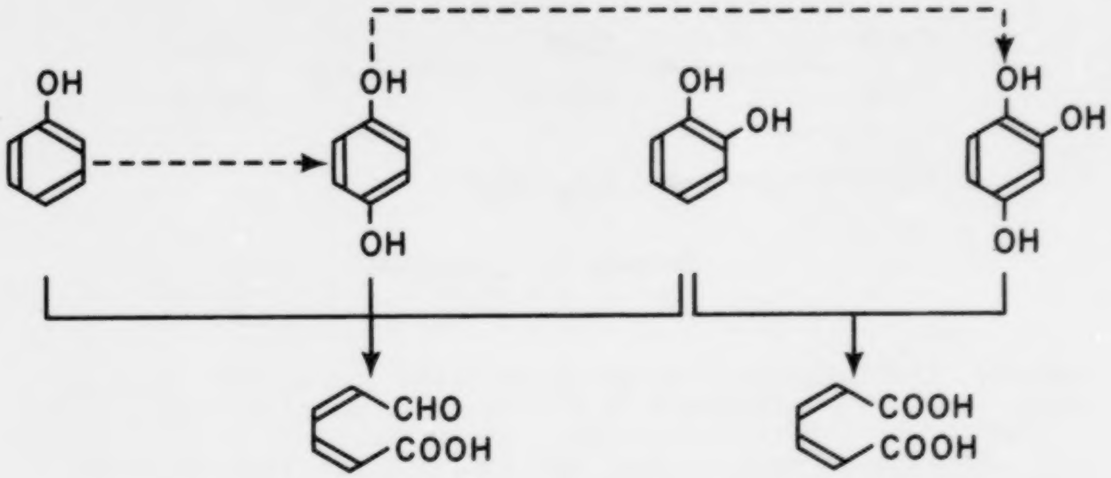
OH
OH
OH
OH
OH
OH
OH
OH
CHO
COOH
COOH
COOH

B. Normal (---) and Anomalous (——) Ozonolysis of α,β-Unsaturated Aldehyde and Acid

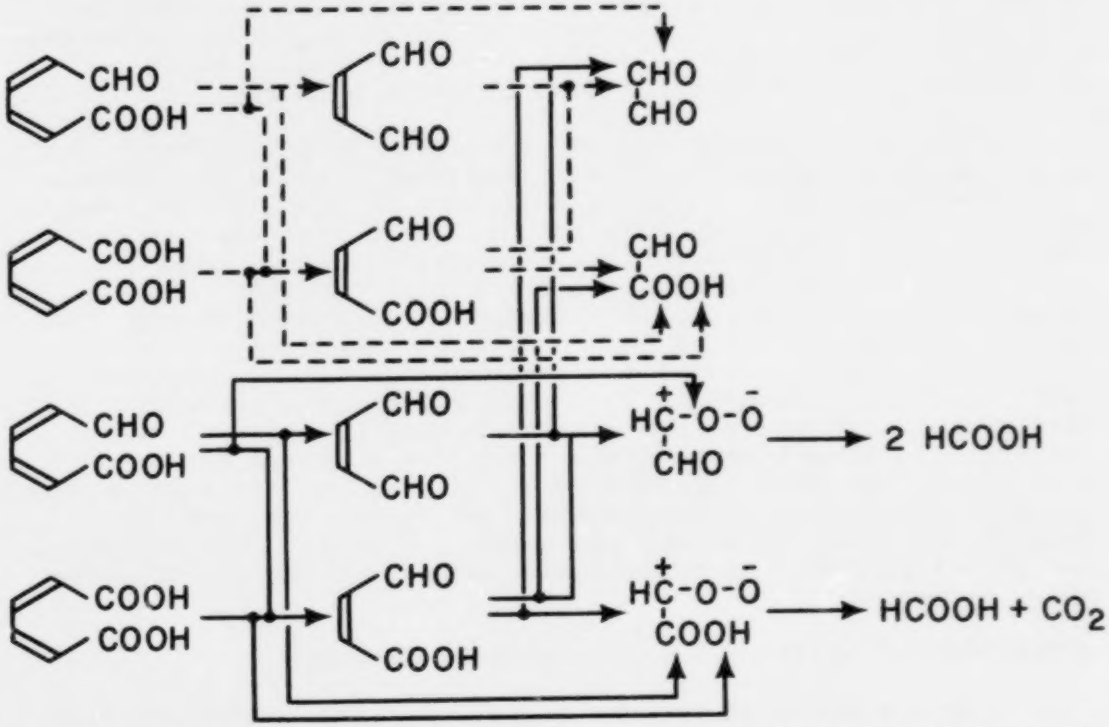
CHO
COOH
CHO
CHO
CHO
CHO
COOH
COOH
CHO
COOH
CHO
COOH
CHO
COOH
CHO
CHO
HC-O-O
CHO
2 HCOOH
COOH
COOH
CHO
COOH
HC-O-O
COOH
HCOOH + CO₂

Figure 2. Proposed major reaction pathways in the ozonation of phenol in water (65) (Continued-next page).

C. Oxidation of Aldehyde and Decarboxylation of Formic Acid

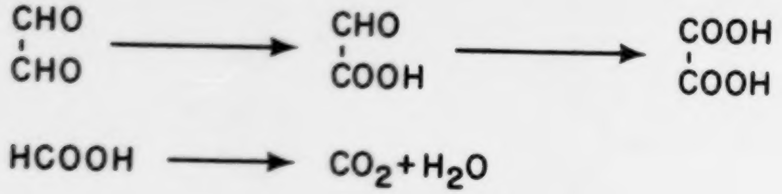

(Figure 2. Continued)

However, 4-chlorophenol produced chloride ion at the start of ozonation. The difference in the rates of dechlorination might be due to the different distributions of electron density on the aromatic rings. Besides chloride ion, Gilbert also detected formic acid and oxalic acid from the ozonation of 2,4-dichlorophenol.

Bauch and co-workers (68) detected chlorotartaric acid, o-;m-and p-chlorophenols and chloride as the ozonation products of chlorobenzene. The hydroxylation of the ring by ozone is interesting since it activates the aromatic ring towards further degradation. Aliphatic oxidation products similar to those found from phenol were also found by these workers.

Ozonation of one of the major classes of pollutants, polychlorinated biphenyls (PCBs), has been studied by Yokoyama and co-workers (69). An aqueous mixture of PCBs, KC-300, was ozonated for 24 hours and the products were monitored by gas chromatography. Major products were chlorobenzoic acids, glyoxylic acid, oxalic acid, chloride ion, hydrogen peroxide, carbon dioxide and white precipitates which showed strong carbonyl group vibrations in the infrared spectrum. A degradation mechanism of 4,4'-dichlorobiphenyl was proposed (see Figure 3). According to this view, ozone attacks the Π-electrons of the phenyl nucleus and causes cleavage of the nucleus. It is interesting that only one ring was ruptured in many cases, and that the ring ruptured products are similar to those of phenol and chlorophenols. No direct evidence to support the reaction scheme was given. Moreover, the active specie was proposed to be molecular ozone without any confirmatory evidence.

GENERATION OF ACTIVE SPECIES IN AQUEOUS SOLUTION

From the previous review, it is generally recognized that both the decomposition products of ozone and ozone itself are involved in the oxidation process. In many cases, the former are more important; therefore, better utilization of ozone may be accomplished by more efficient generation of decomposition products which are reactive towards organic substrates.

Adjustment of pH has been proven to be effective in accelerating both the decomposition of ozone and the ozonation rates of organic substrates (40,42,47,51,70). Higher reactivity of ozone under basic conditions is now understood to involve the formation of hydroxyl radical intermediate which is more reactive than molecular ozone in general. However, except in few cases, complete removal of organic compounds at higher pH has not been obtained.

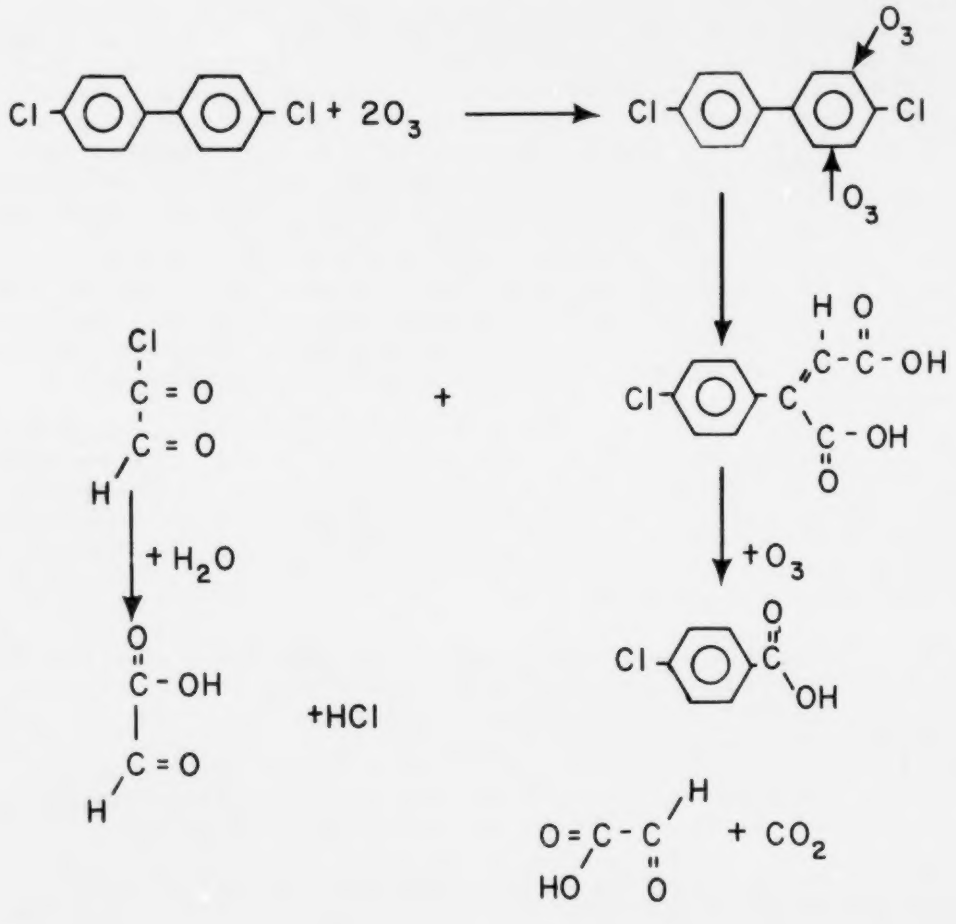
Cl
Cl + 2O3
O3
Cl
Cl
O3
H O
C-C-OH
Cl
C = O
C = O
H
+
Cl
C
C-OH
O
+H2O
+O3
O
C-OH
+HCl
C = O
H
O
Cl
C
OH
H
O=C-C
HO
O
+ CO2

Figure 3. Proposed degradation mechanism for the ozonation of 4,4' - dichlorobiphenyl.

The effect of temperature on ozone decomposition has been studied by Kuo and co-workers (71). They demonstrated that the Arrhenius equation could be employed to express the temperature dependence of the decomposition rate constant of ozone. Hewes and Davison (51) observed a similar dependence on temperature and found experimentally that ozonation at elevated temperature reduced the COD of pretreated secondary municipal wastewater effluent more effectively. Auguliaro and Rizzuti (72) studied the temperature enhancement of the ozonation of aqueous phenol solutions. For actual water treatment processes, however, the practice of elevating the temperature in order to provide better oxidation is impractical. Also, the low solubility of ozone at higher temperatures might adversely affect the rate of organic oxidation.

Chen and co-workers (73) developed catalytic ozonation in a steady state reactor using a special ferric oxide catalyst. The authors stated that the catalyst enabled them to use at least two oxygen atoms in the ozone molecule for oxidations. They postulated that in catalytic ozonation ozone molecules are adsorbed on the surface of the catalyst to form ozone-catalyst complexes which then would form reactive oxygen species for oxidation. The removal of COD in aqueous systems by ozone with glass beads and ozone with catalyst, Fe_2O_3, were compared in this work. The latter system effectively removed COD at a rate of about three times that of former system. The better utilization of ozone was proven, but the cost and life time of the catalyst system was not well-investigated. Moreover, inhibition of the catalyst by chemical poisons is likely to occur in the treatment of wastewaters containing complex components.

Ultraviolet (UV) radiation is one of the most effective methods to accelerate the decomposition of ozone. Ozone absorbs UV light and decomposes very rapidly in water. In a typical reactor, ozone transfers from the gas phase to the liquid phase to reach an equilibrium value. When the UV light is turned on, the concentration of ozone drops almost instantaneously to a very low value. (Figure 4).

The decomposition of ozone by UV in the gas phase has been studied intensively. Ozone absorbs radiation in two regions, one in the red part of the visible spectrum (λ_{max}-600 nm) and the other in the ultraviolet (λ_{max}-254 nm). The photochemical behavior is distinct in the two regions (74). From the UV-absorption spectrum by Inn and Tanaka (75) the large absorption coefficient of ozone at 254 nm is noted (Figure 5).

Heidt and Forbes (76,77,78), Norrish and Wayne (79) studied the UV-photolysis of dry ozone and found the quantum yield is in excess of two. Addition of water vapor gives even higher quantum yields. Kistiakowsky (80), Castellano and Schumacher (81) found the quantum yield for the decomposition of

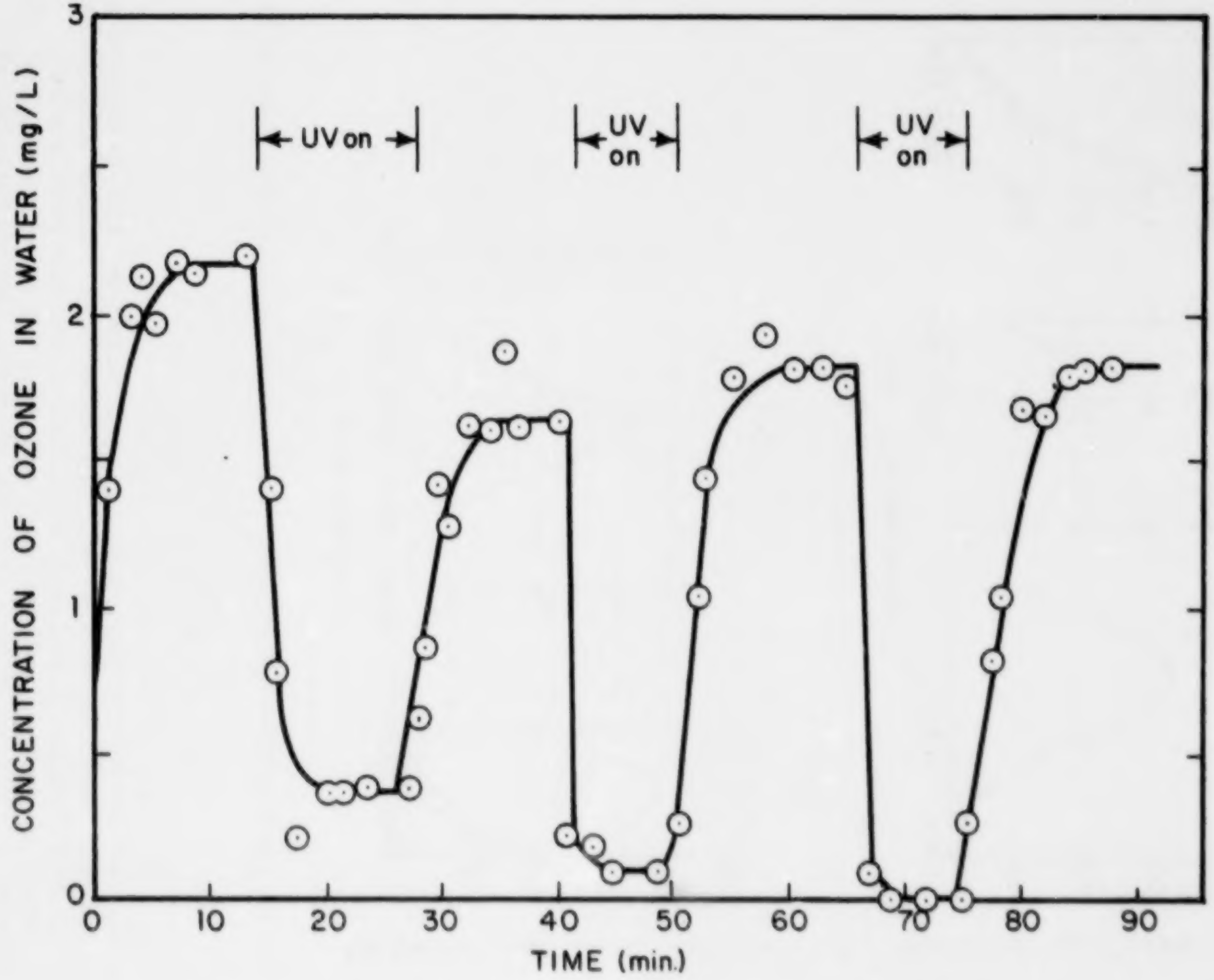

Figure 4. The effect of UV light on ozone decomposition. (Ozone Dose Rate = 7.2 mg/min-L, Flow Rate =1.0 L/min).

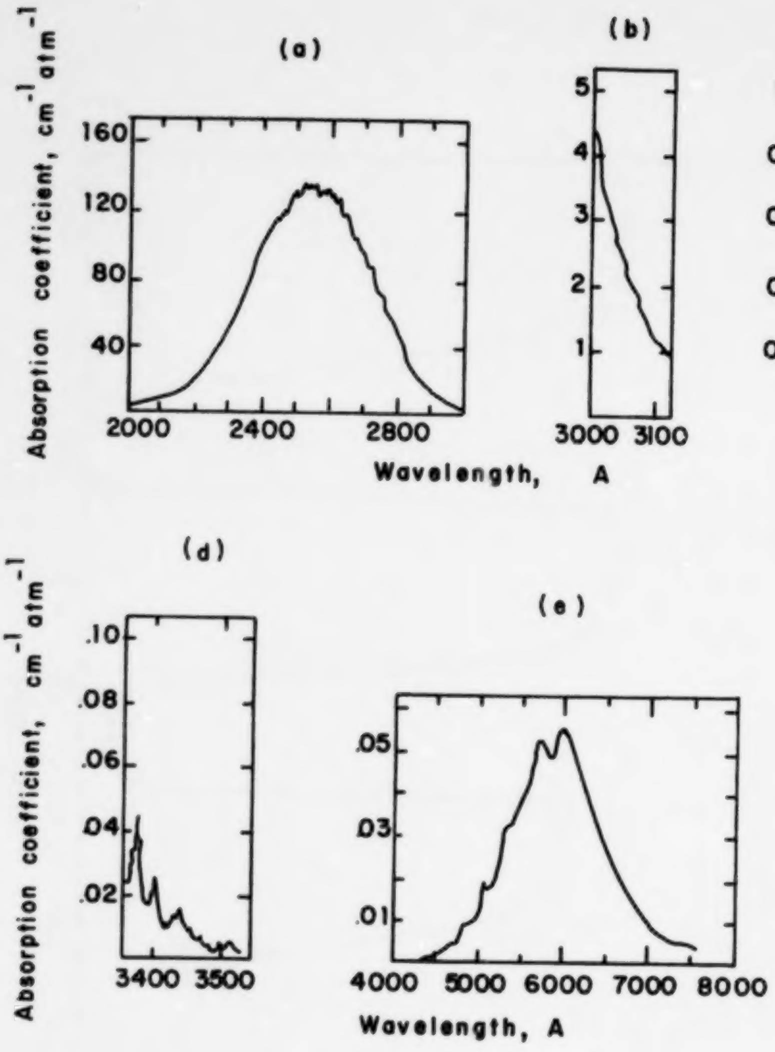

Figure 5. Absorption spectrum of O_3 from Inn and Tanaka. (75)

ozone by red light is two, and is unaffected by the presence of water vapor. Norrish and Wayne (79) observed strong absorption bands of the hydroxyl radical in flash photolysis of ozone-water vapor mixture, and McGrath and Norrish (82) suggested that the hydroxyl radical takes part in a chain decomposition of ozone to give the high quantum yield observed:

$$O_3 + h\nu \longrightarrow O^* + O_2^* \qquad [11]$$

$$O^* + H_2O \longrightarrow 2\ OH\cdot \qquad [12]$$

$$OH\cdot + O_3 \longrightarrow HO_2\cdot + O_2 \qquad [13]$$

$$HO_2\cdot + O_3 \longrightarrow OH\cdot + 2\ O_2 \qquad [14]$$

where O* is in the ^1D excited state. In contrast to the $O(^3P)$ ground state which has all orbitals occupied and which will tend to act as a radical, $O(^1D)$ corresponds to an electronic structure in which a 2p orbital is vacant, so that it is expected to be a strongly "acidic" reagent (eq. [12]). Fortin and co-workers 83) and a number of other researchers (84,85,86) confirmed the reaction of $O(^1D)$ with H_2O to be one of the principal mechanisms for producing hydroxyl radicals.

The photochemistry of ozone in water presumably is somewhat similar, but the large number of water molecules will quench the excited ozone molecule and consequently the quantum yield is expected to be lower in the liquid phase. Ozone decomposition by photolysis to form hydrogen peroxide in aqueous solution has been reported by Taube (87). In mildly acidic solution (dilute hydrochloric or acetic acid) which inhibits the chain reaction of O_3 and H_2O_2, the reaction

$$O_3 + H_2O + h\nu \longrightarrow O_2 + H_2O_2 \qquad [15]$$

takes place with almost exact stochiometry. The quantum yields for the disappearance of ozone at λ=254 nm, 310 nm and 600 nm are 0.62, 0.23 and 0.002-0.005 respectively. When light in the longer wavelength region is absorbed, no hydrogen peroxide is formed. The above observations are in complete agreement with predictions made on the basis of the gas-phase photochemistry of ozone discussed earlier. Reaction [11] occurs followed by direct formation of hydrogen peroxide by the addition of $O(^1D)$ to H_2O. Tracer experiments have shown that H_2O_2 formed derives approximately one-half its oxygen from the water, the other half from the ozone. Taube concluded that in mildly acidic system, a mechanism with OH· as an intermediate would not yield a linear build-up of H_2O_2, nor would the stoichiometry of eq. [13] be followed. Thomas (88) suggested that OH· radicals might dimerize to form H_2O_2 which consequently would react with more OH to form $HO_2\cdot$ and H_2O in the absence of acids.

On the other hand, H_2O_2 itself can be photolyzed to generate hydroxyl radicals. Baxendale and Wilson (89) showed at high intensities that

$$H_2O_2 + h\nu \longrightarrow 2\ OH\cdot \qquad [16]$$

is the primary process of the decomposition. Volman and Chen (90), Hunt and Taube (91) demonstrated that allyl alcohol, a radical scavenger, can remove the OH· and further reduce the quantum yield. They found at λ=254 nm, in aqueous solution, the quantum yield for the decomposition of hydrogen peroxide is 0.94 ± .06, while in the presence of allyl alcohol the number drops to 0.54 ± 0.05. Tetrahydroxyhexane was found as a product which must be formed by the addition of hydroxyl radicals to allyl alcohol followed by the association of the intermediate. Confirmation of the formation of hydroxyl radicals from the photolysis of H_2O_2 at λ=254 nm was also made by Buxton and Wilmarth (92).

Hydroxyl radicals can be obtained from the decomposition of H_2O_2 by other means; such as the titanium trichloride method of Dixon and Normann (93); generation by ferrous ion in the famous Fenton's reagent (94,95), and high energy radiation of aqueous solutions as by Currie and Dainton (96).

As one may expect, H_2O_2 is capable of acting as an oxidant in aqueous solution. Recently, Ogata and co-workers (97) studied the photo-induced oxidation of diethyleneglycol dimethyl ether (DEDE) and analogs with aqueous hydrogen peroxide. They stated that the oxidation is initiated by hydrogen atom abstraction by hydroxyl radical formed by the photolysis of H_2O_2. This is a model reaction for the photo-oxidative removal of nonionic surfactants in wastewater which are difficult to remove biologically. The absorption coefficient for H_2O_2 is larger than that of DEDE at 250 and 300 nm, so it is assumed the photolysis of DEDE itself is negligible. The hydroxyl radicals are supposedly the only active specie to react with DEDE. Ogata and co-workers reported that destruction of up to 67.2% of substrate could be reached after an irradiation time of 60 min. for a mixture of 0.937 M H_2O_2 and 0.184 M DEDE in aqueous solution at 20°C. The products found were methanol, ethylene glycol monomethyl ether (EME), methoxylacetaldehyde, methoxyacetic acid and methyl formate. These presumably were formed by the abstraction of hydrogen atoms at various sites followed by bond cleavage. No complete removal has been reported by this process.

Dore and co-workers (98) used the UV/H_2O_2 system for the oxidation of phenol solutions and compared the results with ozonation. Solutions were chlorinated after treatment and chloroform yields determined. It was reported that both systems gave the same result in that the quantity of chloroform produced by post-chlorination passes through a maximum value which depends on the time of pre-treatment. Photolytic oxidation by UV/H_2O_2 thus was proved to have similar effect on the degradation of organic compounds as ozonation. One may expect, however, that the quantum yield of hydroxyl radicals from hydrogen peroxide might be too low to effectively oxidize organic compounds for practical application. The difficulty in preparation and storage of hydrogen peroxide also discourages the use of this oxidant in large scale water treatment.

APPLICATIONS OF PHOTOLYTIC OZONATION IN AQUEOUS SOLUTION

The ultraviolet-ozone (O_3/UV) system has been used for oxidation of dieldrin in nonaqueous solution by Nagl and Korte (99), and the oxidation of carbon tetrachloride and chlorofluoromethanes in the vapor phase by Jayanty and co-workers (100). More recently, application of the process in aqueous solutions have been developed by a group at Houston Research Inc. It has been established that photolytic ozonation rates of dissolved organic compounds are ten to one thousand fold greater than with ozonation alone. Garrison and co-workers (101) applied O_3/UV for the destruction of complexed cyanides in water. They reported that for a fixed concentration of ozone, increasing the intensity of UV light increased the reaction rate markedly. Likewise, for a fixed intensity of UV light, increasing the ozone concentration also increased the reaction rate markedly. Ozonation alone is very slow compared to any combination of ozone concentration and UV intensity studied. Fochtman and Huff (102) reported that wastewater containing small concentrations of TNT was completely oxidized to carbon dioxide with ozone while being irradiated simultaneously with ultraviolet light. When ozone only was applied to three liters of "pink" water which contained 63 mg/L organic carbon, the TOC dropped to 56 mg/L over the first 60 minutes. No further decrease was observed, even after an additional 2.5 hours of ozonation. Under the same conditions, but with UV radiation, the total organic carbon decreased to 17 mg/L in a period of two hours. From the carbon mass balance studies. Fochtman and Huff found that 85% of the carbon lost from TNT solution under O_3/UV was accounted for as CO_2. Within experimental error, they concluded that TNT had been completely destroyed. No light molecular weight organics were found.

Prengle and co-workers (103) studied the rates of oxidation of refractory chemical species, ethanol, acetic acid, glycine, glycerol and palmitic acid, with ozone and ultraviolet light. A Refractory Index (RFI) parameter was defined to give a measure of the difficulty of oxidation of a given molecule. The lower its RFI, the less refractory is the compound to ozone oxidation. The authors monitored the changes of TOC to indicate the destruction rate of each substance with O_3/UV. The results were as expected in that ozone together with UV light enhanced the destruction significantly. In discussing the mechanisms for the oxidation processes in the O_3/UV system, the authors postulated two models of the kinetics of O_3/UV process. When the amount of UV radiation is small, and the chemical reactions are rate controlling, the authors visualized the reaction as being predominantly a three-step sequence consisting of simultaneous interaction of substrates with ozone and UV light. However, when the intensity of UV radiation is larger, the reaction becomes mass transfer controlled and substrates may be photolyzed to form free radicals which then react with ozone to form CO_2 and H_2O as final products. Apparently the authors applied "classical ozonation" in the model and omitted the possibility of ozone being decomposed to provide active species which carried the major reaction. Ozone/UV oxidation of several chlorinated compounds also had been studied by Prengle's group (104). They examined the oxidation rates of the following five compounds: pentachlorophenol, o-dichlorobenzene, dichlorobutane, chloroform and polychlorinated biphenyls, Aroclor 1254. In general, none of the above compounds are oxidized to the desired lower limits of concentration by ozone treatment alone, but are effectively destroyed by O_3/UV. The original and partial oxidation species reportedly are completely oxidized to Cl^-, Cl_2, CO_2, and H_2O. It was also concluded that UV absorption correlates with reactivity, e.g., aromatics absorb more UV and are more reactive than aliphatic compounds. The fate of chlorine on these compounds was described by one of two processes: dechlorination to form chloride ion from those compounds with substantial UV absorption, or transformed to chlorine and then to hypochlorous acid. The latter case reportedly occurred when the compound had small UV absorption such as chloroform. No evidence was given to verify the formation of free chlorine. Later, Prengle and Mauk (105) carried out photolytic ozonations of four pesticides: Malathion, Baygon, Vapam and DDT in aqueous solution. All were destroyed, as well as subsequent partial oxidation products, to yield TOC values below detectable limit. Postulated mechanisms were presented which indicate the chemical routes from initial to final oxidation species. The authors stated that O_3/UV photooxidation of dissolved substance (M-species) occurs primarily by a combination of ozone photolysis and M-photolysis. For low level UV absorbers the oxidation rate is controlled by the photolysis of ozone. The authors also stated that the species, H and OH radicals formed from photolysis of water, as well as H^+ and OH^-, are involved in the photooxidation of substrates. Neither the intermediate nor the final residues from photolytic oxidation of any of the organic compounds discussed were characterized.

The reduction of COD in wastewater by O_3/UV has been demonstrated by Wako and co-workers (106). A wastewater with 40.2 ppm COD and 110 ppm dispersion dye was treated with ozone while being exposed to UV light at 210-350 nm. After treatment the water had a COD of 2.8 ppm. When the wastewater was treated with ozone alone, the treated water had a COD of 37.3 ppm. In another report, Wako (107) studied the photooxidation of phenol with ozone and UV radiation. The yield of decomposition products was determined by liquid chromotography. The products were not identified but the relations between the peak heights of products and reaction time for each decomposition were recorded. The possible intermediates of ozonation of phenol, such as catechol, hydroquinone, resorcinol and maleic acid were also subjected to O_3/UV at various pH values. As expected, decomposition of phenol was found to be accelerated by increasing the concentrations of base (potassium hydroxide).

Ozonations with and without UV irradiation of 2-propanol, acetic acid, acetone and oxalic acid were conducted by Kuo and co-workers (108). Ozonation and O_3/UV products from these model compounds were identical. Upon ozonation, 2-propanol was converted to acetone which in turn was oxidized to acetic and oxalic acids. Trace amounts of formaldehyde and formic acid were detected in the ozonated acetone solution. Further ozonation of acetic acid resulted in the formation of glyoxylic acid that was oxidized readily to oxalic acid which in turn was oxidized directly to carbon dioxide. The destruction rate of each compound was observed to be faster during O_3/UV process than with ozone alone. The results of Kuo and co-workers suggest a very interesting aspect of the O_3/UV processes for the photo-oxidation of organic compounds. It has been recognized that saturated carbonyl compounds undergo photo-induced decarboxylation in the gas-phase. The process was first observed by R.G.W. Norrish and is known as the Norrish Type I or α-cleavage process (109). The solution-phase reaction is less common due to more rapid vibrational relaxation by collision with solvent molecules, but still many reports of the reaction occurring in solution phase have been made:

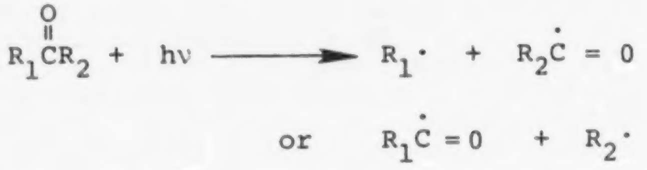

$$R_1\overset{\overset{O}{\|}}{C}R_2 + h\nu \longrightarrow R_1\cdot + R_2\dot{C} = O$$

$$\text{or} \quad R_1\dot{C} = O + R_2\cdot$$

[17]

The free radicals formed are believed to react with solvent or other radicals. In other cases, once the carbonyl groups are excited they commonly undergo intramolecular hydrogen abstraction from the side chain by the photo-excited carbonyl group with the formation of a 1,4-biradical. This species can be cleaved to an olefin and an enol. These reactions are now referred to as Norrish Type II reactions:

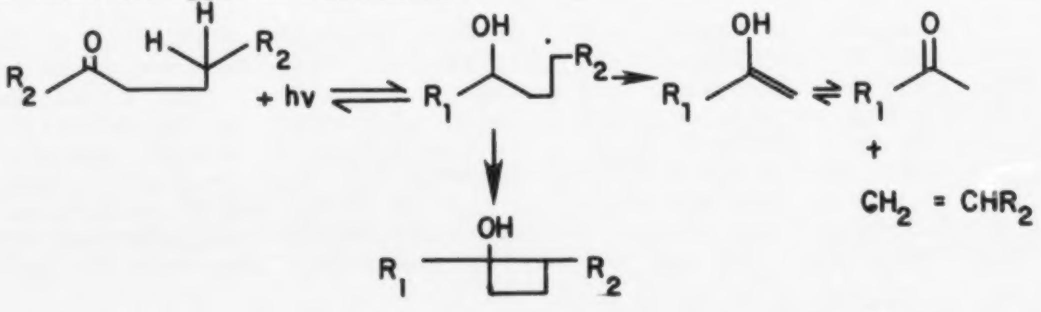

Acetone, then, may be oxidized by the Norrish Type I process followed by reaction with OH· from the decomposition of ozone under UV radiation as follows:

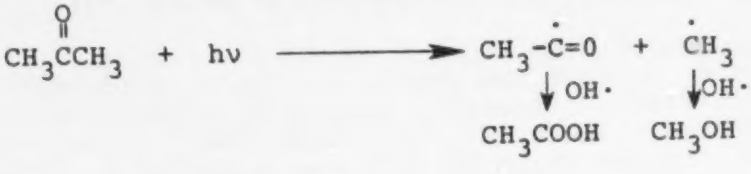

$$\begin{array}{ccccc} CH_3\overset{\overset{O}{\|}}{C}CH_3 + h\nu & \longrightarrow & CH_3-\dot{C}=O & + & \dot{C}H_3 \\ & & \downarrow OH\cdot & & \downarrow OH\cdot \\ & & CH_3COOH & & CH_3OH \end{array} \qquad [19]$$

Acetic acid may be oxidized in the following manner (110):

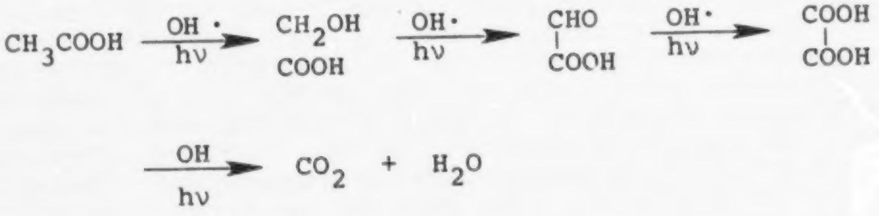

$$CH_3COOH \xrightarrow[h\nu]{OH\cdot} \begin{array}{c}CH_2OH\\COOH\end{array} \xrightarrow[h\nu]{OH\cdot} \begin{array}{c}CHO\\|\\COOH\end{array} \xrightarrow[h\nu]{OH\cdot} \begin{array}{c}COOH\\|\\COOH\end{array} \qquad [20]$$

$$\xrightarrow[h\nu]{OH} CO_2 + H_2O$$

In accordance with the postulated pathway, all the intermediates except $CH_2OHCOOH$ were identified during O_3/UV of acetone by McCarthy (111).

The fate of methanol under O_3/UV was shown by the experimental data of Chian (112). By successive abstraction of hydrogen, addition of hydroxyl radicals or oxygen, and rearrangement of unstable intermediates, methanol may be oxidized through formaldehyde to formic acid. Further oxidation of acids would result in the production of carbon dioxide and water:

$$CH_3OH \xrightarrow[h\nu]{OH\cdot} HCHO \xrightarrow[h\nu]{OH\cdot} HCOOH \xrightarrow[h\nu]{OH\cdot} CO_2 + H_2O \qquad [21]$$

Complete removal of the substance thus occurs once the decarboxylation occurs.

Smetana and Bulusu (113) studied methods of removal of RDX, hexahydro-1,3,5-trinitro-1,3,5-triazine, from wastewater of munitions manufacturing and processing plants. They found that aqueous RDX solutions undergo rapid photochemical degradation with 254 nm radiation leading to low molecular weight gaseous products. Ozone was found to degrade RDX much less efficiently than UV alone, and the combined use of ozone and UV exhibited a marked synergistic effect in that the combined degradation rate is greater than the sum of the two individual degradation rates.

Total destruction of substrate was observed, with CO_2, N_2O, NO, CO, HCN, CH_2O and H_2O found as the products.

In addition to their work on ozonation for destruction of halomethane precursors from humic acid and river water, Glaze and co-workers (33) also applied O_3/UV in the same system. It was found that both ozone and O_3/UV effectively reduce THM formation potential. O_3/UV was found to be more effective than ozone alone.

Leitis and co-workers (115) studied the nature of oxygenating species by determining the ratio of hydroxylation products formed by ozonation and O_3/UV. They attempted to show that hydroxyl radical was not the active specie in ozone and ozone/UV treatment by comparing the relative proportion of ortho-, meta-, and para-nitrophenols which were found as products using ozone, ozone/UV, UV alone, hydrogen peroxide, Fenton's reagent, NaOCl/H_2O_2, and H_2O_2/UV both with air and nitrogen present. Although very little data was given in the paper, it appears that the authors were basing their conclusions on products which, although purportedly representing the first of a multi-stage process, accounted for only about 1% of the substrate which had been destroyed up to that point. The relative amounts of those products remaining would of course be related to their relative rates in subsequent processes, as well as to the manner and amount in which active specie was generated, the initial concentration of substrate, and the length of the treatment time. Since the ozonation was performed at approximately neutral pH, hydroxyl radical is not expected to play an important part in their experiments using ozone without UV, and the results are therefore not in contradiction with the conclusions of Hoigne and Bader (44-46).

The above authors found that ozonation and O_3/UV of nitrobenzene, selected as a primary model compound, gave similar ratios of all major peaks in the chromatograms of the reaction mixtures from ozone and ozone/UV treatment. The major stable intermediates were oxalic acid, formic acid and glyoxal. It was stated that the reactivities of some of the model compounds during both processes were similar indicating that the same reactive species is involved in the reactions. However, the reactivities of the intermediates, oxalic and formic acids, were greatly enhanced by O_3/UV over ozonation. The authors concluded that the first steps of the ozone and ozone/UV degradation are probably not free radical in nature, but gave no direct evidence other than the fact that the reactivities of nitrobenzene, benzoic acid, and anisole with ozone/UV were inconsistent with electrophilic aromatic substitution.

In the treatment of water by ozonation and combined ozone/ultraviolet radiation, ozone at 1-5% by weight in air or oxygen is normally applied at a certain rate into the reactor. Under UV radiation, there remains the question as to whether the interaction of oxygen and ultraviolet radiation contributes to the destruction of substrates. In order to examine this question, two groups, Fochtman and Huff (102) and Prengle and coworkers (105) conducted experiments in which oxygen was used to replace the ozone-oxygen mixture for photolytic oxidation. Fochtman and Huff reported that very little effect could be noted for the destruction of TNT. However, Prengle and coworkers found that oxygen with low pressure mercury radiation led to some degree of destruction of reactant species, such as pesticides. They stated that the effect was a result of a combination of mechanisms which included the production of trace amounts of ozone, activated oxygen, and activated reactant molecules.

The absorption spectrum of oxygen obtained by McNesby and Okabe (116), Figure 6, shows that it strongly absorbs radiation

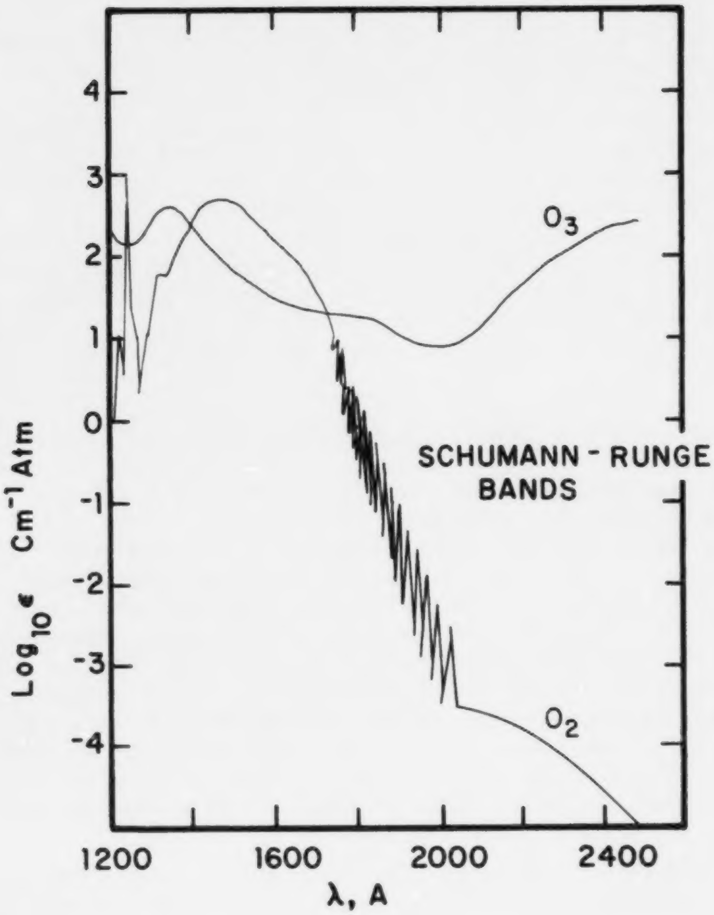

Figure 6. Absorption coefficients of O_2 and O_3.

of wavelengths below 176 nm. Although oxygen weakly absorbs radiation within the forbidden Herzberg band, originating near 254 nm (117),

$$O_2(^3\Sigma^-g) + h\nu \longrightarrow O_2(^3\Sigma^+u) \longrightarrow 2\ O(^3P) \qquad [22]$$

only ground state oxygen O (^{3}P) atoms, not excited molecular oxygen can be formed to act as active oxidative species (eq.[22]). Oxygen must absorb radiation with wavelength below 176 nm to gain enough energy to be promoted to the $O_2(^3\Sigma^-u)$ state which may subsequently dissociate to form $O(^1D)$:

$$O_2(^3\Sigma^-g) + h\nu \longrightarrow O_2(^3\Sigma^-u) \longrightarrow O(^1D) + O(^3P) \qquad [23]$$

Compared with the facile decomposition of ozone at 254 nm, the dissociation of oxygen is far less important in the O_3/UV process. On the other hand, molecular oxygen can undoubtedly take part in the reaction when substances form radicals by other pathways. Galen and Smith (118) have studied the photodecomposition of phenol in a tubular-flow reactor in which phenol was dissociated initially to form the phenoxy radical. The authors propose that this radical then was attacked by molecular oxygen to form peroxy radicals which ultimately yield organic acids and other products.

Jacob, Balakrishnan and Reddy (148) proposed mechanisms which explained the production of phenol and hydroxymucondialdehyde from the reaction of benzene with hydroxyl radicals in which molecular oxygen played a very important role. Correspondingly, Mathews and Sangster (149) showed a threefold decrease in carbon dioxide yield from the hydroxyl radical-involved decarboxylation of benzoic acid when the aqueous solution was deoxygenated. In fact, for reactions of hydroxyl radical in dilute aqueous solution, the oxygen molecule is probably a very important contributor, since it provides the mechanism by which an intermediate can rid itself of the unpaired electron; for example (148),

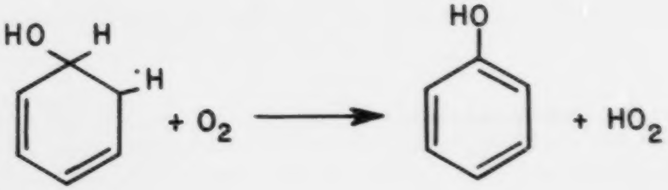

UV PHOTOLYSIS OF HALOGENATED COMPOUNDS IN AQUEOUS SOLUTION

The nonoxidative reactions of organic compounds in aqueous solution caused by UV-irradiation would also be expected to occur. The principles of photochemical reaction in aqueous solution have been reviewed by Owen (119). Water provides a transparent and sometimes reactive medium in which chemical reactions are effectively energized by UV. Ultraviolet light has been shown to exert drastic changes in many pesticides under laboratory conditions. It is well known that, in the presence of hydroxide ions or other nucleophiles, photonucleophilic displacement reactions result in hydrolysis and the conversion of aromatic halides to phenols and eventually to insoluble polymers. Crosby and Tutass (120) studied the photodecomposition of 2,4-dichlorophenoxyacetic acid (2,4-D) at 254 nm. The decomposition products found were 2,4-dichlorophenol, 4-chlorocatechol, 2-hydroxyl-4-chlorophenoxyacetic acid, 1,2,4-benzentriol, and polymeric "humic acid." The proposed mechanism is shown in Figure 7.

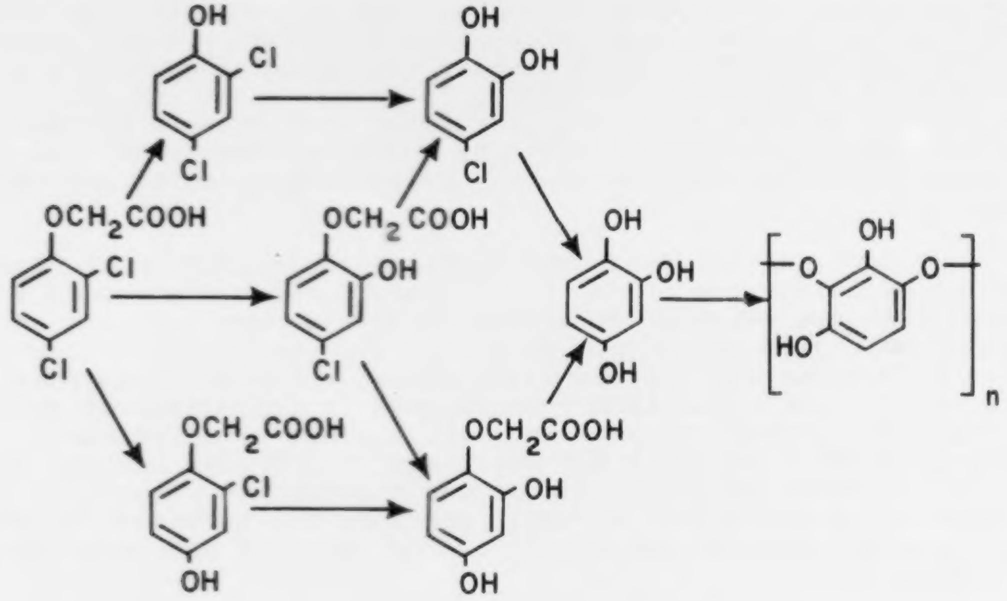

Figure 7. Proposed mechanism of 2,4-D photodecomposition.

Apparently, from the excited state, the carbon-halogen bond undergoes fission giving rise to aryl and halogen radicals. The radicals then abstract hydrogen from the medium or dimerize. Prior to bond fission an alternative reaction between the excited state and a nucleophilic species may occur giving the appropriate substitution at the carbon-halogen bond (121).

Figure 8 shows the nonoxidative photolysis of haloaromatics.

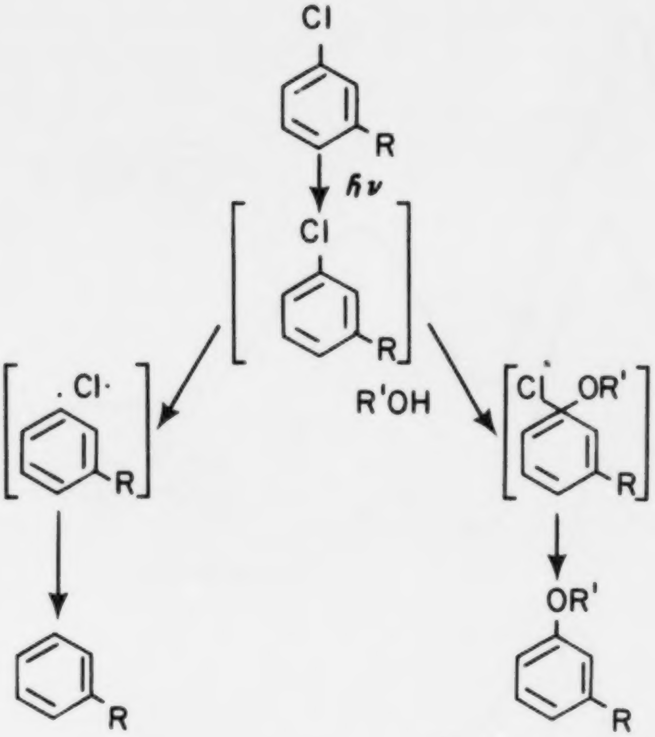

Figure 8. Photolysis of haloaromatics.

Polychlorinated biphenyls are known to be stable towards oxidation, hydrolysis and other chemical reaction might occur in the environment. However, the photochemically-induced degradation of PCBs has been reported by a number of groups, such as Ruzo and co-workers (122-124), Safe and Hutzinger (125, 126) and Hustert and Korte (127). Most of the photochemical experiments were conducted in organic solvents such as hexane and methanol. Dechlorination is the common reaction observed. The isomeric effects play an important role in the rate of dechlorination of PCBs. The spectra of these compounds show a wide range of absorptions which are related to the individual isomeric structure. MacNeil and co-workers (128) examined UV spectra of twenty-nine chlorobiphenyls. It is noted that with increasing chloro substitution in which there are less than two chlorine groups ortho to the ring-ring bond the λ_{max} values for the K bands are shifted to longer wavelengths. Introduction of two or more chlorine atoms ortho to the ph-ph bond results in a decrease in the intensity of K band (see Figure 9 and 10).

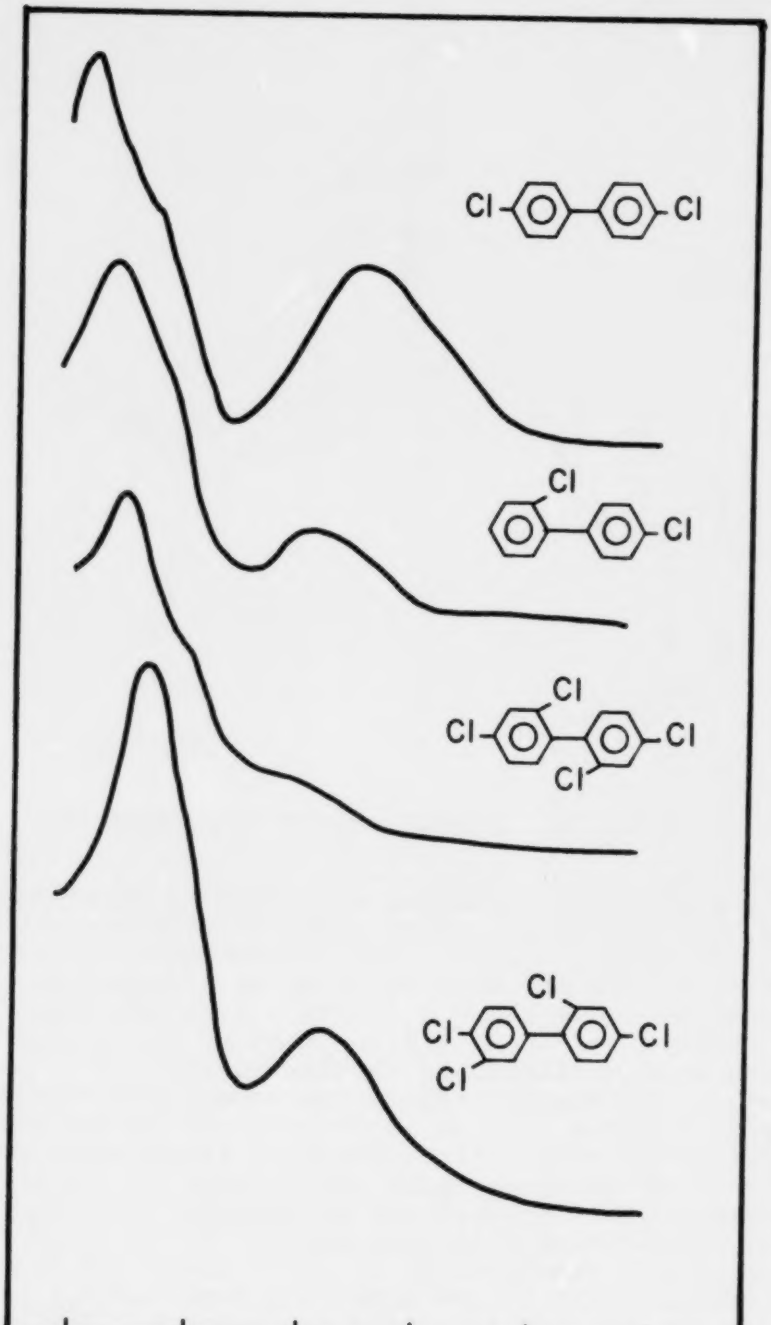

Figure 9. UV spectra of four isomeric tetrachlorobiphenyls.

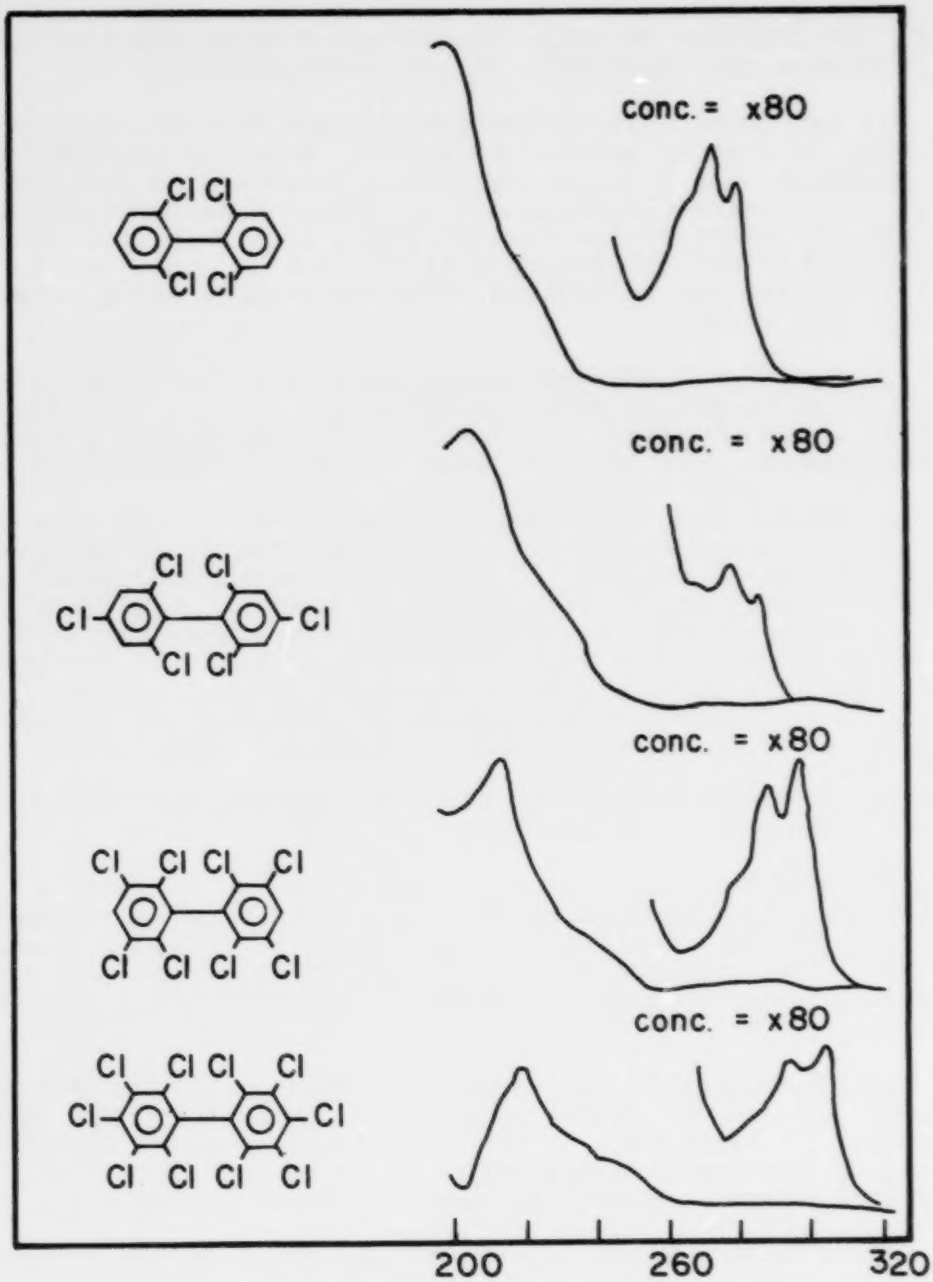

Figure 10. UV spectra of chlorobiphenyls.

Since biphenyl itself has a planar excited state geometry, under radiation the coplanarity between the ring would increase conjugation and stabilize the excited state molecules. However, the ortho chlorine substituents sterically hinder the coplanarity between the phenyl rings, and these groups are specifically cleaved in preference to substituents at the met and para positions. An increase in ortho substituents decreases the lifetime and increases the reactivity of the excited state.

It was found that oxygen retards the photochemical degradation rate of PCBs in aerated solution. Ruzo and co-workers (123) also observed that 1,3-cyclohexadiene quenched the excited state of 2,2',4,4'-tetrachlorobiphenyl in degassed methanol solution. Both results indicate the excited state is a triplet. The authors concluded that PCBs should be excited from ground state to excited singlet and to excited reactive triplet state from which radicals are formed.

2,2',4,4',6,6'-Hexachlorobiphenyl (HCB) had been irradiated at 310 nm in hexane by Safe and Hutzinger (125). They found some products formed by loss of chlorine, rearrangement and condensation; however, the products were not well-characterized.

As noted, most photochemical reactions of PCBs have been conducted in nonaqueous solution. In an attempt to demonstrate the photochemical reaction of PCBs in "natural condition" which is close to that in the environment. Hutzinger and co-workers (126) irradiated PCBs in aqueous suspensions and films covered with water. They identified hydroxychlorobiphenyls and "carboxyl" type compounds, which showed hydroxy and carbonyl stretching, besides dechlorinated PCBs which were identified by gas chromatography, mass spectrometry and infrared spectrometry.

KINETICS OF THE DECOMPOSITION OF OZONE AND ITS REACTION WITH ORGANIC COMPOUNDS IN WATER

The rapid decomposition process of ozone in aqueous solution has been studied by many investigators, as reviewed in a previous section. These investigations have included a number of studies on the kinetics of ozone decomposition; however, the findings are conflicting. In particular, there is a disagreement over the kinetic order of reaction.

Autodecomposition of ozone in water, as it is often called, has been reported to follow a variety of kinetic orders which are apparently pH dependent. A summary of the range of variables covered by various investigators and their conclusions concerning the reaction order related to ozone is shown in Table 2.

There is presently no general agreement on the mechanism of autodecomposition nor has there been any adequate explanation of the variations in the kinetic results obtained by various

TABLE 2. SUMMARY OF RESEARCH ON OZONE DECOMPOSITION IN WATER

Investigators		ph Range	Temperature range, C^o	Reaction order with respect to ozone
Alder and Hill	(129)	1-2.8	0-27	1
Chang	(130)	9	25	1
Czapski and co-workers	(70)	10-13	25	1
Hewes and Davison	(51)	2-4, 6, 8	30-60,10-50,10-20	2, 3/2-2,1
Kilpatrick and co-workers	(41)	0-6.8, 13	25	3/2,2
Kuo and co-workers	(71)	2.2-11.0	15-35	3/2
Merkulova and co-workers	(131)	0.22-1.9	5-40	1,2
Rankas and co-workers	(132)	5.4-8.5	5-25	3/2
Cizzufi and Marrucci	(133)	8.5-13.5	18-27	1
Rogozhkin	(134)	9.6-11.9	25	1
Rothmund and Burgstaliker	(135)	2-4	0	2
Sennewald	(136)	5.3-8	0	2
Shambaugh and Melnyk	(137)	9.0	25	1
Stumm	(42)	7.6-10.4	1.2-19.8	1
Weiss	(138)	2-8	0	3/2

investigators. Several investigators include pH dependent terms in the rate expression such as Stumm (42).

$$\frac{-d[O_3]}{dt} = k\,[OH^-]^{0.75}[O_3] \qquad [24]$$

and Weiss (138)

$$\frac{-d[O_3]}{dt} = k_1\,[OH^-]\,[O_3] + k_2\,[OH^-]^{0.5}\,[O_3]^{3/2} \qquad [25]$$

The mechanism proposed by Peleg which combines proposals by Stumm and others is shown in equations [1] through [8] .

The kinetics of the ozonation of some substances in water and wastewater have been studied. Khandelwal and co-workers (139) reported that cyanide removal appeared to follow one-third order with respect to cyanide concentration:

$$\frac{-d\,[CN^-]}{dt} = k\,[CN^-]^{1/3} \qquad [26]$$

where k the reaction rate constant contains substantially constant ozone concentration in the liquid. Kirk and co-workers (140) proposed the following expressions based on their experiments of the removal of COD by ozonation. The removal or organics followed either the pseudo-first-order kinetics as shown in equation (27)

$$-\frac{d\,[COD]}{dt} = k_1\,[COD] \qquad [27]$$

or second-order kinetics as in (28):

$$-\frac{d\,[COD]}{dt} = k_2[O_3]\,[COD] \qquad [28]$$

In [27] and [28] k_1 is the pseudo-first-order rate constant, [COD] is the concentration of COD at time t, k_2 is the second-order rate constant, $[O_3]$ is the dissolved ozone concentration at time t.

Chang (130) as well as Kuo and Wen (141) studied the kinetics of the ozonation of methanol and its degradation products in aqueous solution. They obtained the following expression for the ozonation of methanol:

$$-\frac{d\,[CH_3OH]}{dt} = k_2[O_3]^p[CH_3OH] \qquad [29]$$

where p = 3/2 to 1/2 as pH varied from 7.2 to 11.0. Their data also showed that the ozonation of formaldehyde and formic acid, degradation products of methanol, are also first-order with respect to the substrates, however, the order with respect to ozone concentration varies. For formaldehyde

$$-\frac{d[HCHO]}{dt} = k[O_3]^q[HCHO] \qquad [30]$$

where q = 1/2 as reported by Kuo and Wen (141) and one by Chang (130). For formic acid

$$-\frac{d[HCOOH]}{dt} = k[O_3]^r[HCOOH] \qquad [31]$$

where r = 1.2 to 0.74 as pH increases from 1.7 to 11.0. With substrate at an initial concentration, the degradation should be proportional to the substrate concentration and to the quantity of ozone used to degrade it.

Eisenhauer (142) defined the "ozone dose rate" as follows:

$$R = \frac{[O_3]\ F}{P_o\ V} \qquad [32]$$

where O_3 = ozone concentration in the feed gas (moles/L)

F = ozone gas flow rate (L/min)

P_o = initial phenol concentration (mole/L), and

V = reaction volume (L).

Thus, the degradation rate of phenol could be expressed as

$$-\frac{d\,[P]}{dt} = k\cdot R\cdot [P] \qquad [33]$$

where [P] = concentration of phenol at time t. Since phenol [P] is oxidized to catechol (C) which in turn is degraded to other oxidation products (D), Eisenhauer used the kinetics of consecutive reactions of the type:

$$P \xrightarrow{k_1} C \xrightarrow{k_2} D \qquad [34]$$

The rate expression for concentration of catechol at time t may be derived from this expression; yielding 35 :

$$[C] = \frac{k_1 P_o}{k_2 - k_1} \left(e^{-k_1 \cdot R \cdot t/F^{1/3}} - e^{-k_2 \cdot R \cdot t/F^{1/3}}\right) \qquad [35]$$

where P_o, R and F are defined in equations [32] and [33] . Gould and Weber (64) in another study of the ozonation of phenol also found that the degradation of phenol follows the expression [33] proposed by Eisenhauer. They stated that the removal of COD may be expressed by the similar relationship

$$[COD] = [COD]_o \, e^{-k \cdot R \cdot t} \qquad [36]$$

MODELS FOR OZONE MASS TRANSFER AND SIMULTANEOUS CHEMICAL REACTION

Since ozone is only slightly soluble in aqueous solution, the rate of absorption of ozone is of main concern in considering the ozone injection process. Eisenhauer (142) as well as Gould and Weber (64) had demonstrated the dependency of ozonation rate on the ozone dose rate. Mass transfer, therefore, plays an important role in the semi-batch type reactor system. The relationship between the dose rate and dissolved ozone concentration is the subject of the study of mass transfer. Numerous studies have been done on models for ozone mass transfer (137, 141, 143-145). The mathematical model which can describe the mass transfer process of ozone from air or oxygen into the water is analogous to heat transfer or conduction of electric charge through resisting medium. Film theory is commonly applied for the mass transfer model, according to which, the ozone reaction mechanism for treating water can be visualized as follows for the case where the ozone-substrate reaction is very fast (145):

a) Ozone diffuses through the gas film to the gas-liquid interface.

b) Ozone transfers across the interface into the liquid film.

c) The liquid reactant diffuses from the bulk liquid into the liquid film.

d) Ozone oxidizes the liquid reactant to form a product.

e) The product can continue to react or diffuse into the bulk liquid.

Using film theory, Shambaugh and Melynk (137) developed the following model to describe the concentration of ozone, A^o, in the liquid as a function of time.

$$A^o = \frac{\frac{G}{V} m_o [1-e^{-PRh}]}{k_1 + \frac{GHe}{VP} [1-e^{-PRh}]} \cdot [1-e^{-[k_1 + \frac{GHe}{VP} (1-e^{-PRh})]t}] \quad [37]$$

where

$$R = \frac{V}{Gh} [\frac{k_L \; k_G a'}{k_L + k_G H_e}] \quad [38]$$

G = inert gas flow rate, g mole/sec.

V = volume of reactor, cm^3

m = molar fraction of ozone in the gas feed

P = reaction operating pressure, atm.

h = distance from sintered glass plate to surface of liquid in reactor, cm.

k_1 = first-order rate constant for ozone decomposition, sec^{-1}.

k_L = liquid-film mass transfer coefficient, cm/sec.

k_G = gas-phase mass transfer coefficient, g mole/cm^2-sec-atm.

a' = interfacial area per unit volume of liquid, cm^{-1}.

He = Henry's law constant, atm-cm^3/g-mole.

From equation [37], the steady state concentration of ozone can be expressed as

$$A^o_{ss} = \frac{\frac{G}{V} \cdot m_o \cdot [1-e^{-PRh}]}{k_1 + \frac{GHe}{VP} [1-e^{-PRh}]} \quad [39]$$

$A^{o}ss$ is less than the equilibrium ozone concentration predicted by Henry's law due to rapid ozone decomposition, particularly under alkaline conditions (pH = 9 and above).

In an attempt to obtain $k_L a$, the overall liquid-phase mass transfer coefficient, Yocum (145) derived the following expression also using film theory:

$$k_L a = \left[\frac{C_1}{\eta - \beta C_1}\right] \frac{L}{V} \qquad [40]$$

with

$$C_1 = \frac{-1}{t} \ln \left[1 - \frac{X_B}{X_B^*}\right] \qquad [41]$$

and

$$\eta = 1 + \frac{k_o}{k_L a} = \frac{X_B^*}{X_{Be}} \qquad [42]$$

where X_B = mole fraction of ozone in liquid

X_B^* = theoretical mole fraction of ozone in liquid at equilibrium with feed gas as predicted by Henry's law

X_{Be} = mole fraction of ozone in liquid at equilibrium

k_o = ozone decomposition reaction rate constant, lb. mole/ft^3 min.

L = moles of liquid, lb moles

V = volume of liquid in reactor, ft^3.

β = $P_t L/HG$

Pt = total pressure, atm.

H = Henry's law constant, atm.

G = gas molar flow rate, lb mole/min.

This coefficient is also a function of turbine power input and superficial gas velocity.

Equations [40] - [42] were derived in part from the equation which describes the change of ozone concentration in the liquid. Writing slightly differently from reference 145,

$$\frac{dC_B}{dt} = K_{la}(C_{Be} - C_B) - k_o C_B \quad , \qquad [43]$$

where C_B = bulk concentration of ozone in liquid,

C_{Be} = concentration of ozone in liquid, which would be in Henry's Law equilibrium with the gas,

and other symbols are as before. Mass transfer coefficients were calculated from the measurement of ozone adsorption into distilled water as a function of time.

When other substances are present which could also react to remove ozone from solution,

$$\text{OZONE REMOVAL RATE}_i = k_i S_i^a C_B^b = -R_i \quad , \qquad [44]$$

$$\frac{dC_B}{dt} = K_{la}(C_{Be} - C_B) - k_o C_B - \sum_j R_i \quad . \qquad [45]$$

When there is only one term in $\sum_i R_i$ and it is first order in C_B then

$$\sum_i R_i = k_a C_B \qquad [46]$$

and

$$\eta = \left(1 + \frac{k_o + k_a}{K_{la}}\right) = \frac{C_B^*}{C_{Be}} \quad . \qquad [47]$$

As will be seen later, this is the case for ozone photolysis.

KINETIC MODELS FOR PHOTOLYTIC OZONATION IN AQUEOUS SOLUTION

Very little work has been done on the kinetics of ozonation under UV irradiation. According to Wako (107), the reaction rate of the O_3/UV oxidation of phenol can be expressed as

$$\frac{-d[P]}{dt} = k'[P]^{0.5} = k''[O_3][P]^{0.5} \qquad [48]$$

where $k' = 0.63 \exp(-3.18x10^3/T), k''=1.24x10^4 \exp(-3.18x10^3/T)$

P = concentration of phenol in solution, mol/L

O_3 = the ozone dose rate, mol/L(O_2)/sec.

T = temperature of solution

Since the decomposition is also reported to be catalyzed by base (potassium hydroxide), Wako derived the following equation for the disappearance of phenol under O_3/UV:

$$[P]_{KOH=0}-[P] = [P]_{t=0}\{1-\exp(-1.3x10^3[KOH][O_3]t)\}. \qquad [49]$$

Prengle and co-workers (105) developed kinetic expressions for the O_3/UV process. The expressions were based on the assumption that reaction mechanisms were different under low and high intensities of UV radiation. The authors stated that when the UV intensity is low, then

$$A \xrightarrow[h_\nu,O_3]{k_o} P_1 \xrightarrow[h_\nu,O_3]{k_1} P_2 \xrightarrow[h_\nu,O_3]{k_2} P_3(CO_2+H_2O) \qquad [50]$$

and

$$\left(\frac{TOC}{TOC_o}\right) = \Omega_o e^{-w_o t} - \Omega_1 e^{-w_1 t} - (\Omega_o-\Omega_1-1)e^{-w_2 t} \qquad [51]$$

where w_o, w_1, w_2 are the reaction rate moduli containing k_o, k_1, k_2, and

$$\Omega_o \equiv \frac{w_1 \quad w_2}{(w_o-w_o)(w_2-w_o)} \; ; \; \Omega \equiv \frac{w_o \quad w_2}{(w_1-w_o)(w_2-w_1)} \qquad [52]$$

However, when UV is larger,

$$A = h\nu \longrightarrow R\cdot's \qquad [53]$$

$$R\cdot's + O_3 \longrightarrow CO_2 + H_2O + \ldots \qquad [54]$$

and the generation rate of free radicals is

$$-\frac{dR\cdot{}'S}{dt} = \frac{\mu\phi a\ \dot{I}}{N_o\ h\nu} \equiv k_\nu\ a\ \dot{I}_\nu \qquad [55]$$

where $k_\nu a$ is the radiation transfer coefficient. The final expression obtained is

$$\frac{TOC}{TOC_o} = f_1(t)f_2(t) = (1-\theta t)[\Omega_o e^{-w_o t}-\Omega_1 e^{-w_1 t}-(\Omega_o-\Omega_1-1)e^{-w_2 t}] \qquad [56]$$

where $\theta = k_\nu a(\frac{V}{m_{Ao}})\ \dot{I}_{\nu c}$, $f_1(t) = 1-\theta t$,

$f_2(t) = \Omega_o e^{-w_o t} - \Omega_1 e^{-w_1 t} - (\Omega_o-\Omega_1-1)e^{-w_2 t}$, $\dot{I}_{\nu c}$ is the critical UV. input

When UV input is small, $f_1(t) = 1$ and $(\frac{TOC}{TOC_o}) = f_2(t)$, and when UV input is larger, t is small, $f_2(t) = 1$ and $(\frac{TOC}{TOC_o}) = f_1(t)$.

No investigations have been reported in which there is sufficient detail of data to confirm this model or to evaluate the reaction rate moduli, but it would appear that the validity of the assumption in equation [53] could easily be deduced from the results of photolysis experiments on the individual substrate compounds.

Taking a completely different approach from that of Prengle and co-workers, Lee and co-workers (110) developed a mathematical model describing the O_3/UV removal of total organic carbon (TOC) from water. The authors assumed that under UV radiation, the only important active species are hydroxyl radicals which are generated from the decomposition of ozone which previously had transferred into the liquid phase. According to this view, the radicals either react with the organic substances or react with each other to terminate the chain reaction. The decomposition rate constant k_d is a function of pH and UV intensity; at high UV intensity and high pH,

$$k_L'a/k_d \ll 1 \qquad [57]$$

where $k_L'a$ is the overall mass transfer coefficient.

Their models are described as follows:

a) When the total organic carbon concentration $C_B \longrightarrow \infty$

$$C_{BO} - C_B = \alpha k_L' a \; P_A t/[H(1 + k_L' a/k_d)] \qquad [58]$$

where C_{BO} = initial concentration of TOC

C_B = concentration of TOC at time t

P_A = partial pressure of ozone in the gas phase

H = Henry's law constant

α = ratio of stoichiometric constants c/b, which come from

$$O_3 + h\nu \longrightarrow c\,R\cdot \qquad [59]$$

$$B + bR\cdot \xrightarrow{k_o(B)} \text{products } (CO_2 + H_2O) \qquad [60]$$

and

$$-r_B = -d\,C_B/dt = k_o C_R^{\,m} C_B^{\,n} \qquad [61]$$

b) When $C_B \longrightarrow 0$

$$\ln(C_{BN}/C_B) = k_2 P_A^{\,m/1} t, \text{ for } n = 1 \qquad [62]$$

$$C_B^{\,1-n} - C_{BN}^{\,1-n} = (n-1) k_2 P_A^{\,m/1} t, \text{ for } n \neq 1 \qquad [63]$$

where $C_B = C_{BN}$, at $t = t_n$

The order 1 in the last equation is derived from the suicidal reaction for free radicals

$$-r_{R,S} = k_S\, C_R^{\,1} \qquad [64]$$

For an intermediate range of C_B concentration, the following expression was applied,

$$-r_B = -\,d\,C_B/dt = k\,C_B^{\,n} = k' V_s^p\, \bar{P}_A^q\, C_B^n \qquad [65]$$

where k' = f(Iuv, T, pH, H)

V_S = gas superficial velocity

$\bar{P}_A$ = logarithmic mean of ozone partial pressure in the reactor and

$$Iuv = \frac{\text{Total output of UV lamp (W)}}{\text{Reactor wet volume (L)}} \qquad [66]$$

Based on the experimental data, the authors obtained $n = 1$, $q = 1.5$ and $p = 1.5$ for the O_3/UV of TOC in hospital wastewater; Equation [65] thus illustrates the dependency of rate on UV intensity, ozone input rate, and mass transfer efficiency.

In the next chapter expressions will be developed which utilize and combine various features of the previous treatments, in order to describe the kinetics of ozone/UV-induced reactions and allow prediction of reaction rates from specified values of the independent variables.

CONCLUSIONS FROM LITERATURE SURVEY

a) Ozonation has been used as a disinfectant of drinking water for decades, without report of serious negative consequences.

b) Ozone decomposes fairly rapidly in water, but there is not general agreement as to the kinetics or mechanism. Hydrogen peroxide and oxygen were found as final products and hydroxyl radical (·OH) as an intermediate. The decomposition rate increases with increasing pH, up to about pH 13.

c) The rate of oxidation of organic compounds increases under conditions which favor decomposition of ozone,

d) The active species formed upon ozone autodecomposition in water is the hydroxyl radical.

e) Reactivity of the hydroxyl radical is considerably faster and more non-specific than ozone itself.

f) Ozonation products include carboxylic acids and aldehydes predicted by cleavage of double bonds. Phenols yield polyhydroxy compounds which then degrade to smaller non-aromatic acids. Hydrogen peroxide has also been found. 4,4'-dichlorobiphenyl gave 4-chlorobenzoic acid.

g) Organohalogen is converted to chloride but not necessarily at the same rate as substrate disappears providing there is a site for attack which does not include the chlorine-bound carbon atom.

h) Ultraviolet light accelerates the decomposition of ozone and therefore may provide a specie more reactive than ozone.

i) Photolysis of dry ozone in the vapor phase gives a quantum yield of two; greater if water vapor is present. Photolysis products are oxygen atoms and hydroxyl radicals.

j) In aqueous solution hydrogen peroxide is a product of ozone photolysis, probably due to combination of oxygen atoms with H_2O. Half of the oxygen in H_2O_2 comes from ozone, half from water.

k) Hydrogen peroxide also photolyzes in water to produce hydroxyl radical.

l) Treatment of phenol with ozone or H_2O_2/UV each gives an initial increase in the chloroform formation potential.

m) An initial increase in trihalomethane formation potential, followed by a decrease is observed upon ozonation of natural water.

n) Rates of aqueous photolytic ozonations are ten to one thousand times faster than ozonation alone.

o) Mechanisms postulated for the ozone/UV reaction are:

    1) Simultaneous interaction of substrate, ozone, and UV

    2) Photolysis of substrate to free radical which reacts with ozone.

    3) Photolysis of ozone to form active species.

    4) Photolysis of water to form the transients ·H and ·OH

    5) Excitation of substrate which then reacts with ozone.

    6) Excitation of ozone which then reacts with substrate.

p) Ozonolysis generally results in a plateau in TOC representing refractory species while photolytic ozonation will destroy these species.

q) Molecular oxygen is expected to play an important role, not as the active species, but in secondary reactions with intermediate products.

r) Water quality will play an important role in determining the rate of an ozone or ozone/UV reaction, and it would therefore be necessary to study the reaction in natural water as well as in purified water.

s) Photonucleophilic displacement reactions result in the conversion of aromatic organohalides to phenols and halide ion.

t) Models for simultaneous ozone mass transfer and chemical reaction indicate that ozone dose rate (amount of ozone applied per unit time per unit volume of liquid to be treated) would be the correct parameter to use in the rate expressions for ozone-related reactions. Depending on the efficiency of the mass transfer process, there may be an efficiency coefficient imbedded in the rate constants determined using ozone dose rate as the intensity factor.

SECTION 5

CHEMICAL KINETICS OF OZONE/ULTRAVIOLET-INDUCED REACTIONS OF ORGANIC COMPOUNDS IN WATER

EXPERIMENTAL PROCEDURES

The Quartz Photochemical Reactor used in these studies was cylindrical with a somewhat rounded bottom, and approximately 10 inches in height by 6 inches wide, into which 3L of sample was placed (Figure 11). It has four baffles on the walls to aid mixing, a six-bladed paddle impeller turned by a stirring motor at 300-500 rpm, and several ports in the lid for introduction of ozone, exiting of off-gas, taking of samples, etc. The gas stream from the ozone generator was run through a modified liquid chromatography UV absorbance detector where the concentration of ozone in the inlet stream could be measured spectrophotometrically. After being bubbled into the bottom of the reactor and up through the liquid, ozone in the off-gas was measured as above, then destroyed thermally. The entire quartz reactor could be lowered into a chamber surrounded by UV lamps. A description of the reactor itself and other experimental details are presented more thoroughly in Appendix B.

During a typical kinetic run in purified water, the desired ozone dose rate was equilibrated with the UV lamps on, then a concentrated aqueous solution of the substrate was added through a port in the reactor head. Samples were withdrawn as a function of time and analyzed by gas chromatography. Ozone in the liquid was measured iodimetrically, and the UV intensity reaching the solution in the reactor was measured by ferrioxalate actinometry.

Total Organic Carbon, where desirable, was measured by a Dohrmann low-level DC-54 and trihalomethane potential was measured by chlorinating the sample at a given level and then measuring trihalomethanes after a specified waiting period (3-8 days) at 26°C.

Because of its relative insolubility, hexachlorobiphenyl (HCB) was dissolved in methanol, 18 µL of which was spiked into the reactor to give the desired concentrations.

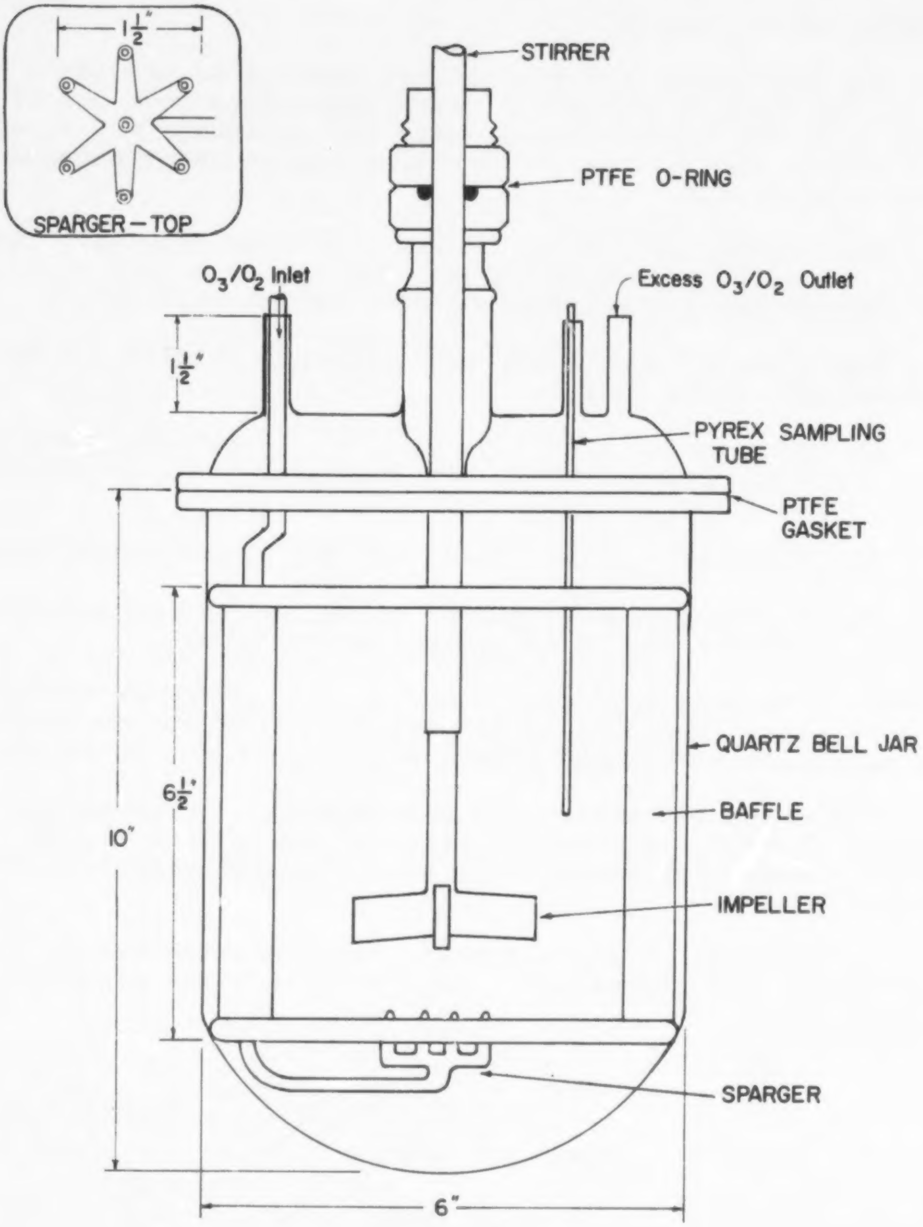

$1\frac{1}{2}"$
SPARGER — TOP
STIRRER
PTFE O-RING
O_3/O_2 Inlet
Excess O_3/O_2 Outlet
$1\frac{1}{2}"$
PYREX SAMPLING TUBE
PTFE GASKET
QUARTZ BELL JAR
$6\frac{1}{2}"$
10"
BAFFLE
IMPELLER
SPARGER
6"

Figure 11. NTSU photochemical reactor.

During the kinetic runs using lake or river water, the sample was placed in the reactor with no ozone flow or UV, then the ozone and UV turned on at the beginning of the experiment. Sampling and analysis was as above.

RESULTS AND DISCUSSION

The purpose of the kinetic analysis is to provide a general expression from which, for a given ozone dose rate and UV intensity, the disappearance curve for substrate may be predicted. This can in turn be used to optimize the ozone/UV process for a given application.

The methods of kinetic analysis and the resulting rate equations will be treated below, after which a more qualitative and comprehensive discussion of the results will follow.

The kinetic results for the compounds studied can be grouped into three classes:

1) Those which are first order in substrate, specifically chloroform, bromodichloromethane, and tetrachloroethylene.

2) Those of complex order, in this case hexachlorobiphenyl.

3) Non-homogenous systems; trihalomethane precursors (TTHMP) and total organic carbon (TOC).

Since a different approach to the kinetic analysis was utilized in each case, they will be discussed in separate sections below. The generalized starting point, however, is the following.

The rate expression for disappearance of substrate is assumed to be the sum of the rates of the individual reactions taking place. For simplicity, the following reactions were assumed:

1) Removal of the substrate from solution due to purging by the sparge gas O_3/O_2; a first order process.

$$-\frac{dS}{dt} = k_{purge}S \qquad [67]$$

where S = substrate, and

k_{purge} = first order rate constant

2) Photolysis of the substrate in the presence of UV radiation;

$$-\frac{dS}{dt} = k_p I^a S^b \qquad [68]$$

where I = intensity of ultraviolet radiation, in W/L

3) Ozonolysis of substrate

$$-\frac{dS}{dt} = k_o [O_3]_\ell^c S^d \qquad [69]$$

where $O_{3\,\ell}$ = ozone concentration in the liquid

4) Ozone/UV reaction

$$-\frac{dS}{dt} = k_u I^e D^f S^g \qquad [70]$$

where D = ozone dose rate, in mg/L-min

The first three rate expressions should be correct independently of the fourth, that is, for example, the ozonolysis reaction should proceed at an instantaneous rate which is proportional to some power of the ozone concentration, and should therefore be measureable in a separate experiment. This assumption is valid when the "ozone-only" reaction is not so fast that the solution becomes depleted of ozone and the rate of reaction is so mass transfer limited that reaction takes place at the bubble surface. The same assumption of independence is used for the photolysis and purging reactions. On the other hand, there may be several reactions lumped into the fourth term, particularly where the substrate is a good UV absorber. Reaction of substrate with the active specie generated from the photolysis of ozone is probably the major reaction which takes place, although, as discussed later, reaction of photoexcited substrate with ozone is a possibility. The reaction of substrate with photoexcited ozone would also appear in the fourth term, should it occur. The general approach used was to evaluate the first three terms from independent experiments, then to subtract their contribution from the experimentally determined total rate of the ozone/UV experiment. The "remainder" of the rate was then empirically fit to the form $k_u I^e D^f S^g$. As mentioned in the preceding section, the use of the "ozone dose rate" in the kinetic expression was previously suggested by Eisenhauer (142) and indirectly by Lee and co-workers (110). The implication that it should be correct for ozone without UV in the case of dilute solutions of substrate in pure water in a semi-batch reactor is not so obvious, since the equilibrium value of dissolved ozone concentration is proportional to the concentration of ozone in the gas stream, not the absolute amount. However, the greater quantity of a gas of a given concentration that is present, the less that gas stream is depleted. In the case of the ozone/UV experiments in this investigation, very little (2-8% of the incoming ozone concentration) ozone was found in the off-gas from the reactor, and ozone in the liquid phase was below the detectable limit in almost all cases, so that dose rate was the logical parameter. Details are explained by compound in the following section.

Because of the complexities of the processes and the inhomogeneity of the substrate, the above procedure was not used to analyze the trihalomethane precursor destruction data. Analysis of that data will be discussed in a separate section below.

Kinetic Analysis of Ozone/UV Reactions Which are First-Order in Substrate

In the case of chloroform (CF), bromodichloromethane (BDM), and tetrachloroethylene (TCE), the sum of the terms representing the individual reactions (eq. 67-70) can be condensed to a pseudo-first-order rate constant since the overall reaction rate during an ozone/UV experiment is found to be first-order with respect to (directly proportional to) substrate, as were the individual processes [67] through [69] ,

$$-\frac{dS}{dt} = k_{purge}S + k_{p}I^{a}S^{b} + k_{o}[O_3]_1^{c}S^{d} + k_{u}I^{e}D^{f}S^{g} = \sum_i [RATE]_i \quad [71]$$

$$= \sum_i K_i S = KS .$$

This pseudo-first-order rate constant, K, is itself a sum of pseudo-first-order rate constants, the relative values of which represent the relative importance of the processes comprising the total reaction.

I. Purified Water as the Reaction Medium

Details of the kinetic analysis, being necessarily mathematical, are given in Appendix C, Section I. The results are discussed in Section III below.

II. Lake Water as the Reaction Medium

In an actual drinking water treatment situation the water will not be highly purified. The presence of substances other than the substrate of interest will decrease the rate at which that substrate is destroyed, due to competition for the active species. Hoigne' and Bader have published several papers (40,44, 45,46) in which they discuss the effect of TOC, ammonia, bicarbonate, and carbonate on the destruction rate of micropollutants by ozone, particularly in the high pH range, where they give evidence that hydroxyl radical is the active specie generated by the decomposition of ozone. Since a similar effect is expected with ozone/UV, the reaction rates of the model compounds were also studied in a natural water matrix, Lewisville Lake Water (LLW).

This water was partially characterized as follows:

pH	8.1
Suspended Solids	<10 mg/L
Total Dissolved Solids	130 mg/L
Chemical Oxygen Demand	10 mg/L
Total Organic Carbon	4.3 mg/L
NH_3/NH_4^+ (as N)	120 µg/L
$CO_3^=/HCO_3^-$	1 mM

If the expression of Hoigne' and Bader (45) is used to calculate the decrease in reaction rate in going from pure water to Lewisville Lake Water, the rate changes by the ratio of the "competition values," Ω. Since

$$\Omega_{M,\text{matrix a}} = (\eta'\eta''k_M)^{-1} \sum_i k_i S_i \quad , \qquad [72]$$

where M is the test compound, η's are fractional efficiencies characteristic of pH and compound M, k's are PFO rate constants and S_i is the concentration of component i, the ratio is given by

$$\frac{\Omega_{M,\text{ pure water}}}{\Omega_{M,\text{ LLW}}} = \frac{k_M S_M}{\sum_i k_i S_i} \qquad [73]$$

Evaluation of this expression using reference 45 and the above data on Lake Lewisville water gives

$$k_{CHCl_3} = 1.9 \times 10^{7}\ M^{-1}sec^{-1} \quad , \quad [CHCl_3] = 8.5 \times 10^{-7}\ M$$

$$k_{TOC} = 1 \times 10^{9}\ M^{-1}\ sec^{-1} \quad , \quad [TOC] = 4.3 \times 10^{-5} M$$

$$k_{CO_3^=} = 3 \times 10^{8}\ M^{-1}\ sec^{-1} \quad , \quad [CO_3^=] = 7 \times 10^{-6}\ M$$

$$k_{HCO_3^-} = 1.7 \times 10^{7}\ M^{-1}\ sec^{-1} \quad , \quad [HCO_3^-] = 10^{-3}\ M$$

$$k_{NH_3/NH_4^+} = 1.3 \times 10^{7} M^{-1}\ sec^{-1} \quad , \quad [NH_3/NH_4^+] = 6.5 \times 10^{-6}\ M$$

and

$$\frac{\Omega_{M,pw}}{\Omega_{M,LLW}} = \frac{CHCl_3}{CHCl_3 + TOC + CO_3^= + HCO_3^- + NH_3/NH_4^+}$$

$$= \frac{16.15}{1.6\text{X}10^{1} + 4.3\text{X}10^{4} + 2.1\text{X}10^{3} + 1.7\text{X}10^{4} + 8.5\text{X}10^{1}} = \frac{1.6\text{X}10^{1}}{6.2\text{X}10^{4}}$$

$$= 2.6 \times 10^{-4}.$$

Since the water used in the purified water experients is not strictly pure but contains typically 0.2-0.4 mg/L of TOC, this factor of 10^4 difference in rates is not to be expected experimentally, but rather

$$\frac{\Omega_{M,\ \text{purified water}}}{\Omega_{M,\ LLW}} = \frac{1.6\text{X}10^{1} + 3\text{X}10^{-6}(10^{9})}{6.2 \times 10^{4}} \cong \frac{3 \times 10^{3}}{6.2\text{X}10^{4}} \cong \frac{1}{20}$$

where an average figure of 0.3 mg/L has been used for the TOC of purified water. This calculation shows that if the active specie were hydroxyl radical, the rate could be expected to slow by a factor of twenty in going from purified water to this natural water matrix. Although the identity of the ozone/UV active specie is not known, all evidence in this study indicated a very reactive free radical species, so that the possibility of a similar matrix effect existed. In view of this large difference in reaction rate, it was necessary to perform kinetic studies in natural water and to use that kinetic analysis as the basis for the engineering calculations. Appendix C, Section II describes the kinetic analysis on a compound-by-compound basis, and the results are discussed in Section III, below.

III. Discussion of Kinetic Results for Tetrachloroethylene, Chloroform, and Bromodichloromethane

Because of the complexity of the kinetic analyses described in Appendix C it is difficult to visualize the differences and similarities between rate expressions and to make comparisons between compounds and matrices. The choice of model compounds, based at the time of choosing on the interest in those compounds as potential pollutants, was a fortunate choice. Hexachlorobiphenyl, described in another section of this report, is an aromatic compound. Tetrachloroethylene (TCE) contains a double bond but is not aromatic, while chloroform (CF) and bromodichloromethane (BDM) contains no double bonds. The latter two compounds do, however, have one important dissimilarity: BDM absorbs ultraviolet radiation in the region of the important mercury lines while CF does not.

The ozone/UV reactions of TCE, CF, and BDM are all first order in substrate, which makes them somewhat easier to compare, since their rate equations all have the same general form,

$$\mathrm{RATE} = - S = - \frac{dS}{dt} = KS \ .$$

which states that the rate of reaction is proportional to the concentration of substrate present. For a given substrate concentration, then, the relative rate of reaction of two compounds is the same as the relative size of the rate constants. Since the functional dependence of the rate constants on ozone dose rate and UV intensity has been determined in the previous section, it is instructive to compare the form of those rate constants as well as the contribution of the various reactions. Table 3 summarizes the general form of the rate equation and the more specific variations which each compound takes in the two matrices, as determined in Appendix C.

Points which should be especially noted are:

1) Increasing the UV intensity has less effect on TCE in lake water than in purified water.

2) The ozone/UV term of chloroform in purified water has a very weak UV dependency. Upon changing to lake water that UV dependence drops to zero.

3) The odd orders of dose rate dependence for chloroform indicate that its reaction is kinetically very complicated. This point is discussed further in the products section of this report, where further evidence for a chain reaction is given.

TABLE 3. KINETIC FORM OF PSEUDO-FIRST ORDER RATE CONSTANTS FOR TETRACHLOROETHYLENE, CHLOROFORM, AND BROMODICHLOROMETHANE

(a) Compound	(b) Matrix	Purging	(c) Ozonolysis	(d) Photolysis	Ozone/UV	Notes
GENERAL	---	k_{purge}	$k_o D_{eff}^w$	$k_p I^X$	$k_u I^y D^Z$	
TCE	PW	k_{purge}	$k_o D_{eff}$(e)	$k_p I$	$k_u I D$	
	LLW	k_{purge}	$k_o D_{eff}$	$k_p I^{0.670}$	$k_u I^{0.419} D$	
CF	PW	k_{purge}	$k_o D_{eff}$	$k_p I$	$k_u I^{0.266} D^{1.5}$	(f)
	LLW	k_{purge}	$k_o D_{eff}$	$k_p I$	$k_u D^{0.562}$	
BDM	PW	k_{purge}(g)	$k_o D_{eff}$	$k_p I$	$k_u I^{-0.466} D$	(h)
	LLW	k_{purge}	$k_o D_{eff}$	$k_p I$(i)	$k_u I^{-0.481}$	(j)

a) TCE=tetrachloroethylene, CF=chloroform, BDM=bromodichloromethane
b) PW=purified water, LLW=Lewisville Lake Water
c) In which no UV is involved
d) In which no ozone is involved
e) Converted to this form from that given in the text using the experimental relationship $[O_3]_\ell \cong 2.46 \times 10^{-4} D$ for ozonolysis experiments.
f) In the curve fit only the ozone/UV term was used because of its greater magnitude compared to the other terms
g) The small correction term, k_c, is not included in this table; see text.
h) Provided D is below the cut-off point; see Appendix C
i) Only two data points; assumed first order, checked by prediction of k_p. See Appendix C.
j) Restriction of correspondence of terms to different chemical reactions relaxed. See Appendix C.

TABLE 4. REACTION RATE CONSTANTS k_i FOR INDIVIDUAL TERMS IN RATE EXPRESSION OF TETRACHLOROETHYLENE, CHLOROFORM, AND BROMODICHLOROMETHANE (a)

Compound	Matrix	Purging k_{purge}	Ozonolysis k_o	Photolysis k_p	Ozone/UV k_u	Notes
TCE	PW	$1.24X10^{-2}$	$8.66X10^{-2}$	$5.68X10^{-1}$	6.54	
	LLW	$9.96X10^{-3}$	$3.68X10^{-2}$	$7.86X10^{-2}$	$1.78X10^{-1}$	
CF	PW	$1.5 X 10^{-3}$	$8.0 X 10^{-3}$	$2.5 X 10^{-2}$	$4.78X10^{-1}$	(b)
	LLW	$9.54X10^{-4}$	$2.56X10^{-3}$	$4.58X10^{-3}$	$9.18X10^{-3}$	
BDM	PW	$1.43X10^{-3}$	$3.45X10^{-3}$	$5.62X10^{-2}$	$6.56X10^{-2}$ (c)	
	LLW	$2.65X10^{-4}$	$4.86X10^{-3}$	$2.99X10^{-2}$	---	(d)
	LLW	$-7.39X10^{-3}$	---	$8.95X10^{-2}$	$5.04X10^{-3}$	(e)

a) Units of time - minutes, of ozone dose rate - mg/L min, of UV intensity - W/L. Powers of units consistent with Table 3.

b) Rate constants for purging, ozonolysis, and photolysis are evaluated from separate experiment; the ozone/UV rate constant given is for the total reaction.

c) Does not include $k_c = 8.78 X 10^{-3}$. See Appendix C.

d) Determined from separate experiments.

e) Empirical expression to be used for calculating O_3/UV runs only (see Appendix C).

TABLE 5. CONTRIBUTIONS TO PSEUDO-FIRST-ORDER RATE CONSTANTS BY THE VARIOUS COMPONENT TERMS.(a)

(b) Compound	(c) Matrix	Purging	Ozonolysis	Photolysis	Ozone/UV	Total
TCE	PW	1.24×10^{-2}	0	1.14×10^{-1}	1.01	1.13
	LLW	9.96×10^{-3}	0	2.67×10^{-2}	7.03×10^{-2}	1.07×10^{-1}
CF	PW	1.5×10^{-3}	0	5.0×10^{-3}	2.13×10^{-1}	2.20×10^{-1}
	LLW	9.54×10^{-4}	3.1×10^{-5}	9.16×10^{-4}	7.95×10^{-3}	9.85×10^{-3}
BDM	PW	1.43×10^{-3}	0	1.12×10^{-2}	1.08×10^{-1}	1.20×10^{-1}
	LLW	2.65×10^{-4}	0	5.98×10^{-3}	1.28×10^{-2}	1.90×10^{-2}
		(d)		(d)	(f)	(e)

a) All values in minutes^{-1}. Values of reaction conditions assumed are I = 0.20 W/L, D = 0.775 mg/L min.

b) TCE = tetrachloroethylene, CF = chloroform, BDM = bromodichloromethane

c) PW = purified water, LLW = Lewisville Lake Water

d) From line 6 of Table 4

e) From line 7 of Table 4

f) by difference

TABLE 6. PERCENTAGE CONTRIBUTION TO PSEUDO-FIRST-ORDER RATE CONSTANTS BY THE VARIOUS COMPONENT TERMS(a)

Compound	Matrix	Purging	Ozonolysis	Photolysis	O_3/UV
TCE	PW	1.9	0	10	89
	LLW	9.3	0	25	66
CF	PW	0.7	0	2.3	97
	LLW	9.7	0.3	9.3	81
BDM	PW	1.2	0	9.3	90
	LLW	1.4	0	31	67

a) calculated from the values in Table 5

TABLE 7. RATIO OF RATE CONSTANTS IN PURIFIED WATER TO THOSE IN LAKE LEWISVILLE WATER

Compounds	Purging	Photolysis	O_3/UV	Total
TCE	1.2	4.3	14.4	10.6
CF	1.6	5.5	26.8	22.3
BDM	5.4	1.9	8.4	6.3

4) The negative order of the BDM-O_3/UV reaction with respect to UV intensity is unlike any other compound studied, and may indicate competing reactions.

5) Not shown in Table 3, but indicated earlier is the fact that for bromodichloromethane in purified water, increased ozone dose rate past a certain value results in no further increase in rate constant. This cut-off value of D seems to double when the UV intensity is doubled, indicating a direct relationship.

The rate constants, K_i, are collected in Table 4 in the units appropriate to Table 3. By tabulating values of the pseudo-first-order rate constants representing the individual reactions, evaluated for a given set of reaction conditions, the relative contributions from each term to the total can be seen. This is done in Table 5 for values of ozone dose rate = 0.775 mg/L min and UV intensity of 0.2 W/L. The chosen values of I and D represent the middle of the experimentally investigated range of these parameters. In the last column in Table 5 are shown the total PFO rate constants for comparison with the contributed parts. The relative contributions of the various terms is made more clear in Table 6 where the percent of the PFO rate constant contributed by each reaction is shown. Finally, the results are shown in another way in Table 7, where the ratios of the PFO rate constants for the various reactions in purified water compared to Lake Lewisville water are tabulated. These are the factors by which the reaction rate decreases when going from purified water to Lewisville Lake Water.

Several points concerning the results tabulated in Tables 4 - 7 are worthy of note:

a) Because of the destruction of ozone by UV there was no ozone present in solution in 90% of the purified water experiments. Only for the highest dose rates with the lowest UV intensities was ozone found in solution, and then only in amounts equivalent to an effective dose rate of 0.05 mg/L min and less. In the lake water experiments the natural components of the water absorbed some of the UV so that the actual intensity available to an effective dose rate of only 0.13 mg/L min, approximately equal to the lowest actual dose rate used in any of the experiments. Because of this, the ozonolysis contribution to these reactions is essentially zero, as seen in Table 6.

b) Although TCE and BDM are quite different chemically and have very different rates of reaction, they have approximately the same ratio of purging and photolysis rate to the total PFO rate constant, as shown in Table 6. Chloroform, which does not appreciably absorb in the UV region naturally has much lower photolysis contribution, ∿2% in PW compared to 9-10% for TCE and BDM. However, because of the rate of the ozone/UV reaction, CF is intermediate in reaction rate between TCE and BDM.

c) Rather than experiencing a "salting out" effect, all three compounds appear to purge more slowly from lake water than from purified water (Table 7). This may indicate a tendency of the compounds to complex in some way with the constituents of the lake water.

d) Next to purging, photolysis of the model compounds appears to slow down the least in going to a natural matrix, as seen from the ratios in Table 7. This is as expected, since the UV absorbance of LLW is not large. It should be noted that ratios for ozonolysis, k_o; can be calculated from the data in Table 4 and give lower values than those listed for photolysis in Table 7. The k_o values listed in Table 4, however, are based on very limited data so that the ratio must be regarded carefully.

e) The O_3/UV reaction rate of chloroform is seen in Table 7 to decrease by the greatest factor upon the addition of the natural matrix. If indeed a chain reaction is involved in the destruction of chloroform, introduction of the natural matrix could not only compete for the original active species but also for the chain carrier.

f) In purified water the total reaction of TCE is about five times faster than chloroform which is in turn twice as fast as bromodichloromethane. In natural water, TCE is about five times as fast as BDM which is twice as fast as chloroform (Table 5).

g) The decrease in reaction rate of the model compounds in going from purified water to natural water is by a factor of 6 - 22. It should be noted again here that the rate in purified water is not the same as the rate in pure water, as calculated in section II above.

h) If the substrate is a UV-absorber, the photolysis contribution to the total rate of an ozone/UV reaction is likely to be appreciable, while, as mentioned above, the ozonolysis contribution may be quite negligible.

i) Most importantly, for a given does rate, ozone/UV is considerably faster than ozone alone, as shown in the following table of relative rates, calculated for the same values of I = 0.2 W/L and D = 0.775 mg/L min as in the previous example.

	OZONOLYSIS ONLY	PHOTOLYSIS ONLY	OZONE+UV
	(D = 0.775)	(I = 0.20)	
TCE/PW	.059	.10	1
/LLW	.27	.25	1
CF/PW	.028	.023	1
/LLW	.20	.093	1
BDM/PW	.022	.093	1
/LLW	.20	.31	1

It is seen that even in the least favorable case, the combination of ozone and UV is four times as fast as either ozone or UV alone, and in the most favorable cases is fifty times as fast as ozone and forty times as fast as UV alone. It is also seen that there is a striking similarity between all three compounds in the decreasing efficiency of O_3/UV relative to ozone when going from purified water to a natural matrix.

j) Finally, although previously unanticipated, UV alone suggests itself as a treatment method which has the specificity for certain undesirable micropollutants which ozone/UV seems to lack. Since the major expenses of an ozone/UV system are the ozone generator and power to run it, plus the contactor, ultraviolet radiation could prove to be very cost-effective for the compounds for which it was specific. This point will be discussed in more detail later in this report.

The effect of the ozone dose rate, and UV intensity on the pseudo-first-order rate constant, and thus on the reaction rate is shown in Figures 12-15 for the entire range of experimental values. The situation for tetrachloroethylene (Figure 12) is seen to be first-order in dose rate. In Figure 13 the lake water portion of the plot is magnified to show its behavior as well as for comparison with the other two compounds. In Figure 14, the results for chloroform, are seen the concave curves which indicate the reaction to be

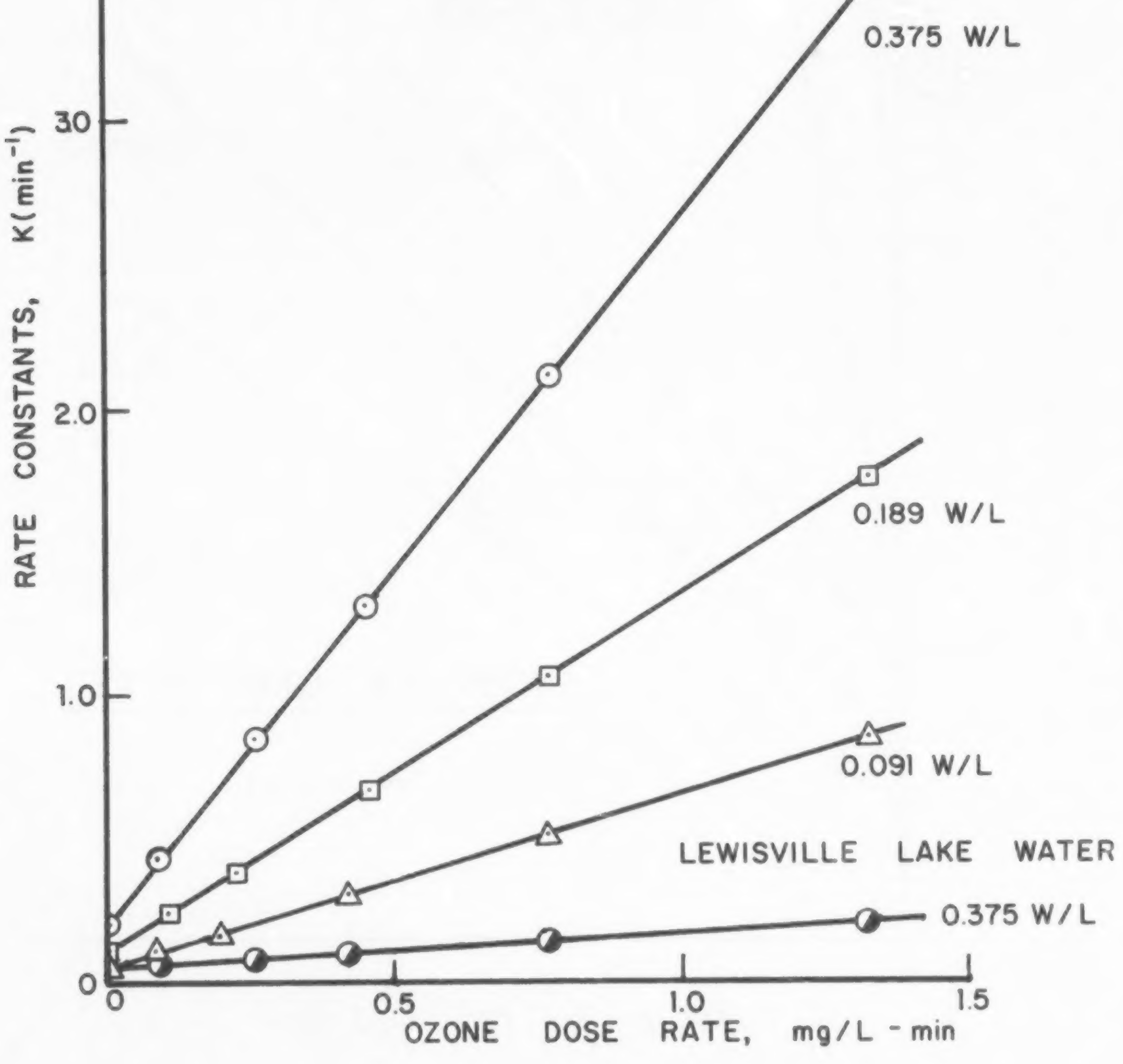

Figure 12. Pseudo-first-order rate constants for ozone/UV destruction of tetrachloroethylene.

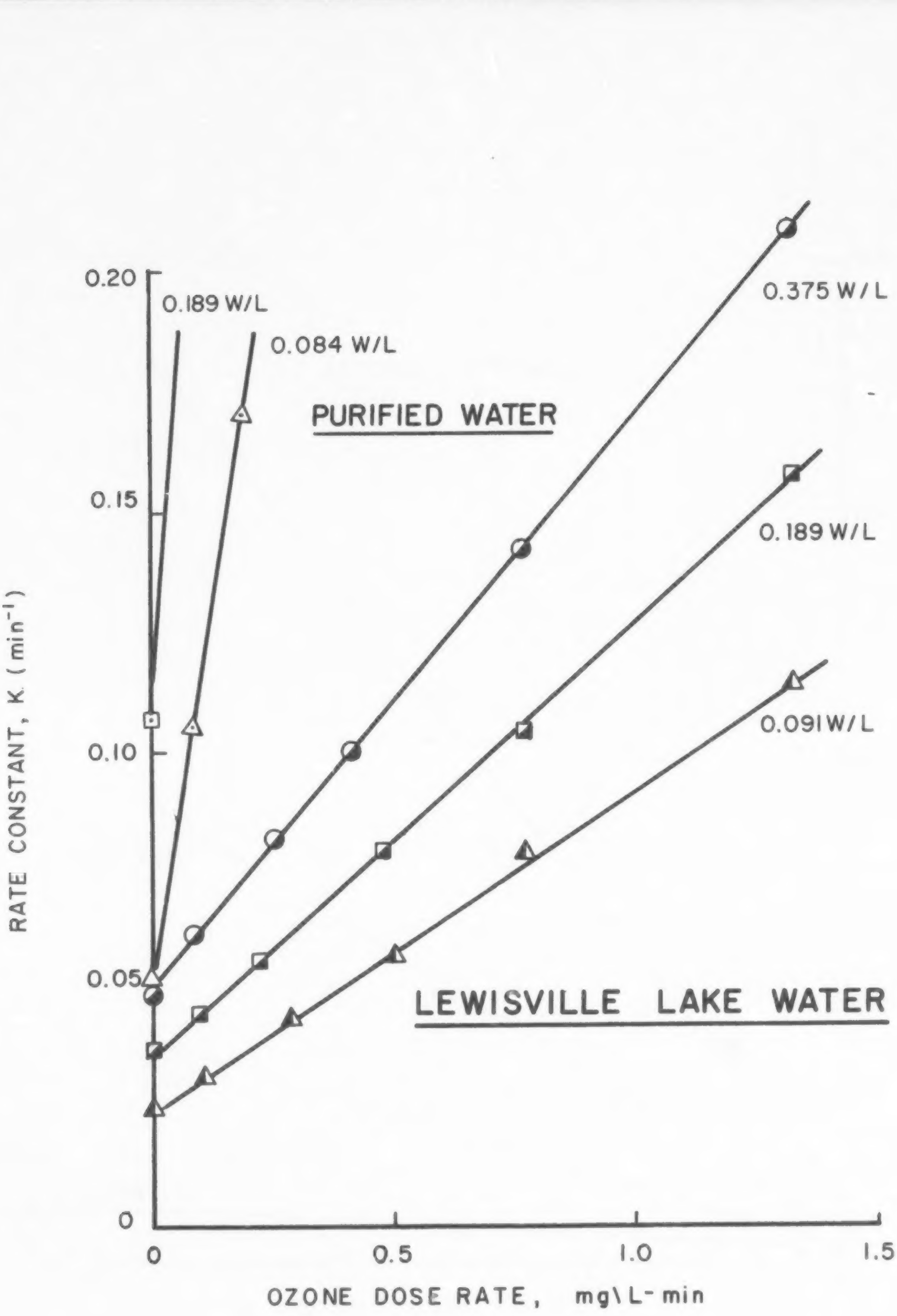

Figure 13. Pseudo-first-order rate constants for ozone/UV destruction of tetrachloroethylene, detail.

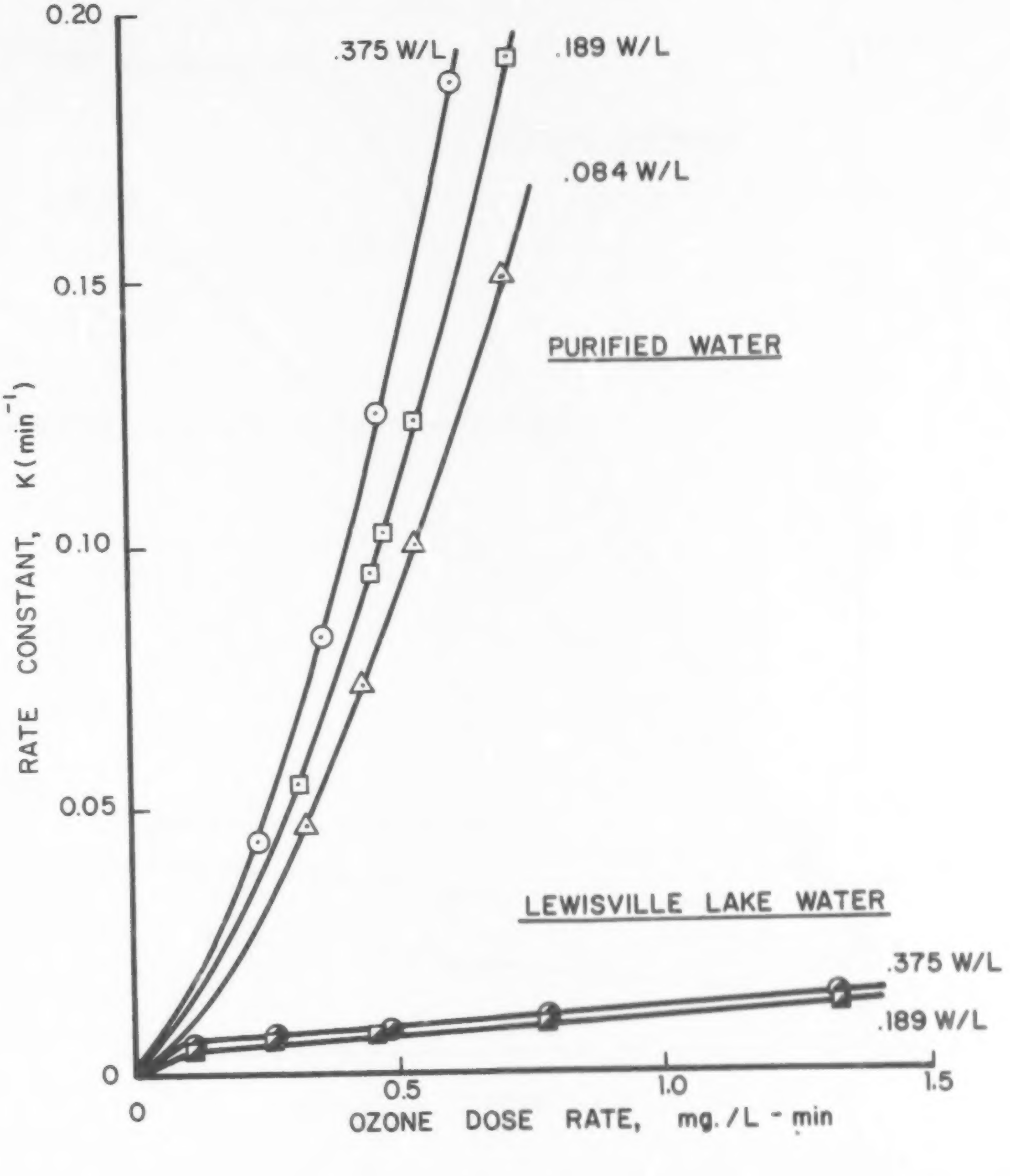

Figure 14. Pseudo-first-order rate constants for ozone/UV destruction of chloroform.

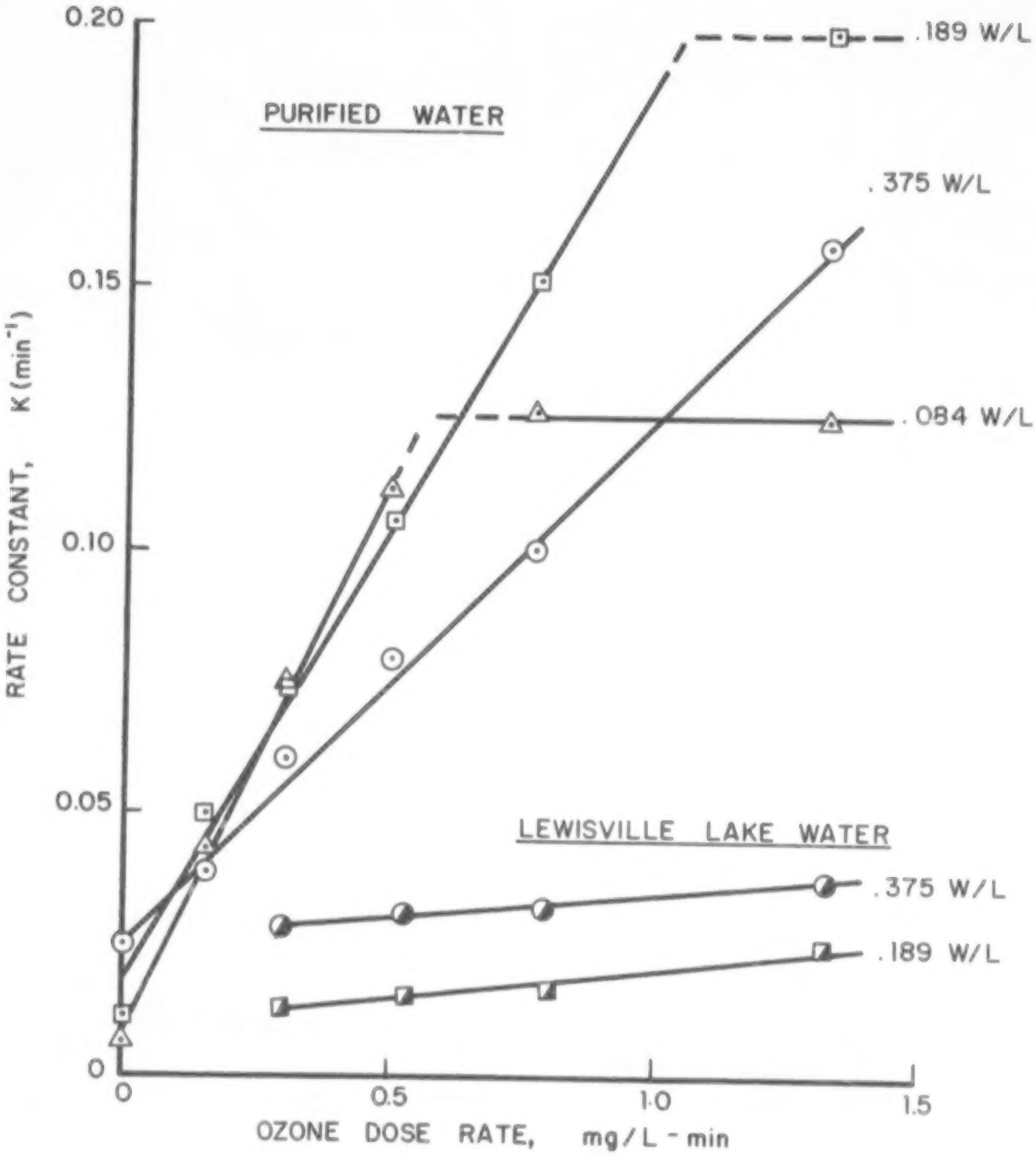

Figure 15. Pseudo-first-order rate constants for ozone/UV destruction of bromodichloromethane.

greater than first-order in dose rate in purified water. Also obvious is the much greater difference between the rate in pure water and lake water, compared to TCE.

Shown in Figure 15 is the most complicated case discussed so far, that of bromodichloromethane. The cut-off dose rate at approximately 0.56 and 1.07 mg/L min for one and two lamps, respectively, is most obvious in this plot, while the negative dependency of the lake water rates on the UV intensity can barely be discerned.

IV. The Effect of pH on the Reaction Rates of Tetrachloroethylene, Chloroform, and Bromodichloromethane.

Because of the great amount of data collection and analysis necessary for the completion of the previous and subsequent sections, the effect of pH on the rate of ozone/UV destruction of tetrachloroethylene, chloroform, and bromodichloromethane was not investigated comprehensively enough to allow a kinetic analysis. There is, however, interesting and important information which can be gathered from the pH studies which were performed.

A. Tetrachloroethylene--Destruction of tetrachloroethylene by ozone is fairly rapid compared to chloroform. Comparison of $\tau(3)$ (95% removal) for pH 4, 6.9, and 10 is shown in Figure 16, where it is seen for example that for an ozone dose rate of 0.8 mg/L min, the reaction at pH 10 is five times as fast as that at pH 4. This order is consistent with the suggested (42) hydroxyl radical mechanism at high pH. On the other hand, the ozone UV process takes four times as long at pH 10 as at pH 7 which is 1.5 times slower than pH 4. The data is shown in Table 8.

TABLE 8. ELIMINATION TIME, $\tau^{(a)}$, FOR TETRACHLOROETHYLENE BY OZONE AND OZONE/UV FOR VARIOUS pH VALUES$^{(b)}$

Process	pH 4	pH 7	pH 10
Ozone	5000 sec	2750 sec	450 sec
Ozone/UV	53 sec	89 sec	395 sec

(a) corresponding to 95% removal

(b) ozone dose rate = 0.8 mg/L min, UV intensity = 0.375 W/L

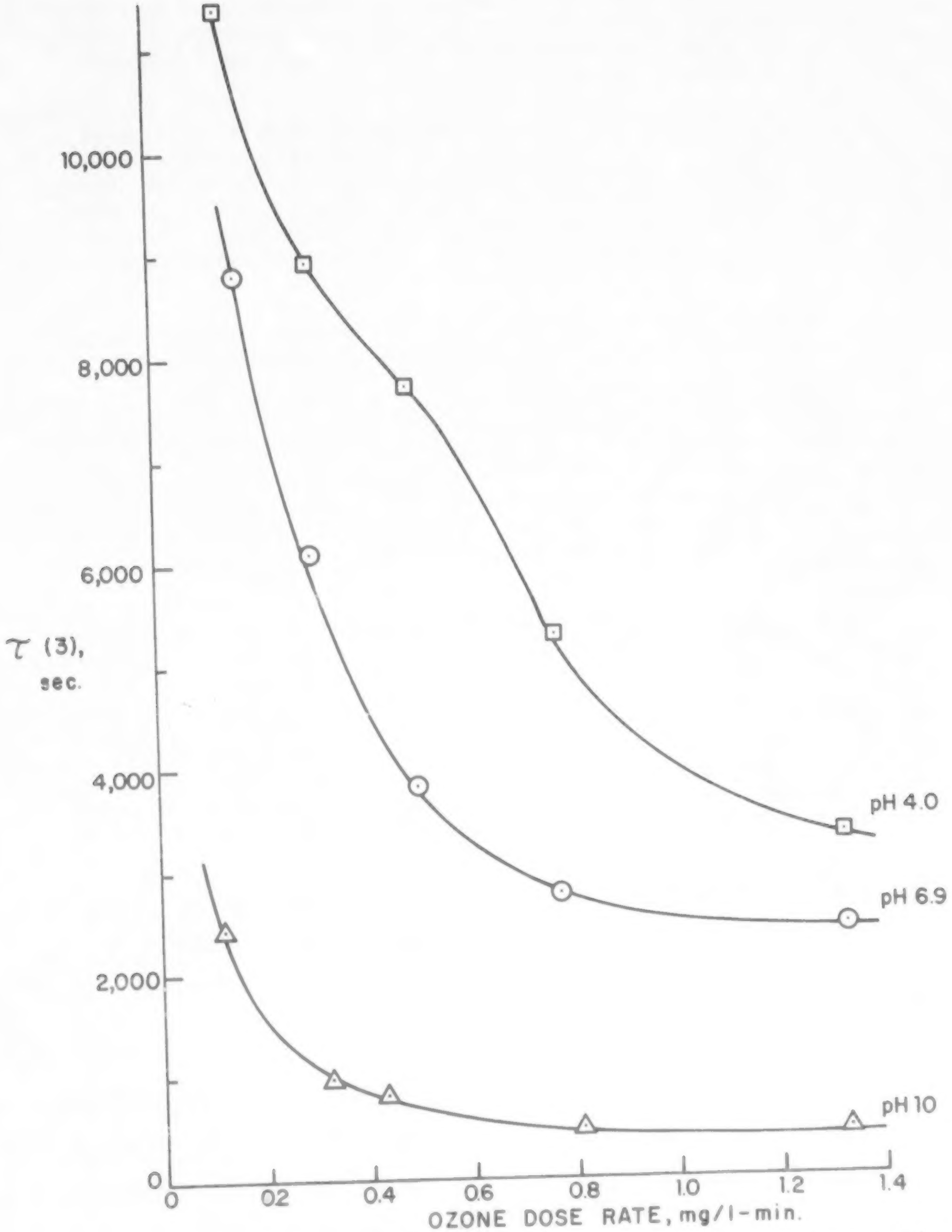

Figure 16. Tetrachloroethylene - effect of pH on treatment time (95% removal from 100 µg/L ozone only (no UV)).

B. Chloroform--Chloroform behaves in much the same manner as tetrachloroethylene in the response of its reaction rate to pH. Figure 17 shows the effect of pH on the ozonolysis of chloroform. It is seen that at the end of 100 minutes, about 18% of the chloroform has been removed by ozone at pH 7, while a similar dose rate at pH 10 has removed 56%. On the other hand, similar doses of ozone with UV leave 12% remaining after 120 minutes at pH 9.8 while at pH 6.5, less than 3% remains after 15 minutes (Figure 18).

C. Bromodichloromethane--Figure 19 shows the removal due to ozonolysis of bromodichloromethane from solution at pH 3.2, 6.5 and 10. It is seen that BDM, like TCE and CF, is removed much more quickly at pH 10. Experiments in which no UV or ozone was present showed that there was some basic hydrolysis of BDM taking place at pH 10, but it is not fast enough to contribute appreciably to the rate. Also as in the case of TCE and CF, the removal of BDM by ozone/UV is enhanced by low pH, as shown in Figure 20.

Thus all three of the model compounds discussed thus far react similarly in that high pH speeds the ozonolysis process while the ozone/UV process is fastest at low pH. This similarity is interesting in view of the markedly different rates of reaction and the unusual differences in the rate equations of the three compounds. This pH behavior may contain important information about the identity of the primary active species, since the behavior is constant for different substrates. This point will be discussed further after additional data is introduced.

Kinetic Analysis of the Ozone/UV Destruction of Hexachlorobiphenyl

The study of the model compound 2,2',4,4',6,6'-hexachlorobiphenyl presented unique difficulties. First of all, its very low solubility made it necessary to perform the experiments using an initial concentration of 60 μg/L. This fact, coupled with the compound's electron capture response made it necessary to perform a concentration step on each of the individual samples, thereby affecting the precision of the measurements. Studies were performed using initial concentrations lower than 60 μg/L to ensure that the solubility limits had not been exceeded and that the same rate law was applicable.

The fact that HCB was very slowly soluble in water made it necessary to dissolve the compound in methanol and then to spike water with the concentrate to obtain the desired initial concentration. This procedure introduced 6 μl of methanol per liter of solution which could alter the reaction rate considerably in purified water. That quantity of methanol is equivalent to 4.7 mg MeOH per liter, as compared with a TOC value of 4.3 mg/L for the lake water.

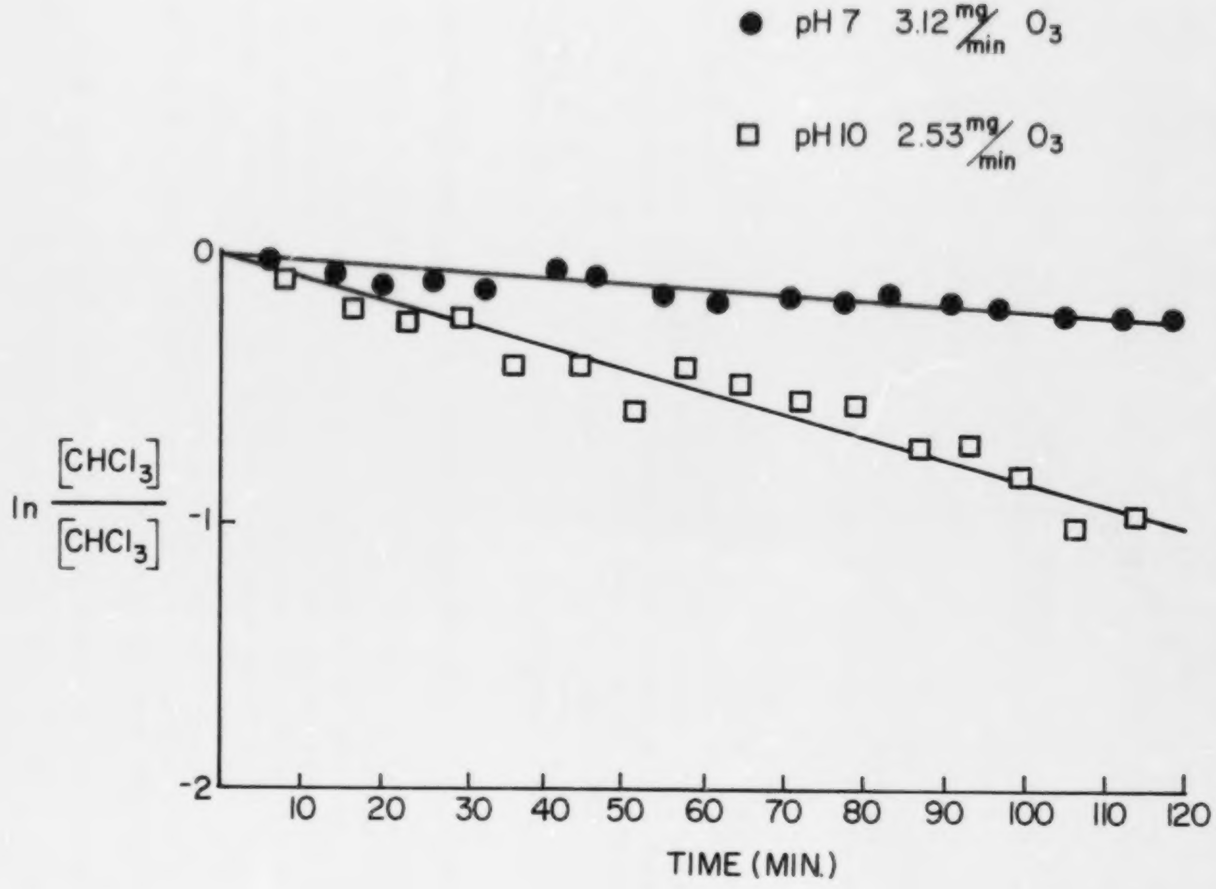

Figure 17. Effect of pH on ozonolysis of chloroform.

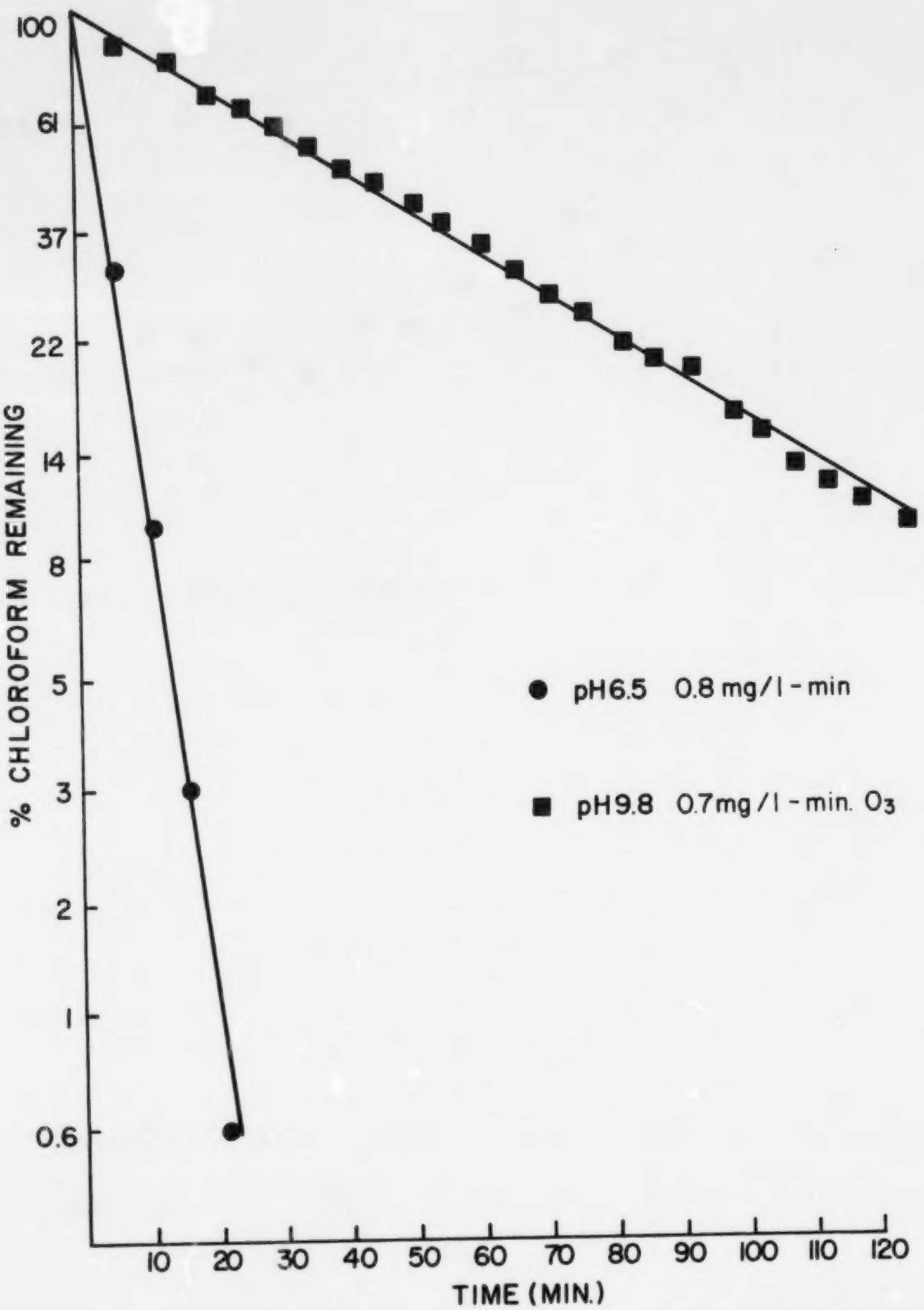

Figure 18. Effect of pH on photolytic ozonolysis of chloroform.

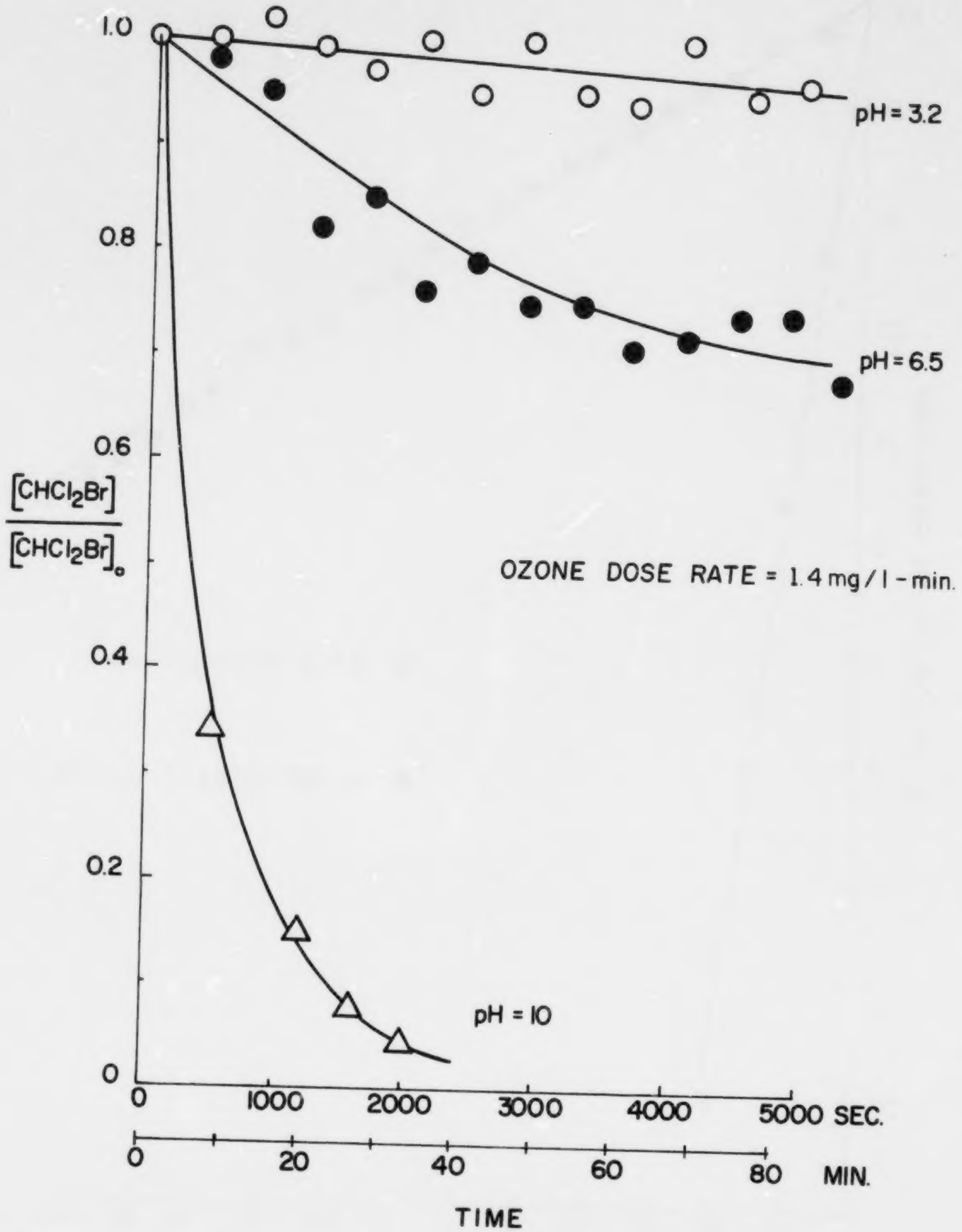

Figure 19. Effect of pH on BDM destruction by ozone.

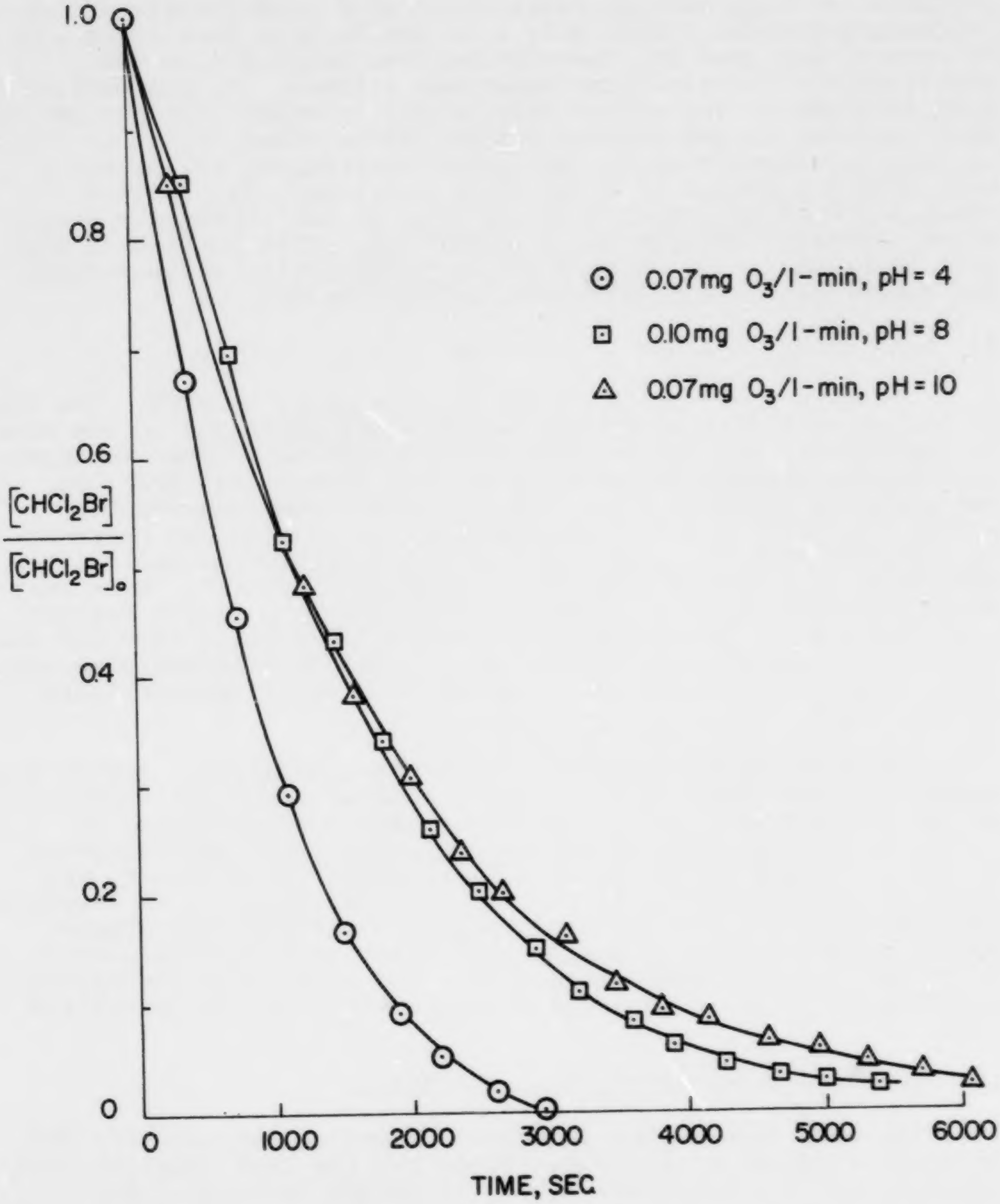

Figure 20. Effect of pH on ozone/UV destruction of BDM.

The HCB reaction was of apparent kinetic order greater than one for both photolysis and ozone/UV. High apparent orders are amplified by high initial rates which slow tremendously as the reaction proceeds. Thus, only with the highest dose rates and UV intensities used did destruction ever reach 90% in the eighty-minute reaction time which was allowed. It was because of this slowness in the second half of the reaction that HCB has not been included in the process design calculations, since it would obscure information about the other substrates, all of which were closer together in their reaction rates. The kinetic results are of interest, however, even if not completely understood, and are included for completeness. This portion of the work is presented in more detail by Huang (161), whose results are summarized in Appendix D and briefly below.

I. Lake Water as a Reaction Medium

The direct ozonation of HCB in lake water is slow, just 50% of the 60 μg/L initial concentration being destroyed in one hour at the highest ozone dose rate used, 4 mg/L min. The disappearance curves (Figure 21) have an unusual appearance, the rate being fairly rapid at first, then slowing down considerably within the first five or ten minutes. In all figures pertaining to HCB, the points are actual data points while the solid lines are curve fits from the empirical equations derived. Runs were conducted with no UV or ozone and with sparging of the reactor with nitrogen to determine if the drastic change in rate was due to some phenomenon such as adsorption, but no disappearance was seen. The initial rate was found to be directly proportional to dose rate.

The photolytic ozonation of HCB was considerably faster than ozonation, but still slow, taking 1 hour to reach 90% destruction at the highest dose rate (4 mg/L min) and a UV intensity of 0.25 W/L (Figure 22). After the photolysis rate (proportional to the 1/2 power of the UV intensity) was subtracted out, the ozone/UV portion of the rate expression was found to be directly proportional to ozone dose rate and UV intensity, and proportional to the square of the concentration of substrate present. It is worth noting that at long reaction times, the photolytic ozonation rate is in many cases very similar to the photolysis rate.

II. Purified Water as the Reaction Medium

The same form of the photolysis equation was used for HCB in purified water as for lake water, but the rate constant (and consequently the rate) was about 1/3 larger (faster). Subtraction of the photolysis contribution from the total rate of disappearance of HCB gave an expression which was 1½ order in dose rate, first order in UV intensity, and proportional to the cube of the substrate concentration. It should be stressed again

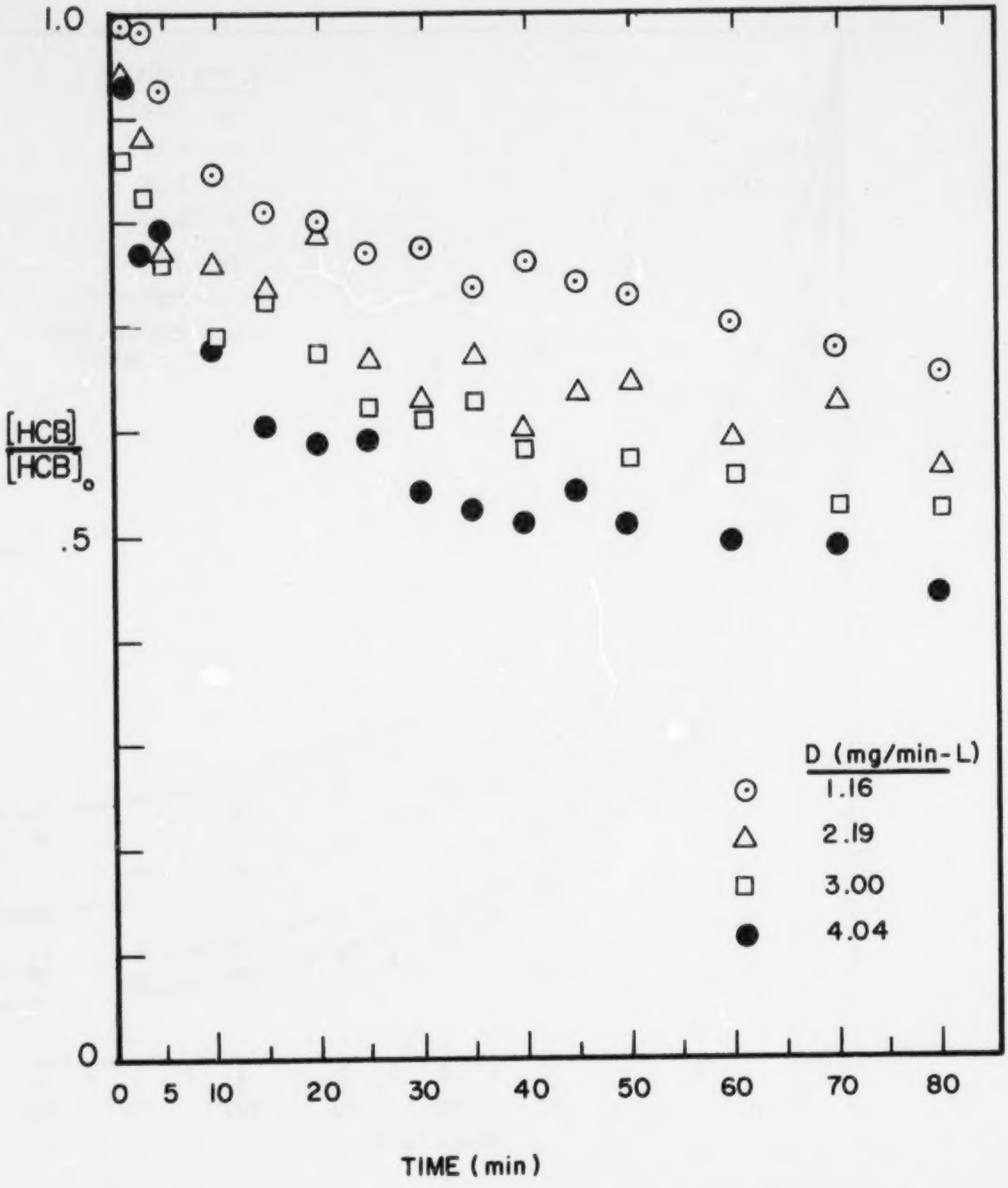

Figure 21. Effects of dose rate on the direct ozonation of HCB in lake water.

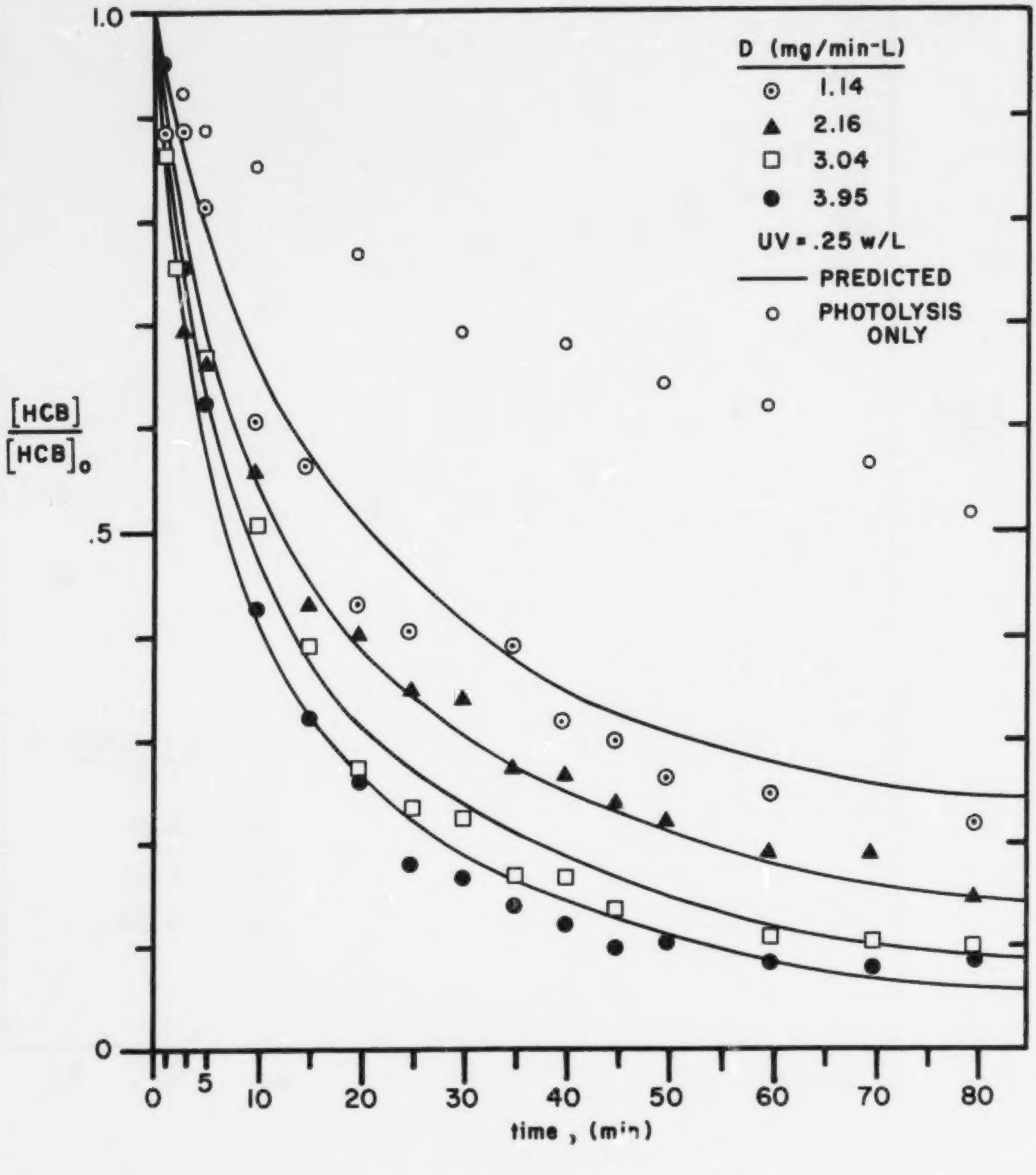

Figure 22. Effects of dose rate on the photolytic ozonation of HCB in lake water.

that these are empirical fits to the data, useful for prediction, and no mechanistic explanation can be offered, being totally beyond the scope of the project.

HCB differed from the compounds previously discussed in that elevation of the pH increased the destruction rate of both ozonation and photolytic ozonation. It also differed in that its destruction rates in lake water were very similar to those in pure water and the two were, in some cases, indistinguishable in the final stages. This may be due to the methanol which was present in the pure water experiments, as discussed earlier. These results are discussed in more technical detail in Appendix D.

Kinetic Analysis of Ozone/UV Reactions with Nonhomogeneous Systems: Trihalomethane Formation Potential and TOC:

The term nonhomogeneous systems in the context of this report means that the substrate is not a chemically well-defined species. More specifically, the systems of interest in this study are trihalomethane formation potential (THMFP) and, to the extent that it affects THMFP, total organic carbon (TOC).

So far, the entities responsible for THMFP have eluded investigators, although several functional groups have been discussed as contributors to the formation potential of a water. The consensus seems to be that THMFP should be thought of as sites, probably located on macromolecules such as those which comprise humic and fulvic acids. This view is consistent with the finding of certain functionalities which yield trihalomethanes upon chlorination. If this is the case, an important issue is whether one can destroy the site without having to remove or destroy the entire organic matrix. For this reason it is important to monitor the TOC destruction in a process which is designed to chemically destroy THMFP, even though removal of the TOC may not in itself be a primary goal.

In preliminary experiments run in the reactor at Houston Research, Inc., in Houston, Texas, and analyzed at North Texas State University, it was indicated that photolytic ozonation might actually produce THMFP as well as destroy it, an effect which was also reported by Rook (15), Lawrence (32), by Riley (162) for ozonation. These data are presented in Figure 23, where it is also seen that the rate of destruction seems to be roughly the same for ozone and ozone/UV down to approximately $S/S_o = 0.5$, but the asymptotic limit reached by ozone was quite different from that reached by ozone/UV. Although this was in agreement with similar previous claims for the ozone versus ozone/UV destruction of model substrates (103), it was not in agreement with results obtained previously in this project for

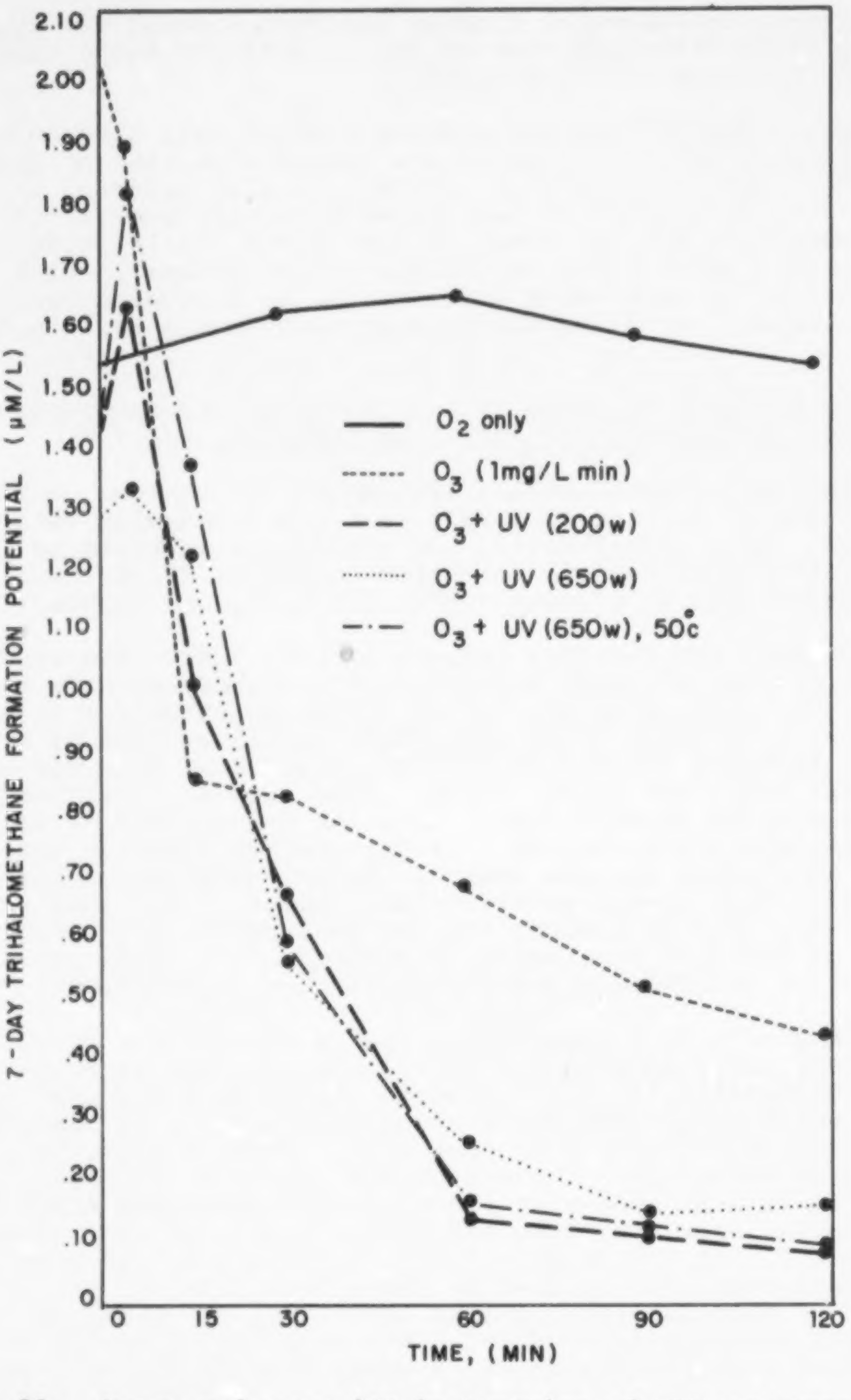

Figure 23. Ozone and ozone/UV destruction of THM precursors - Ohio River water (2/77).

Ohio River water as well as for 1 mg/L solutions of commercial humid acid solution (Aldrich), as shown in Figures 24 and 25 respectively.

Thus, it was decided to repeat these studies at lower ozone dose rates which are more realistic for purposes of future applications, and which also would be more likely to show differences between the effectiveness of O_3 and O_3/UV. For this purpose, water from Caddo Lake in East Texas was chosen as the test medium. This water represents surface water sources in the south and southeastern parts of the USA where total organic carbon levels reach high values and where THM values are expected to be correspondingly high after chlorination. Caddo Lake water at the time of our sampling showed a TOC value of 25 mg/L and a DOC of about 12 mg/L.

Figure 26 shows the destruction of THM precursors in Caddo Lake water with ozone doses of 0.14, 0.28 and 0.42 mg O_3/L-min, which correspond to 2.9, 5.8 and 8.8 µmoles/L-min. The essential features of this data are as follows:

a) Under the conditions utilized, ozone initially destroys high THM precursor levels in Caddo Lake water at a very rapid rate. Initial slopes of the THM precursor destruction curves for the 2.9 and 5.8 µm O_3/L-min runs are 0.011 and 0.016 µmole THMFP/L-min.

b) Complete destruction of THM precursor levels is not achieved in any of the runs. Indeed there appears to be evidence for the formation of precursors as the ozonation of the natural organics in the water proceeds. Figure 27 is a plot of the data shown in Figure 26 after subtraction of an exponential THMFP-destruction curve obtained from the initial slopes of Figure 26. The residual curves suggested a mechanism such as the following, in which precursor P_2 is formed by ozonolysis of "natural carbon" C. P_1 is precursor initially present in the water, and presumably differs from P_2 in chemical type and relative reactivity with ozone.

$$P_1 + O_3 \xrightarrow{k_1} X \qquad X,Y = \text{non-precursors}$$

$$C + O_3 \xrightarrow{k_2} P_2 \qquad k_1 > k_2 \approx k_3$$

$$P_2 + O_3 \xrightarrow{k_3} Y$$

Shown in Figure 28 is a comparison of one run in which a dose rate of 0.42 mg O_3/L min was used, with an O_3/UV run at

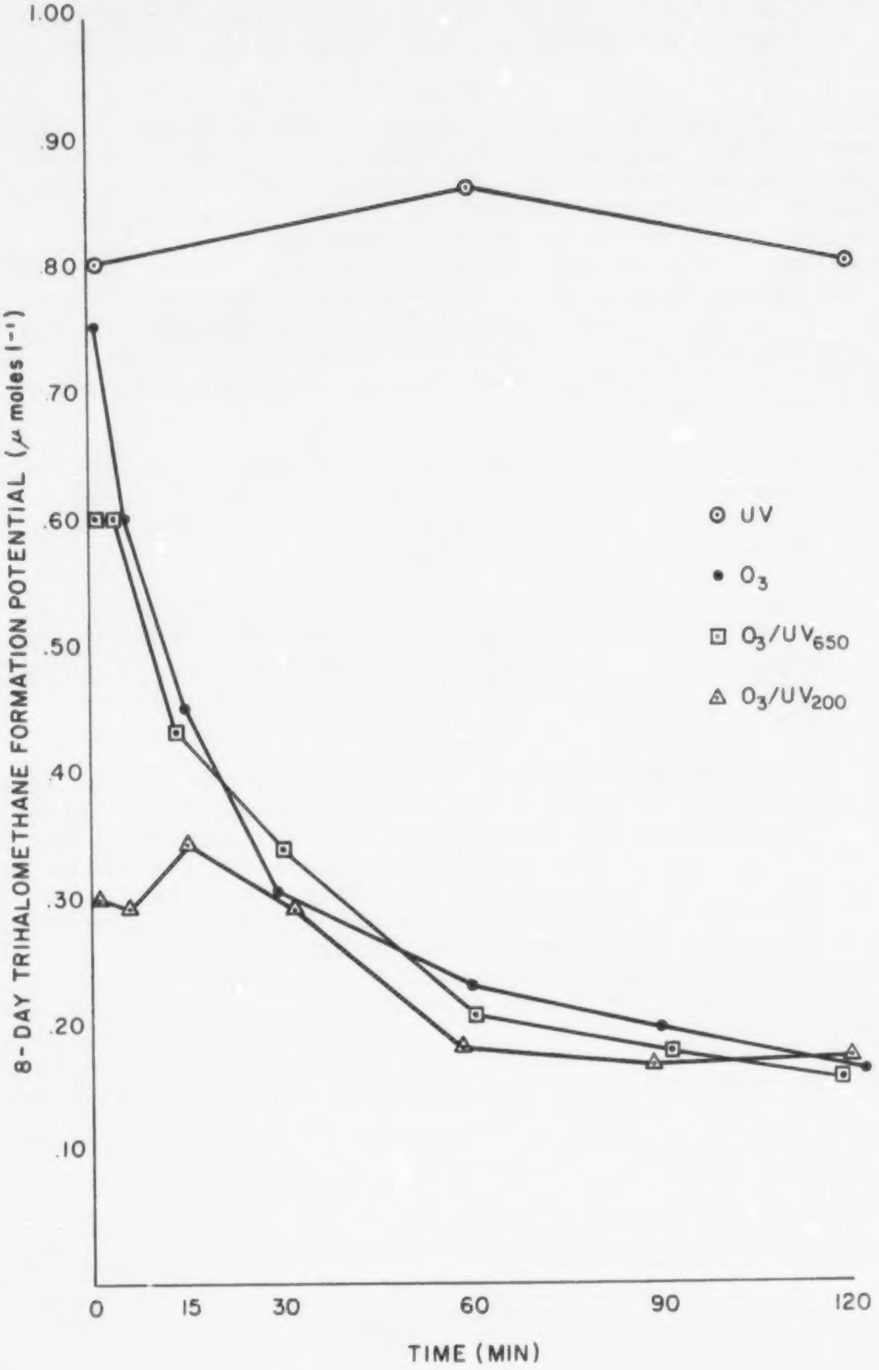

Figure 24. Ozone and ozone/UV destruction of THM precursors - Ohio River water (2/76).

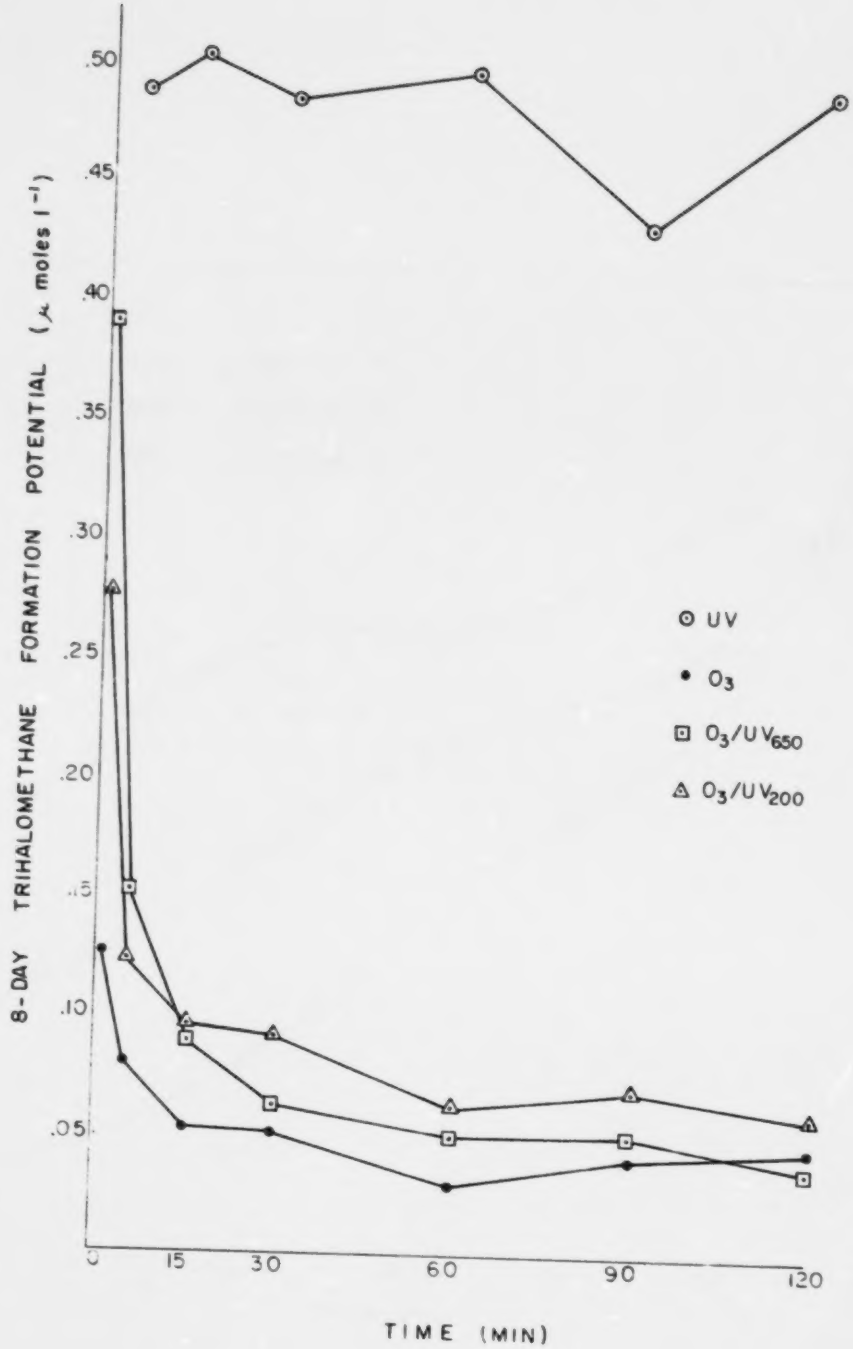

Figure 25. Ozone and ozone/UV destruction of THM precursors - humic acid (1ppm).

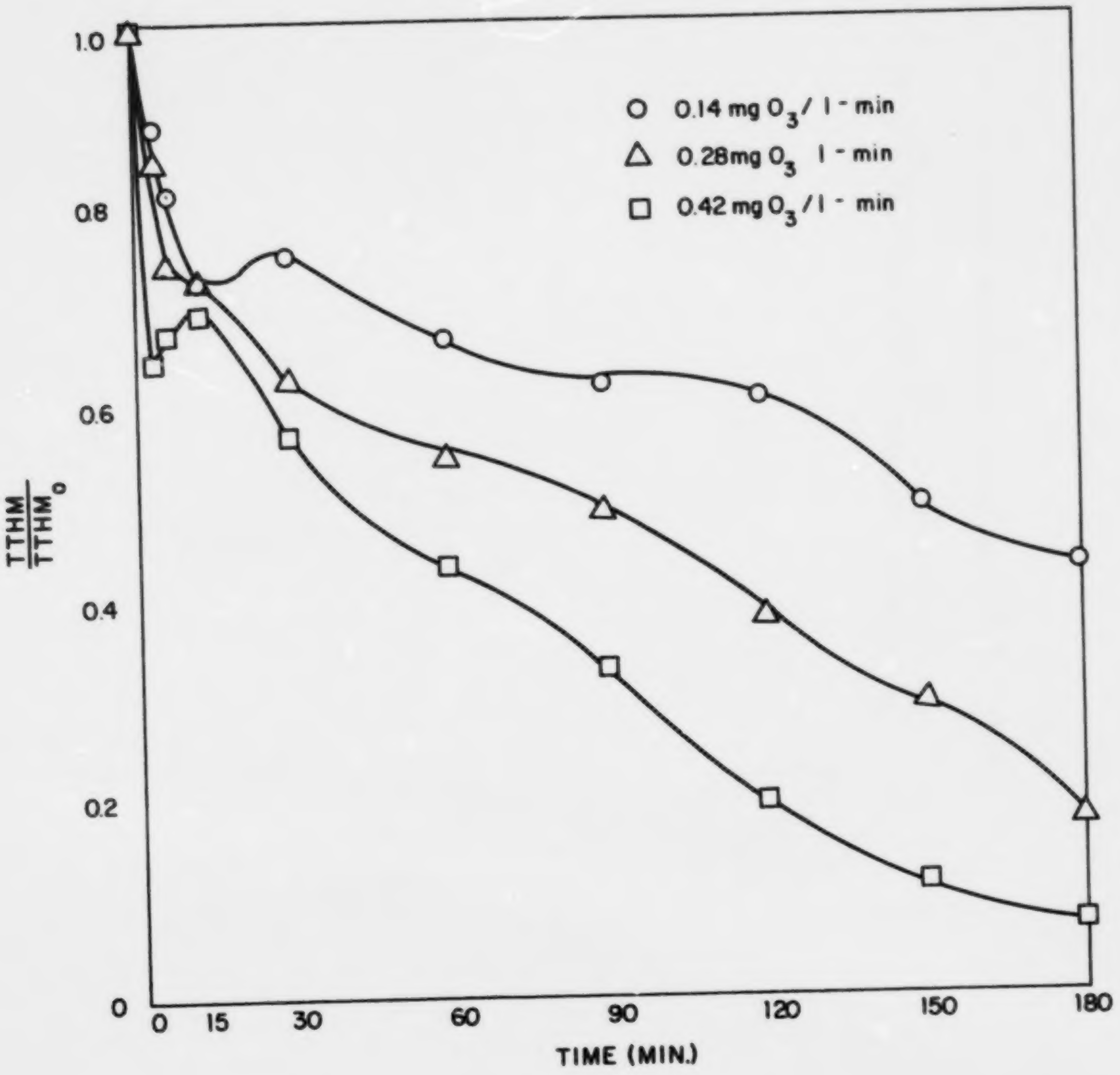

Figure 26. Normalized THM formation potential: Ozone destruction of THM precursors - Caddo Lake water .

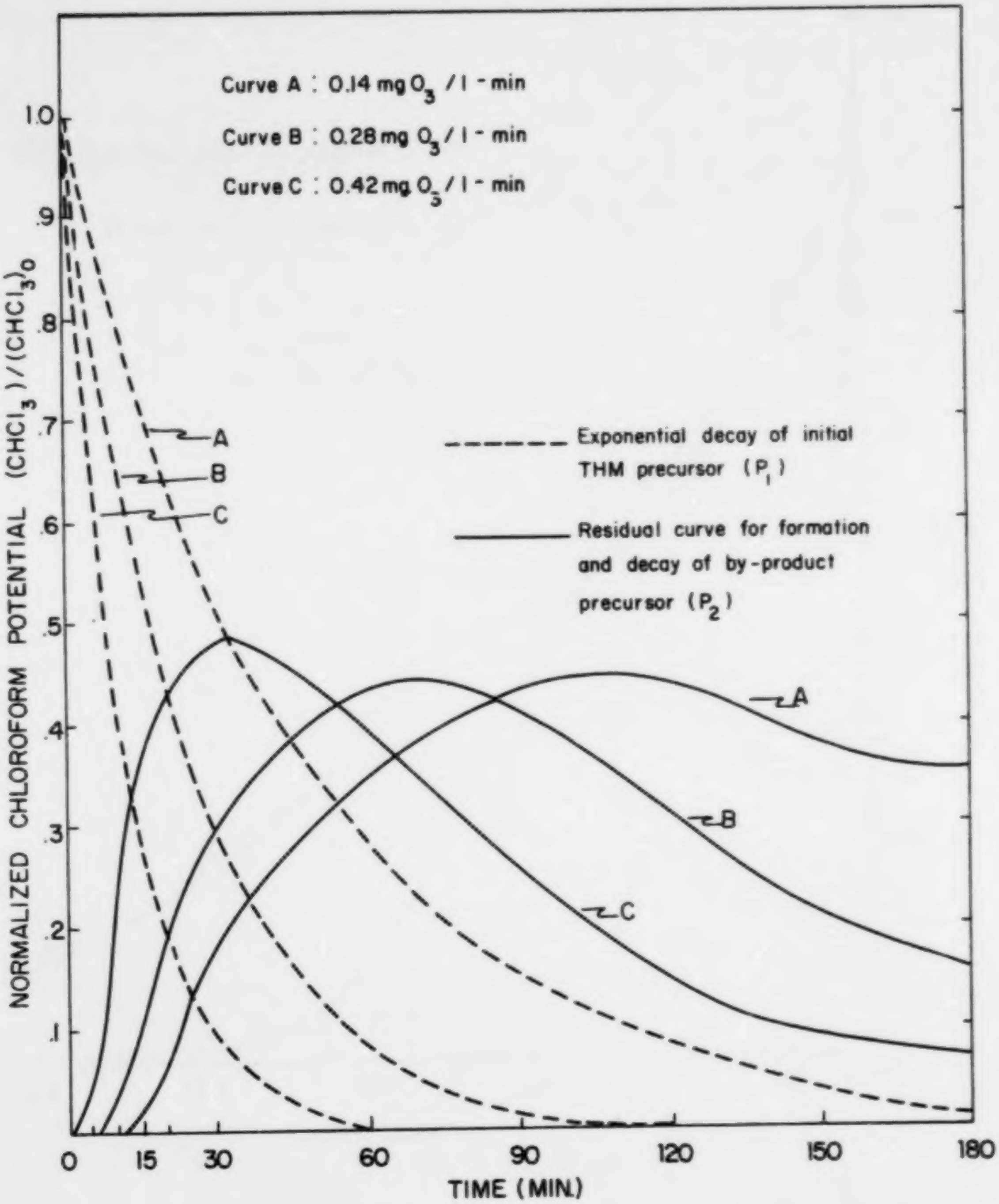

Figure 27. Analysis of THMFP destruction curves - Caddo Lake water.

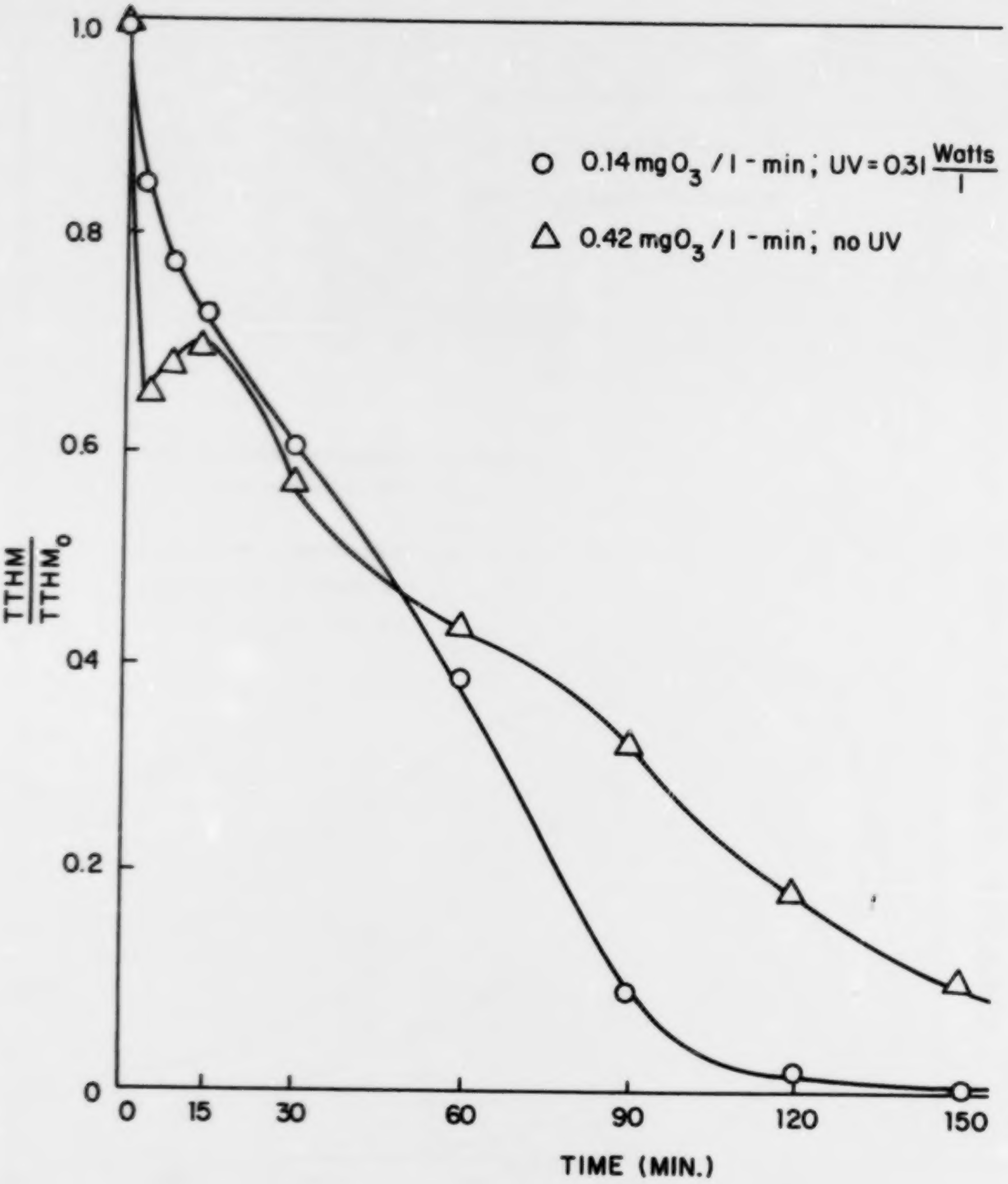

Figure 28. Normalized THM formation potential: Ozone destruction of THM precursors - Caddo Lake water.

0.14 mg O_3/L min and 0.31 W/L of UV radiation from medium pressure mercury lamps. A comparison of the curves shows two distinguishing features: (a) the O_3/UV treatment destroys THM precursor levels at a more rapid rate, and (b) no residual THMFP remains in the case of the ozone/UV runs, whereas ozone alone does not completely destroy THMFP after a net consumption of 930 mg of O_3 (dose rate minus off-gas minus residual) during 180 minutes. It should also be noted that in this example, ozone has produced additional precursor, as shown by the hump in the destruction curve, whereas O_3/UV did not, exactly the opposite as was found for Ohio River water.

Following a decision to construct a reactor at NTSU, more THMFP destruction runs were made using a single large water sample. A more complete matrix of run conditions was used and the data was accumulated as quickly as possible in order to avoid deterioration of the water sample between runs. The results of this matrix of experiments are shown in Figures 29 - 31. Experimental data is denoted by points while the curve fit of the kinetic analysis is shown by the solid lines. Several qualitative features of the data points stand out:

a) For a given UV intensity, destruction rate has an obvious dependence on ozone dose rate.

b) There is clearly some sort of precursor generation at the beginning of many of the runs. The size of the error bars and the general smoothness of the data attest to the reliability of the results, even with the inherent imprecision of the THMFP analysis. Secondary humps can clearly be seen in the following runs:

   I = 0.196   D = 6.36   t = 30
   I = 0.096   D = 4.00   t = 45

   Secondary humps have been ignored in the kinetic analysis.

c) A general increase in THMFP destruction rate is seen as UV intensity increases. There are, however, exceptions to that trend:

   1) I = 0.196, D = 6.36 > I = 0.40, D = 6.18
   2) I = 0.196, D = 2.09 < I = 0.096, D = 2.23

   In both of these cases, it can be seen that the run which is slower than expected had to overcome a greater initial buildup of precursor.

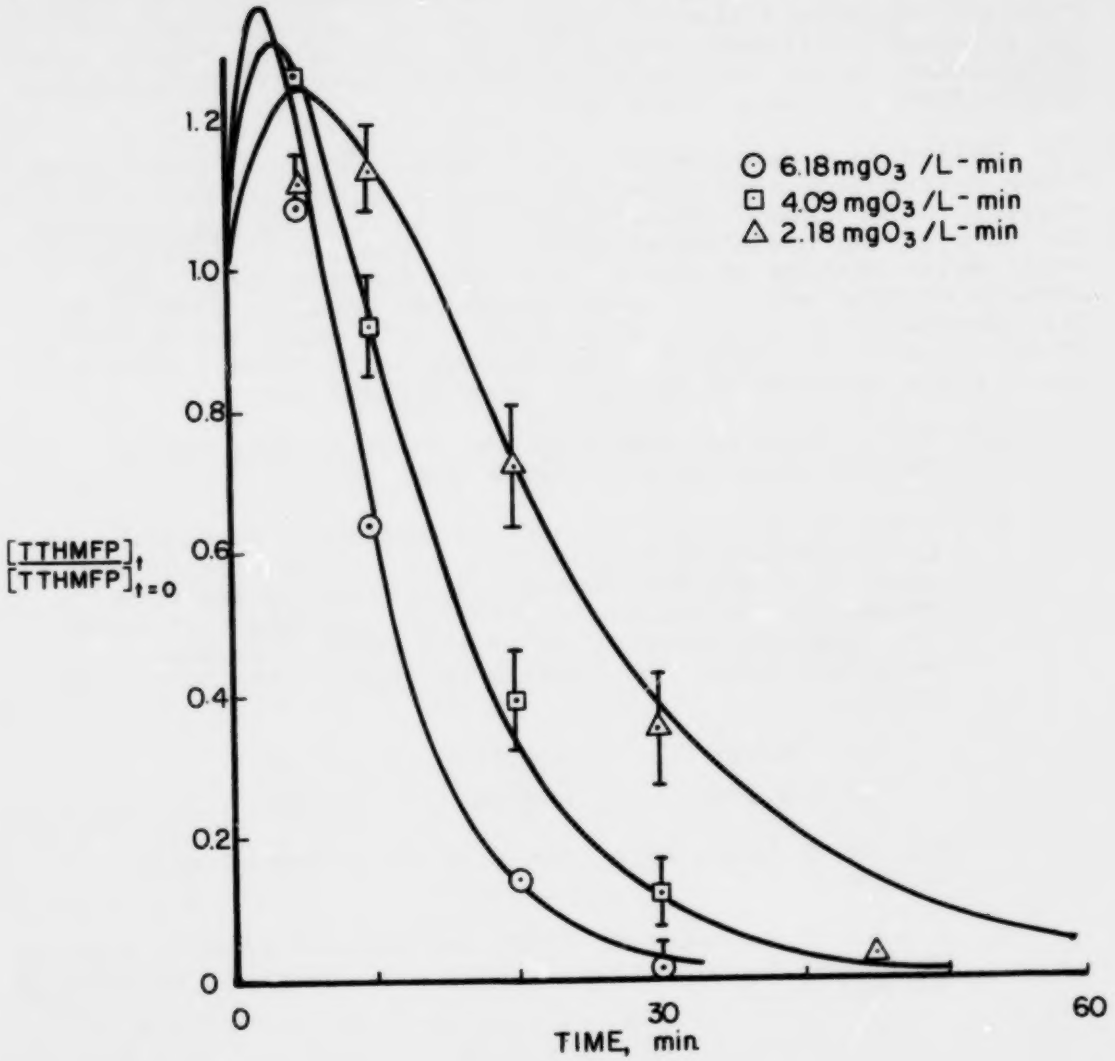

Figure 29. Trihalomethane precursor destruction by ozone/UV: [UV] = 0.40 W/L.

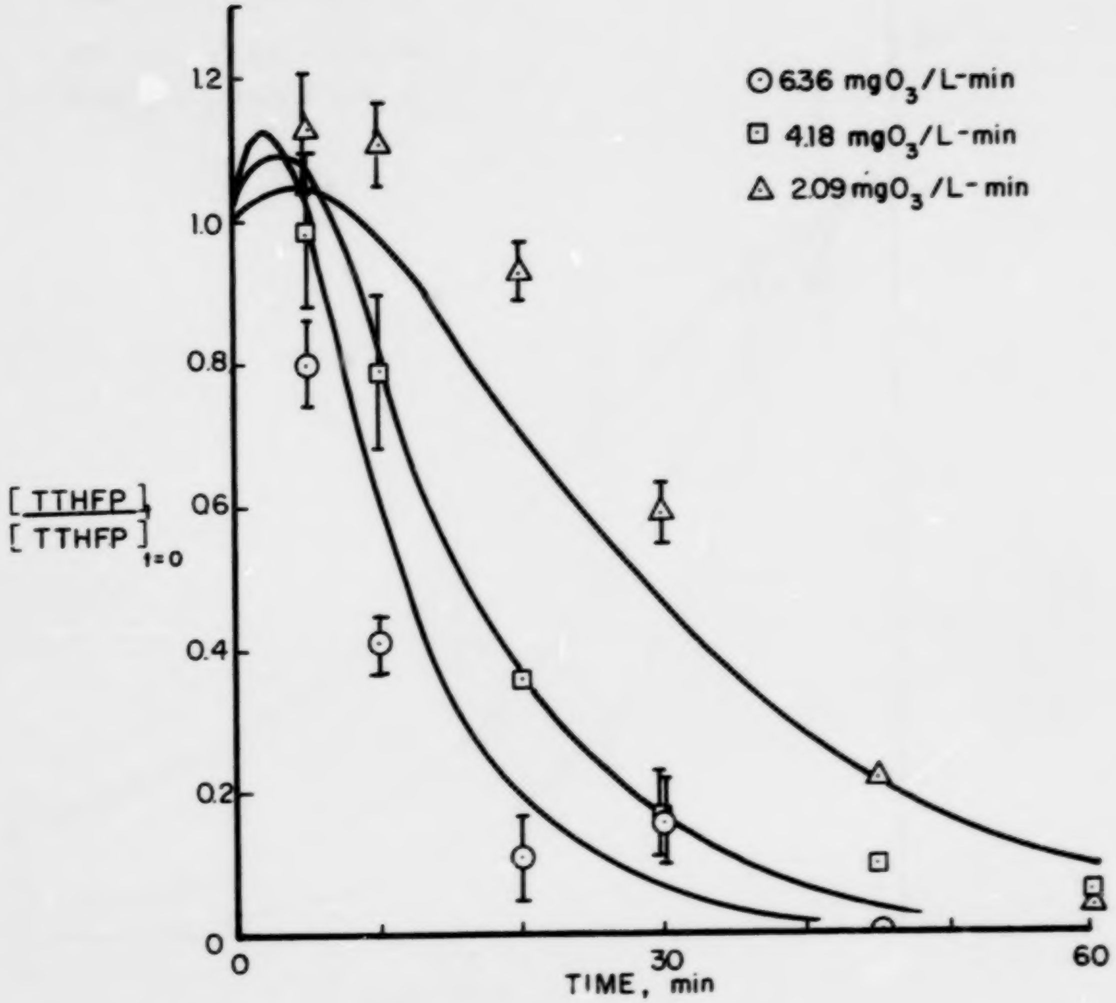

Figure 30. Trihalomethane precursor destruction by ozone/UV: [UV] = 0.196 W/L.

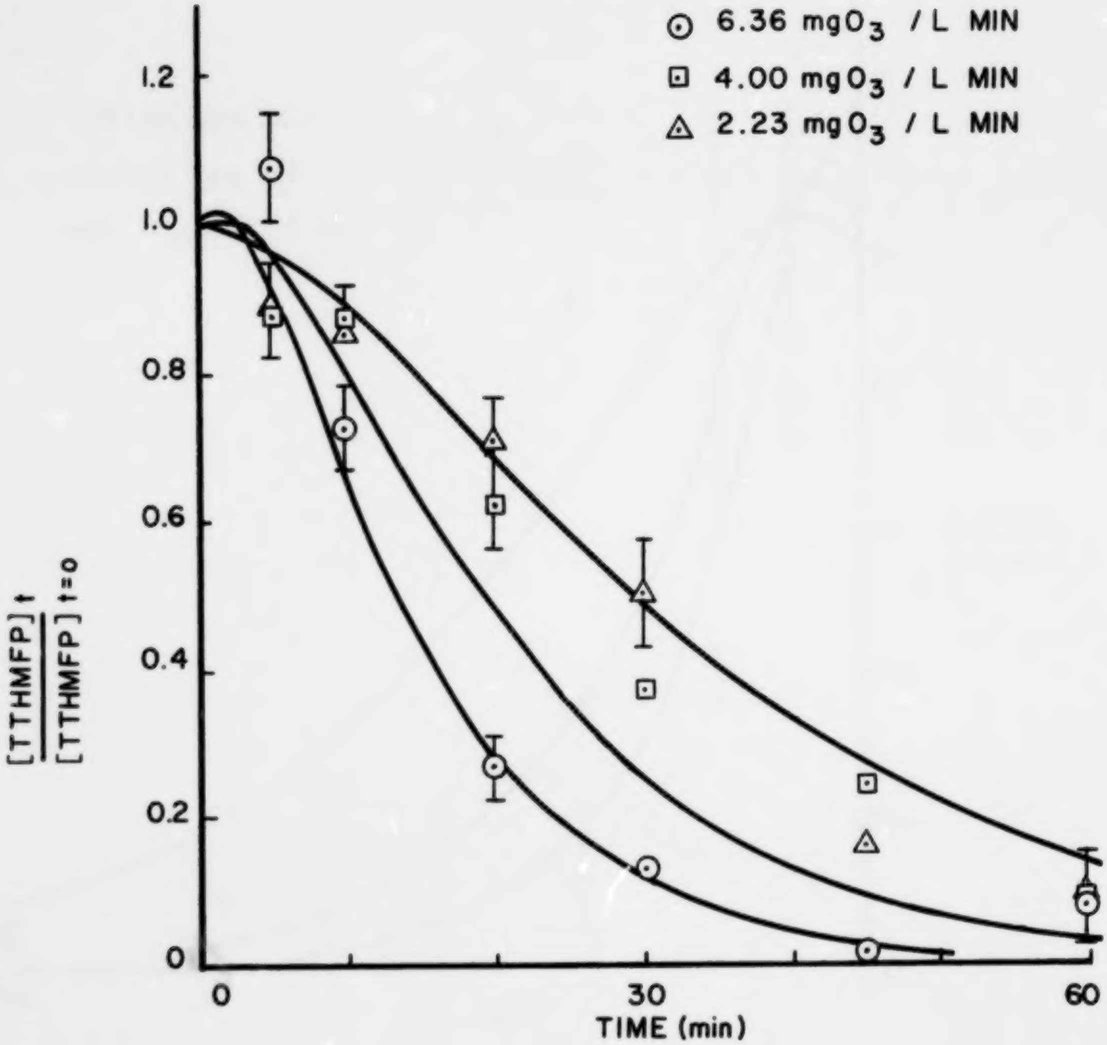

Figure 31. Trihalomethane precursor destruction by ozone/UV: [UV] = 0.096 W/L.

d) In the runs

$I = 0.40, \quad D = 2.18$
$I = 0.096, \quad D = 4.00$
$I = 0.096, \quad D = 2.23,$

the primary hump appears to have been delayed from the beginning and appears less intense than the others.

During this series of experiments, TOC was monitored as well as THMFP. The TOC data is given in Table 9. The major point of interest here is that comparison of Table 9 with the THMFP data in Table 10 shows that THMFP is destroyed long before TOC is eliminated. Thus, it appears that only specific portions of the organic carbon macromolecules can be converted to precursor sites, and so the model was altered to the following:

$$\text{Precursor (P)} \xrightarrow[K_1]{O_3/UV} \text{Non-Precursor} \qquad [74]$$

$$\begin{tikzcd}
\text{Potential Precursor Sites (M)} \arrow[r, "O_3/UV \quad \overset{+}{K_1}"] \arrow[dr, "K_M"'] & \text{Precursor} \\
& \text{Non-Precursor}
\end{tikzcd} \qquad [75]$$

Integration of the resultant differential equations yields

$$P/P_o = e^{-K_1 t} \{1 + \rho/\delta \; (1-e^{-\delta t})\} \qquad [76]$$

where

$$\rho = \overset{+}{K_1} \, M_o/P_o$$

$$\delta = K_M - K_1$$

Note that if destruction of a potential precursor site M (K_M) is considerably faster than that of precursor (K_1) it does not take long before $e^{-\delta t}$ is small compared to 1 and the disappearance of P is basically exponential. If, however, precursor formation ($\overset{+}{K_1}$) is fast compared to destruction (K_1), some precursor is built up before its source, M, is destroyed.

At this point the mathematical characteristics of the problem must be considered briefly. What is desired is a model which serves as a basis for simulating the rate equation. Furthermore it must be a model which allows prediction of the reaction rate, provided values of the parameters of interest

TABLE 9. TOC DESTRUCTION IN CROSS LAKE WATER BY OZONE AND OZONE/UV

UV Intensity, W/L	Ozone Dose Rate mg/L min	Treatment Time, Minutes					Pseudo-first-order rate constant(a) (c) $[\frac{-\ln C/C_o}{t}]_{avg}$
		0	15	35	65	95	
	2.18	8.92±0.01	8.10±0.02	7.83±0.06	6.95	6.47±0.02	$3.39X10^{-3}$ ±0.031[b]
0	4.00	9.35±0.01	7.78±0.02	$6.93\pm0.00_3$	5.75±0.01	4.78±0.01	$6.54X10^{-3}$ ±0.030
	6.00	8.97±0.07	7.11±0.07	6.23±0.02	5.84±0.08	4.39±0.03	$6.70X10^{-3}$ ±0.076
	2.23	8.08±0.07	5.90±0.06	4.36±0.04	$2.16\pm0.00_2$	2.04±0.03	$1.11X10^{-2}$ ±0.004
0.096	4.00	8.26±0.16	7.37±0.02	4.90±0.17	4.00±0.28	1.95±0.03	$1.38X10^{-2}$ ±0.0027
	6.36	7.97±0.05	6.50±0.04	5.82±0.14	3.95	2.77±0.01	$1.54X10^{-2}$ ±0.080
	2.09	$8.27\pm0.00_1$	6.99±0.06	5.18±0.02	3.31±0.04	$3.26\pm0.00_0$	$1.10X10^{-2}$ ±0.074
0.196	4.18	9.11±0.01	6.49±0.02	4.24±0.03	2.95±0.02	2.47±0.04	$1.34X10^{-2}$ ±0.107
	6.36	8.66±0.01	5.64±0.01	4.46+0.01	2.57±0.03	1.63±0.05	$1.71X10^{-2}$ ±0.080
	2.18	9.14±0.94	5.97±0.27	4.17±0.17	2.15±0.02	1.32±0.32	$1.78X10^{-2}$ ±0.062
0.40	4.09	8.85±0.155	6.23±0.16	3.73±0.06	2.40±0.03	1.82±0.02	$1.68X10^{-2}$ ±0.126
	6.18	8.974±0.02	6.35±0.01	4.24±0.03	2.61±0.02	1.61±0.01	$2.01X10^{-2}$ ±0.060

a) Outlying values have been eliminated by the 4σ rule, reference 160

b) The standard deviation should also be multiplied by the appropriate power of ten, i.e. $0.031 X 10^{-3}$.

c) For predictive purposes, the values of K for the ozone/UV experiments (i.e. exclusive of the ozone-only experiments) approximately fit the relationship:

$$K(D,I) = 2.43X10^{-3} + 4.29X10^{2}I + 2.96X10^{-4}I^{-0.883}D$$

TABLE 10. THMFP DESTRUCTION IN CROSS LAKE WATER BY OZONE/UV

Intensity, W/L	Ozone Dose Rate mg/L min	Treatment Time, Minutes							
		0	5	10	20	30	45	60	90
.096	2.23	378 ± 2[a]	338 ± 16	326 ± 10	267 ± 19	188 ± 26	62 ± 1	33 ± 9	0
	4.00	348 ± 33	305 ± 12	306 ± 12	215 ± 17	128 ± 3	84 ± 5	33 ± 16	0
	6.36	343 ± 24	372 ± 19	249 ± 16	91 ± 11	43 ± 2	3 ± 5	29 ± 9	0
.196	2.09	352 ± 20	397 ± 23	391 ± 20	326 ± 14	207 ± 15	78 ± 8	13 ± 4	0
	4.18	346 ± 21	341 ± 39	273 ± 37	124 ± 5	58 ± 20	33 ± 5	20 ± 6	0
	6.36	290 ± 18	232 ± 12	119 ± 22	32 ± 17	45 ± 17	1 ± 19	---	-
0.40	2.18	314 ± 10	351 ± 12	357 ± 20	226 ± 28	109 ± 3	8 ± 9	---	-
	4.09	282 ± 10	358 ± 3	260 ± 19	111 ± 19	35 ± 14	---	---	-
	6.18	316 ± 9	346 ± 7	203 ± 10	45 ± 7	3 ± 12	---	---	-

(a) THMFP is the sum of the chlorine and bromine trihalomethanes produced by chlorination, in μg/L. Experimental details in Appendix B.

(UV intensity and ozone dose rate) are specified. Three subordinate parameters emerge in the model in the form of rate constants:

K_1 = The rate constant for precursor destruction

$\rho = K_1^+ M_o / P_o$ = The rate of formation of precursor from site M, normalized by the amount already present

$\delta = K_M - K_1$ = The difference in rate constant between site M destruction and precursor destruction

Within any specified degree of convergence of the curve fit and the data, there are not unique values of the parameters, K_1, ρ, and δ, so that if these values are iterated until they give good reproduction of one curve, they will still not necessarily be related to the values which fit the next curve. It is therefore desirable to fix the form of the dependence of these rate constants on the parameters I = UV intensity, D = ozone dose rate, M = potential precursor site concentration, and P = precursor site concentration.

The model selected was that all reaction rates in equations [74] and [75] were first order in substrate and had the form

$$\text{Rate} = \frac{-dS_i}{dt} = K_i S_i = k_i I^a D^b S_i \qquad [77]$$

This is a reasonable, simple equation which has been used successfully in the foregoing sections of this report. Since the dependence on dose rate was obvious, the assumption of first order in dose rate was used initially. A general fit was done on all curves, the parameters linearized with respect to D, curves replotted, K's adjusted to improve the fit, relinearized, etc. This iteration was performed until the process failed to converge further. At this point, the restriction that dose rate be first order in K_1 was relaxed, and considerable improvement was obtained. Inspection of the resulting curves indicated that further iteration would not produce a significantly better fit within the model used. The resulting values are

$K_1 = k_1 I^a D^b$, where $k_1 = 6.38\text{X}10^{-2}$, $a=0.406$, $b=0.727$

$\rho = k_1^+ I^c D^d M_o / P_o$, where $k_1^+ M_o / P_o = 0.215$, $c = d = 1$

$K_M = k_M I^e D^f$, where $k_M = 7.76\text{X}10^{-2}$, $e = 0.325$, $f = 1$

where time is in minutes, dose rate in mg/L min, UV intensity in W/L and the concentration of M and P are in the same units.

These values were used in equation [76] to produce the curves shown in Figures 29-31, where as stated before, no attempt has been made to reproduce the secondary humps such as appear at t = 30 in the I = 0.196, D = 6.36 curve.

Agreement of the model with experiment is seen to be excellent for I = 0.40 and at its worst for I = 0.196. Overall the fit is adequate for the purpose for which it is intended since slight variations in the matrix can cause more change in the destruction curves than the amount by which the curve fits miss the points in Figure 30. Of the other models tried, the assumption that the oroginal precursor was different from that produced by potential precursor M did not give the added flexibility needed to better fit the data while still introducing an additional variable.

It is interesting to compare the initial increase in trihalomethane potential upon treatment with ozone or ozone/UV with results obtained by other investigators studying different systems. Dore, Merlet and Blanchard (98) found that treatment of phenol with hydrogen peroxide/UV, a known hydroxyl radical producer, or with ozone alone, increased the chloroform potential of the solution before decreasing it. Martin (179) has reported the production of humic acid-like materials upon treatment of a mixture of various phenols and carboxylic acids with hydrogen peroxide and the enzyme peroxidase, but at this time there has been no report of the investigation of the haloform potential of the substances produced. In all of these systems, there appears to be an oxygen-containing active species reacting with aromatic ring-containing systems. Since hydroxyl radical, for example, adds to aromatic rings rather than abstracting a hydrogen atom, this is consistent with the m-dihydroxybenzene precursor site theory suggested by Rook (180). In the ozone and ozone/UV systems, precursors may even be re-synthesized from the small molecule resulting from the degradation of larger molecules. Knowledge and control of the precursor-forming part of the ozone/UV reaction with organics could be quite important in the optimization of precursor removal by that process, as is obvious from inspection of Figures 29-31.

Returning to the model which was used, calculation of the pseudo-first-order rate constants for the case I = 0.40 W/L and D = 4.09 yields the following values of rate constants.

$$K_1 = 1.22 \times 10^{-1}\ \text{min}^{-1}$$

$$\rho = 3.52 \times 10^{-1}\ \text{min}^{-1}$$

$$K_M = 2.36 \times 10^{-1}\ \text{min}^{-1}$$

and the following interpretation. At t = 0, this model predicts production of precursor occurs about three times as fast as it is destroyed ($\rho/K_1 = \rho P_o/K_1 P_o = K_1^+ M_o/K_1 P_o \cong 3$). Destruction of potential precursor sites, M, is however twice as fast as that of precursor itself (which is in turn a few times faster than the destruction of TOC), so that after a while no more precursor can be formed. Furthermore, an increase in UV intensity initially favors precursor formation more than it favors precursor destruction or destruction of M. The supply of M runs out, however, whereupon the increased UV is seen to aid in the destruction of remaining precursor.

The chemistry of trihalomethane precursors and their reaction with ozone and ozone/UV is obviously complicated, but the following general scenario emerges from past work of other researchers combined with the above observations. Humic materials, as well as other macromolecular precursors, consist of a diversified collection of chemical functionalities and situations, both aromatic and aliphatic. Several of these functionalities are known to be trihalomethane precursors. Still others are within one or two oxidation steps of being precursors, i.e. they are potential precursors. Evidence is presented in the product section of this report that in hexachlorobiphenyl, once a ring is broken it is degraded to a number of products, all containing carbonyl or carboxyl groups, while the other ring remains intact. This mechanism provides a means of producing new oxygenated functionalities as well as reactive double bonds which can serve as precursors as well. Balikrishnan and Reddy (148) have discussed the reaction of hydroxyl radicals with benzene to produce phenol as well as α-and β-hydroxymucondialdehyde. The structure of β-hydroxymucondialdehyde, shown below, makes it a likely precursor candidate.

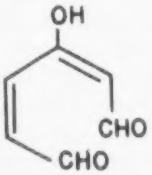

Rook (15) has shown that even non-aromatic β-diones such as 1,3-cyclohexanedione yield chloroform upon chlorination. Since hydroxyl and many other oxy-radicals are known to add to double bonds rather than abstract hydrogen, it is logical that as a complicated molecule is degraded by ozonation or O_3/UV treatment, intermediates are formed which, if chlorinated, would produce chloroform. Apparently, most of these situations are produced early in the O_3/UV reaction, and correspond to immediate conversion of $M \longrightarrow P$. The fact that is particularly striking, however, is the occurrence of the secondary humps, which are seen in Figures 30 and 31, and even more clearly and with more regularity in Figure 26. A delayed accumulation of precursor as shown in these figures, may indicate a homogeneity of some sort in the substrate molecules, rather than a mixture of molecular debris. If this idea were borne out by experiment, a significant contribution would be made toward understanding the treatment chemistry of natural water.

Summary

a) Ozone/UV destroys THMFP and TOC faster than ozone alone, for a given ozone dose.

b) Ozone/UV appears able to entirely destroy the THMFP of a natural water. Ozone does not.

c) Precursors in addition to those originally present may be produced during the treatment process but are later destroyed as the treatment continues.

d) The rate at which the THMFP of a particular water is formed and destroyed by ozone/UV is very sensitive to changes in the matrix which may occur over a short time, either upon storage in the laboratory or in its natural source.

e) The rate of destruction of THMFP in Cross Lake water by ozone/UV could not be described by a simple kinetic relationship of the type used for micropollutants in previous sections. However, THMFP destruction was described with fair adequacy by the simple model

$$\text{Precursor} \xrightarrow[O_3/UV]{K_1} \text{Non-Precursor}$$

$$\text{Potential Precursor} \xrightarrow{O_3/UV} \left\{ \begin{array}{l} \xrightarrow{K_1^+} \text{Precursor} \\ \xrightarrow{K_M} \text{Non-Precursor} \end{array} \right.$$

where each reaction is assumed to be first order in substrate, and each of the K's is described by the equation

$$K_i = k_i I^a D^b \quad .$$

A more accurate description of the details of the destruction curves would require a more complicated model.

f) THMFP is seen to be destroyed more quickly than TOC.

Mass Transfer Characteristics of the NTSU Photochemical Reactor

I. Applicability of Ozone Mass Transfer Information to the Ozone/UV System

The most frequent criticism of early ozone work is the failure of workers to measure the amount of ozone which was actually consumed in a process. Most early work and even some recent work was carried out using a glass cylinder as a reaction vessel with a fritted glass sparger at the bottom, and either no stirring or a magnetic stir bar for agitation. It was common to bubble a known concentration of ozone through the solution for a given length of time, but rarely was the concentration in the off-gas measured, so that the actual amount of ozone reacting was not known.

The reactor system used in this investigation was modeled after that which has been used by Houston Research, Inc. for a number of years. The reason for using a highly efficient stirred-tank reactor was twofold: 1) the electrical power necessary for the generation of ozone is a major expense, so that the power used in stirring is more than compensated for in ozone utilization; and 2) this type of reactor is said to be easy to scale up (163). One important parameter in the scale-up which must be correlatable between laboratory and full size reactor is the ability to transfer the gaseous reactant into the liquid. Applying the models normally used for mass transfer, however, is complicated by several factors in the case of the ozone/UV system. For example, it is not known whether the majority of the ozone is photolyzed in the gas bubbles or in the liquid. Obviously this could effect the ozone mass transfer process, particularly if the photolysis of ozone produces a specie which is very reactive with water. For example, in the gas phase, photolysis of ozone produces $O(^1D)$ oxygen atoms which can react exceedingly quickly with water to produce hydroxyl radicals (82-86). For the case where $O(^1D)$ reacts with the bubble wall, a secondary active specie, ·OH radical, would be simultaneously produced in the liquid by the chemical reaction. If the $O(^1D)$ instead reacted with water vapor in the bubble, hydroxyl radical would be generated in the gas phase which then could be transferred into the liquid, react with another ·OH or some other specie in the gas, etc. If however, ozone was photolyzed in the liquid phase, the second reaction to form hydroxyl radical would probably occur extremely rapidly.

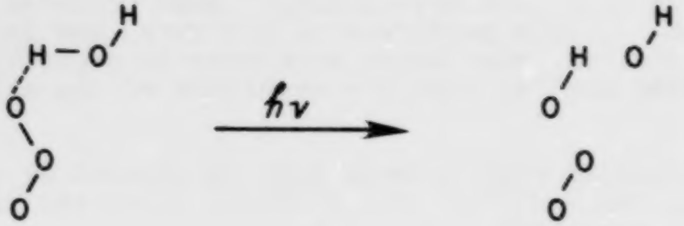

The possibility of radical caging to form H_2O_2 or ·OOH is obvious, and will be discussed at a later point.

In fact the identity of the active specie responsible for the rapid destruction of substrate in an ozone/UV experiment is not known. The three processes cited above, and others probably contribute active specie to the solution, all with their individual transfer characteristics. Analysis of some preliminary data collected here indicate that in our reactor, ozone photolyzed in the gas phase is just as effective at destroying substrate as ozone which was photolyzed in the liquid phase. This preliminary finding indicates that the usual ozone mass transfer considerations are not appropriate for an ozone/UV situation. Because of the nature of this investigation and the unavailability of resources necessary to pursue answers to the above questions, it was decided that the ozone mass transfer characteristics of the NTSU reactor would be evaluated to ensure that it was performing adequately, at least by ozone mass transfer standards.

II. Ozone Mass Transfer in Absence of UV Radiation

Since UV catalyzes the decomposition of ozone, one convenient way to perform consecutive mass transfer experiments is to destroy ozone from a previous mass transfer run using the UV lamps which were present for the ozone/UV runs. Using this procedure it was noted that the first time a mass transfer run was performed on a fresh batch of purified water, not only the equilibrium level of ozone in solution, but also the calculated value of the mass transfer coefficient was higher than on successive runs. This effect could be explained by the production of a substance during the UV period of the first run which catalyzed the decomposition rate of ozone in successive runs. Alternately, one may postulate that the organic matter present in the water reacted with the ozone during the first run, a situation which is known to enhance mass transfer (169, 170). In addition, the reaction might have produced compounds or complexes which were still reactive enough to give a positive test with iodide. The results of one such series of experiments is shown in Figure 32. The erratic first run followed by a series of reproducible and regular subsequent runs made the second possibility seem more likely. Mass transfer calculations, described below, were performed on all runs, and in the discussion which follows, the larger more erratic first runs are labeled "first run" so that the magnitude of the effect can be seen.

Mass transfer coefficients were calculated by the method published by Yocum (145). His starting point was the molar mass balance equations

$$G(Y_{BF} - Y_{BE}) = K_{la}(C_{Be} - C_B) \qquad [78]$$

and

$$\frac{dC_B}{dt} = \frac{K_{la}}{V}(C_{Be} - C_B)\ k_oC \qquad [79]$$

where G = molar flow rate of the gas

Y_{BF} = mole fraction of ozone in feed gas

Y_{BE} = mole fraction of ozone in exit gas

K_{la} = mass transfer coefficient

C_{Be} = liquid concentration of ozone in equilibrium with gas concentration in the bubbles

C_B = concentration of ozone in bulk liquid

V = volume of liqud

k_u = ozone autodecomposition constant

The equations resulting from Yocum's treatment are

$$\ln(1 - C_B\eta/C_B^*) = -C_1t \qquad [80]$$

$$\eta = (1 + k_o/k_{La}) = C_B^*/C_{Be} \qquad [81]$$

and

$$k_{La} = \left[\frac{C_1}{\eta - \beta C_1}\right]\frac{L}{V} \qquad [82]$$

where C_B^* = liquid ozone concentration predicted to be in equilibrium with feed gas

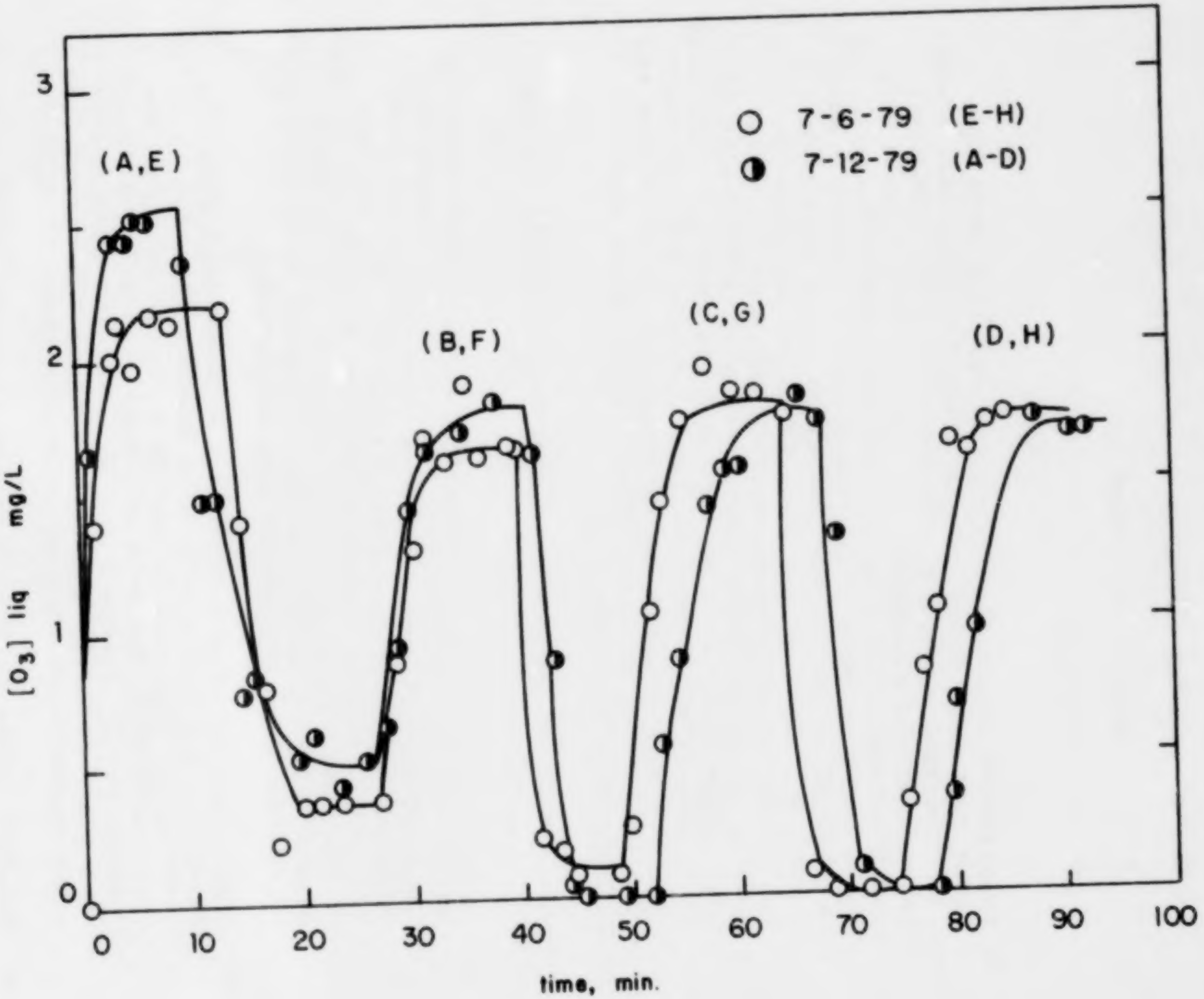

Figure 32. Mass transfer experiments showing "first run" and subsequesnt results.

C_{Be} = experimental equilibrium ozone level in liquid

$\beta = \frac{PL}{HG}$

L = Number of moles of liquid in reactor

H = Henry's law constant

P = Pressure

At superficial velocities (ratio of gas flow rate to reactor cross sectional area) usually used for good mass transfer into stirred-tank reactors, the volatile model compounds chloroform, bromodichloromethane and tetrachloroethylene were purged from the reactor at a rate which was comparable with the reaction rate found in some of the experiments. Thus, a much lower flow rate of 25 mL/min was chosen in order to avoid excessive purging. This is the same ratio of gas flow to reactor volume which was used at Houston Research in their initial runs on trihalomethane precursors at the beginning of the project. Mass transfer runs were made at this gas flow rate as well as at 200 mL/min, the flow rate used for HCB and THMFP destruction, and at 1.0 L/min for comparison. These values are shown in Table 11 along with the other values which were available from the literature.

Several important points about the data in Table 11 are noteworthy:

1) Comparison of line 1 with lines 2 and 3 indicates that while fairly constant mass transfer coefficients are observed at 500 rpm and 200 or 1000 mL/min gas flow, lowering the stirring speed to 300 rpm and the gas flow to 25 mL/min causes a decrease by a factor of two in the mass transfer coefficient. In all of these experiments the water had been "burned" with ozone and UV before the experiments were performed.

2) Comparison of line 3 with line 4 shows that when the water had not previously been burned, the mass transfer coefficient appeared larger by a factor of five, and comparable with the data of Yocum (lines 5 and 7) and Prengle et al. (lines 8 and 9). The two experiments in line 4 are actually the first runs in two series, the other consecutive runs of which are shown in line 3.

3) The data given in line 8 is the first run in the series which produced line 10 as the second run. The numbers in line 10 were calculated from the data presented graphically in Figure 16 of reference 103. Since there is no mention of UV in reference 145, it was assumed that

the water is changed between runs. This was later verified in a private conversation with that author. In other words, lines 5, 6 and 7 are also "first run" values. The tabulated values of the mass transfer coefficients in Table 11 are seen to break into two groups plus the low value of run (1).

TABLE 11. MASS TRANSFER COEFFICIENTS DETERMINED FOR NTSU REACTOR (a) COMPARED WITH LITERATURE VALUES

Gas flow rate ml/min	Dose Rate, mg/L min	Superficial Velocity cm/min	Stirring Rate, RPM	k_La g Moles L min Δ X	Number of Determinations	Reference
1) 25	0.47	0.145	300	2.69±1.53	3(f)	NTSU
2) 200	0.95-3.82	1.16	500	5.26±1.71	5(f)	NTSU
3) 1000	7.2	5.8	500	5.30±1.66	6(f)	NTSU
4) 1000	7.2	5.8	500	28.1±2.3	2	NTSU
5) 4240	n.a.	6.1	300	19.2	n.a.	(b)
6) 4240	n.a.	6.1	500	54.5	n.a.	(e)
7) 323	1.33	1.88	n.a.	28.6	n.a.	(b)
8) 1000	2.08	2.4	548	21.3	1	(c)
9) 1000	2.08	2.4	720	22.9	1	(c)
10) 1000	2.08	2.4	548	5.30	1(f)	(d)

a) V=3.0L, cross sectional area=172 cm^2. Other dimensions given in experimental - Appendix B.

b) Calculated by Houston Research from the data of Yocum (ref.145).

c) Given by Prengle, Hewes, and Mauk in Reference 103.

d) Calculated from the data shown in Figure 16 of Reference 103 by assuming t_o= 130 minutes and using the three points at t=136,141, and 150 min. C_B was assumed zero at $t=t_o$ whereas it was actually 2.7 mg/L.

e) Yocum, ref. 145, Figure 8.

f) Water which has been "burned" by ozone/UV. Results in line 4 are for water which had not previously been "burned." See text for explanation of "First Run" results

k_{la}, $\frac{\text{y-moles}}{\text{L-min }\Delta X}$	NTSU	Reference 145	Reference 103
"First Run" Values	28.1	19.2, 28.6, 54.5	21.3, 22.9
"Burned" Water	5.26, 5.30	--	5.30

The fact that the NTSU reactor behaves approximately as the reactors described in references 103 and 145 is not surprising since, to the extent practical, it was build according to the design presented in those two references. The difference between the "first run" and subsequent mass transfer coefficients, however, is to these investigators knowledge, previously unreported, and further study is needed to determine the reason for this effect. The data in line 10 of Table 11 is reported to be at 29°C rather than at 26°C which is the temperature for the data in line 8. The change is, however, too large to be explained by a change in the Henry's Law constant. Furthermore, this effect is seen in NTSU experiments when no temperature change is seen. There is one additional piece of data which indicates that the effect is due to reaction with substances during the first run, which are destroyed when the UV is applied the first time. The value of the autodecomposition rate constant, which reflects the rate at which ozone decomposes in solution, was found to be 54.5 ± 1.8 for the "first run" experiments, while it was 15.5 ± 4.9 for subsequent experiments using the same water after ozone/UV treatment. Although not conclusive, this larger value of k_o for the first run, compared with the lower value consistently found in the subsequent runs is consistent with the concept of "burning" the impurities out when the UV is switched on.

Summary

a) The NTSU reactor was modeled along the lines of the standard stirred-tank reactor design (103,145,163,168) to the extent practical for the fabrication material (quartz), since use of this design is said to eliminate some scale-up difficulties.

b) Mass transfer experiments using ozone and purified water which has never been treated with ozone appear to give higher values of the mass transfer coefficient than the same experiments using water which has been "burned" with ozone/UV prior to determination of K_{la}. Use of an analytical procedure for aqueous ozone which did not respond to other oxidants might resolve this question, which is fundamental to ozone technology. One such test may be the indigo test proposed by Hoigne' and Bader (171). The above effect is also seen in the published data of other investigators (103).

c) Within the framework of b) above, the mass transfer coefficient of the NTSU reactor calculated by the method of Yocum, does appear to be in the range reported (103,145) for larger engineering reactors, except at much lower flow and stir rates, as in line 1, Table 11.

d) Above a UV intensity to ozone dose ratio, I/D, of about 0.15 $W(mg/min)^{-1}$ no ozone or other KI-detectable oxidant is found in solution during an ozone/UV experiment when either no substrate or very dilute substrate (a few tenths of a mg/L) is present.

e) Because of d) above and the apparent ability of active species or their precursors to transfer from the gas into the liquid, it may be inappropriate to use ozone mass transfer considerations to describe what occurs in an ozone/UV experiment.

f) The autodecomposition of ozone was found to be higher in the quartz NTSU reactor than that reported by other investigators (103,145).

g) On a stoichiometric basis, ozone utilization for substrate destruction at low concentrations (100 µg/L) is low (Table 12). The reasons for this low efficiency are not known, but definitely warrant study, as a sizable increase in efficiency would yield a very powerful treatment tool. Along these lines it is very important to study the mechanisms and species involved, since the key to increased efficiency is in understanding what is occurring in this complex system.

TABLE 12. EFFICIENCY OF CHLOROFORM DESTRUCTION BY OZONE/UV (50% REMOVAL)

INITIAL CHLOROFORM CONCENTRATION	MOLES CHLOROFORM DESTROYED / MOLE OZONE DESTROYED
20 µg/L	.00095
50 µg/L	.0023
100 µg/L	.0046
1.9 µg/L	14.5

SECTION 6

IDENTIFICATION OF CHEMICAL BY-PRODUCTS FROM OZONE/ ULTRAVIOLET-INDUCED REACTIONS OF ORGANIC COMPOUNDS IN WATER

EXPERIMENTAL PROCEDURES

Product runs for hexachlorobiphenyl were conducted in a smaller reaction vessel than the one described previously for the kinetic runs. The larger vessel was, however, used for product runs on chloroform and lake water. No attempt was made to determine ozone utilization except in the case of chloroform, described below.

HCB and lake water reaction products were identified by GC/MS after extraction and derivatization of the acidic fraction, sometimes preceded by liquid chromatographic separation. An electrochemical detector was used to check for easily reducible compounds, but this investigation was cut short by the changes in emphasis as the project progressed. Carbon dioxide was trapped in base and titrated, and chloride ion was titrated microcoulometrically. The details of the experimental procedures are given in Appendix E.

RESULTS AND DISCUSSION

I. Chloroform, Bromodichloromethane, and Tetrachloroethylene

Product studies were not conducted on bromodichloromethane because of limited time and the decision to deemphasize products in favor of additional kinetic work in natural water. Because of its lower stability and the small likelihood of finding bromine and oxygen atoms on the same carbon, the products resulting from bromodichloromethane are expected to be innocuous, and chloroform was chosen as the representative compound.

One recurrent peak was noticed during the photolysis kinetic studies on TCE. Attempts to extract it into ether or pentane failed initially, but finally succeeded once the pH was lowered to 0.8. Comparison of retention times and mass spectra with those from an authentic sample of trichloroacetic acid showed that they were identical. The mass spectrum is also very similar to that of chloroform, which is expected to be the decarboxylation product of the somewhat unstable acid. Further confirmation of the compounds identity was made from its odor.

The products resulting from ozone/UV treatment of chloroform were studied by treating a concentrated solution of chloroform (1.9g/L) with 0.57 mg/L min of ozone and 0.40 W/L of UV radiation for one hour, during which time the off-gas from the reactor was bubbled through sodium hydroxide solution to trap carbon dioxide, then through pentane to trap any purgable organics which formed. At the end of the reaction period, the ozone was shut off and the reaction mixture purged with 75 mL/minute of oxygen for 45 minutes to purge remaining CO_2 and products from solution and the reactor headspace. Portions of the aqueous reaction mixture were extracted and analyzed for halogenated compounds by gas chromatography with electron capture detection, and by GC/MS. The pentane solution was analyzed similarly, and in both cases, no compounds other than chloroform were found. The solutions were analyzed by selected ion monitoring for tetrachloroethylene and hexachloroethane with negative results. The increase in carbonate in the trap was measured and a portion of the reaction mixture titrated for hydrogen ion increase. Another portion of the reaction mixture was derivatized and analyzed for formic acid as the benzyl ester, as described in Appendix E. The results are shown in Table 13.

TABLE 13. PRODUCTS RESULTING FROM OZONE/UV TREATMENT OF CHLOROFORM

Substance	Concentration $\frac{\text{m moles}}{\text{L}}$	Ratio to Chloroform
Chloroform (destroyed)	7.32 ± 0.73	---
H^+	23.6 ± 0.4	3.22 ± 0.38
Cl^-	19.4 ± 0.2	2.65 ± 0.29
CO_2	5.1 ± 0.2	0.70 ± 0.10
Halogenated Organics	n.d.	---
Formic Acid	n.d.	---
Ozone Destroyed	0.713	0.097

It can be seen from the last column that the reaction

$$CHCl_3 \longrightarrow 3H^+ + 3Cl^- + CO_2$$

appears to have occurred. Within experimental error the products are those expected from the equation (Cl^- lacks 3% of fulfilling the stoichiometry while CO_2 lacks 20%, probably due to the method of collection), thus it is seen that the products are inorganic and innocuous, organic halogen being mineralized to halide ion. Several mechanisms can be written which would give this stoichiometry, but these are the products which are expected whenever one of two things happens: 1) an oxygen atom in any form is attached to the carbon, whereupon an acid chloride situation develops, which is unstable enough in water that the acid chloride itself ($HCOCl$, $ClCO_2H$, $COCl_2$, etc.) probably never forms, but passes on to the hydrolysis products shown in the above equation; or 2) the hydrogen atom is abstracted by a free radical in the presence of water (the autooxidation product of chloroform is phosgene). In either case, once the integrity of the chloroform molecule is destroyed it probably collapses completely to products, resulting in the very rapid reaction rate observed and the lack of intermediate products. Judging from the last entry in Table 13, this appears to be a chain reaction. It is not presently known what species carries the chain, but possible coupling products between CH_iCl_j species were specifically looked for in the chromatograms of both reaction mixture and pentane trap and not found. The above considerations probably hold for most halogenated compounds, consistent with the claim by Westgate Research Corporation for example, that their ozone/UV system is particularly effective in removing chlorinated compounds (115).

II. Hexachlorobiphenyl

As an aid to understanding and predicting what types of products will be produced upon ozone/UV treatment of complex halogenated molecules, the degradation of 2, 2', 4, 4', 6, 6'-hexachlorobiphenyl was studied rather extensively. Although the concentration of PCB in water and wastewater is usually at the µg/L level, the experiments in this work were conducted at higher concentration (suspension) in order to obtain a larger quantity of products for identification. The small reactor as described in the experimental section was used for all the experiments. In the case of photolysis, nitrogen or oxygen gas at the same flow rate was used. At the end of each reaction time, the whole solution was extracted according to the procedures described in Appendix E. Products were identified by using gas chromatography combined with mass spectrometry. Chromatograms and mass spectra are collected in Appendix E, section II, but are referred to from the text.

Photolysis Products of HCB--

The photolysis of HCB in nonaqueous solution has been studied by Safe and Hutzinger (172) with 310 nm radiation. The authors found that chlorine is removed rather rapidly from HCB yielding di-, tri-, tetra- and penta-chlorobiphenyls. The reconstructed GC/MS scans of HCB photolysis products found in the neutral fraction in this work are shown in Figures E-3 and E-4. No acidic products were found. In the neutral fraction of the solution after four hours radiation, dechlorinated product pentachlorobiphenyl was found and heptachlorobiphenyl was also identified. Safe and Hutzinger found other dechlorinated products besides pentachlorobiphenyl and some other compounds caused by rearrangement or condensation. However, in this work only products resulting from dechlorination were found. The product heptachlorobiphenyl is believed to be produced from the attack of HCB by chlorine radicals. It should be noted that the solution used is a suspension with high concentration of HCB and the heptachlorobiphenyl is an unlikely product in dilute solution. Figure 33 shows the production of chloride ion during the photolysis process as measured by microcoulometry. The yield appears to be approaching 1 mole of chloride ion per initial mole of HCB.

When the HCB molecule is excited by UV radiation, the C-Cl bonding is apparently cleaved. According to Ruzo et al (173), this process proceeds through the triplet state and is driven by the need to remove strain in the excited molecule in which the planar configuration is most stable. The formation of heptachlorobiphenyl suggest that free chloride radicals are formed (path A). However, it is possible that the pentachlorobiphenyl product is the result of a concerted process in which solvent water attacks the excited HCB molecule (path B), Figure 34.

The mass spectra of HCB, penta chlorobiphenyl and heptachlorobiphenyl are shown in Figures E-5, E-6 and E-7. From Figures E-3 and E-4, and from the rate data reported before, it is apparent that oxygen does not change the rate or mechanism of the photolysis of HCB in aqueous solution. It has been reported that the presence of oxygen in nonaqueous solution retards the photolysis of PCBs, presumably due to triplet quenching by oxygen.

Ozonation and Photolytic Ozonation Products--

Yokayama and co-workers (174) ozonated a mixture of PCBs in aqueous solution for 24 hours to obtain a variety of small degradation products which were rationalized in terms of a ring opening process. Chlorine elimination was found as a secondary process, and it was noted that PCBs with several chlorine atoms produced fewer products. No detailed study of the ozonation products of HCB has been conducted in this work; however, in one ozonation run, traces of pentachlorobiphenyl were found along

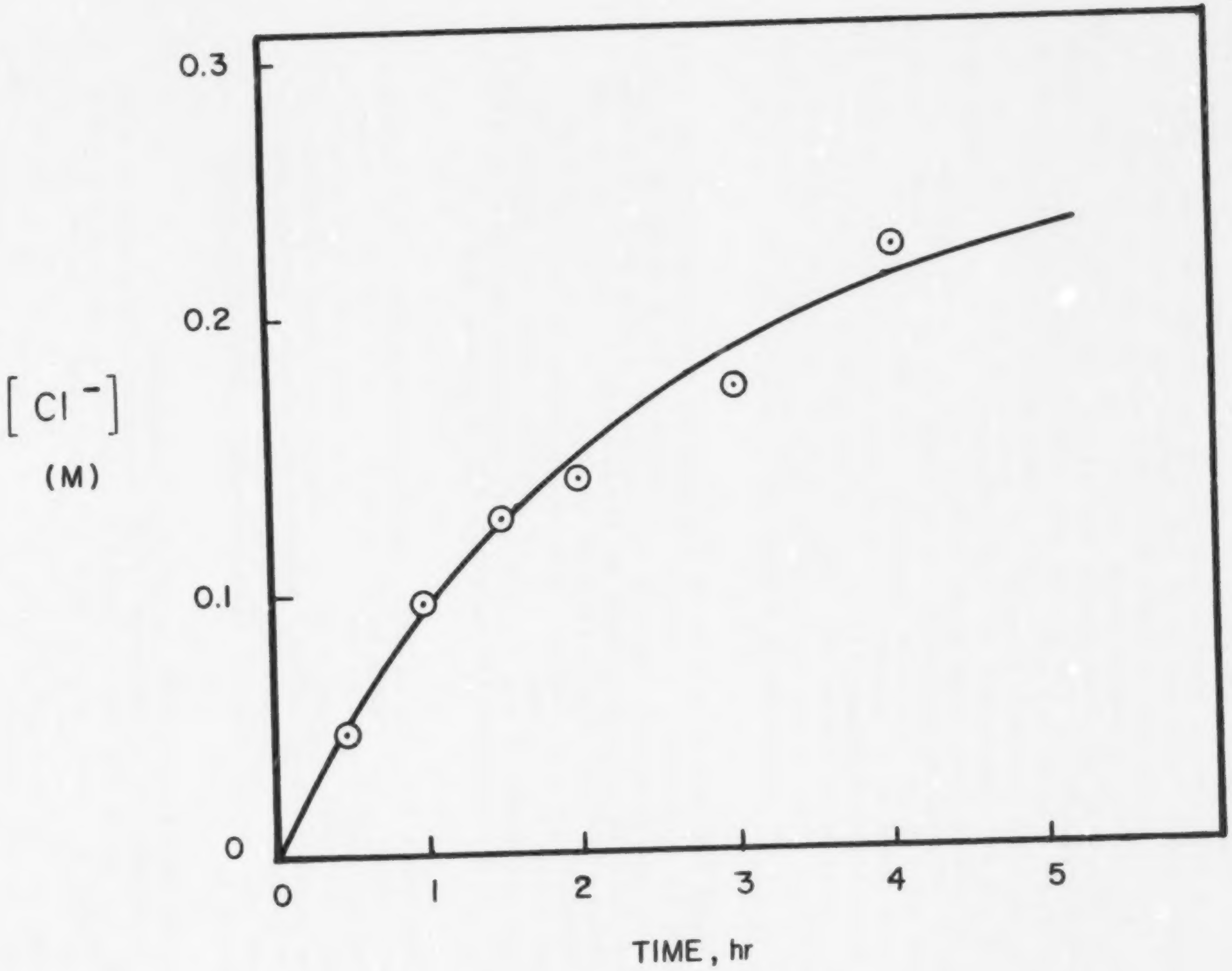

Figure 33. Production of chloride from the photolysis of HCB in water.

with a compound with $M^+ = 372$ with a six chlorine cluster. The compound was not identified. No chloride production during the reaction period of four hours was found.

Photolytic ozonation of HCB was conducted in the small reactor and the products identified by either GC or GC/MS. The reactor is shown and extraction and derivatization schemes described in Appendix E. In order to study the pathways of the reactions, the concentrations of the major products at different reaction times were determined. The proposed reaction scheme

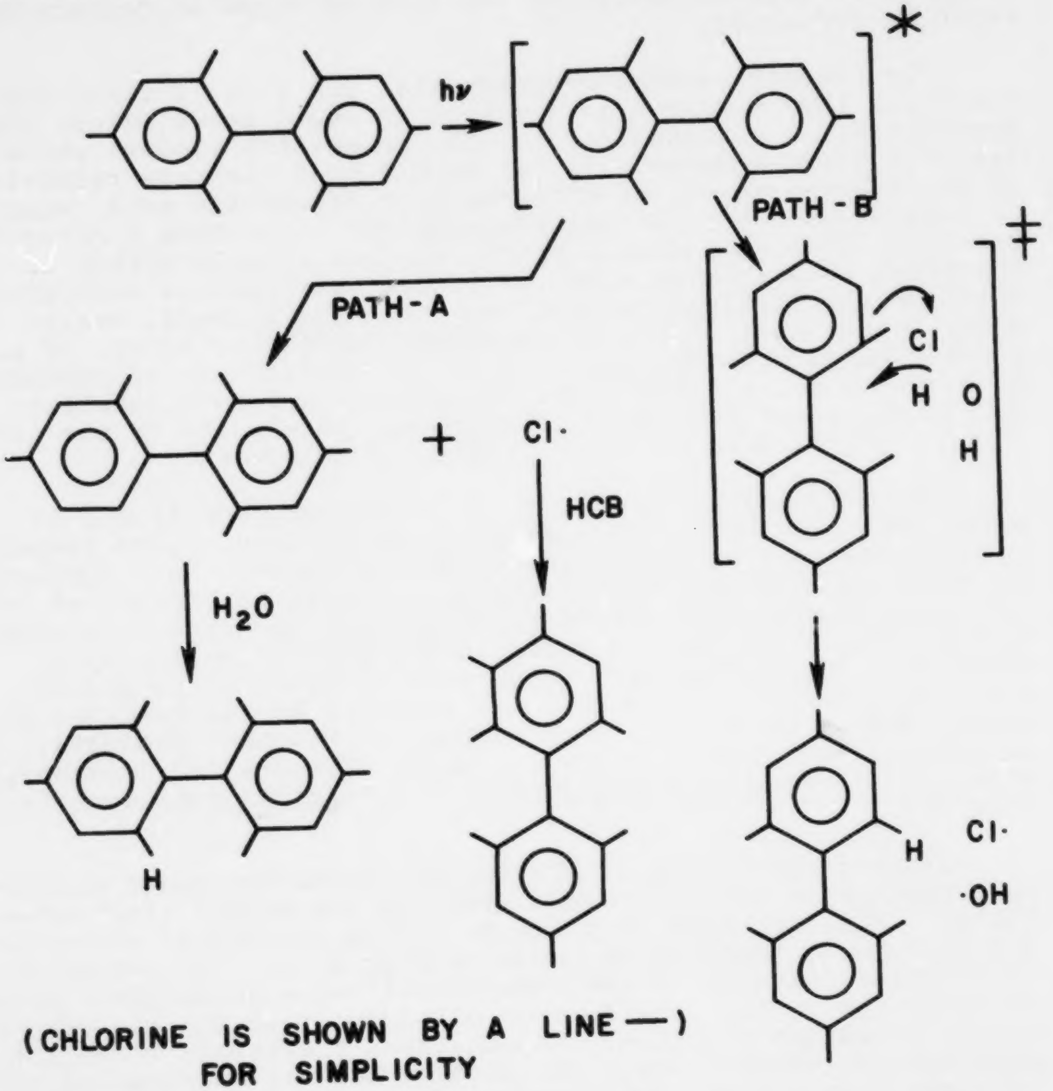
hν
*
PATH - B
‡
PATH - A
Cl
H O
H
+
Cl·
HCB
H_2O
H
H
Cl·
·OH
(CHLORINE IS SHOWN BY A LINE —)
FOR SIMPLICITY

Figure 34. Hexachlorobiphenyl photolysis pathway according to Ruzo (173) (chlorine is shown by a line — for simplicity).

for ozone/UV degradation of HCB is shown in Figure 35. The scheme utilized five types of reactions which are not uncommon in ozone (176) and photochemistry (175). Double bonds are cleaved in aqueous solution (C in Figure 35) to yield acids and carbonyl compounds. Decarboxylation (D in Figure 35) and replacement of halogen by hydroxyl (R) are known photochemical processes (175). Oxidation of an aldehyde to an acid and hydrolysis of an acid chloride are the remaining two reactions which are employed in the scheme. This scheme is not intended to rationalize all of the products which were found, but is meant to be representative of the type of stepwise degradation which is occurring.

The reaction scheme proposes that one ring is first ruptured and then degraded in a series of rapid steps before the second ring is attacked (177). The repetitive process which destroys these compounds is, a) double bond cleavage resulting in an aldehyde which, b) oxidizes to a carboxylic acid, which c) decarboxylates. Further cleavage may occur when a molecule contains additional double bonds, so that organic carbon in converted to carbon dioxide via either intermediate carboxylic acids or the terminal compound in the ozone process, oxalic acid. Since most of the products are carboxylic acids, pH presumably plays an important role in the degradation of products. At elevated pH, the acids are dissociated and more reactive toward electrophilic reagents; however, pH effects in the production of products were not studied in this work.

The compound 2-chloro-3-(2,4,6-trichlorophenyl)-maleic acid, (CTMA) is a major intermediate which is produced rather quickly and reaches a maximum at about 3 hours. This compound is believed to be the first stable ring-opening product of HCB. Upon ring opening the HCB molecule apparently quickly oxidizes by the loss of two carbon atoms in the form of oxalic acid, which also is produced at a high rate as shown in Figure 36. 2,4,6-trichlorobenzoic acid forms steadily as the reaction proceeds, and is relatively stable compared to other products. It is significant to note, however, under UV radiation decarboxylation (175) occurs and the product 2,4,6-trichlorobenzene is observed.

After ring-opening of HCB further oxidation seems to proceed rapidly on the open chain, leaving the second ring undisturbed. The formation of chloride in the photolytic ozonation system occurs steadily as shown in Figure 37. The percentage of chloride relative to the theoretical value is slightly high, possibly due to the interference of products in the microcoulometric titration reaction. Nonetheless, the steady formation of chloride ion suggests that chlorine on HCB may be attacked to initiate ring rupture and subsequent oxidation reactions. Although peroxides are assumed intermediates from the oxidation of organics, high pressure liquid chromatography with an elec-

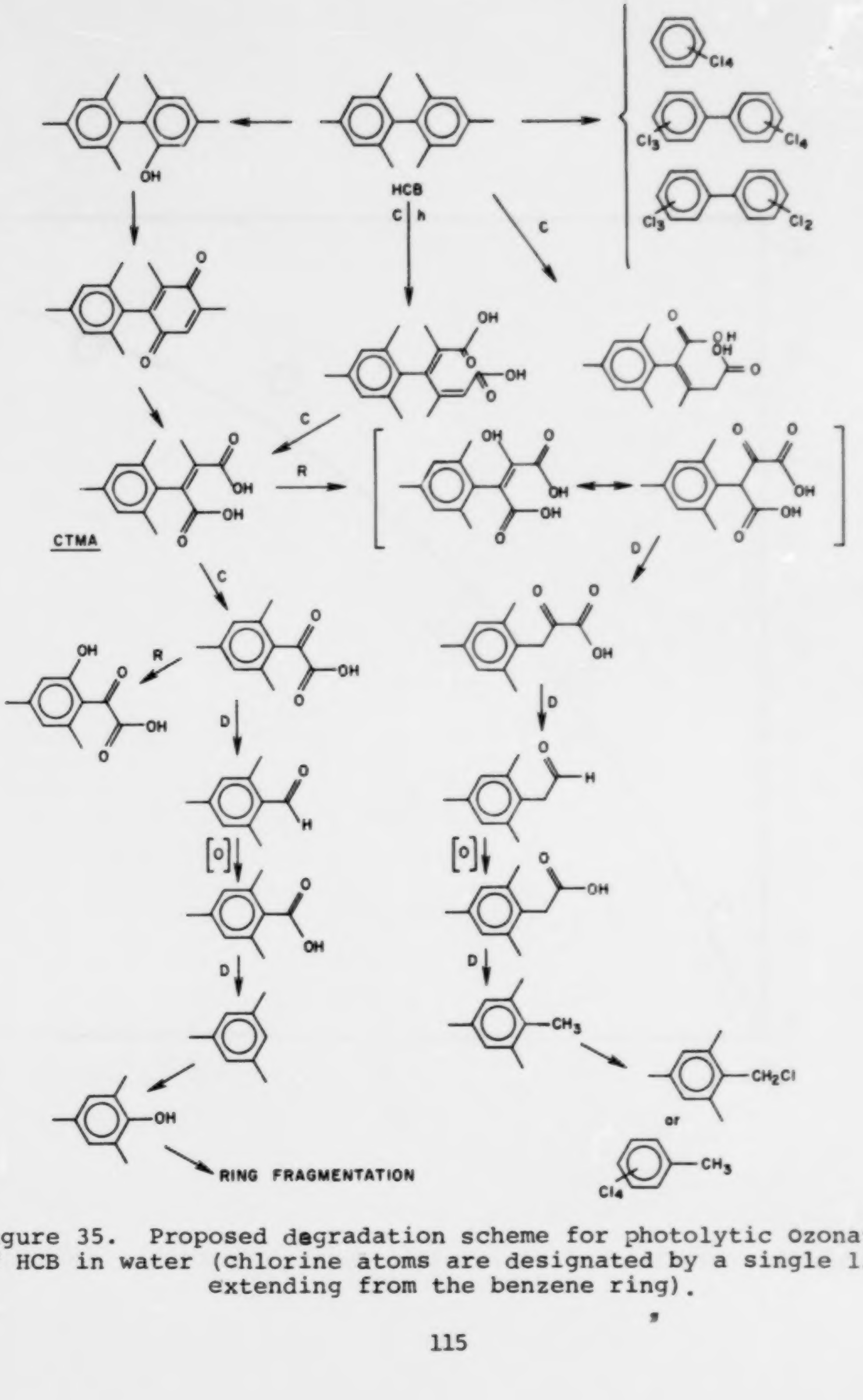

HCB
C
h
C
Cl4
Cl3
Cl4
Cl3
Cl2
OH
O
OH
OH
O
OH
O
C
R
CTMA
OH
OH
O
D
C
R
OH
D
H
[O]
OH
D
CH3
CH2Cl
or
CH3
Cl4
RING FRAGMENTATION

Figure 35. Proposed degradation scheme for photolytic ozonation of HCB in water (chlorine atoms are designated by a single line extending from the benzene ring).

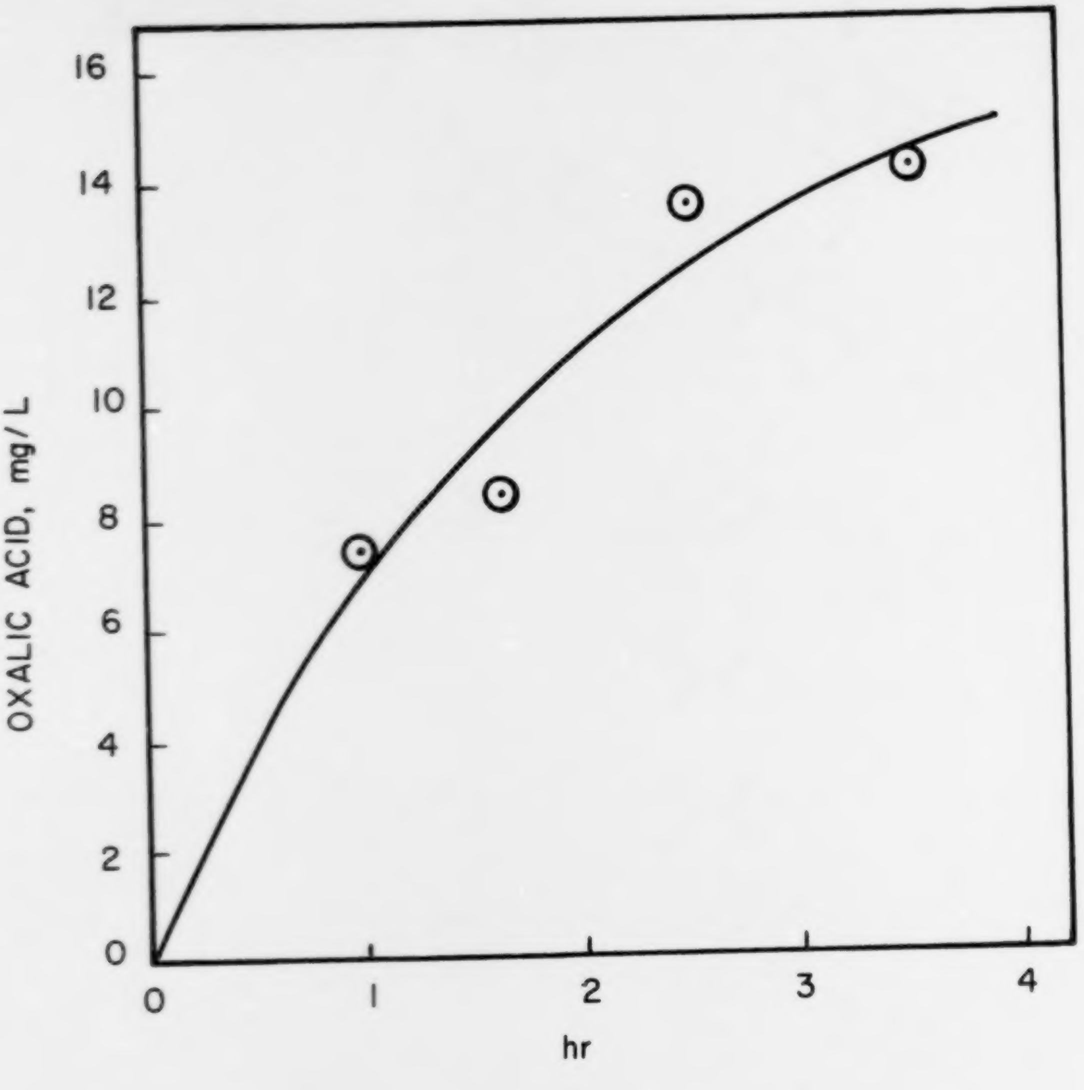

Figure 36. Formation of oxalic acid during photolytic ozonation of HCB in water.

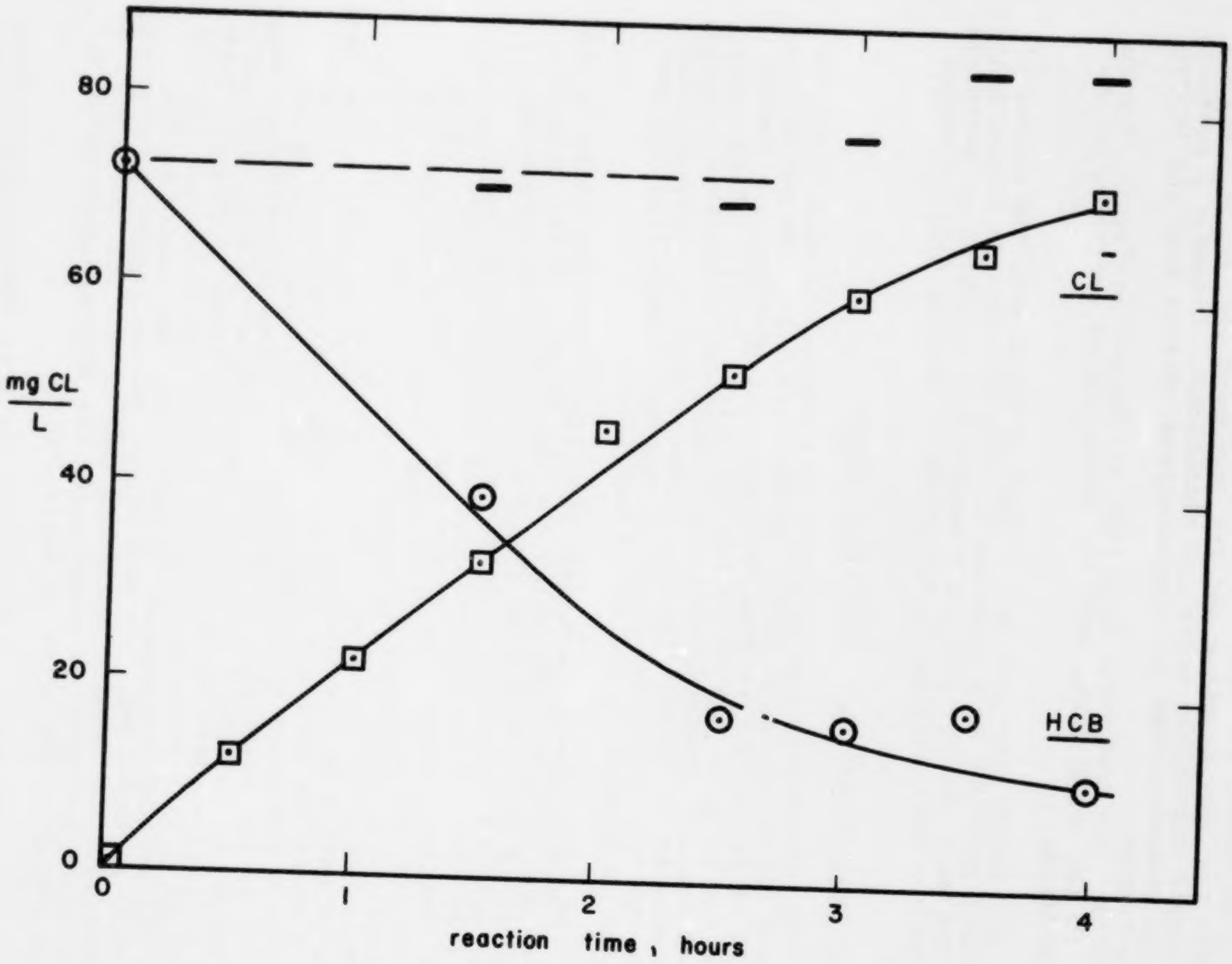

Figure 37. Chlorine balance during ozone/UV treatment of HCB.

trochemical detector failed to detect easily reducible peroxides as HCB oxidation products. Presumably these intermediates, if formed, are very reactive and are destroyed very quickly under the severe photolytic ozonation conditions. Appendix E contains typical reconstructed gas chromatograms (Figure E-8) and GC/FID chromatogram
products. All compounds from CTMA and beyond in Figure 35 were seen in the GC/MS data, with the exception of trichlorophenylacetaldehyde.

The major compounds are listed in Table E-1, the amount of products produced as a function of time is shown in Figure E-10, and the mass spectra and the fragmentation patterns on which the identifications were based are shown in Figures E-11 to Figure E-19.

III. Natural Water: Caddo Lake, Texas

In considering the ozone/UV treatment of natural water to remove micropollutants and trihalomethane formation potential, it is of importance to know what kinds of products are formed from the ozone/UV reaction with the matrix itself. Caddo Lake water has been ozonated with and without UV, products extracted, and studied by GC/MS. The experimental details, reconstructed mass chromatograms, and lists of compounds identified are presented in Appendix E and summarized below.

The only peaks which have been identified are those in the ozone and ozone/UV runs which are not present in the control. Methods of confirmation of peak identity include comparison with spectra collected in Registry of Mass Spectral Data (164) or published in the literature, and computer matching through the Chemical Information System (166). Those spectra which could not be found in the literature have been rationalized according to fragmentation patterns and compared with actual samples whenever possible. The scheme shown in Figure E-2 for concentration of HCB products is also the extraction scheme used to concentrate products from the Caddo Lake water ozonations, neutrals and basic compounds being extracted at high pH and acids at the lower pH. Glass capillary mass chromatograms were obtained by splitless injection onto a 30 m. SP-2100 WCOT column in a Finnigan 3200 GC/MS system, and are shown in Figures E-18 through E-23. Peaks which occur in the ozonation runs but not in the control are labeled by letter and the compounds are listed in Table E-2. In many cases, the compounds have not been identified but several peaks are seen to exhibit the same fragmentation pattern. In these cases the fragmentation patterns are listed in the notes to Table E-2.

The most striking feature of the mass chromatograms shown in Figures E-18 through E-23 is that treatment of Caddo water with ozone greatly increases the number of lower molecular weight (i.e. chromatographable) compounds, as can be seen by comparing Figure E-18 with Figure E-20 and Figure E-21 with Figure E-23. Ozone/UV treatment, however, produces much fewer such compounds, many of which are thought to be innocuous at low levels (e.g. aliphatic hydrocarbons) and most of which are at much lower levels than with ozone alone. (Compare Figures E-19 and E-28 with E-18, E-20, E-21, and E-23.) Quantitation has not been attempted but peak f is the internal standard, trichlorobenzene, the height of which corresponds to 1 µg/L in the original water, assuming 100% extraction efficiency.

In order to avoid altering the nature of the products, the remaining ozone residual was not quenched by the addition of some reducing agent. Peak C is thought to be related to ethyl ether peroxide and has the empirical formula $C_4H_8O_2$. Striking is the number of nitrogen compounds found in the chromatograms, but more expected is the abundance of organic acids produced in the experiments using ozone without UV. Hydrocarbons in the O_3/UV neutral fraction are though to originate by photolysis of carboxylic acids (175),

$$RCO_2H \xrightarrow{hv} RH + CO_2 \quad ,$$

or by reaction with an active free radical. Seivers (60) has reported their production in a non-UV ozonation system. Absence of organic acids in the O_3/UV acid fraction is conspicuous, and is consistent with the findings of other investigators (103).

Of interest from a health effects viewpoint is compound n. Fetizon and Audier (14) reported the mass spectra of I and II and discussed the possibility of their interconversion through the epoxide III. The spectra obtained in our experiment was intermediate between the published spectra of I and II, making the presence of the epoxide a possibility. There is, however, no direct evidence for the presence of the epoxide.

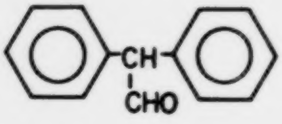
I

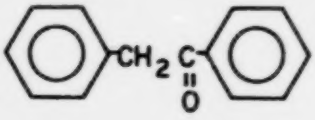
II

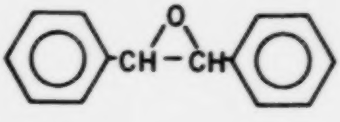
III

Summary

It can be seen from the ozonation products of Caddo Lake water that the number of chromatographable products, both from ozone and from ozone/UV, is larger than that found for the control, indicating breakdown of larger natural organics into smaller molecules. Ozone/UV treatment, however, while showing considerably greater destruction of the organic matter (TOC) present, gives considerably fewer products than ozonation alone. Seen from the work on hexachlorobiphenyl is the fact that once an aromatic ring is ruptured, it appears to continue to degrade more rapidly than scission of the other ring occurs. Furthermore, with HCB, as in the case with chloroform, chlorine atoms are eliminated from the degrading portion of the molecule very early in the process, as the first oxygen atoms are introduced. Because of the decrease in TOC in the case of chloroform, it is seen that organic compounds actually are converted to carbon dioxide and organohalogen to halides by ozone/UV, as opposed to the situation for ozone alone, where degradation usually stops at some organic compound such as oxalic acid. This difference is reinforced by comparison of the ozone and ozone/UV products from natural waters, referred to above. One strength of the ozone/UV process over ozone alone seems to be the ability of the ozone/UV process to decarboxylate organic acids.

Comparison of the effect of ozone and ozone/UV on aqueous chloroform is particularly instructive since many of the early investigations of nonaqueous ozone chemistry were performed using chloroform as a solvent. The ozone/UV process is seen from the present work on chloroform to involve a chain reaction, at least in the case of some substrates. It was observed that several chloroform molecules are destroyed by photolysis of one ozone molecule at high substrate concentrations, while at very low substrate concentrations the ratio of chloroform to ozone molecules destroyed went as low as 10^{-3} for 20 μg chloroform per liter. This observation is in agreement with the chain reaction hypothesis in that the ratio of the rates of the chain termination reactions to propogation reactions is very large when the chain carrier finds it difficult to locate substrate. Similarly, when a natural matrix is added, additional possibilities for chain termination and other reactions are introduced.

SECTION 7

PROCESS ENGINEERING ANALYSIS AND SIZING AND COSTING OF FULL SCALE UNITS*

A consulting engineering firm was hired to design a full scale process for removal of chloroform, bromodichloromethane, and tetrachloroethylene from lake water in one set of cases, and to remove trihalomethane precursors from lake water in a second set of cases, utilizing the kinetic data collected in this project and presented in preceding sections. This design would be utilized by the firm to estimate treatment costs for the process. As test cases, 1, 10, and 50 million gallon per day capacities were selected, and facilities were designed to remove 90% of the undesirable substances.

This section contains the final report submitted by the subcontracted engineering firm, Houston Research, Inc., selected as representative of the best currently available technology, due to their experience in the field of ozone/UV treatment. The critical assumption which has been made in performing the following calculations is that of how much the efficiency of the process can be increased in going to full scale equipment. Houston Research, based on their previous experience, has estimated that an ozone utilization efficiency of 35 to 50% may be expected from the full scale unit, whereas maximum efficiencies of 17% in the case of trihalomethane precursors and 13% in the case of the micropollutants were calculated from the experiment, as based on reaction stoichiometries assumed by Houston Research. Whether this difference is due to the low concentration of substrate, some characteristic of the laboratory scale reactor, or some other factor is presently unknown. However, efficiency calculations performed using data similar to that shown in Figure 32 but with a model substrate present, indicate that all ozone photolyzed, whether in the liquid or the bubbles, was utilized to the same extent in the destruction of model compound. These results indicate that a more likely cause of the low efficiency was the competition of side reactions with useful ones. While examination of that question was beyond the scope of this investigation, the study of the mechanism and active species of the ozone/UV process would be of importance in the process optimization. A pilot study would be needed before the assumed increase in efficiency could actually be demonstrated.

---

*This section of the report was prepared by H. William Prengle, Jr., Arthur E. Nall, and Dilip S. Joshi of Houston Research, Inc., Houston, Texas.

The following list defines the symbols and nomenclature used in this section.

SYMBOLS & NOMENCLATURE

Chemical Species

A	TOC or other organic components
B	Ozone
C	Chloroform (CF)
D	Bromodichloromethane (BCM)
E	Tetrachloroethylene (TCE)
M	Trihalomethane Precursors (THMP)
S	Substrate of interest; or total of all organic species

Upper Case

B_c	Cumulative ozone supplied
C_B, C_B^*	Concentration of ozone; Henry's law concentration of ozone, respectively
D	Ozone dose rate
D_I, D_T	Impeller diameter; tank or reactor diameter, respectively
E_ν, $E_{\nu S}$	UV energy; UV energy per gram of S removed
H	Henry's law constant
H_I, H_ℓ, H_S	Height of impeller above bottom of reactor; height of liquid, height of sparger, respectively
I	UV-intensity
K_A, K_C, K_D, K_E, K_M	Component chemical reaction rate constants
K, K_o, K_u^+, K_u	Reaction rate constant; for O_3-only; for UV only; preliminary UV rate constant, respectively
K_L, K_g	Overall mass transfer coefficients, liquid side, gas side, respectively
K_ν^*	UV-energy transfer coefficient
L	Path length
N, N_g, N_R, N_B	Rotation rate; gas flow number; Reynolds number; O_3 mass transfer number, respectively
$P, \mathcal{P}$	Pressure; power input
Q	Gas flow rate
R, r	Reactor radius; bulb to reactor distance, respectively
V	Reactor volume
X_B, X_B^*	Ozone liquid phase mole fraction; Henry's law value, respectively

Lower Case

a	Interfacial area for mass transfer; liquid phase attenuation coefficient, respectively
b, b_a, b'	Turbine blade width; apparent O_3 requirement; stoichiometric O_3 requirement, respectively
$f(N_g)$	Gas flow dispersion function
g, g_c	UV irradiation geometric factor; dimensional constant (fm lbm/lbf sec^2); respectively
h	Turbine blade height
k_L, k_g	Individual mass transfer coefficients, liquid and gas, respectively
$k_L a, k_g a$	Mass transfer coefficients including interfacial area
$\dot{m}_B, \dot{m}_C$	Ozone supply rate; volatile component desorption rate, respectively
n	UV-intensity exponent
$p^{\neq}$	Vapor pressure
r	Correlation coefficient
t	Time variable
u_g	Superficial gas velocity
w_b	Reactor quadrant baffle width
w_n, w_u	Nominal UV bulb wattage; UV-wattage, respectively
y_B	Vapor phase mole fraction of ozone

Greek

$\alpha, \alpha_o, \alpha_o^+$	O_3-utilization fraction; for O_3 only; intrinsic value
γ	Liquid phase activity coefficient
η	Preliminary analysis optimization parameter
μ	Liquid phase viscosity
ρ	Liquid phase density
τ	Wall transmission factor

Operators

< >	Denotes average
Sub o	Denotes initial value
Super o	Denotes standard state values
•	"Dot" above symbol denotes a time derivative

A. PROCESS ENGINEERING ANALYSIS BASIS

The Ozone/UV process for photo-oxidation of refractory and toxic inorganic and organic species was developed in the early 1970's. The first quantitative reaction rate data were presented in 1973 [1], and followed by extensive data on oxidation of organic compounds in 1975 [2] and 1976 [3,4]. A substantial body of research has been completed on a broad range of inorganic compounds: metal cyanide complexes; organic and amino acids; alcohols; insecticides; organic nitrogen, phosphorous, and sulfur compounds; chlorinated organics; inorganic anions and cations; and numerous composite industrial mixtures. Three major areas of application exist for treatment of: a) industrial waste water, b) municipal waste water and c) raw source water. To date, three patents have been granted [5,6,7].

And now detailed research, presented in this report, has been carried out on application of the process to removal of micropollutants and trihalomethane precursors from raw water.

The objective of this part of the report is to carry out a reaction engineering analysis of the experimental data, adding the necessary important aspects of reactor dynamics, in order to produce,

1) - a process configuration, and

2) - sizing and costing of the equipment for certain full-scale units.

The work presented in the first part of the report is not sufficient, of itself, to permit design of the reaction equipment. Other aspects, such as mass and energy transfer and optimization must be added in order to do the full-scale designs. Prengle has developed the methods, used herein, from hundreds of Houston Research, Inc. O_3/UV data points and basic chemical engineering theory and practice.

At the outset, some comments are necessary concerning the reaction rate equations used. Peyton, Glaze and co-workers in the first part of this report have used the forms, e.g. for the tetrachloroethylene data,

$$\begin{array}{cccccc} -\dot{S} & = K_u & I & D & S & \text{(1a)} \\ \left(\frac{\text{mols S}}{\ell\ \text{sec}}\right), & \left(\frac{\ell\ \text{min}}{\text{sec}, \text{mgO}_3, \text{watts}/\ell}\right), & \left(\frac{\text{watts}}{\ell}\right), & \left(\frac{\text{mgO}_3}{\ell\ \text{min}}\right), & \left(\frac{\text{mols s}}{\ell}\right) & \end{array}$$

integrating to,

$$\ell n\ S_o/S = K_u\ I\ D\ t \qquad \text{(1b)}$$

and gives a hybrid non-consistent set of dimensions for the overall reaction rate constant, K_u, (ℓ, min/sec, mgO_3, watts/ℓ). An alternate form has been used in the reaction engineering analysis that follows:

$$\begin{array}{ccccc} -\dot{S} & = K_u & I & (\frac{\dot{m}_B}{V}) & (\frac{S}{S^o}) \\ (\frac{mg\ S}{\ell min}), & (\frac{mg\ S}{mgO_3\ watt/\ell}), & (\frac{watts}{\ell}), & (\frac{mg\ O_3}{\ell\ min}), & (\frac{mg\ S/\ell}{mg\ S/\ell}) \end{array} \qquad (2a)$$

S^o, a standard state concentration (taken as 1.0 mg/ℓ) is inserted to make the concentration variable dimensionless. The equation integrates to,

$$\ell n(S_o/S) = K_u\ I(\dot{m}_B/V)t = K_u I B_c \qquad (2b)$$

Since the sequence of reactions taking place by photolysis and photo-oxidation are driven by UV-energy input, the ozonalysis being almost negligible, the dimensions of K_u[(mgS removed/mgO_3, watts/ℓ)] = [(mgS removed/mgO_3, (joules/sec ℓ)], is a dimensionally consistent concept.

B. ENGINEERING ANALYSIS OF THE REACTION DATA

Each set of experimental data obtained was analyzed to determine certain quantities necessary to carry out the process engineering calculations and sizing of the full scale units.

The characteristics of the lake water used in the experiments are shown in Table 14.

TABLE 14. CHARACTERISTICS OF THE LAKE WATER

Characteristic	Lewisville Lake (A)	Cross Lake (B)
pH	8.1	7.6
SS (mg/ℓ)	<10	<10
TDS (mg/ℓ)	130	100
COD (mg/ℓ)	10.0	34.6
TOD (mg/ℓ)	4.3	8.7
THM Precursor (μg/ℓ)	-	<330>
COD/TOC	2.33	3.98

An important parameter missing from the above list is a measure of the "total oxidizables, TO," or the total oxygen demand, TOD. Such information is very important in determining the total O_3-utilization, since Houston Research, Inc. experiments have amply demonstrated that inorganic species -- certain metals, cations, anions, etc. are also oxidized by O_3 and O_3/UV, producing an additional ozone demand. However, at present a satisfactory TO test procedure is not available. The data sets are analyzed in Table 15.

TABLE 15. ANALYSIS OF DATA SETS

System	Initial Concentration (mg/ℓ)	Table
1) Tetrachloroethylene, TCE in purified water	0.100	II-1
2) TCE in Lake Water (A)	0.100	II-2
3) Chloroform, CF in purified water	0.100	II-3
4) CF in Lake Water (a)	0.100	II-4
5) Bromodichloromethane, BCM in Lake Water (a)	0.100	II-5
6) Trihalomethane Formation Potential (5 days, 26°C)	<0.330>	II-7

In order to carry out the engineering analysis of the data, the following functions were used as "screening" parameters.

1) The cumulative O_3(B) supplied,

$$B_c \equiv \left(\frac{\dot{m}_B}{V}\right)t, \text{ (mgO}_3\text{ supplied/}\ell) \tag{3}$$

2) The apparent O_3 requirement,

$$b_a(\text{based on S}) \equiv \left(\frac{B_c}{\Delta S}\right), \quad (\text{mgO}_3/\text{mgS removed}) \tag{4a}$$

$$b_a(\text{based on TOC}) \equiv \left(\frac{B_c}{\Delta TOC}\right), \quad (\text{mgO}_3/\text{mg TOC removed}) \tag{4b}$$

3) The fraction of O_3 utilized,

$$\alpha(\text{on S}) \equiv \left(\frac{b'\Delta S}{B_c}\right), \quad b' = \text{stoichiometric O}_3 \text{ required} \tag{5a}$$

$$\alpha(\text{on TOC}) = \left(\frac{COD}{TOC}\right)_o \frac{\Delta(TOC)}{B_c} \tag{5b}$$

4) The reaction rate constant,

$$K_u(\text{on S}) \equiv \frac{\ell n(S_o/S)}{I(B_c/B^o)}, \quad \frac{\text{mg S removed}}{\text{mgO}_3\text{, joules/sec }\ell}) \qquad (6a)$$

$$K_u(\text{on TOC}) \equiv \frac{n(\text{TOC}_o/\text{TOC})}{I(B_c/B^o)}, \quad (\frac{\text{mg TOC removed}}{\text{mgO}_3\text{, joules/sec}}) \qquad (6b)$$

These K_u-rate constants used for screening assume first order in I and B_c; therefore, for a given set of runs, a drift in the K_u-value will be an indicator of whether or not first order is adequate to account for the results. In addition, the question arises: How constant is constant? Some take the view that if rate constants fall within "an order of magnitude," they are constant, and there are literature data for gas phase reaction which only satisfy such a criterion. Here, at the outset, we would consider values constant if they are within a factor of 2 to 3.

5) Energy input per unit volume,

$$E \equiv (\frac{It}{60}), \quad (\frac{\text{watt hrs}}{\ell}) \qquad (7a)$$

6) Energy input per gram of material removed,

$$E_{\nu S} \equiv (\frac{E_\nu}{10^{-3}\Delta S}) \quad \text{(watt hrs/g. S removed)} \qquad (8a)$$

$$E_{\nu TOC} \equiv (\frac{E_\nu}{10^{-3}\Delta TOC}), \quad \text{(watt hrs/g. TOC removed)} \qquad (8b)$$

7) An approximate optimization parameter can be defined and calculated from the data based on the following concept. Best process economics for a given situation would dictate that the size of reaction equipment, amount of ozone, and amount of energy input be minimized. That is, maximum S or TOC removal, per unit of O_3 input, per unit of energy input, per unit residence time. The requirements can be incorporated in the parameter, η, which is used only for screening purposes,

$$\eta \equiv (\frac{\Delta S}{B_c\ E_\nu t}), \quad (\frac{\text{mg S removed}}{\text{mgO}_3\text{, (watt hrs/}\ell\text{)min}}) \qquad (9)$$

Analysis of the individual data sets follows.

1. Tetrachloroethylene Destruction in Purified Water

Example: $I = 0.375$ watts/ℓ, $(\dot{m}_B/V) = 1.33$(mg O_3/min),

$t = 0.917$ min

$S_o = 0.100$ mg/ℓ, $\Delta S = 0.095$, $\ell n\, S_o/S = 3.00$

$$B_c = (\dot{m}_B/V)t = (1.33)(0.917) = 1.22 \text{ mgO}_3 \text{ supplied}/\ell$$

$$b_a = (B_c/\Delta S) = 1.22/0.095 = 12.8 \ (\text{mgO}_3/\text{mg } \Delta S)$$

$$K_u = \frac{\ell n\, S_o/S}{I(B_c/B^o)} = \frac{3.00}{(0.375)(1.22/1.00)} = 6.56 \ \left(\frac{\text{mg S removed}}{\text{mgO}_3,\ \text{watts}/\ell}\right)$$

$$\alpha = \frac{b'\Delta S}{B_c} = \frac{(1.158)(0.095)}{1.22} = 0.0902 \ (\text{fraction } O_3 \text{ utilized})$$

$$E_\nu = (It/60) = \frac{(0.375)(0.917)}{60} = 0.00573 \text{ watt hrs}/\ell$$

$$E_{\nu A} = \frac{E_\nu}{\Delta S(10^{-3})} = \frac{0.00573}{0.059(10^{-3})} = 60.3\left(\frac{\text{watt hrs}}{\text{g}.\Delta S}\right)$$

$$\eta = \left(\frac{\Delta S}{B_c E_\nu t}\right) = \frac{0.095}{(1.22)(0.00573)(0.917)} = 14.8 \ \frac{\text{mg } \Delta S}{\text{mgO}_3\left(\frac{\text{watt hrs}}{\ell}\right)\text{min}}$$

Values of these parameters for all conditions of TCE in purified water are summarized in Table 16.

2. Tetrachloroethylene Destruction in Lake Water (A)

Example:

$I = 0.375$, $(\dot{m}_B/V) = 1.33$, $t = 11.1$ min, $S_o = 0.100$,

$\Delta S = 0.090$, $TOC_o = 4.3$, $(TOC/TOC_o) = 0.81$,

$\Delta TOC = 0.82$ mg/ℓ

TABLE 16. SUMMARY DATA ANALYSIS, TETRACHLOROETHYLENE DESTRUCTION IN PURIFIED WATER

I (watts/ℓ)	$(\frac{\dot{m}_B}{V})$ (mgO$_3$/min)	t (min)	B_c (mgO$_3$/ℓ)	b_a (mgO$_3$/mgΔS)	K_u (watts/ℓ)$^{-1}$	α	$E_{\nu S}$ (watt hrs/gΔS)	η
0.091	1.33	9.83	13.1	136	2.52	0.0085	155	0.0495
	0.775	7.83	6.07	63.2	5.43	0.0183	124	0.168
	0.420	16.7	7.01	73.0	4.70	0.0158	264	0.0323
	0.200	-	-	-	-	-	-	-
	0.090	33.0	2.97	3094	11.1	0.0371	521	0.0194
0.189	1.33	1.53	2.03	21.1	7.82	0.055	50.2	6.42
	0.775	2.58	1.99	20.7	7.98	0.056	84.7	2.30
	0.460	5.33	2.45	25.5	6.48	0.045	175	0.438
	0.230	9.33	2.14	22.3	7.41	0.052	307	0.164
	0.110	10.1	1.11	11.6	14.3	0.100	332	0.268
0.375	1.33	0.917	1.22	12.0	6.56	0.0902	60.3	14.8
	0.775	1.57	1.22	12.7	6.56	0.091	102	5.11
	0.450	2.23	1.00	10.4	8.00	0.111	146	3.09
	0.260	3.17	0.824	8.58	9.71	0.135	207	1.86
	0.090	6.60	0.594	6.19	13.5	0.187	431	0.593
					<8.01>			

Constants for this Set of Data: $b' = 1.158$, $S_o = 0.100$ mg/ℓ, $\ell n(S_o/S) = 3.00$;
$\Delta S = 0.095$ mg/ℓ.

$B_c = (1.33)(11.1) = 14.76 \ (\mathrm{mgO_3/\ell min})$

$b_a(\text{on S}) = (B_c/\Delta S) = (14.76/0.090) = 164$

$b_a(\text{on TOC}) = (B_c/\Delta\text{TOC}) = 14.76/(0.19)(4.3) = 18.07$

$$K_u(\text{on S}) = \frac{\ell n\ S_o/S}{I(B_c/B^o)} = \frac{2.303}{(0.375)(14.76)} = 0.416$$

$$K_u(\text{on TOC}) = \frac{\ell n\ 4.3/3.48}{(0.375)(14.76)} = 0.0382$$

$$\alpha(\text{on S}) = \frac{b'\Delta S}{B_c} = \frac{(1.158)(0.090)}{14.76} = 0.00706$$

$$\alpha(\text{on TOC}) = \frac{2.33(0.82)}{14.76} = 0.129$$

$$E_\nu = \frac{It}{60} = \frac{(0.375)(11.1)}{60} = 0.0694$$

$$E_{\nu S} = \frac{E_\nu}{\Delta S(10^{-3})} = \frac{0.0694\ (1000)}{0.090} = 771$$

$$E_{\nu TOC} = \frac{E_\nu}{\Delta TOC(10^{-3})} = \frac{(0.0694)10^3}{0.82} = \frac{69.4}{0.82} = 84.6$$

$$\eta_{TOC} = \frac{\Delta\ TOC}{B_c E_\nu t} = \frac{0.82}{(14.76)(0.0694)(11.1)} = 0.0721$$

Values of these parameters for all conditions are summarized in Table 17.

3. Chloroform Destruction in Purified Water

Example: (CFM in purified water)

$I = 0.184,\ (\dot{m}_B/V) = 0.733,\ t = 12.0,\ S_o = 0.100$

$\Delta S = 0.090,\ \ell n\ S_o/S = 2.303$

$B_c = 0.733(12.0) = 8.80$

$b_a = (8.80/0.090) = 97.8$

TABLE 17. SUMMARY DATA ANALYSIS, TCE DESTRUCTION IN LAKE WATER (A)

					- Based on S -				- Based on TOC -				
I	$(\frac{\dot{m}_B}{V})$	t	B_c	$(\frac{TOC}{TOC_o})$	b_a	K_u	α	$E_{\nu S}$	b_a	K_u	α	$E_{\nu TOC}$	η
(watts/ℓ)	(mgO$_3$/min)	(min)	(mgO$_3$/ℓ)		(mgO$_3$/mgΔA)	(watts/ℓ)$^{-1}$							
0.084	1.33	20.3	27.0	0.92	300	1.02	0.00386	316	78.5	0.0367	0.0297	34.6	0.0221
	0.775	29.5	22.9	0.91	254	1.20	0.00456	459	59.2	0.0490	0.0394	50.4	0.0139
	0.510	40.4	20.6	0.91	229	1.33	0.00505	629	53.2	0.0545	0.0438	69.0	0.0082
	0.295	52.9	15.6	0.93	173	1.76	0.00665	823	51.8	0.0554	0.0450	90.4	0.0049
	0.11	72.3	8.0	-	89	3.12	0.0131	1124	-	-	-	-	-
0.189	1.33	14.6	19.4	0.87	216	0.628	0.00855	511	34.7	0.0380	0.0671	56.1	0.0429
	0.775	22.1	17.1	0.86	190	0.713	0.00610	773	28.4	0.0467	0.0820	84.9	0.0229
	0.480	29.3	14.1	0.87	157	0.863	0.00740	1026	25.2	0.0523	0.0924	113	0.0147
	0.230	41.0	9.4	0.91	104	1.30	0.0111	1436	24.3	0.0531	0.0959	158	0.0078
	0.10	51.7	5.2	0.94	58	2.35	0.0202	1811	20.2	0.0630	0.1156	199	0.0059
0.375	1.33	11.1	14.76	0.81	164	0.416	0.00706	771	18.1	0.0382	0.129	84.6	0.0721
	0.775	16.2	12.5	0.81	139	0.492	0.00805	1165	15.3	0.0450	0.152	124	0.0400
	0.420	23.0	9.7	0.83	108	0.633	0.0108	1597	13.3	0.0512	0.176	175	0.0256
	0.260	28.2	7.3	0.84	81	0.842	0.0142	1958	10.6	0.0637	0.220	215	0.0262
	0.096	37.3	3.6	0.92	40	1.56	0.0292	2590	10.5	0.0618	0.223	284	0.0110
						<1.22>				<0.0506>			

Constants for this Data Set: b' = 1.158, S_o = 0.100 mg/ℓ, S = 0.090 mg/ℓ, ℓn S_o/S = 2.303

For TOC: TOC_o = 4.3 mg/ℓ, b' = 2.33

$$K_u = \frac{\ell n\ S_o/S}{I(B_c/B^o)} = \frac{2.303}{(0.184)(8.80)} = 1.42$$

$$\alpha = \frac{b'\Delta S}{B_c} = \frac{(1.004)(0.090)}{(8.80)} = 0.0103$$

$$E_\nu = \frac{(0.184)(12.0)}{60} = 0.0368$$

$$E_{\nu A} = \frac{E_\nu}{\Delta S(10^{-3})} = \frac{0.0368}{(0.090 \times 10^{-3})} = 409$$

$$\eta = \frac{\Delta S}{B_c E_\nu t} = \frac{0.090}{(8.80)(0.0368)(12.0)} = 0.0232$$

Values of these parameters for all conditions of chloroform in purified water are summarized in Table 18.

4. Chloroform Destruction in Lake Water (A)

Example:

$I = 0.375$, $(\dot{m}_B/V) = 1.33$, $t = 171$ min, $S_o = 0.100$,

$\Delta S = 0.090$, $(\ell n\ S_o/S) = 2.303$, $TOC_o = 413$,

$(TOC/TOC_o) = 0.037$; $\Delta TOC = 4.14$

$$B_c = (\dot{m}_B/V)t = 1.33(171) = 227$$

$$b_a(\text{on S}) = (B_c/\Delta S) = (227/0.090) = 2522$$

$$b_a(\text{on TOC}) = (B_c/\Delta TOC) = (227/4.14) = 54.8$$

$$K_u(\text{on S}) = \frac{\ell n\ S_o/S}{I(B_c/B^o)} = \frac{2.303}{(0.375)(227/1)} = 0.0271$$

$$K_u(\text{on TOC}) = \frac{\ell n(TOC_o/TOC)}{I(B_c/B^o)} = \frac{3.297}{0.375(227/1)} = 0.0387$$

TABLE 18. SUMMARY DATA ANALYSIS, CHLOROFORM DESTRUCTION IN PURIFIED WATER

I (watts/ℓ)	$(\frac{\dot{m}_B}{V})$ $(\frac{mgO_3}{min})$	t (min)	B_c $(mgO_3/ℓ)$	b_a $(\frac{mgO_3}{mg\Delta A})$	K_u $(watts/ℓ)^{-1}$	α	$E_{\nu S}$ (watt hrs/ gΔA)	η $(X\ 10^3)$
0.084	0.716	15.4	11.0	122	2.49	0.00910	240	0.0246
	0.545	23.1	12.6	140	2.18	0.00795	359	0.00955
	0.443	31.5	14.0	156	1.96	0.00715	490	0.00463
	0.330	49.2	16.2	180	1.69	0.00600	765	0.00163
0.184	0.733	12.0	8.80	97.8	1.43	0.0103	409	0.0232
	0.545	1818	10.3	114	1.22	0.00880	640	0.00805
	0.483	22.5	10.9	121	1.15	0.00830	767	0.00535
	0.458	24.3	11.2	124	1.12	0.00810	829	0.00444
	0.318	42.1	13.4	149	0.934	0.00675	1435	0.00124
0.417	0.625	12.5	7.69	85.4	0.718	0.0118	950	0.0108
	0.477	18.4	8.78	97.6	0.629	0.0103	1421	0.00436
	0.364	27.7	10.1	112	0.547	0.00895	2140	0.00167
	0.238	52.1	12.4	138	0.445	0.00725	4020	0.00385
					<1.27>			

Constants for this Data Set: $b' = 1.004$, $S_o = 0.100$ mg/ℓ, $\Delta S = 0.090$ mg/ℓ, $\ln(S_o/S) = 2.303$

$$\alpha(\text{on S}) = \frac{b'\Delta S}{B_c} = \frac{(1.004)(0.090)}{227} = 0.000398$$

$$\alpha(\text{on TOC}) = \frac{(2.33)(4.14)}{227} = 0.0425$$

$$E_\nu = \frac{It}{60} = \frac{(0.375)(171)}{60} = 1.069$$

$$E_{\nu S} = \frac{E_\nu}{\Delta S(10^{-3})} = \frac{1.069}{(0.090 \times 10^{-3})} = 11{,}880$$

$$E_{\nu TOC} = \frac{E_\nu}{\Delta(TOC)10^{-3}} = \frac{1.069}{(4.14 \times 10^{-3})} = 258$$

$$\eta_{TOC} = \left(\frac{\Delta\ TOC}{B_c\ E_\nu t}\right) = \frac{60(\Delta TOC)}{B_c\ I\ t^2} = \frac{(60)(4.14)}{(227)(0.375)(171)^2} = 0.98 \times 10^{-4}$$

Values of these parameters for all conditions of chloroform in lake water are summarized in Table 19.

5. Bromodichloromethane Destruction in Lake Water (A)

Example:

$I = 0.375$, $(\dot{m}_B/V) = 1.33$, $t = 62.2$ min,

$S_o = 0.100$ mg/ℓ, $\Delta S = 0.090$; $TOC_o = 4.3$,

$(TOC/TOC_o) = 0.305$, $\Delta TOC = 0.695(4.3) = 2.99$

$$B_c = (1.33)(62.2) = 82.7$$

$$b_a(\text{on S}) = (B_c/\Delta S) = (82.7/0.090) = 920$$

$$b_a\ (\text{on TOC}) = (B_c/\Delta TOC) = (82.7/2.99) = 27.7$$

$$K_u(\text{on S}) = \frac{\ell n\ S_o/S}{I(B_c/B^o)} = \frac{2.303}{(0.375)(82.7/1)} = 0.0743$$

TABLE 19. SUMMARY DATA ANALYSIS, CHLOROFORM IN LAKE WATER

					- Based on S -				- Based on TOC -				
I	$(\frac{\dot{m}_B}{V})$	t	B_c	$(\frac{TOC}{TOC_o})$	b_a	K_u	α	E_ν	b_a	K_u	α	$E_{\nu TOC}$	η
		(min)					$(\times 10^5)$	$(\times 10^{-4})$					$(\times 10^4)$
0.189	1.33	182	242.1	0.17	2,680	0.0503	7.46	3.19	67.8	0.0387	0.0344	161	1.41
	0.775	235	182.1	0.20	2,024	0.0669	9.94	4.11	52.9	0.0468	0.0440	215	1.09
	0.454	298	135.3	0.26	1,504	0.0900	13.4	5.22	42.5	0.0527	0.0548	295	0.840
	0.260	376	97.8	0.35	1,086	0.125	18.5	6.58	35.0	0.0568	0.0667	423	0.643
	0.113	510	57.6	0.52	640	0.257	31.4	8.93	27.9	0.0601	0.0833	7	0.437
0.375	1.33	171	227.7	0.037	2,522	0.0270	39.8	1.19	54.8	0.0387	0.0424	258	0.998
	0.775	216	167.7	0.053	1,864	0.0366	10.8	7.50	41.2	0.0467	0.0566	332	0.832
	0.488	261	127.3	0.084	1,414	0.0482	14.2	9.06	32.3	0.0519	0.0721	414	0.732
	0.260	329	85.4	0.160	948	0.0719	21.2	11.4	23.6	0.0572	0.0984	570	0.625
	0.110	431	47.4	0.340	526	0.130	38.2	14.5	16.7	0.0607		935	0.516
						<0.0903>				<0.0510>			

Constants for this Data Set: $b' = 1.004$, $S_o = 0.100$ mg/ℓ, $\Delta S = 0.090$ mg/ℓ, $\ell n(S_o/S) = 2.303$

For TOC: $TOC_o = 4.3$ mg/ℓ, $b' = 2.33$

$$K_u(\text{on TOC}) = \frac{\ell n\ 4.3/1.31}{(0.375)(82.7/1)} = 0.0383$$

$$\alpha(\text{on S}) = \frac{b'\Delta S}{B_c} = \frac{(0.7324)(0.090)}{82.7} = 0.000796$$

$$\alpha(\text{on TOC}) = \frac{(2.33)(2.99)}{82.7} = 0.0842$$

$$E_\nu = \frac{It}{60} = \frac{(0.375)(62.2)}{60} = 0.389$$

$$E_{\nu S} = \frac{E_\nu}{\Delta S(10^{-3})} = \frac{(0.389)(1000)}{0.090} = 4340$$

$$E_{\nu TOC} = \frac{0.389(1000)}{2.99} = 130$$

$$\eta_{TOC} = \frac{\Delta TOC}{B_c\ E_\nu t} = \frac{(2.99)}{(82.7)(0.389)62.2} = 0.00149$$

Values of these parameters for all conditions are summarized in Table 20.

6. Simultaneous CF, BCM, TCE and TOC Destruction

A composite run was made to determine the simultaneous disappearance of CF, BCM, TCE and TOC in Lake Water (A) at a specified set of run conditions. The results are presented in Table 21. It will be noted that for 90% removal of CF and BDM, ~99% of the other TOC was removed. It appears that the UV-intensity was beyond the optimum, permitting greater reduction of other TOC than is necessary, cf. lower I-value, to get the desired 90% reduction of the micropollutants.

TABLE 20. SUMMARY DATA ANALYSIS, BROMODICHLOROMETHANE DESTRUCTION IN LAKE WATER (A)

					- Based on S -				- Based on TOC -				
I	$(\frac{\dot{m}_B}{V})$	t	B_c	$(\frac{TOC}{TOC_o})$	b_a	K_u	α	E_ν	b_a	K_u	α	$E_{\nu TOC}$	η
watts/ℓ	$(\frac{mgO_3}{min})$	(min)	$(\frac{mgO_3}{\ell})$				$(X\ 10^3)$						$(X\ 10^3)$
0.189	1.33	93.6	124.5	0.407	1383	0.0979	0.530	3276	48.8	0.0382	0.0497	116	0.740
	0.80	123.8	99.1	0.440	1101	0.123	0.665	4333	41.1	0.0438	0.0567	162	0.500
	0.53	148.6	78.7	0.471	874	0.155	0.838	5201	34.7	0.0506	0.0672	206	0.410
	0.30	178.5	53.6	0.572	596	0.227	1.230	6248	29.1	0.0551	0.0800	306	0.340
0.375	1.33	62.2	82.8	0.305	920	0.0742	0.796	4340	27.7	0.0383	0.0842	130	1.49
	0.80	70.4	46.3	0.379	626	0.109	1.171	4889	21.1	0.0460	0.1105	165	1.53
	0.53	73.5	40.0	0.466	444	0.153	1.648	5243	17.4	0.0509	0.1340	205	1.61
	0.30	80.5	24.2	0.607	269	0.254	2.724	5590	14.3	0.0550	0.1627	298	1.72
						<0.149>				<0.0472>			

Constants for this Data Set: $b' = 0.7324$, $S_o = 0.100$ mg/ℓ, $\Delta S = 0.090$, $\ell n\ S_o/S = 2.303$

For TOC: $TOC_o = 4.3$ mg/ℓ, $b' = 2.33$

TABLE 21. COMPOSITE RUN, CF, BCM AND TCE IN LAKE WATER (A)

t (min)	B_c (mg O_3/ℓ)	C/C_o	K_u	(C/S)	(D/D_o)	K_u	(D/S)	(E/E_o)	K_u	(E/S)	(A/A_o)	α
0	0	1.00	-	0.0222	1.000		0.0222	1.000		0.0043	1.000	-
4.75	47.5	0.700	0.0189	0.0450	0.733	0.0165	0.0475	0.123	0.111	0.00158	0.490	0.108
9.67	96.7	0.484	0.0189	0.0935	0.518	0.0171	0.100	(0.0141)	0.111	0.00054	0.234	0.079
15.5	155	0.253	0.0223	0.181	0.257	0.0221	0.184	-			0.0977	0.058
20.0	200	0.178	0.0217	0.349	0.166	0.0226	0.326	-			0.0498	0.048
25.0	250	0.126	0.0209	0.756	0.115	0.0218	0.930	-			0.0235	0.039
30.3	303	0.0969	0.0194	1.90	0.0814	0.0209	1.60	-			0.0106	0.0330
35.4	354	0.0761	0.0183	4.70	0.0635	0.0196	3.92	-			0.0049	0.0282
41.4	414	0.0641	0.0167		-			-				
45.6	456	0.0433	0.0173		-			-				
51.2	512	0.0404	0.0158		-			-				
			<0.0190>			<0.0201>			0.111			

$$\left(\frac{TOC}{TOC_o}\right) = \frac{A}{A_o} = \exp[-0.0378IB_c] = \exp[-0.0150B_c]$$

Gas Flow = 0.666 ℓ/min @ 23°C, $\dot{m}_B/V$ = 10 mg/ℓ min, I = 0.397 watts/ℓ

C_o(CF) = 0.100 mg/ℓ, D_o(BCM) = 0.100 mg/ℓ, E_o(TCE) = 0.020 mg/ℓ; A_o(TOC) = 4.30; S_o = 4.51

7. THM Precursor Destruction in Lake Water (B)

Example:

$I = 0.196$ watts/ℓ, $m_B/V = 2.09$, $t = 60$ min,

$THMP_o \equiv M_o = 0.352$ mg/ℓ, $M/M_o = 0.04$; $TOC_o = 8.7$ mg/ℓ,

$b' = 3.98$, $TOC/TOC_o = 0.416$

$$B_c = (2.09)(60) = 125$$

$$b_a = B_c/\Delta M = 125/0.96(0.352) = 370$$

$$b_a(\text{on TOC}) = B_c/\Delta TOC = 125/0.584(8.7) = 24.6 \text{ mgO}_3/\text{mg}\Delta TOC$$

$$K_u(\text{on M}) = \frac{\ell n\ M_o/M}{I\ B_c/B^o} = \frac{3.219}{(0.196)(125)} = 0.313$$

$$K_u(\text{on TOC}) = \frac{\ell n\ TOC_o/TOC}{I\ B_c/B^c} = 0.0220$$

$$\alpha(\text{on TOC}) = \frac{b'\Delta TOC}{B_c} = \frac{(3.98)0.584(8.7)}{125} = 0.162$$

$$E = (\frac{It}{60}) = \frac{(0.196)(60)}{60} = 0.196 \text{ watt hrs/}\ell$$

$$E_{\nu M} = \frac{E_\nu}{\Delta M(10^{-3})} = \frac{0.196}{(0.96)(0.352)(10^{-3})} = 580\ (\frac{\text{watt hrs}}{\text{g}})$$

$$E_{\nu TOC} = \frac{0.196}{(0.584)(8.7)10^{-3}} = 38.6\ (\frac{\text{watt hrs}}{\text{g}})$$

$$\eta_{TOC} = \frac{\Delta TOC}{B_c E_\nu t} = \frac{(0.584)(8.7)}{(125)(0.196)(60)} = 0.00346$$

Values of these parameters for all conditions are summarized in Table 22.

TABLE 22. SUMMARY OF DATA ANALYSIS, THMP DESTRUCTION IN LAKE WATER (B)

I	$(\frac{\dot{m}_B}{V})$	t	B_c	(M/M_o)	b_a	K_u	$E_{\nu M}$	$(\frac{TOC}{TOC_o})$	α	$E_{\nu TOC}$	η
(watts/ℓ)	$(\frac{mgO_3/\ell}{min})$	(min)	(mgO_3/ℓ)		($mgO_3/mg\Delta M$)		(watt hrs/g)				
0.096	2.23	60	140	0.09	466	0.179	320	0.516	0.120	22.8	0.00522
	4.00	60	240	0.09	799	0.105	320	0.436	0.081	19.6	0.00355
	6.36	45	286	0.01	875	0.168	220	0.412	0.071	14.1	0.00552
0.196	2.09	60	125	0.04	370	0.131	580	0.416	0.162	38.6	0.00346
	4.18	45	188	0.10	633	0.0625	619	0.429	0.105	29.6	0.00399
	6.36	30	191	0.16	689	0.0490	354	0.530	0.085	84.0	0.00728
0.40	2.18	45	98.1	0.03	306	0.0894	937	0.415	0.171	59.0	0.00384
	4.09	30	123	0.12	424	0.0431	689	0.521	0.135	48.0	0.00565
	6.18	20	124	0.14	437	0.0396	470	0.745	0.071	60.1	0.00671
						<0.0963>					

Constants for this Data Set: THMP ≡ M; $\langle M \rangle = 0.330$ mg/ℓ

For TOC: $TOC_o = 8.7$ mg/ℓ; $b' = 3.98$

C. REACTION RATES FOR MIXTURES

Examination of the data in Tables 16 to 22 incl. indicates a substantial difference in the rate constants in lake water compared to in purified water. Also, a substantial reduction in other organic carbon is necessary to reduce the micropollutants to the desired level of 90% removal. Obviously, all oxidizable species present are oxidized to some extent and thereby exert an ozone demand. By choice, the experimental work tracked the disappearance of TOC, the micropollutants, and the THM precursors, but not any inorganic species.

A model is needed which will account for the simultaneous disappearance of TOC as well as the other species of primary interest. Tables 23 and 24 present the laboratory data obtained for TOC reduction. The most complete set is for Cross Lake water giving values for ozone supply rate as well as at three levels of UV-intensity. Several striking features of the data will be noted.

1) - the O_3 utilization values, α, are quite low, and are not constant at different O_3 supply rates. α-values increase with increasing UV-intensity, but decrease with increasing ozone supply rate. Concerning the latter, it is true that increasing the O_3 supply rate without limit would lead to decreased α; however, over the operating range used, it is not clear, at the outset, why this decrease should occur. Mass transfer calculations presented later are revealing.

2) - the rate constants, calculated by $\ell n(A_o/A)/(B_c/B^o)$ vary somewhat for different supply rates, primarily because the ozone utilization is not the same.

Using the two sets of data, the constants were determined for the following functions:

$$\ell n(A_o/A) = \left(\frac{K_o}{A^o B^o}\right)\left(1 + \frac{K_u^+}{K_o} I^n\right) B_c = \frac{K_A}{A^o}(B_c/B_o) \qquad (10a)$$

$$K_A = K_o\left(1 + \frac{K_u^+}{K_o} I^n\right) \qquad (10b)$$

and for the reactor used, $\alpha = \alpha_o\left(1 + \frac{K_u^+}{K_o} I^n\right)$. (10c)

TABLE 23. TOC DISAPPEARANCE, CROSS LAKE WATER

I	$(\frac{\dot{m}_B}{V})$	$(\frac{\ln A_o/A}{t(\min)}) \times 10^3$	$(\frac{\ln A_o/A}{B_c/B^o})$	α $(\text{at} \frac{A}{A_o} = 0.40)$
0	2.00	3.39 ± 0.031	0.00170	0.0385
	4.00	6.54 ± 0.030	0.00164	0.0372
	6.00	6.70 ± 0.076	0.00112	0.0254
			<0.00149>	<0.0377>
0.096	2.23	11.1 ± 0.04	0.00498	0.113
	4.00	13.8 ± 0.30	0.00345	0.0783
	6.36	15.4 ± 0.80	0.00242	0.0549
			<0.00372>	<0.0820>
0.196	2.09	11.0 ± 0.70	0.00526	0.119
	4.18	13.4 ± 1.10	0.00321	0.0728
	6.36	17.1 ± 0.80	0.00269	0.0610
			<0.00372>	<0.0843>
0.400	2.18	17.8 ± 0.60	0.00817	0.185
	4.09	16.8 ± 1.3	0.00411	0.0932
	6.18	20.1 ± 0.60	0.00325	0.0739
			<0.00518>	<0.1174>

Correlation Constants: $K_o = 0.00149$; $K_u^+/K_o = 5.54$; $n = 0.842$, $r = 0.996$, $\alpha_o = 0.0380$, $A \equiv \text{TOC}$

And the differential rate equation becomes,

$$\frac{d\ln A_o/A}{dt} = -\frac{1}{A}\left(\frac{dA}{dt}\right) = \frac{K_o}{A^o B^o}\left(1 + \frac{K_u^+}{K_o} I^n\right)\left(\frac{\dot{m}_B}{V}\right)$$

$$-\dot{A} = K_o\left(1 + \frac{K_u^+}{K_o} I^n\right)\left(\frac{\dot{m}_B}{VB^o}\right)\left(\frac{A}{A^o}\right) = K_A\left(\frac{\dot{m}_B}{VB^o}\right)\left(\frac{A}{A^o}\right) \qquad (10d)$$

TABLE 24. TOC DISAPPEARANCE, LEWISVILLE LAKE WATER

I	B_c	(A/A_o)	$\langle\alpha\rangle$	$\left(\frac{\ln A_o/A}{B_c/B^o}\right)$	$\left(\frac{\ln A_o/A}{\alpha B_c/B^o}\right)$
0.084	20	0.915	0.0425	0.00444	0.105
	40	0.835	0.0413	0.00450	0.109
	52	0.800	0.0385	0.00427	0.111
			<0.0408>	<0.00440>	<0.108>
0.189	20	0.800	0.100	0.0112	0.112
	60	0.625	0.0626	0.00783	0.125
	100	0.340	0.0661	0.0108	0.163
	140	0.255	0.0533	0.00975	0.183
			<0.0705>	<0.00990>	<0.146>
0.375	20	0.620	0.240	0.0239	0.0996
	60	0.257	0.124	0.0226	0.183
	100	0.127	0.0875	0.0207	0.236
	120	0.092	0.0758	0.0199	0.262
			<0.132>	<0.0218>	<0.195>

Constants: $K_o = 0.0010$; $\frac{K_u^+}{K_u} = 47.7$; $n = 1.00$; $r = 0.997$; $\alpha_o = 0.048$

$A \equiv \text{TOC}$

The effect of UV-input shows up in the model as the K_u^+/K_o ratio and the exponent "n" on the intensity. One would expect K_u^+/K_o to be several-fold to many-fold greater than unity, and "n" to be in the range 1/2 to 3/2.

A composite model for all organic components including TOC can be constructed in the following manner; the components are defined for convenience as,

$S \equiv$ total organic substrate components
$A \equiv$ other organic carbon components
$B \equiv$ ozone
$C \equiv$ chloroform (CF)
$D \equiv$ bromodichloromethane (BDM)
$E \equiv$ tetrachloroethylene (TCE)
$M \equiv$ trihalomethane precursors (THMP)

Then for CF, BCM and TCE in Lewisville Lake water,

$$\begin{array}{ccccccccc} S & = & A & + & C & + & D & + & E \\ (4.52\ \mathrm{mg}/\ell) & & (4.3) & & (0.100) & & (0.100) & & (0.020) \end{array} \tag{11a}$$

Assuming simultaneous disappearance of all components,

$$\dot{S} = \dot{A} + \dot{C} + \dot{D} + \dot{E} \tag{11b}$$

$$-\dot{S} = K_A(\dot{m}_B/VB^o)(A/A^o) + K_C(\dot{m}_B/VB^o)(C/C^o) + K_D(\dot{m}_B/VB^o(D/D^o)$$

$$K_E(\dot{m}_B/VB^o)(E/E^o) \tag{11c}$$

$$-\dot{S} = (\dot{m}_B/VB^o)[K_A(A/A^o) + K_C(C/C^o) + K_D(D/D^o) + K_E(E/E^o)]$$

Dividing by S,

$$-\frac{\dot{S}}{S} = (\dot{m}_B/VB^o)\ [\frac{K_A}{A^o}\ \frac{A}{S} + \frac{K_C}{C^o}\ \frac{C}{S} + \frac{K_D}{D^o}\ \frac{D}{S} + \frac{K_E}{E^o}\ \frac{E}{S}] \tag{11d}$$

Integrating,

$$-\int_{S_o}^{S} \frac{dS}{S} = (\dot{m}_B/VB^o)\frac{t}{t}\ (\frac{K_A}{A^o})\int_o^t \frac{A}{S}\,dt + \ldots\ ) \tag{11e}$$

$$\ell n\ (\frac{S_o}{S}) = (B_c/B^o)\ \ [(\frac{K_A}{A^o t}\int_o^t (\frac{A}{S})dt + \ldots] \tag{11f}$$

and as an approximation,

$$\simeq K_A(\cdot\frac{B_c}{A^o B^o})\ \ [1 + (\frac{K_C}{K_A})\ \frac{1}{t}\int_o^t (\frac{C}{S})dt + \ldots] \tag{11g}$$

where the total rate constant K_A breaks down into the two parts, for ozone only and ozone-UV, as shown by Equation 10b.

By the mean-value theorem, the mean value of C/S over the time interval involved is,

$$\langle\frac{C}{S}\rangle = \frac{1}{t}\int_{o}^{t} (\frac{C}{S})\,dt = \frac{1}{B_c}\int_{o}^{B_c} (\frac{C}{S})\,dB_c \tag{11h}$$

Obviously, if the rate of disappearance of S is greater than C, then the ratio C/S will increase, going from a low initial value to a high value, perhaps approaching unity. Actual values are shown in Table 21 for the three components.

The final model involves three equations; one for the total disappearance of S, a second for the disappearance of the component requiring the longest time to attain the desired reduction, and the third is Equation 10b, giving:

$$\ln(\frac{S_o}{S}) = K_A(\frac{B_c}{A^oB^o})[1 + \sum_i (\frac{K_{Ci}}{K_A}) \frac{Ci}{S}] \tag{11i}$$

$$\ln(\frac{C_o}{C}) = K_C(I)\ (B_c/A^oB^o) \tag{11j}$$

In order to use the equations, values for the rate constant ratios and concentration ratios are required. For the micropollutants values are presented in Table 25. It will be noted that the rate constant ratios are for the most part substantially greater than unity; however, since the concentrations are very low, the rate of removal is low cf. TOC removal. The rate limiting component is chloroform, requiring 60-90% removal of TOC.

For removal of THMP (≡M) the equation is,

$$\ln(\frac{S_o}{S}) = K_A(\frac{B_c}{A^oB^o})\ [1 + (\frac{K_M}{K_A})\ \langle\frac{M}{S}\rangle] \tag{11k}$$

and the values of the rate constant ratio and the concentration ratio are given in Table 26. In this case, it will be noted that these ratios are essentially constant over a wide range of ozone supply rates and UV-intensities. In order to get 90% removal of THMP, approximately 50% removal of the TOC was necessary.

TABLE 25. REACTION PARAMETERS, MICROPOLLUTANTS IN LAKE WATER (A)

Component	I	B_C	K	$<\frac{Comp}{S}>$	$<\frac{TOC}{TOC_o}>$	K_A	$(\frac{K}{K_A})$	$<\alpha>$
TCE (E)	0.084	8.0 ⟶ 27.0	K_E 0.000	0.00257	0.92	0.00411	27.0	0.0395
	0.189	5.2 ⟶ 19.4	0.221	0.00259	0.87	0.00956	23.1	0.0906
	0.357	3.6 ⟶ 14.8	0.296	0.00260	0.84	0.0195	15.2	0.128
	0.397	97	0.0441	0.00301	0.30	0.0224	1.97	0.130
CF (C)	0.189	58 ⟶ 242	K_C 0.0223	0.00309	0.30	0.00947	2.35	0.0566
	0.375	47 ⟶ 228	0.0235	0.00410	0.13	0.0191	1.23	0.0674
	0.397	250	0.00754	0.241	0.004	0.0224	0.337	0.0400
BCM(D)	0.189	54 ⟶ 125	K_D 0.0285	0.0138	0.47	0.00886	3.22	0.0634
	0.375	24 ⟶ 83	0.0555	0.0140	0.44	0.0179	3.10	0.123
	0.397	250	0.00798	0.268	0.004	0.0224	0.356	0.0400

TABLE 26. REACTION PARAMETERS, THMP IN LAKE WATER (B)

I	$(\dot{m}_B/V)$	(M/M_o)	K_M	A/A_o	K_A	K_M/K_A	$<M/A>$	α
0.096	2.23	0.09	0.0172	0.516	0.00498	3.45	0.0223	0.120
	4.00	0.09	0.0101	0.436	0.00345	2.93	0.0229	0.081
	6.36	0.01	0.0161	0.412	0.00242	6.65	0.0194	0.071
0.196	2.09	0.04	0.0257	0.416	0.00526	4.89	0.0208	0.162
	4.18	0.10	0.0123	0.429	0.00321	3.83	0.0234	0.105
	6.36	0.16	0.00960	0.530	0.00269	3.57	0.0247	0.085
0.400	2.18	0.03	0.358	0.415	0.00817	4.38	0.0203	0.171
	4.09	0.12	0.0172	0.521	0.00411	4.18	0.0233	0.135
	6.18	0.14	0.0158	0.745	0.00325	4.86	0.0225	0.071
		<0.087>		<0.491>		<4.30>	<0.0222>	

THMP ≡ M, $<M_o> = 0.330$ mg/ℓ, TOC ≡ A; $A_o = 8.7$ mg/ℓ; $M_o/A_o = 0.0379$

D. REACTOR DYNAMICS -- MASS AND ENERGY TRANSFER

There are numerous aspects of "reactor dynamics" involved in the scale-up from laboratory scale experiments to full-scale design. In this instance, the laboratory work was carried out in a 3.0 liter (0.106 ft^3) liquid volume reactor; whereas the full-scale reactors will be in the range of 100 to 1000 ft^3 liquid volume. For various gas and liquid flow rates, and stirring rates, the following considerations enter into the dynamical problems involved:

1) the mixing patterns, degree of mixing, and power input;
2) the mass transfer of O_3 from gas phase to liquid phase;
3) the mass transfer of volatile components from liquid phase to gas phase; and
4) the energy (UV-range) transfer across semi-transparent boundaries into the liquid.

The reactor used in the experiments is described in the first part of the report and can be compared to the standard reactor configuration, described previously and used by others [2,8]. A comparison of the dimensional ratios, laboratory reactor vs. standard reactor is made in Table 27.

TABLE 27. COMPARISON OF REACTOR DIMENSIONS

Dimensional Ratio	Lab Reactor	Standard Reactor
H/D_T	1.11	1.00
D_I/D_T	0.547	0.333
w_b/D_T	0.135	0.100
h/D_I	0.222	0.200
b/D_I	0.395	0.25
H_I/D_I	1.21	1.00
H_S/H	0.39	0
Average gas path length	12 cm	30 cm*

*For engineering laboratory reactor [2,8]

In the standard reactor, the gas is introduced through a sparger located at the bottom of the reactor. Whereas, in the lab reactor used, the sparger was located at approximately 0.50 D_T above the bottom, thereby reducing the gas path length significantly.

Also, the UV radiators were externally located for the lab reactor used. Whereas, in a standard reactor of engineering scale and above, the radiators are inside the reactor, mounted axially in the horizontal plane quadrants, thereby giving significantly greater UV-radiation transfer into the liquid. However, for the lab reactor the photon transfer was actually determined by directly measured actinometry experiments.

Mixing Variables

In order to produce the necessary mixing patterns for complete mixing, good UV-energy transfer, and high interfacial area for mass transfer, the following are required for a standard reactor,

$$N_R(\text{Reynolds number}) \equiv \left(\frac{D_I^2 N \rho}{\mu}\right) = 10^4 \rightarrow 10^7 \qquad (12a)$$

$$N_g(\text{gas flow number}) \equiv (100\ Q/D_I^3 N) = 1 \rightarrow 10 \qquad (12b)$$

$$P(\text{Power input}) = 1 \rightarrow 10 \text{ horsepower/1000 gals} \qquad (12c)$$

The Bates and Moo-Young [9,10] correlations can be combined to obtain the power input for the above range of N_R and N_g.

$$P = \left(\frac{0.679\ \rho_L D_I^5 N^3}{g_c V}\right) N_R^{0.045}\ f(N_g),\ (\text{HP/1000 gal}) \qquad (12d)$$

$$f(N_g) = 0.45 \exp\left(\frac{-0.413}{N_g}\right) + \exp(-0.525\ N_g) \qquad (12e)$$

Example Calculation -- values of the above parameters can be calculated for a typical run of the lab reactor.

$$D_I = \left(\frac{8.1}{30.48}\right) = 0.266 \text{ ft},\ N = 300 \text{ rpm},\ Q = \frac{0.323}{(28.32)60} = 1.90\times 10^{-4}\left(\frac{\text{ft}^3}{\text{sec}}\right)$$

$$V = 3.00/28.32 = 0.106 \text{ ft}^3.$$

$$N_R = \frac{(0.266)^2(300/60)(62.2)}{(6.38 \times 10^{-4})} = \underline{3.45} \times 10^4$$

$$N_g = \frac{100(1.90 \times 10^{-4})}{(0.266)^3(300/60)} = \underline{0.202}$$

$$f(N_g) = 0.45 \exp(\frac{-0.413}{0.202}) + \exp(-0.525)(0.202) = \underline{0.958}$$

$$P = [\frac{(0.679)(62.2)(0.266)^5(300/60)^3}{(32.2)(0.106)}] (3.45 \times 10^4)^{0.045}(0.958)$$

$$= 3.15 \text{ (HP/1000 gals)}$$

The calculation indicates a low gas flow number, and hence gas velocity, as compared to an engineering scale or full scale reactor, which would operate at 10 to 100 times greater N_g-values

Ozone Mass Transfer

Ozone, like oxygen, is relatively insoluble in water. Maximum liquid phase concentrations at room temperature depend on the gas phase concentration and lie in the range of 1 → 20 mg/ℓ. Henry's law provides the equilibrium relationship,

$$\frac{y_B}{X_B} = \frac{H_B}{P} = \frac{\gamma_B \rho_B^{\neq}}{P} \tag{13a}$$

H_B, the Henry's law constant being of the order of 10^4. Therefore, the overall mass transfer coefficient,

$$\frac{1}{K_L} = \frac{1}{k_L} + \frac{1}{H_B k_g} \simeq \frac{1}{k_L} \ ; \quad K_L = k_L \tag{13b}$$

is liquid side controlled; hence the ozone mass transfer can be described by,

$$(\frac{\dot{m}_B}{V})_{max} = k_L a(C_B^* - C_B) = k_L a(X_B^* - X_B) \tag{13c}$$

For a given situation of flow, etc., equation (13c) determines the upper limit of O_3 transfer into the liquid. If the actual supply rate, $(\dot{m}_B/V)$, is less, all will be transferred; but if greater, some of the O_3 will remain in the bubbles and bypass the liquid, flowing out the top of the reactor.

Ozone mass transfer coefficients have been determined and correlated by Yocum [11] for a standard reactor configuration of engineering laboratory scale. His data gave the relationship,

$$k_La = 6.85\ u_g^{0.67}\ P^{0.454},\ \left(\frac{\text{lb mols}}{\text{ft}^3\text{min},\Delta X}\right) \tag{13d}$$

which can be normalized by introducing u_g = 0.60 ft/min, and P = 10 HP/1000 gals, giving,

$$k_La = 13.8\ \left(\frac{u_g}{0.60}\right)^{0.67}\ \left(\frac{P}{10}\right)^{0.454} \tag{13e}$$

This equation is consistent with the correlation function found by Prengle and students [12] for O_2 mass transfer in an engineering laboratory scale standard reactor.

$$k_La = 11.0\left(\frac{u_g}{0.60}\right)^{0.41}\left(\frac{P}{10}\right)^{1/2} \tag{13f}$$

The mass transfer coefficients obtained for the lab reactor in this project at various conditions are summarized in Table 28.

Example Calculation -- assume the following set of conditions for the lab reactor:

$\dot{G}$ = 0.323 sℓ/min; w%O_3 = 2.5, $\dot{m}_B$ = 3.99 mg O_3/min

$(\dot{m}_B/V)$ = 1.33 (mgO_3/minℓ). T = 23°C; H = 4.20×10^3 atm.

Other conditions are the same as previous example (p. 152).

$$C_B^* = \left(\frac{w\%\ O_3}{100}\right)\left(\frac{M_{cg}}{M_w}\right)\ \frac{P \cdot 10^6}{H} = \frac{(0.025)(28.9)(1.0 \times 10^6)}{(18)(4.20 \times 10^3)} =$$

$$9.56\left(\frac{\text{mg}O_3}{\ell}\right)$$

$$X^* = \frac{9.56 \times 10^{-3}}{(48)(55.5)} = 3.59 \times 10^{-6} \quad (\frac{\text{g mols } O_3}{\text{g mol water}})$$

$$u_g = \frac{323 \text{ m}\ell\text{/min}}{172 \text{ cm}^2} = 1.88 \text{ cm/min} = 0.0617 \text{ ft/min}$$

Using Yocum's correlation,

$$k_La = 13.8(\frac{0.0616}{0.60})^{0.67} (\frac{3.15}{10})^{0.454} = 1.78(\frac{\text{lb mols}}{\text{ft}^3\text{min}\Delta X})$$

$$= 28.6 \ (\frac{\text{g mols}}{\ell\text{min } \Delta X})$$

We note from Table 2 8 that the value for the lab reactor be approximately 5 → 6.

Now we can calculate the O_3 transferred and compared with the supply rate,

$$(\dot{m}_B/V)_L = (48 \times 10^3)k_La(X^* - X) = (48 \times 10^3)(6)(3.59 \times 10^{-6})$$

$$= 1.03 \ (\frac{\text{mgO}_3}{\text{min } \ell}) \ \underline{\text{cf}}.\ 1.33(\frac{\text{mgO}_3\text{supplied}}{\text{min } \ell})$$

Defining, N_B(O_3 mass transfer number) $\equiv (\frac{k_La\ X^*}{\dot{m}_B/V})$ (13g)

Then, $N_B = (1.03/1.33) = 0.774$

Since $N_B < 1$, not all the ozone was transferred into the liquid phase in the lab reactor, for this case.

Table 2 8 also shows the N_B-values for the cases listed plus four calculated cases which fall in the range of the operating conditions used, indicating that in numerous instances mass transfer was not complete.

Ozone Utilization

Since we are dealing with a heterogeneous process, gas to liquid transfer followed by reaction in the liquid phase, reactor dynamics enter into the efficiency of utilization of ozone. This fact has been amply demonstrated previously [13].

TABLE 28. SUMMARY OF O_3 MASS TRANSFER COEFFICIENTS AND TRANSFER NUMBERS

Gas Rate	O_3 Rate	u_g	N	k_a/K_La	$<k_La>$		k_LaX^*	N_B
(mℓ/min)	(mg/min ℓ)	(cm/min)	(rpm)		$(\frac{\text{g mols}}{\ell \text{min} \Delta X})$	$(\frac{\text{lb mols}}{\text{ft}^3 \text{min} \Delta X})$	$(\frac{\text{mgO}_3}{\text{min } \ell})$	
25.0	0.47	0.145	300	1.98	4.44	0.277	0.765	1.76
200	3.82	1.16	500	2.22	7.75	0.483	1.34	0.350
200	2.86	1.16	500	2.60	5.73	0.357	0.987	0.345
200	1.75	1.16	500	2.43	9.95	0.621	1.71	0.977
200	0.954	1.16	500	2.15	8.11	0.506	1.40	1.47
1000	7.2	5.8	500		5.30	0.331	0.913	0.127
1000	7.2	5.8	500		28.1	1.75	4.84	0.672
Some other calculated cases -								
323	1.33	1.88	300	-	(6.0)*	-	1.03	0.774
300	6.00	1.74	300	-	(12.0)*	-	2.07	0.345
300	6.00	1.74	300	-	(30.0)*	-	5.17	0.862
666	10.0	3.86	300	-	(30.0)*	-	5.17	0.517

---

*Estimated from the above data.

By decreasing mixing, for both O_3 only and O_3/UV reactions, one can lower the reaction rate, and hence the O_3 utilization value, α, for a given ozone supply rate.

Consider as a point of departure an O_3-only experiment. For a very well mixed complete mass transfer situation, defined by,

$$N_R = 10^4 \rightarrow 10^7,\ N_g = 2 \rightarrow 10,\ P = 5 \rightarrow 10,\ N_B > 1$$

there will be an intrinsic α-value, determined only by chemical reaction rate. In addition, as observed from the data, for UV-input the value of α increases significantly. Consequently, can be represented functionally as,

$$\alpha = f(\alpha_o^+,\ k_L a,\ \dot{m}_B/V,\ I,\ \text{dynamic variables}) \qquad (13h)$$

By equations 13e, 12d and 13g, N_B contains all the dynamical effects and can be expressed as,

$$\alpha = \alpha_o^+ N_B^n (1 + aI^m) \qquad (13i)$$

where, $n \simeq 1/2 \rightarrow 1$, $m = 1/2 \rightarrow 3/2$, and $a \simeq (\frac{K_u^+}{K_o})$

Volatile Components Mass Transfer

Under operating conditions of full-scale equipment, volatile components will be partially desorbed or stripped from the liquid. These components, e.g. chloroform, are much more soluble than substances like oxygen and ozone; and therefore have much smaller Henry's law constants. Consequently, the overall mass transfer coefficient,

$$\frac{1}{K_g} = \frac{H}{k_L} + \frac{1}{k_g} \simeq \frac{1}{k_g};\quad K_g = k_g \qquad (14a)$$

is essentially gas side controlled. The mass transfer can be described by,

$$(\frac{\dot{m}_c}{V}) = k_g a(y_c^* - y_c) \simeq k_g a(\frac{P_c^{\neq}}{P})\ \frac{C}{C_o} \qquad (14b)$$

Data were obtained for chloroform using the lab reactor at different gas velocities and stirring rates. The results are summarized in Table 29. lines 1-6 incl. There is a fair amount of scatter in the mass transfer coefficients, but they can be correlated by functions similar to equations (13e) and (13f); giving,

$$k_g a = 6.20 \times 10^{-6} \left(\frac{u_g}{0.60}\right)^{1.05} \left(\frac{P}{10}\right)^{0.50}, \left(\frac{g \cdot CF}{\min, \ell}\right) \qquad (14c)$$

The magnitude of the values appear to be low, line 7 in Table 29 is a run obtained by Houston Research, Inc. [13] in an engineering laboratory scale reactor which gives a coefficient ∿10.6 times greater.

Therefore, for large scale reactors, the following function is more realistic:

$$k_g a \left(\frac{\text{lbs CF}}{\min \text{ ft}^3}\right) = 4.098 \text{ X } 10^{-6} \left(\frac{u_g}{0.60}\right) \left(\frac{P}{10}\right)^{\frac{1}{2}} \qquad (14d)$$

Example Calculation: Estimate the loss of volatile components by stripping by gas flow through a continuous flow 2000 ft^3 stirred tank reactor, operating at 26°C and with a residence time of ten minutes. Initial concentrations are: CF and BCM = 0.100 mg/ℓ each and TCE = 0.020 mg/ℓ. The total removal of the compounds of interest by oxidation and stripping is 90%.

TABLE 29. CHLOROFORM MASS TRANSFER DATA

Gas Rate (ℓ/min)	u_g		N (rpm)	N_R	N_g	P (HP/1000 gal)	$\left(\frac{g \cdot CF}{\min \ell}\right)$
	(cm/min)	(ft/min)					
1) 0.200	1.16	0.0381	300	3.45×10^{4}	0.125	3.14	0.195×10^{-6}
2)			500	5.75×10^{4}	0.075	15.6	0.499×10^{-6}
3) 0.660	3.84	0.126	300	3.45×10^{4}	0.413	3.20	0.733×10^{-6}
4)			500	5.75×10^{4}	0.248	15.0	0.781×10^{-6}
5) 1.00	5.81	0.191	300	3.45×10^{4}	0.625	3.14	1.82×10^{-6}
6)			500	5.75×10^{4}	0.375	15.2	2.02×10^{-6}
7) 4.00	9.36	0.307	700	7.40×10^{4}	1.22	8.94	31.8×10^{-6}

The gas velocity is 1.5 ft/min and the mixing power is approximately 7.5 HP/1000 gal.

$$k_g a = (4.098 \times 10^{-6})\left(\frac{1.5}{0.60}\right)\left(\frac{7.5}{10}\right)^{\frac{1}{2}} = 8.87 \times 10^{-6}\left(\frac{\text{lbs}}{\text{min ft}^3}\right)$$

$$\Delta m_c = k_g a\, V\left(\frac{p^{\neq}}{P}\right) \frac{\theta}{\theta}\int_0^{\theta} \left(\frac{C}{C^o}\right) d\theta = k_g a\, V\left(\frac{p^{\neq}}{P}\right)\theta \left\langle\frac{C}{C^o}\right\rangle$$

$$= (8.87\text{x}10^{-6})(2\text{x}10^{3})\left(\frac{245}{760}\right)(10)\left(\frac{0.105}{1.00}\right) = 6.00 \times 10^{-3} \text{ lbs. removed}$$

UV-Energy Transfer

The chemical reactions involved are driven by the UV energy input to the liquid. An energy transfer process is involved and must be dealt with, both for the lab reactor used and scale up to full size.

UV-energy (180 to 400 nm) is transferred into the liquid phase from the UV-radiators located in the reactor, or as in the case of the lab reactor, located external to the reactor. Commercially available UV radiators have a total wattage rating, which measures the power requirement, but only a fraction (15-25%) of the total power (w_n) is converted to UV power (w_u), the remaining being primarily infrared and dissipated as heat. The UV-energy must pass through radiator wall, quartz sheath, and reactor walls, whatever the case may be, and thence into the liquid phase -- the rays being of different path lengths (L). The integrated UV intensity in the liquid can be represented by a transfer equation of the form,

$$\underset{\text{(watt UV in liquid/}\ell\text{)}}{I} = \underset{\text{(watts UV from radiators/}\ell\text{)}}{\left(\frac{w_u}{w_n}\right)\cdot\left(\frac{nw_n}{V}\right)} \cdot \underset{\left(\frac{\text{watts UV in liquid}}{\text{watt UV from radiators}}\right)}{K_\nu^*} \tag{15a}$$

$$= \left(\frac{w_u}{w_n}\right)\left(\frac{nw_n}{V}\right)\left(\frac{\tau g}{aL}\right)(1 - e^{-aL}) \tag{15b}$$

K_ν^* being the UV-energy transfer coefficient accounting for geometry (g, L) and attenuation factors (τ,a). The geometric factor g, is determined by the location of the radiators; if located inside the reactor g = 1, but if located externally,

$$g(r,R) = \frac{1}{2}(1 - \frac{2}{\Pi} \sin^{-1} \frac{R}{R+r}) \qquad (15c)$$

The attenuation coefficient for quartz wall [14], $\tau = 0.90$, and for aqueous media, evaluated from experimental data [15], $a = 0.17$ to 0.21.

Consequently for a given reactor, UV-radiators, and geometry, the UV intensity in the liquid can be calculated using equations 15b and 15c. A calculation for the lab reactor is illustrated by the following example.

Example: Calculate the UV-intensity in the liquid for the lab reactor using 4-14 watt bulbs mounted externally, and compare with 1-bulb immersed in the liquid. UV watts equal 18.8% of nominal watts, $\langle L \rangle = 10.5$ cm; assume $a = 0.175$, $\tau = 0.90$.

$$g = \frac{1}{2}(1 - \frac{2}{\Pi} \sin^{-1} \frac{7.4}{10.8}) = 0.260$$

$$K_\nu^* = \frac{\tau g}{aL}(1-e^{-aL}) = \frac{0.90(0.260)}{0.175(10.5)} [1-e^{-0.175(10.5)}] = 0.107$$

$$I = K^* (\frac{w_u}{w_n}) (\frac{nw_n}{V}) =)0.107)(0.188)(4)(14)/3.0 = 0.375 \text{ watts}/\ell$$

For 1-bulb (rather than four) immersed in the liquid.

$$g = 1;\ K_\nu^* = \frac{(1)(1)}{(0.175)(7.4)} \quad 1-e^{-0.175(7.4)} = 0.561$$

$I = (0.561)(0.188)(1)(14)/3.0 = 0.492$ watts/ℓ, approximately 5-1/4 times greater.

Therefore, UV-transfer coefficients have the following approximate values for different scale reactors:

Reactor Scale	Radiators	K_ν^*
Lab	External	0.10
Engr. Lab	Internal	0.50 - 0.60
Industrial	Internal	0.40 - 0.60

E. CONCLUSIONS FROM THE DATA ANALYSIS

As a result of a detailed engineering analysis of the laboratory data, the following conclusions can be drawn.

1. Destruction of tetrachloroethylene in purified water showed relatively high rate constants, but lower O_3-utilization values than would be expected, even with highest UV-intensity. On the other hand, the rate constants in lake water were 5-10 fold less than in purified water, but the O_3-utilization was somewhat greater when other TOC destruction was included; however, the absolute magnitude of total O_3-utilization was still low.

2. Destruction of chloroform in purified water showed factor of 10 lower rate constants than for TCE, and O_3-utilization was very low. In lake water, the rate contants were further reduced by another factor of 10, but total O_3-utilization, including total TOC removal, was higher. However, the absolute magnitude of O_3-utilization was quite low. Substantial removal of TOC, 50-90%, occurred in order to get 90% removal of CF.

3. Destruction of bromodichloromethane in lake water showed low rate constants, low O_3-utilization values, and substantial removal of TOC, 40 to 70%, to obtain 90% removal. O_3-utilization was improved when the TOC destruction was included, but on an absolute basis the values were still quite low.

4. Destruction of trihalomethane precursors in lake water showed low rate constants, approximately the same level as for chloroform, and low O_3-utilization values including TOC removal. TOC removal amounted to approximately 50% to get 90% removal of THMP.

5. The effect of UV-input is substantial in producing higher rates and greater O_3-utilization for both micropollutants and THMP.

6. Insofar as design of full-scale equipment is concerned, the reaction rate data for the micropollutants studied in purified water provide little information. The rate constants are many-fold less in lake water, which is to be expected since numerous components are competing for oxidizer, and furthermore the components, other than the micropollutants, are in greater concentration. Therefore, the crucial factor is the extent to which other TOC must be removed in order to get 90% removal of the micropollutants.

7. The scale of the laboratory reactor was too small to provide data which can be used to scale up to commercial size for the aspects of: O_3-mass transfer, volatile components mass transfer, and UV-energy transfer. In particular, the location of the sparger at 0.50 D_T, and the actual small gas path length, 12 cm, did not provide sufficient contact time for transfer.

8. In general, the dynamical mixing characteristics of the lab reactor appear to be approximately satisfactory. N_R and P fall in the right range, but N_g-values are low by a factor of 5-10; this coupled with the position of the sparger, adversely affect the mass transfer coefficients.

9. The mass transfer coefficients in the lab reactor were low by approximately a factor of 5-10, and in fact the calculations indicate that for many runs not all of the O_3-supplied was transferred into the liquid, accounting in part for the low values of O_3-utilization.

10. The mass transfer coefficients for volatile components, e.g. chloroform, appear to be low by at least a factor of 10 in the lab reactor.

11. The UV-energy transfer, coming from radiators on the outside of the lab reactor, was substantially less than would be achieved by radiators located inside the reactor, as in a full-scale reactor.

F. SIZING METHODS AND CASES

For purposes of sizing and costing a range of full-scale units, the following six (6) cases were defined:

Cases A-1, A-2, A-3

(a) Matrix: Lake Lewisville, Texas

(b) Influent Micropollutant Levels:

$CHCl_3$, Chloroform: $C_o = 100\ \mu g/\ell$

$CHCl_2Br$, bromodichloromethane: $D_o = 100\ \mu g/\ell$

C_2Cl_4, tetrachloroethylene: $E_o = 20\ \mu g/\ell$

(c) % Removal for all Micropollutants: 90%

(d) Plant Sizes: Case A-1: 1 MGD
Case A-2: 10 MGD
Case A-3: 50 MGD

Cases B-1, B-2, B-3

(a) Matrix: Cross Lake, Louisiana

(b) Influent THM Precursor Level: Ambient

(c) % Removal of THMFP: 90%

(d) Plant Sizes: Case A-1: 1 MGD
Case B-2: 10 MGD
Case B-3: 50 MGD

For a given case defined by:

water flow rate, influent concentrations of TOC and micropollutants or THM precursors, and required removal, a procedure was used involving a sequence of steps to determine: the ozone required, and hence the size of the ozone generation unit, the reactor system size, and the energy required to operate the system. In order to achieve the advantages of higher average concentration of oxidizable components, a multi-staged reactor system of four completely mixed stages in series was used. Also, the combination of the four stages plus choice of the dynamical variables to give complete mass transfer of the O_3 supplied, were incorporated into the design in order to achieve high ozone utilization, $\alpha > 0.50$.

The following mathematical relations -- a total of some 24 equations -- were solved simultaneously, by numerical iteration until the desired convergence was attained.

1. mass balances of the oxidizable components, ozone, and air;
2. reaction rate equations for the disappearance of the TOC and the individual compounds of interest;
3. mass transfer equations for ozone and volatile compounds;
4. UV transfer equations from radiators into liquid phase; and
5. the mixing dynamic equations.

The iteration loop is started by making a first approximation of the design, followed by a calculational check of all the conditions that must be satisfied. Since there are numerous engineering solutions to the design problem, because of trade-offs, the final optimization is based on an "operating cost" (including amortization of the capital cost) object function. Time and funding limitations do not permit presentation of the generalized procedure for the optimization.

Table 30 presents the sizing results for Series A, and Table 31 the results for Series B.

G. TREATING UNIT CONFIGURATION

The process for both cases, A and B, is as shown in Figure 38.

The influent water is pumped to Reactor R1a and by gravity flow goes to Reactor R1b from whence, after treatment, it is discharged for utilization.

Ozone is generated from either air or O_2 and is fed to the bottom of each reactor for best ozone utilization.

The off-gas from the reactors is fed to a gas-liquid separator and in the case of oxygen-generated ozone, the excess oxygen is recycled to the ozone generator.

A transfer pump is provided to feed the reactors from the storage reservoir.

A flow indicator regulator is provided on the input to the reactors to regulate the influent flow.

Ozone monitors are provided at various points in the system to insure proper ozone utilization.

Each of the series reactors, as shown in Figure 38, is continually stirred and contains the UV lamps, fully immersed in quartz wells to insure proper UV energy transfer.

The unit, as pictured is easily adaptable to skid-mounting, thereby reducing the on-site construction costs for small communities.

H. CAPITAL AND OPERATING COSTS

Once the ozone requirements had been determined, the process configuration developed and the reactors sized, the following bases were used to estimate the capital and the operating costs.

PCI-Ozone Corp. was contacted and provided capital estimates for the ozone generation equipment in the various size ranges as well as air preparation equipment or oxygen recycle equipment, depending upon the configuration.

Estimates for reactors with mixers were obtained from local suppliers of comparable equipment to the petrochemical industry. This source was selected since most manufacturers of water and wastewater treatment vessels do not provide sufficient mixing horsepower for this application.

TABLE 30. SUMMARY OF DESIGN CASES SIZINGS, SERIES A

Parameter	A-1	A-2a	A-2b	A-3a*	A-3b*
1) Flow, MGD	1.00	10.0	10.0	50.0	50.0
2) O_3req'd, (lbs/day)	113 (from air)	1193 (from air)	1193 (from O_2)	5965 (from air)	5965 (from O_2)
3) TOC + Micropollutants					
-Influent,(lbs/day)	37.7	377	377	1885	1885
-Removal,(lbs/day)	26.4	264	264	1320	1320
4) Air or O_2 req'd, (lbs/day)	4492	47,720	2386 (make up)	239,000	11,930 (make up)
5) Reactors x Stages	2 x 2	2 x 2	2 x 2	5(2 x 2)	5(2 x 2)
6) Reactor Size,(each) D' x V(ft^3) x H'	5'x236x12' (+ 3'skirt)	10'x1855 x24'(+ 3' skirt)	=	5 units	5 units
7) Mixing req'd,					
HP	25.7	200	=	1000	=
KWH/day	460	3581	=	17,905	=
Motor Size,HP	2(18)	2(180)	=	10(180)	=
8) UV req'd,					
KW	22.3	178	=	1000	=
KWH/day	535	4271	=	21,355	=
9) Pumping req'd,					
HP	12.5	125	=	625	=
KWH/day	224	2238	=	11,190	=
Motor Size,HP	15	150	=	5(150)	=

*5-10MGD units for this case.

Design Basis: CF_o and BCM_o = 0.100 mg/ℓ, TCE_o = 0.020 mg/ℓ, TOC_o = 4.3 mg/ℓ

90% removal of micropollutants, 60-70% removal of TOC.

TABLE 31. SUMMARY OF DESIGN CASE SIZINGS, B-SERIES

Parameter	B-1	B-2a	B-2b	B-3a*	B-3b*
1) Flow, MGD	1.00	10.0	10.0	50.0	50.0
2) O_3 req'd (lbs/day)	255 (from air)	2550 (from air)	2550 (from O_2)	12,750 (from air)	12,750 (from O_2)
3) TOC + THMP					
-Influent, (lbs/day)	72.5	725	725	3625	3625
-Removal, (lbs/day)	38.4	384	384	1920	1920
4) Air or O_2 req'd, (lbs/day)	10,200	102,000	5100 (make up)	510,000	25,500 (make up)
5) Reactors x Stages	2 x 2	2 x 2	2 x 2	5(2 x 2)	5(2 x 2)
6) Reactor Size, (each) D' x Vft^3 x H'	5'x236x12' (+ 3'skirt)	10'x1855x 24'(+ 3' skirt)	=	5 units	5 units
7) Mixing req'd.					
-HP	25.0	200	=	1000	=
-KWH/day	447	3581	=	17,905	=
-Motor Size, HP	2(18)	2(150)	=	10(150)	=
8) UV req'd,					
-KW	22.3	178	=	890	=
-KWH/day	535	4271	=	21,355	=
9) Pumping req'd,					
-HP	12.5	125	=	625	=
-KWH/day	224	2238	=	11,190	=
-Motor Size, HP	15	150	=	5(150)	=

*5-10MGD units for this case.

Design Basis: $THMP_o$ = 0.330 mg/ℓ; 90% removal of THMP; TOC_o = 8.7 mg/ℓ; 50-60% removal of TOC.

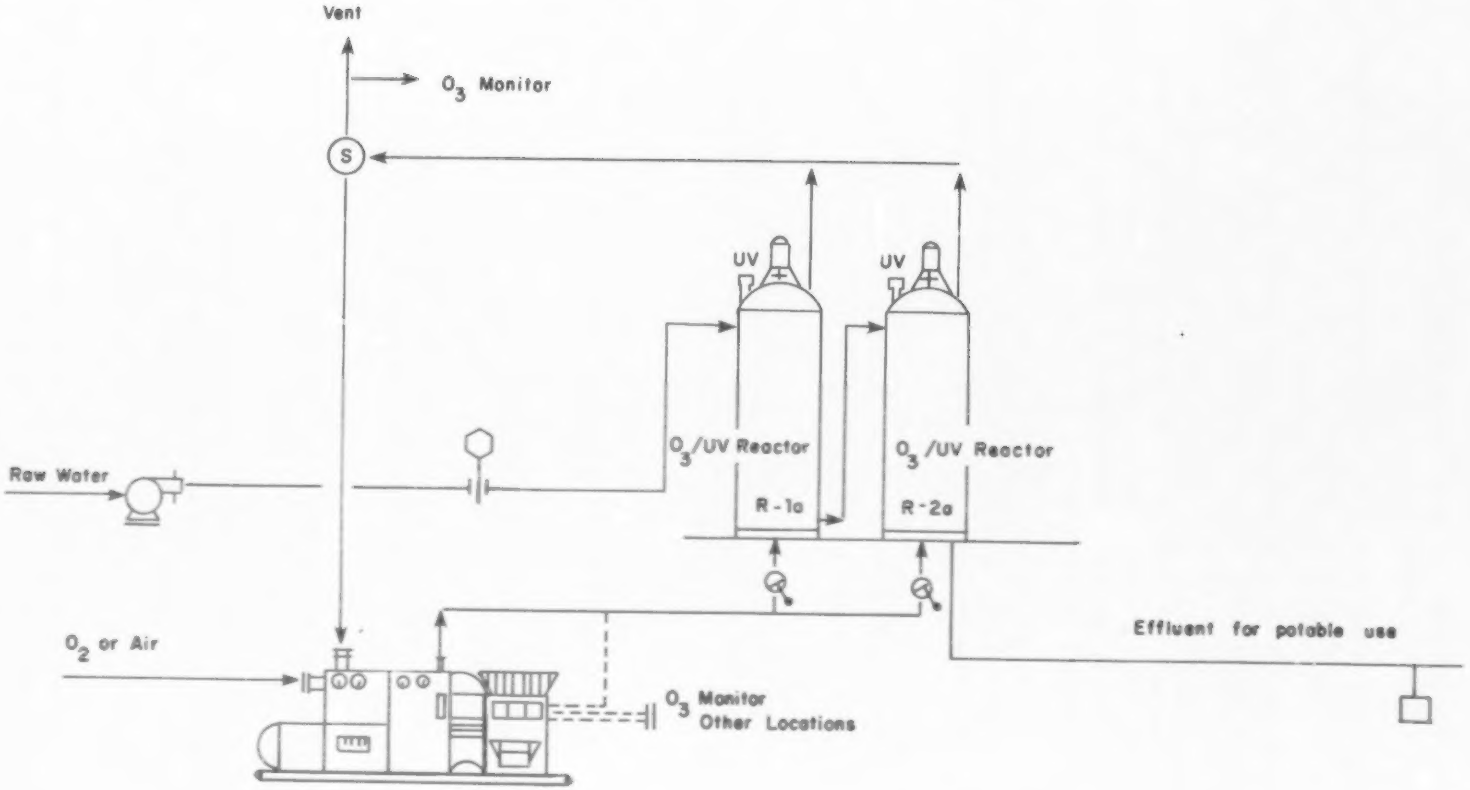
Vent
O_3 Monitor
S
UV
UV
Raw Water
O_3/UV Reactor
O_3/UV Reactor
R-1a
R-2a
O_2 or Air
Effluent for potable use
O_3 Monitor
Other Locations

Figure 38. Oxyphotolysis^{RM} Process Unit for Drinking Water.

UV equipment estimates were provided by Canrad-Hanovia, a supplier of industrial UV lamps.

The estimates for the pumps were provided through Flow - Quip, Inc. using Allis-Chalmers pumps.

The estimates for ozone monitors were provided by PCI and the instrumentation estimate was provided by local suppliers.

Piping, valves and skid-mounted installation, where feasible, was estimated by local fabricators. Design, engineering and fee estimates were based on local industry percentages. A 5% miscellaneous and contingency fee was also included in the estimated capital cost.

The elements of the estimated direct operating cost include operating labor, electrical energy cost, equipment maintenance cost, UV lamp replacement cost and oxygen, where necessary.

Fifteen dollars per hour was used for the estimated cost of operating labor. The daily operating time required ranged from 4 hours/day to 16 hours/day depending upon the size of the treatment unit.

A cost of $0.02/KWH was used to estimate the electrical energy cost. The elements composing the electrical energy load include ozone generation, UV lamp operation, mixing, pumps and instrumentation.

Maintenance is estimated at 1.5% of the capital cost per annum while UV lamp replacements are estimated on the basis of a 4000 hour life.

Oxygen is estimated at $70/ton delivered to the site in those cases where oxygen is used to produce the ozone.

The total operating cost also includes amortization of the capital expenditure. A 20-year amortization period has been used at 7% interest.

Tables 32 through 35 summarize the capital and operating costs for both the A and B series cases.

Larger cases, beyond 50 MGD, were not sized and costed, since it is believed that process economics better than 2X50 MGD, for example, can be achieved by a different design more appropriate to very large volumetric flow rate units. Such designs are in preliminary stages of development.

Recently it has been proposed (16) that for purposes of estimating capital and operating costs, a correlation better

TABLE 32. SUMMARY OF CAPITAL COSTS (A-SERIES)

			Case		
	A-1	A-2a	A-2b	A-3a*	A-3b*
Flow (MGD)	1.00	10.0	10.0	50.0	50.0
O_3 req'd (lbs/day)	113 (from air)	1193 (from air)	1193 (from O_2)	5965 (from air)	5965 (from O_2)
Removal (lbs/day TOC + Micro-pollutants	26.4	264	264	1320	1320
Equipment					
Ozone Generators	$ 81,000	$480,000	$200,000	$2,400,000	$ 900,000
Air Prep or O_2 Recycle	21,000	60,000	60,000	300,000	250,000
Reactors w/mixers	11,000	75,000	75,000	375,000	375,000
UV Equipment	8,920	80,000	80,000	356,000	356,000
Pumps	3,000	20,000	20,000	100,000	100,000
O_3 Monitors	6,000	6,000	6,000	30,000	30,000
Instrumentation	10,000	10,000	10,000	40,000	40,000
Sub-total	$140,920	$731,000	$451,000	$3,601,000	$2,051,000
Piping, Valves, Instl.	90,000	382,750	212,750	1,500,250	1,012,750
Design, Engineering, Fee	41,565	200,475	119,475	918,225	551,475
Misc. & Contingency	13,624	65,711	39,161	300,974	180,781
TOTAL	$286,109	$1,379,936	$822,386	$6,320,449	$3,796,006

*5-10 MGD units for this case.

TABLE 33. SUMMARY OF OPERATING COSTS (A-SERIES) $/DAY

	Case A-1	A-2a	A-2b	A-3a	A-3b
Operating Labor @ $15/hr.	$ 60.00	$ 60.00	$ 60.00	$ 240.00	$ 240.00
Electrical Energy @ ($0.02/KWH)					
O_3 Generation	$ 22.60	$238.60	$109.76	$1,193.00	$ 548.78
UV Lamps	10.70	85.42	85.42	427.10	427.10
Mixing	9.20	71.62	71.62	358.10	358.10
Pumps & Inst.	4.48	44.76	44.76	223.80	223.80
Sub-total	$ 46.98	$440.40	$311.56	$2,202.00	$1,557.78
Maintenance @ $1.5% of capital/ annum	11.76	56.71	33.80	259.74	156.00
UV Lamp Replacement	5.85	46.67	46.67	233.36	233.36
Oxygen @ $70/ton	-	-	83.51	-	417.55
DIRECT OPERATING COST	$124.59	$603.78	$535.54	$2,935.10	$2,604.69
AMORTIZATION (20 years @ 7%)	41.94	202.26	120.54	926.42	556.40
TOTAL OPERATING COST ($/day)	$166.53	$806.04	$656.08	$3,861.52	$3,161.09
TREATMENT COST ($/1000 gals)	$ 0.16	$ 0.081	$ 0.066	$ 0.077	$ 0.063

TABLE 34. SUMMARY OF CAPITAL COSTS (B-SERIES)

	Case				
	B-1	B-2a	B-2b	B-3a[*]	B-3b[*]
Flow (MGD)	1.00	10.0	10.0	50.0	50.0
O_3 req'd (lbs/day)	255 (from air)	2550 (from air)	2550 (from O_2)	12,750 (from air)	12,750 (from O_2)
Removal (lbs/day) TOC + THMP	38.4	384	384	1920	1920
Equipment					
Ozone Generators	$118,400	$1,140,000	$440,000	$5,280,000	$2,100,000
Air Prep or O_2 Recycle	26,600	180,000	100,000	540,000	480,000
Reactors w/mixers	11,000	75,000	75,000	375,000	375,000
UV Equipment	8,920	80,000	80,000	356,000	356,000
Pumps	3,000	20,000	20,000	100,000	100,000
O_3 Monitors	6,000	6,000	6,000	30,000	30,000
Instrumentation	10,000	10,000	10,000	40,000	40,000
Sub-total	$183,920	$1,511,000	$731,000	$6,721,000	$3,481,000
Piping, Valves, Instl.	108,850	906,600	438,600	3,965,390	2,053,790
Design, Engineering, Fee	52,695	435,168	210,528	1,923,550	996,262
Misc.&Contingency	17,273	142,638	69,006	630,497	326,553
TOTAL	$362,738	$2,995,406	$1,449,134	$13,240,437	$6,857,605

[*] 5-10 MGD units for this case.

TABLE 35. SUMMARY OF OPERATING COSTS (B-SERIES) $/DAY

	Case				
	B-1	B-2a	B-2b	B-3a	B-3b
Operating Labor @ $15/hr	$ 60.00	$ 60.00	$ 60.00	$ 360.00	$ 360.00
Electrical Energy @ ($0.02/KWH)					
O_3 Generation	$ 51.00	$510.00	$234.60	$2,550.00	$1,173.00
UV Lamps	10.70	85.42	85.42	427.10	427.10
Mixing	8.95	71.62	71.62	358.10	358.10
Pumps & Inst.	4.50	44.75	44.75	223.80	223.80
Sub-Total	$ 75.15	$711.79	$436.39	$3,559.00	$2,182.00
Maintenance @1.5% of capital/ annum	14.91	123.10	59.55	544.13	281.82
UV Lamp Replacement	5.85	46.67	46.67	233.36	233.36
Oxygen @ $70/ton	-	-	178.50	-	892.50
DIRECT OPERATING COST	$155.91	$941.56	$781.11	$4,696.49	$3,949.68
AMORTIZATION (20 years @ 7%)	53.17	439.05	212.41	1,940.72	1,005.16
TOTAL OPERATING COST ($/day)	$209.08	$1,380.61	$993.52	$6,637.21	$4,954.84
TREATMENT COST ($/1000 gals)	$ 0.20	$ 0.138	$ 0.099	$ 0.133	$ 0.099

than,

$/1000 gals treated vs. MGD

is $/lb oxidizables removed vs. lbs removed/day.

The method is particularly applicable to chemical oxidation since the oxidant required is directly related to the amount of material to be oxidized per unit time.

Figure 39 presents correlation of the costs for Series A and B on the suggested basis. By comparison, data for the OXYPHOTOLYSIS™ process applied to industrial wastewater gives values of $0.75 to $1.00/lb removed, for cases in the range of 100 and greater lbs removed/day. These lower treating costs are to be expected, since in industrial cases, O_3-utilization approaches 100%.

Sensitivity of the Cost Estimates

Examination of Tables 33 and 35 indicates that best economics result when the ozone is generated from oxygen rather than air for unit processing 10 MGD and greater; this fact might also be true for units of 5.0 MGD. In order to determine the sensitivity of the operating cost estimates, four additional cases were estimated, designated A-2b', A-3b', B-2b', and B-3b', assuming that ozone utilization was only 35%. The results are presented in Tables 36 and 37. In the case of the A-case comparisons, the treating cost increased by approximately 15%, whereas for B-case comparisons the increases were approximately 40%, but for all cases the estimates are less than $0.15/1000 gal. treatment cost.

I. ENGINEERING CONCLUSIONS AND RECOMMENDATIONS

In addition to the conclusions in Part E, and as a result of the process engineering sizing and costing, the following engineering conclusions and recommendations are offered:

1. The ozone/UV photo-oxidation process can be used effectively to reduce micropollutants and trihalomethane precursors to the desired limits. Simultaneously, TOC will be reduced and disinfection will be accomplished.
2. The cost estimates indicate that daily operating costs, including amortization of capital equipment and interest on borrowed capital, are in the range of $0.06 to $0.15 per 1000 gals of water treated, for 10-50 MGD units using ozone generated from oxygen.

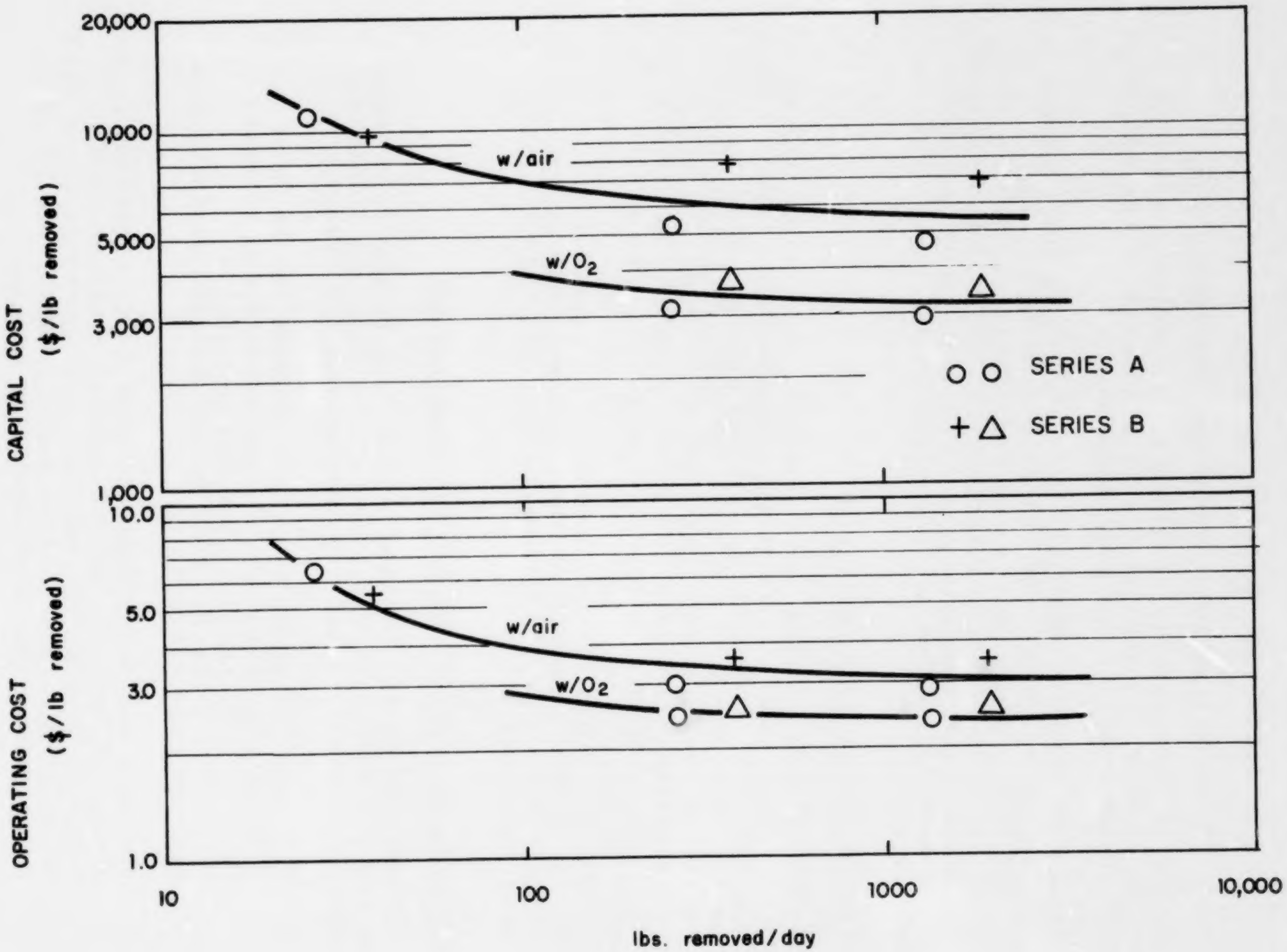

Figure 39. Correlation of Capital and Operating Costs (Assuming 50-60% O_3 Utilization).

TABLE 36. OPERATING COST ESTIMATE SENSITIVITY (A-SERIES)

	A2b	A2b'	A3b	A3b'
1) Flow (MGD)	10.0	10.0	50.0	50.0
2) O_3 Required (lbs/day)	1,193	1,705	5,965	8,524
3) Removal (lbs/day)	264	264	1,320	1,320
4) Capital Cost ($)	822,386	1,133,000	3,796,000	5,426,000
5) Direct Operating Cost ($/day)	535.5	571.0	2605.7	2846.2
6) Amortization (20 years @ 7%)	120.5	165.9	556.4	795.1
7) Total Operating Cost ($/day)	656.0	736.9	3161.1	3641.3
8) Treatment Cost ($/1000 gal)	0.066	0.077	0.063	0.073
($/lb removed)	2.48	2.79	2.39	2.76

TABLE 37. OPERATING COST ESTIMATE SENSITIVITY (B-SERIES)

	B2b	B2b'	B3b	B3b'
1) Flow (MGD)	10.0	10.0	50.0	50.0
2) O_3 Required (lbs/day)	2,550	4,371	12,750	21,854
3) Removal (lbs/day) TOC + THMP	384	384	1,920	1,920
4) Capital Cost ($)	1, 449,134	2,461,000	6,857,605	11,740,000
5) Direct Operating Cost ($/day)	781.1	1057.7	3949.7	5157.2
6) Amortization ($/day) (20 years @ 7%)	212.4	360.7	1005.2	1720.8
7) Total Operating Cost ($/day)	993.5	1418.4	4954.8	6878.0
8) Treatment Cost ($/1000 gal)	0.099	0.142	0.099	0.138
($/lb removed)	2.59	3.69	2.58	3.58

3. A treating cost of \$0.06 to \$0.15/1000 gals for combined micropollutant, trihalomethane and TOC removal, plus disinfection appears reasonable.

4. If higher ozone utilization values can be achieved, the capital and operating cost could be reduced significantly; the latter by as much as 30-40%.

5. For raw water streams containing TOC > 10 mg/L, the possibility of coupling the process with another pre-TOC removal process to minimize total treating cost may be desirable. For high TOC streams, each situation should be examined individually.

In view of the foregoing conclusions, it is recommended that:

> The process should be field tested at the 1.0 MGD, or greater, level for at least one year, using a four-stage reactor system unit, as described in this report, to obtain actual data on performance (operating efficiency, ozone utilization, etc.) and treatment costs. The unit could be completely skid-mounted for use at several locations, if desired.

REFERENCES

1. Robeck, G. G., Dostal, K. A., Cohen, J. M., and Kreisel, J. F., Journal of American Water Works Association, 57, 181 (1965).

2. Glaze, W. H., and Henderson, J. E. IV., Journal of the Water Pollution Control Federation, 47, 2511 (1975).

3. Glaze, W. H., Henderson, J. E. IV, and Smith, G., Analysis of New Chlorinated Organic Compounds in Municipal Wastewaters After Terminal Chlorination, Identification and Analysis of Organic Pollutants in Water. Keith, L. H. editor, Ann Arbor Science, Ann Arbor, Michigan, p. 247, 1976.

4. Jolley, R. L., Environmental Letters, 1, 321 (1974).

5. Jolley, R. L., Journal of the Water Pollution Control Federation, 47 (3), 601 (1975).

6. Harlock, R. M. and Dowlin, R., Journal of American Water Works Association, 50, 29 (1958).

7. Burttschell, R. G., Rosen, A. A., Middleton, F. M., and Ettinger, M. B., Journal of American Water Works Association, 51, 205 (1959).

8. Morris, J. C., Formation of Halogenated Organics by Chlorination of Water Supplies, U.S. EPA, EPA-600/1-75-002, March, 1975.

9. Rook, J. J., Water Treatment and Examination, 23 (2), 234 (1974).

10. Bellar, T. A., Lichtenberg, J. J., Kroner, R. C., Journal of American Water Works Association, 66, 703 (1974).

11. Murphy, K. L., Zaloum, R., and Fulford, D., Water Research, 9, 389 (1975).

12. Symons, J. M., Carswell, J. K., Clark, R. M., Love, O. T., Miltmer, R. J., and Stevens, A. A., Interim Treatment Guide for the Control of Chloroform and Other Trihalomethanes, U.S. EPA, Water Supply Research Division/Municipal Environmental Research Laboratory, Cincinnatti, Ohio, June, 1976.

13. Guinvarch, P., Three Years of Ozone Sterilization of Water in Paris, Ozone Chemistry and Technology, Advances in Chemistry Series No. 21, ACS. Washington, D.C., p. 416,1959.

14. Lebout, H., Fifty Years of Ozonation at Nice, ibid., p. 450, 1959.

15. Rook, J. J., Journal of American Water Works Association, 68, 279 (1976).

16. Diaper, E. W. J., Practical Aspects of Water and Wastewater Treatment by Ozone, Ozone in Water and Wastewater Treatment. Evans, F. L. editor, Ann Arbor Science, Michigan, p. 145, 1972.

17. Katzenelson, E., Kletter, B., and Shuval, H. I., Journal of American Water Works Association, 66, 725 (1974).

18. McNabney, R., and Wynn, J., Water and Wastes Engineering, 8 (8), 46 (1971).

19. Meijers, A. P., Water Research, II, 647 (1977).

20. Rosen, H. M., Ozonation: A Solution to Potential Carcinogens in Drinking Water, Proceedings of 2nd International Symposium on Ozone Technology. Rice, R. G., editor, International Ozone Institute, Syracuse, N.Y., p. 143,1976.

21. Zeng, D., Ozonation Pilot Plant Studies at Chicago, Ozonation in Sewage Treatment. The University of Wisconsin, Milwaukee, November 9, 1971.

22. Feasibility Studies of Applications of Catalytic Oxidation in Wastewater. Report No. 17020 ECILL/71, Water Quality Office, U.S. EPA, December 1971.

23. Elia, V. J., Clark, C. S., McGinnis, K. T., Cody, T. E., and Kinman, R. N., Journal of the Water Pollution Control Federation, 50, 1727 (1978).

24. Foulds, J. M., Water and Sewage Works, 118, 80 (1971).

25. Guirguis, W., Cooper, T., and Ungar, H. A., Journal of the Water Pollution Control Federation, 50, 308 (1978).

26. Glaze, W. H., EPA Project No. R-806157-01.

27. Shambaugh, R. L., and Melnyk, P. B., Journal of the Water Pollution Control Federation, 50, 113 (1978).

28. Williams, P. M., Baldwin, R. J., and Robertson, K. J., Water Research, 12, 385 (1978).

29. Mignot, J., Application of Ozone With or Without Activated Carbon for Drinking Water Treatment, Proceedings of 1st International Symposium on Ozone for Water and Wastewater Treatment. Rice, R. G., and Browning, M. E., editors, International Ozone Institute, Syracuse, N.Y., p. 134, 1975.

30. Collier, H. E., "Ozone Treatment of Waste Aqueous Effluent from Alkyl Lead Manufacture." U.S. Patent No. 3,308,061, (1977).

31. Lapidot, H., Estimated Cost of Ozone Treatment of an Industrial Wastewater, Proceedings of 1st Symposium on Ozone for Water and Wastewater Treatment, December 1973. Rice, R. G., and Browning, M. E., editors, International Ozone Institute, Syracuse, N.Y., p. 712, 1975.

32. Lawrence, J., The Oxidation of Some Haloform Precursors with Ozone. Water Chemistry Section, Canada Centre for Inland Waters, Burlington, Ontario, Canada.

33. Glaze, W. H., Rawley, R., and Lin, S., By-products of Organic Compounds in the Presence of Ozone and Ultraviolet Light: Preliminary Results, Ozone/Chlorine Dioxide Oxidation Products of Organic Materials, Rice, R. G., and Cotruvo, J. A., editors, Ozone Press International, International Ozone Institute, Inc., Cleveland, Ohio, p. 321, 1978.

34. Riley, T. L., Mancy, K. H., and Boettner, E. A., The Effect of Preozonation on Chloroform Production in the Chlorine Disinfection Process. Department of Environmental and Industrial Health, School of Public Health, The University of Michigan, Ann Arbor, Michigan.

35. Regener, V. H., Automatic Chemical Determination of Atmospheric Ozone Chemistry and Technology. Advances in Chemistry, Series 21. ACS, Washington, D.C., p. 124, 1959.

36. Manley, T. C., and Niegowski, S. J., Ozone, Kirk-Othmer Encyclopedia of Chemical Technology, 2nd Ed., 14, 410 (1967). John Wiley and Sons, New York.

37. Trambarulo, R., Ghosh, S. N., Burrus, C. A. Jr., and Gordy, W., Journal of Chemical Physics, 21, 851 (1953).

38. Kinman, R. N., Ozone in Water Disinfection, Ozone in Water and Wastewater Treatment. Evans, F. L., editor, Ann Arbor Science Publishers, Inc., p. 123, 1972.

39. Stumm, W., Journal of Boston Society of Civil Engineering, 45, 68 (1958).

40. Hoigne, J., and Bader, H., Water Research, 10, 377 (1976).

41. Kilpatrick, M. L., Glerrick, C. C., and Kilpatrick, M., Journal of American Chemical Society, 78, 1784 (1956).

42. Stumm, W., Helvitia Chimica Acta, 37, 773 (1954).

43. Gorbenko-Germanov D. S., and Kozlova, I. V., Zhurnal Fizicheskoi Khimii, 48, 166 (1974).

44. Hoigne, J., and Bader, H., Science, 109, 782 (1975).

45. Hoigne, J., and Bader, H., Ozone and Hydroxyl Radical-Initiated Oxidations of Organic and Organometallic Trace Impurities in Water, Organometals and Organometalloids Occurrence and Fate in the Environment, ACS Symposium Series No. 82. Brinckman, F. E., and Bellama, J. M. editors, p. 293, 1978.

46. Hoigne, J., and Bader, H., Environmental Science and Technology, 12, 79 (1978).

47. Peleg, M., Water Research, 10, 361 (1976).

48. Czapski, G., Journal of Physical Chemistry, 71, 1683 (1967).

49. Barr, N. F., and King, C. G., Journal of American Chemical Society, 78, 303 (1956).

50. Baxendale, J. H., Radiation Research Supplement, 4, 114 (1964).

51. Hewes, C. G., and Davison, R. R., Journal of American Institute of Chemical Engineering, 17 (1), 141 (1971).

52. Murray, R. W., Accounts of Chemical Research, 1, 1822 (1968).

53. Bailey, P. S., Reactivity of Ozone With Various Organic Functional Groups Important to Water Purification, Proceedings of 1st International Symposium on Ozone for Water and Wastewater Treatment. Rice, R. G., and Browning, M.E. editors. International Ozone Institute, Syracuse, N.Y., p. 101, 1975.

54. Criegee, R., Products of Ozonation of Some Olefins, Ozone Chemistry and Technology, Advances in Chemistry Series No. 21. ACS. Washington, D.C., p. 133, 1959.

55. Oelschlaeger, H. F., Reactions of Ozone with Organic Compounds, Ozone/Chlorine Dioxide Products of Organic Materials. Rice, R. G., and Cotruvo, J. A. editors, Ozone Press International, Cleveland, Ohio, p. 20, 1978.

56. Maggiolo, A., ibid., p. 59, 1978.

57. Rice, R. G., Reaction Products of Organic Materials with Ozone and with Chlorine Dioxide in Water. presented at International Ozone Institute, Symposium on Advanced Ozone Technology, Toronto, Ontario, Canada, Nov. 17, 1977.

58. Ahmed, M. D., and Kinney, C. R., *Journal of American Chemical Society*, *72*, 559 (1950).

59. Kinney, C. R., and Friedmann, N., ibid., 74, 57 (1952).

60. Sievers, R. E., Barkley, R. M., Eiceman, G. A., Shapiro, R. H., Walton, H. F., Kolenko, K. J., and Field, L. R., Environmental Trace Analysis of Organics in Water by Glass Capillary Column Chromatography and Ancillary Techniques, *Products of Ozonolysis*. Department of Chemistry, University of Colorado, Boulder, Colorado.

61. Lawrence, J., *Identification of Ozonation Products in Natural Waters*. Water Chemistry Section, Ontario Canada Centre for Inland Waters, Burlington, Canada.

62. Shevchenko, M. A., and Taran, P. N., *Ukrainskii Khimicheskii Zhuranal*, *32* (5), 532 (1966).

63. Bailey, P. S., *Chemical Review*, *58*, 957 (1958).

64. Gould, J. P., and Weber, W. J., *Journal of the Water Pollution Control Federation*, *48*, 47 (1976).

65. Yamamoto, Yorihiro; Niki, Etsuo; Shiokaw, Hiroyo; and Kamiya, Yoshio, *Ozonation of Organic Compounds, II, Ozonation of Phenol in Water*. Department of Reaction Chemistry. University of Tokyo, Hongo, Japan, 1978.

66. Shuval, H., and Peleg, M., Studies on Refractory Organic Matter from Wastewater by Ozonation. Progress Report of Work Sponsored by Ges Fur Kernforchung, Karlsruhe, Germany and National Council for R & D, Jerusalem, Israel, 1975.

67. Gilbert, E., Ozonolysis of Chlorophenols and Maleic Acid in Aqueous Solution. *Proceedings of 2nd International Symposium on Ozone Technology*. Rice, R. G. editor, International Ozone Institute, Syracuse, N.Y., p. 253, 1976.

68. Bauch, H., Burchard, H., and Arsovic, H. M., *Gesunheits Ingenieur*, *91* (9), 258 (1970).

69. Yokayama, Kazuo; Sato, Sadao; Yoshiyasu, Ikuyo; and Imamura, Takashi, *Mitsubishi Denki Giho*, *48* (10), 1233 (1974).

70. Czapski, T., Samuni, A., and Yelin, R., *Israel Journal of Chemistry*, *6*, 969 (1968).

71. Kuo, C. H., Li, K. Y., Wen, C. P., and Weeks, J. L. Jr., *Journal of American Institute of Chemical Engineering, Symposium Series*, *73*, 230 (1977).

72. Augugliaro, V., and Rizzuti, L., *Chemical Engineering Communication*, *2*, 219 (1978).

73. Chen, J. W., Hui, C., Keller, T., and Smith, G., *American Institute of Chemical Engineering Symposium Series*, *73*, 206 (1977).

74. Ashmore, P. G., Dainton, F. S., and Sugden, T. M. editors., *Photochemistry and Reaction Kinetics*. Cambridge, the University Printing House, p. 35, 1967.

75. Inn, E. C. Y., and Tanaka, Y., Ozone Absorption Coefficients in the Visible and Ultraviolet Regions, Ozone Chemistry and Technology. *Advances in Chemistry No. 21*. American Chemical Society, Applied Publications, p. 263, 1959.

76. Heidt, L. J., and Forbes, G. S., *Journal of American Chemical Society*, *56*, 1617 (1934).

77. Heidt, L. J., and Forbes, G. S., ibid., 2365 (1934).

78. Heidt, L. J., ibid., 57, 1710 (1935).

79. Norrish, R. G. W., and Wayne, R. P., *Proceedings of the Royal Society A.*, *288*, 200, 361 (1965).

80. Kistiakowsky, G. B. Z., *Physic Chem*, *117*, 337 (1925).

81. Castellano, E., and Shumacher, H. J., *Journal of Chemical Physics*, *36*, 2238 (1962).

82. McGrath, W. D., and Norrish, R. G. W., *Proceedings of the Royal Society A.*, *254*, 317 (1960).

83. Fortin, C. J., Snelling, D. R., and Tardif, A., *Canadian Journal of Chemistry*, *50*, 2747 (1972).

84. Biedenkapp, D., Hartshorn, L. G., and Bair, E. J., *Chemical Physics Letters*, *5*, 379 (1970).

85. Langley, K. F., and McGrath, W. D., *Planetary Space Science*, *19*, 413 (1971).

86. Scott, P., and Cvetanovic, R. J., *Journal of Chemical Physics*, *54*, 1440 (1970).

87. Taube, H., *Transactions of the Faraday Society*, *53*, 656 (1957).

88. Thomas, J. K., ibid., 61, 702 (1965).

89. Baxendale, J. H., and Wilson, J. A., ibid., 53, 344 (1957).

90. Volman, D. H., and Chen, J. C., *Journal of American Chemical Society*, *81*, 4141 (1959).

91. Hunt, J. P., and Taube, H. J., ibid., 74, 5999 (1952).

92. Buxton, G., and Wilmarth, W. K., *Journal of Physical Chemistry*, *67*, 2835 (1963).

93. Dixon, W. T., and Norman, R. O. C., *Journal of the Chemical Society*, 3119 (1963); 3625, 4850, 4857 (1964).

94. Haber, F., and Weiss, J., *Proceedings of the Royal Society*, *A*, *147*, 332 (1934).

95. Walling, C., and Johnson, R. A., *Journal of American Society*, *97*, 363 (1975).

96. Currie, D. J., and Dainton, F. S., *Transactions of the Faraday Society*, *61*, 1156 (1965).

97. Ogata, Yoshiro; Tomizawa, Kohtaro; and Fuju, Kohzo; *Bulletin of the Chemical Society of Japan*, *51*, 2628(1978).

98. Dore, M., Merlet, N., and Blanchard, T., *Water Research*, *12*, 427 (1978).

99. Nagl, H. G., and Korte, F., *Tetrahedron*, *28*, 5445 (1972).

100. Jayanty, R. K. M., Simonaitis, R., and Heicklen, J., *Journal of Photochemistry*, *4*, 203, 381 (1975).

101. Garrison, R. L., Mauk, C. E., and Prengle, H. W. Jr., Advanced Ozone-Oxidation System for Complexed Cyanides, *1st International Symposium on Ozone for Water and Wastewater Treatment*. Rice, R. G., and Browning, M. E. editors, International Ozone Institute, Syracuse, N.Y., p. 551, 1975.

102. Fochtman, E. G., and Huff, J. E., Ozone-Ultraviolet Light Treatment of TNT Wastewaters, *Proceedings of 2nd International Symposium on Ozone Technology*, Rice, R. G., Richet, P., and Vincent, M. A., editors, International Ozone Institute, Syracuse, N.Y., p. 211, 1975.

103. Prengle, H. W. Jr., Hewes, C. G. III, and Mauk, C. E., ibid., 224 (1975).

104. Prengle, H. W. Jr., Mauk, C. E., and Payne, J. E., Ozone/UV Oxidation of Chlorinated Compounds in Water. Presented at the International Ozone Institute Forum on Ozone Disinfection. Chicago, Illinois, June 2-4, 1976.

105. Prengle, H. W. Jr., and Mauk, C. E., Ozone/UV Oxidation of Pesticides in Aqueous Solution, *Ozone/Chlorine Dioxide Oxidation Products of Organic Materials*. Rice, R. G., and Cotruvo, J. A., editors. Ozone Press International, Cleveland, Ohio, p. 302, 1978.

106. Wako, Hikoji; Kanihiko, Horikawa; Ken, Kuroshimai and Isamu, Ono, *Japan Kokai*, *75*, 44, 648 (1975).

107. Wako, Hikoji, *Journal of the Japan Chemical Society*, *10*, 1530 (1976).

108. Kuo, P. P. K., Chian, E. S. K., and Cheng, B. J., *Environmental Science and Technology*, *II*, 1177 (1977).

109. Horspool, W. M., *Aspects of Organic Photochemistry*. Academic Press Inc., New York, 1976.

110. Lee, M. K., See, G. G., and Wynveen, R. A., Reaction Kinetics of UV/Ozone with Organic Compounds in Hospital Wastewater. Presented at the Symposium on Advanced Ozone Technology, Toronto, Ontario, Nov. 16-18, 1977. Sponsored by International Ozone Institute, Inc., Cleveland, Ohio.

111. McCarthyl, J. J., Evaluation of an Air Stripping-Ozone Contactor System. Presented at the 32nd Industrial Water Conference, Purdue University, 1977.

112. Chian, E. S. K., and Kuo, P. P. K., Fundamental Study on the Post Treatment of RO Permeats from Army Wastewaters, Second Annual Summary Report to U.S. Army Medical Research and Development Command, Contract No. DAMD 17-75-C-5506, 1976.

113. Smetana, A. F., and Bulusu, S., Photochemical Studies of Secondary Nitramines Part II. *Ultraviolet Photolysis and Ozonolysis of RDX in Aqueous Solution*. Technique Report ARLCD-TR-77039, U.S. Army Armament Research and Development Command, 1977.

114. Glaze, W. H., unpublished data.

115. Leitis, E., Bryan, E. H., Zeff, J. D., Crosby, D. C., and Smith, M., An Investigation into the Chemistry of the UV-Ozone Purification Process. Presented at the 4th World Ozone Congress, Houston, Texas, November 27-29, 1979.

116. McNesby, J. R., and Okabe, H., Vacuum Ultraviolet Photo-Chemistry, *Advances in Photochemistry*, Vol. III. Noyes, W. A. Jr., Hammond, G. S., and Pitts, J. N. Jr., editors, Interscience Publishers, New York, p. 157, 1964.

117. Calvert, J. G., and Pitts, J. N. Jr., *Photochemistry*, John Wiley and Sons, Inc., New York, 1966.

118. Galan, M. A., and Smith, J. M., *Chemical Engineering Science*, 31, 1047 (1976).

119. Owen, E. D., Principles of Photochemistry in Aqueous Solution, *Organic Compounds in Aquatic Environments*. Faust, S. D., and Hunter, J. V., editors, Marcel Dekker, Inc., New York, p. 387, 1971.

120. Crosby, D. G., and Tutass, H. O., *Journal of Agricultural and Food Chemistry*, 14, 596 (1966).

121. Safe, S., Bunce, N. J., Chittim, B., Hutzinger, O., and Ruzo, L. O., Photodecomposition of Halogenated Aromatic Compounds, *Identification & Analysis of Organic Pollutants in Water*. Keith, L. H., editor, Ann Arbor Science, Michigan, p. 35, 1976.

122. Ruzo, L. O., Zabik, M. J., and Scheutz, R. D., *Bulletin of Environmental Contamination and Toxicology*, 8, 217 (1972).

123. Ruzo, L. O., Zabik, M. J., and Scheutz, R. D., *Journal of the American Chemical Society*, 96, 3809 (1974).

124. Ruzo, L. O., Zabik, M. J., and Scheutz, R. D., *Journal of Agricultural and Food Chemistry*, 22, 199 (1974).

125. Safe, S., Hutzinger, O., *Nature (London)*, 232, 641 (1971).

126. Hutzinger, O., Safe, S., and Zitko, V., *Environmental Health Perspectives*, I, 15 (1972).

127. Hustert, K., and Korte, F., Chemosphere, 1, 7 (1972).

128. MacNeil, J. D., Safe, S., and Hutzinger, O., Bulletin of Environment Contamination & Toxicology, 15, 66 (1976).

129. Alder, G. A., and Hill, G. R., Journal of the American Chemical Society, 72, 1884 (1950).

130. Chang, B. J., A Model Study of Ozone-Sparged Vessels for the Removal of Organics from Water and Wastewater. thesis for the degree of Doctor of Philosophy in civil engineering, University of Illinois at Urbana-Champaign, 1978.

131. Merkulova, V. P., Lorchikov, V. S., and Ivanousk, M. D., Izvestiya Vysshikh Uchebnykh Zavedenii, Khimiya i Khimicheskaya Tekhnologiya, 14, 818 (1971).

132. Rankas, M. M., Siirode, E. K., and Kyulm, S. R., Rate of Ozone Decomposition in Different Water. Tallinna Poluteh. Inst. Toim, Ser. A198, 219 (1962). Chemical Abstract, 60, 2633e (1964).

133. Rizzuti, L., Auguliao, V., and Marrucci, G., Chemical Engineering Science, 31, 877 (1976).

134. Rogozhkin, G. I., Kinetics of Ozone Adsorption by Alkaline Solutions. Chemical Abstract, 73, 81108Y (1971).

135. Rothmund, V., and Burgstaller, A., Decomposition Velocity of Ozone in Aqueous Solution. Mh. Chem. 34, 665 (1970).

136. Senewald, K., Zeitschrift fur Physikalische Chemie. A 164, 305 (1933).

137. Shambaugh, R. L., and Melynk, P. B., The Influence of Spontaneous Decomposition and Mass Transfer Upon Soluble Ozone Concentration. Forum on Ozone Disinfection. International Ozone Institute, Chicago, 1976.

138. Weiss, J., Transactions of the Faraday Society, 31, 668 (1935).

139. Khandewal, K. K., Barduhn, A. J., and Grove, C. S. Jr., Kinetics of Ozonation of Cyanides, Ozone Chemistry and Technology. Advances in Chemistry Series No. 21. American Chemical Society, Washington D.C., p. 78 (1957).

140. Kirk, B. S., McNabney, R., and Wynn, C. S., Pilot Plant Studies of Tertiary Wastewater Treatment with Ozone, Ozone in Water and Wastewater Treatment. Evans, F. L. editor. Ann Arbor Science Publishers, Inc., Ann Arbor, Michigan, 1972.

141. Kuo, C. H., and Wen, C. P., Ozonation of Formic Acid, Formaldehyde and Methanol in Aqueous Solutions. Presented at American Institute of Chemical Engineers, 69th Meeting, Chicago, Illinois, Nov. 28, 1976.

142. Eisenhauer, H. R., *Water Pollution Control Federation*, *40*, 1887 (1968).

143. Majumdar, S. B., Ceckler, W. H., and Sproul, O. J., *American Institute of Chemical Engineers*, *Symposium Series*, *73*, 188 (1977).

144. Richards, D. A., Fleischman, M., and Ebersold, L. P., ibid., 213 (1977).

145. Yocum, F. H., Ozone Mass Transfer in Stirred Vessels. Presented at 86th National Meeting of American Institute of Chemical Engineers, April, 1979.

146. Sherwood, T. K., Pigford, R. L., and Wilke, C. R., *Mass Transfer*, McGraw-Hill Book Co., New York, pp. 178-195, 1975.

147. Hoigne, J., and Bader, H., Ozone Initiated Oxidations of Solutions in Wastewater: A Reaction Kinetic Approach. Presented at International Association on Water Pollution Research, 9th International Conference, Stockholm, June, 1978.

148. Jacob, N., Balakrishnan, I., and Reddy, M. P., *Journal of Physical Chemistry*, *81*, 17 (1977).

149. Mathews, R. W., and Sangster, D. F., *Journal of Physical Chemistry*, *69*, 1938 (1965).

150. Flamm, D. L., *Environmental Science & Technology*, *11*, 978 (1977).

151. Skoog, D. A., and West, D. M., *Fundamentals of Analytical Chemistry*. Holt, Rinehart and Winsten, Inc., New York, N.Y., p. 661, 1969.

152. Parker, C. A., *Proceedings of the Royal Society A*, *220*, 104 (1953).

153. Ullmann, F., *Ann. Chemistry*, *332*, 38 (1904).

154. Hutzinger, O., Safe, S., and Zitko, V., *Bulletin of Environmental Contamination & Toxicology*, *6*, 209 (1971).

155. Kornblum, N., and Kendall, D. L., *Journal of the American Chemical Society*, *74*, 5782 (1952).

156. Horning, E. C. editor-in-chief, Organic Syntheses, Vol.3, John Wiley & Sons, Inc., London, p. 339, 1955.

157. Standard Methods -- for the Examination of Water and Wastewater. 14th edition, American Public Health Assoc., New York, N.Y., pp. 278-282, 407-416, 1975.

158. Keith, L., Current Practice in GC-MS Analysis of Organic in Water. Environmental Practice Technology Series. EPA Rz-73-277, Appendix Two, p. 88, 1973.

159. Bethge, P. O., and Lindstrom, K., Analyst, 99, 137 (1974).

160. Skoog, D. A., and West, D. M., Analytical Chemistry. Holt, Rinehart and Winston, Chicago, p.57, 1963.

161. Huang, Francis, Ph.D. Dissertation. North Texas State University, Denton, Texas, 1980.

162. Riley, T., Paper presented at IOI Symposium on Advanced Ozone Technology, Toronto, Canada, Nov. 16-18, 1977.

163. Prengle, H. W., Jr., and Barona, N., Hydrocarbon Processing, 49, 159 (1970).

164. Stenhagen, E., Abrahamsson, S., McLafferty, F. W., Registry of Mass Spectral Data. John Wiley, New York, 1974.

165. Heller, S. R., and Milne, G. W. A., GPA/NIH Mass Spectral Data Base. NSRDS-NBS, U.S. Govt. Printing Office, Wash., D.C.

166. Chemical Information System. (Now, Information Sciences Corporation, Suite 500, 918 16th St., N.W., Washington, D.C., 20006) Brookhaven National Laboratory, Upton, N.Y.

167. Henderson, J.E., IV., Peyton, Gary R., and Glaze, W.H. in Keith, L.H. (editor), Identification and Analysis of Organic Pollutants in Water. John Wiley, p. 105, 1976.

168. Horak, J., and Pasek, J., Design of Industrial Chemical Reactors from Laboratory Data. Heyden & Son, Inc., Philadelphia, p.358, 1978.

169. Perry, R. H., and Pigford, R. L., Indust. and Eng. Chem, 45, 1247 (1953); 49, 1400 (1957).

170. Danckwerts, P.V., Trans. Farad. Soc., 46, 300 (1950).

171. Hoigne, J., and Bader, H., Presented at 4th World Ozone Conference, Houston, Texas, Nov. 27-29, 1979.

172. Safe, S., Hutzinger, O., Nature, 232, 641 (1971).

173. Ruzo, L. O., Safe, S., and Zabik, M. J., Journal of Agricultural and Food Chemistry, 23, 594 (1975).

174. Yokayama, Kazuo; Sato, Sadao, Yoshiyasu, Ikuyo; and Imamura, Takashi, Mitsubishi Denki Giho, 48 (10), 1233 (1974).

175. Calvert, J. G., and Pitts, J. N., Photochemistry. John Wiley & Sons, Inc., New York, p. 432, 1966.

176. Bailey, P. S., Chemical Review, 58, 957 (1958).

177. Gould, J. P., and Weber, W. J., Journal of Water Pollution Control Federation, 48, 47 (1976).

178. Fetizon, M. and Audier, H., Organic Mass Spectrometry 8 (1974) 201.

179. Martin, J. P., Haider, K., and Linhares, L. F. J., Soil. Sci. Soc. Am., 43, 100 (1979).

180. Rook, Johannes J., Environ. Sci. Technol., 11, 478 (1977).

181. Garrison, R. L. , Mauk, C. E., and Prengle, H. W., Jr., "Advanced O_3-Oxidation System for Complexed Cyanides;" First International Symposium, International Ozone Institute, Washington, D.C., December 1973.

182. Prengle, H. W., Jr., Hewes, C. G. III, and Mauk, C. E., "Oxidation of Refractory Materials by Ozone with Ultraviolet Radiation;" Second International Ozone Symposium, International Ozone Institute, Montreal, Canada, May, 1975.

183. Prengle, H. W., Jr., Mauk, C. E., and Payne, J. E., "Ozone/UV Oxidation of Chlorinated Compounds in Water;" International Ozone Institute Forum, Chicago, Illinois, June, 1976.

184. Prengle, H. W., Jr. and Mauk, C. E., "Ozone/UV Oxidation of Pesticides in Aqueous Solution;" EPA/IOI Workshop, Cincinnati, Ohio, November 1976.

185. U.S. Patent #3,920,547: "Method of Destroying Cyanides," November 1975; Assignee: Houston Research, Inc.

186. British Patent #1,543,225: "Improvements in or Relating to Oxidation of Organic Refractories in an Aqueous Medium," April 1976; Assignee: Houston Research, Inc.

187. French Patent #2,309,480: "Procédé d'oxydation de matieres réfractaires organiques contenues dans l'eau," November 1976; Assignee: Houston Research, Inc.

188. Yocum, F. H., "Oxidation of Styrene with Ozone in Aqueous Solution;" EPA/IOI Workshop, Cincinnati, Ohio, November 1976.

189. Bates, R., Fondy, P. L., and Corpstein, R. R., Ind. Eng. Chem. Proc. Res. Dev. 2, 310 (1968).

190. Moo-Young, M. B., Ph.D. Dissertation, University of London (1961).

191. Yocum, F. H., "Ozone Mass Transfer in Stirred Vessels;" 86th National Meeting, AIChE, Houston, Texas, April 1979.

192. Prengle, H. W., Jr., private communication, Chemical Engineering Department, University of Houston (1974).

193. Nall, A. E., private communication, Houston Research, Inc. (1979).

194. Canrad-Hanovia Brochure: "Photochemical Equipment," 100 Chestnut St., Newark, New Jersey 07105, November 1974.

195. Jacob, S. M. and Dranoff, J. S., "Light Intensity Profiles in a Perfectly Mixed Photoreactor, "AIChE Journal, 16, 359 (1970).

196. Prengle, H. W. Jr. and Joshi, D. S., "New Developments in the O_2, O_3/UV Photo-Oxidation Process for Industrial Wastewater Treatment;" 86th National Meeting, AIChE, Houston, Texas, April 1979.

APPENDIX A

DESTRUCTION CURVES FOR FIRST-ORDER SUBSTRATES

Shown in Figures A-1 through A-16 are the disappearance curves for substrates which are first-order in substrate. Points are actual experimental data while the solid lines are the results of the curve fits given in Appendix C. All curves are normalized to the initial concentration of substrate, 100 μg/L in all uses.

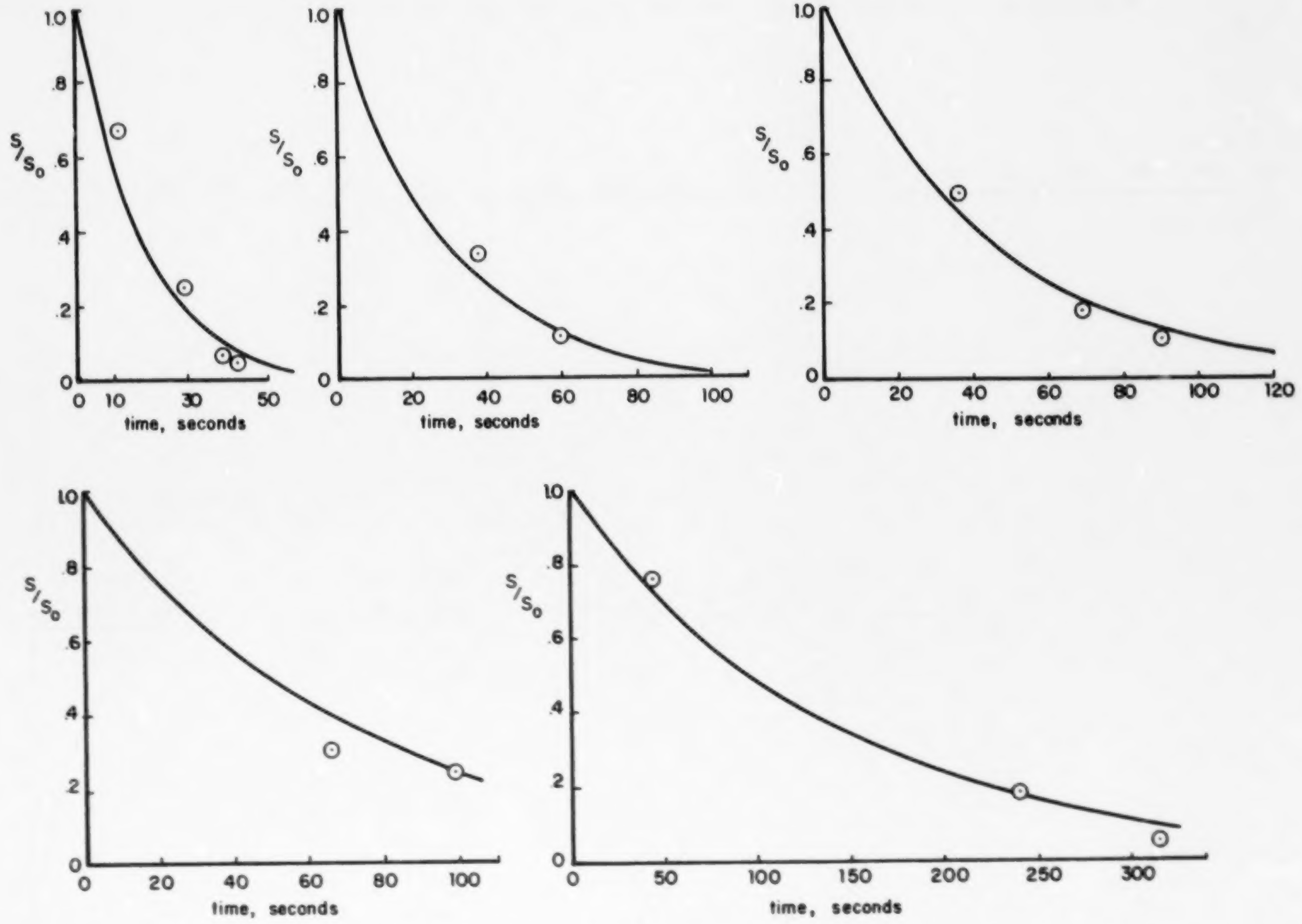

Figure A-1. Tetrachloroethylene in purified water. UV intensity = 0.375 W/L.

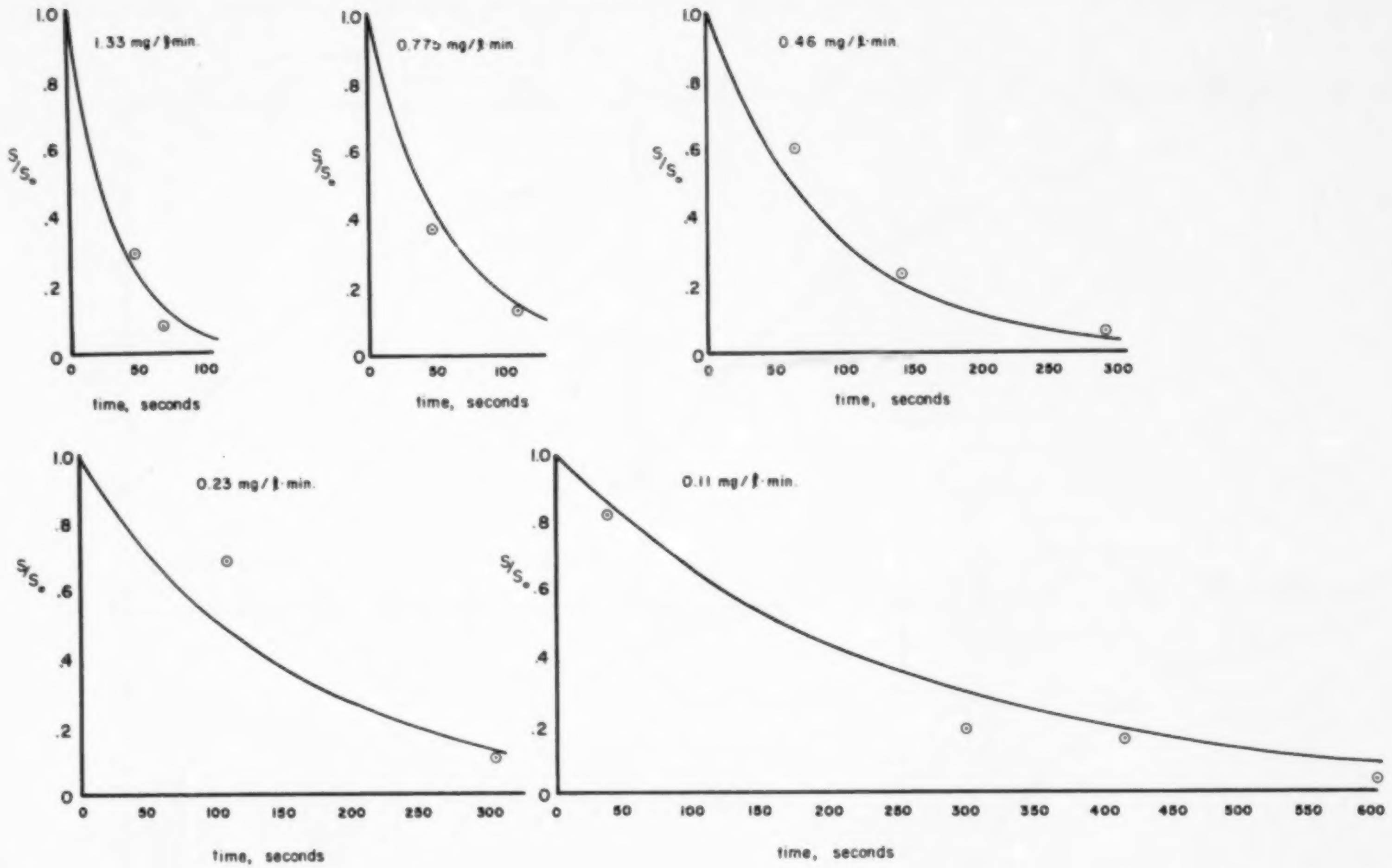

Figure A-2. Tetrachloroethylene in purified water. UV intensity = 0.189 W/L.

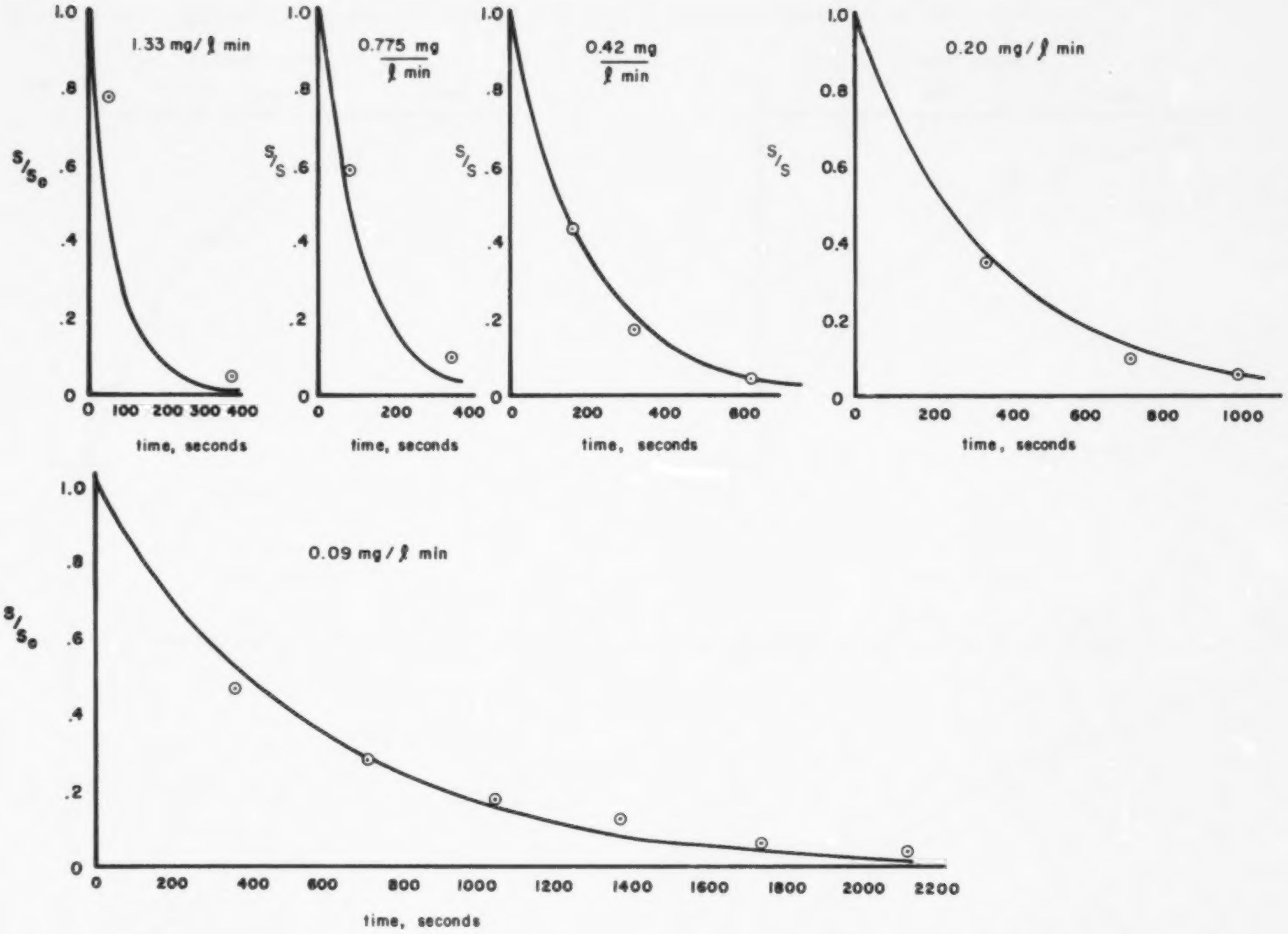

Figure A-3. Tetrachloroethylene in purified water. UV intensity = 0.091 W/L.

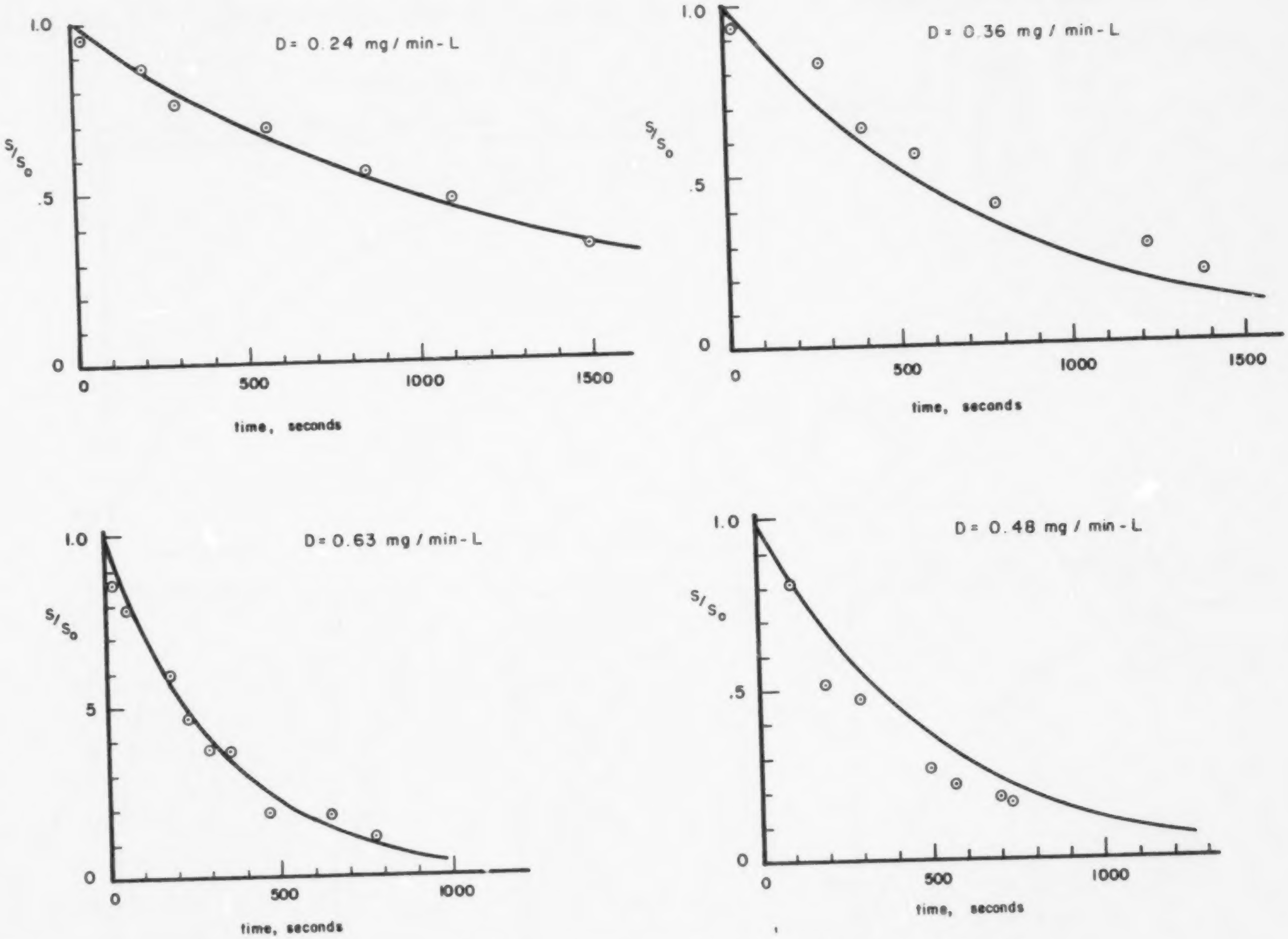

Figure A-4. Chloroform in purified water. UV intensity = 0.417 W/L.

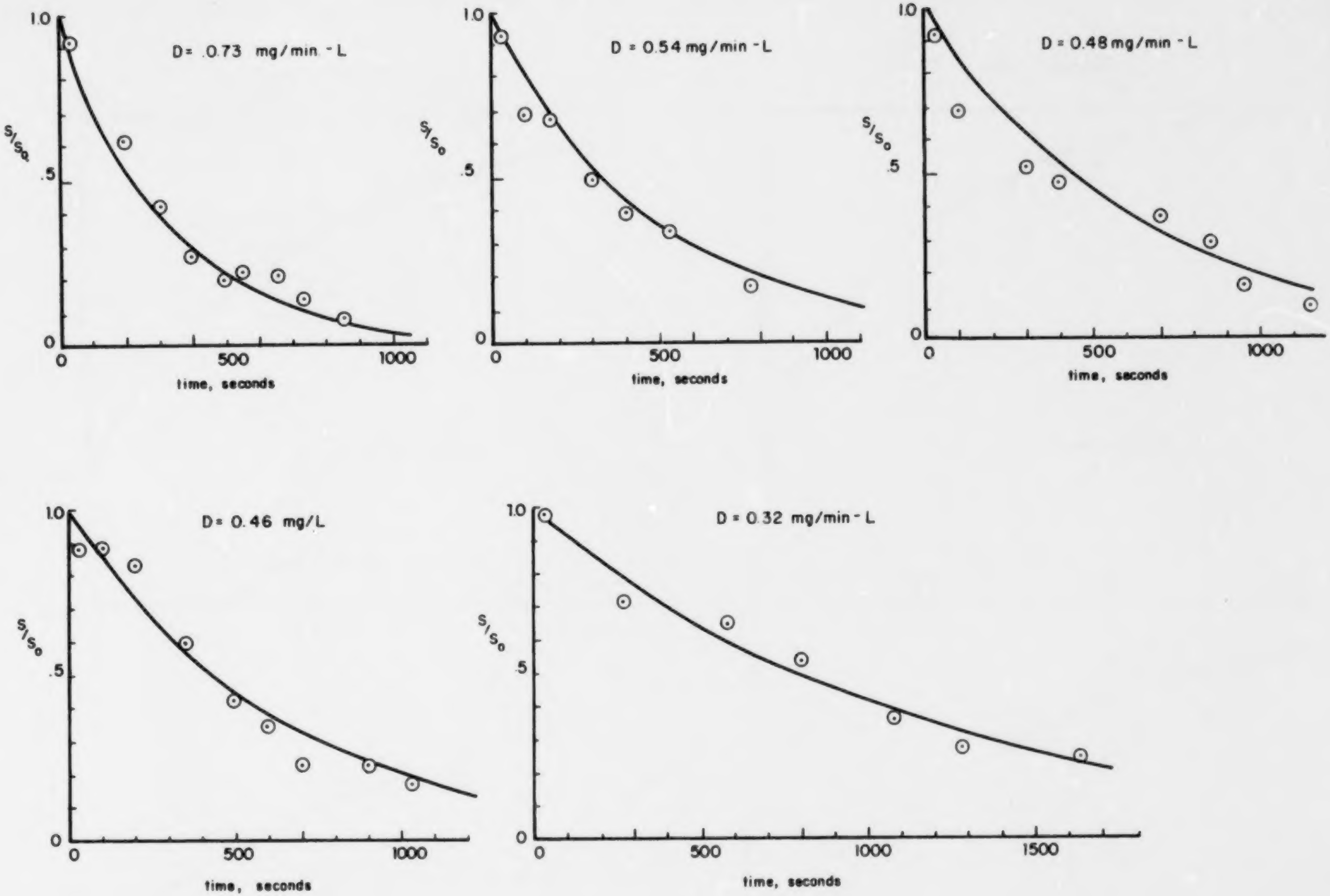

Figure A-5. Chloroform in purified water. UV intensity = 0.184 W/L.

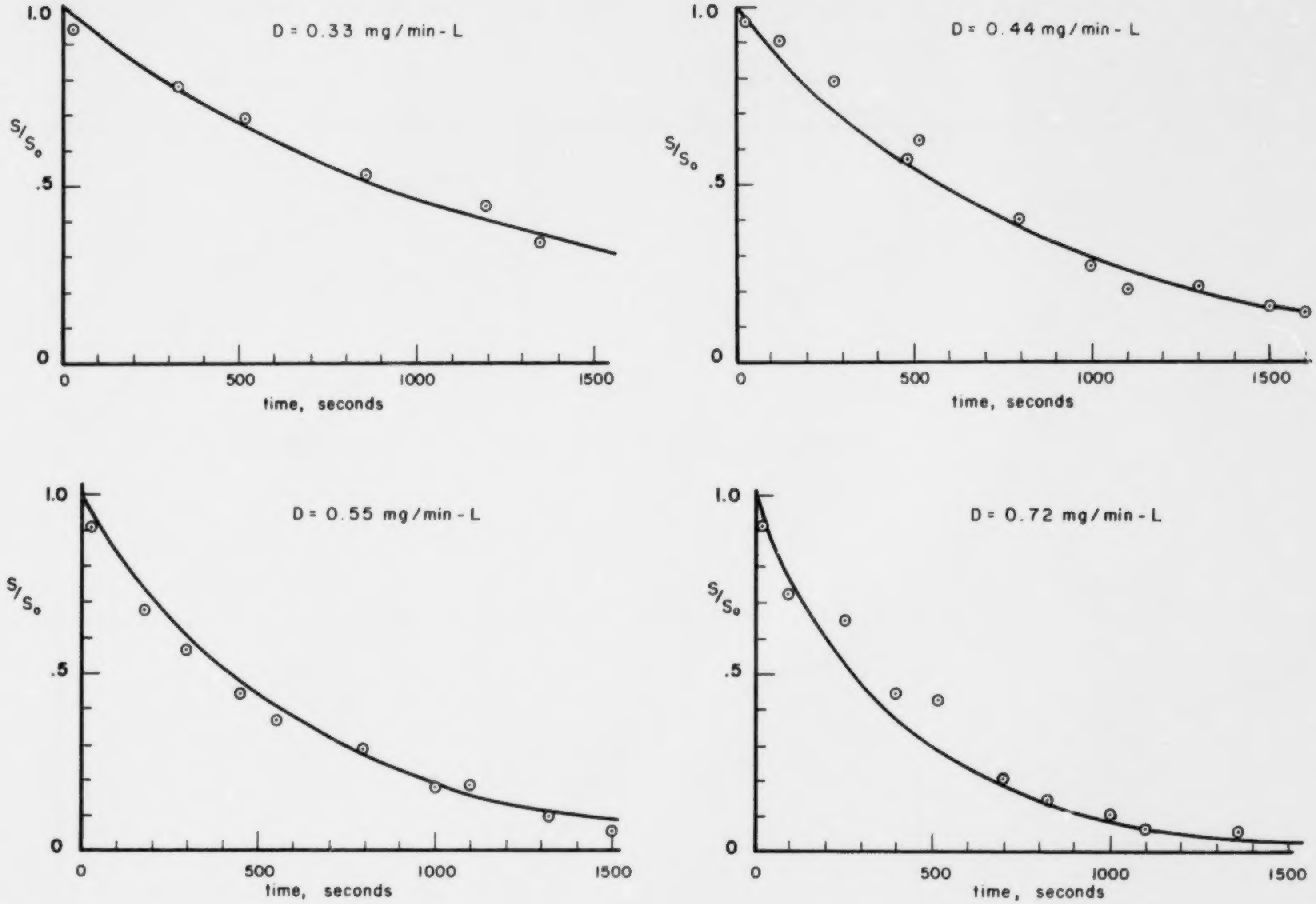

Figure A-6. Chloroform in purified water. UV intensity = 0.084 W/L.

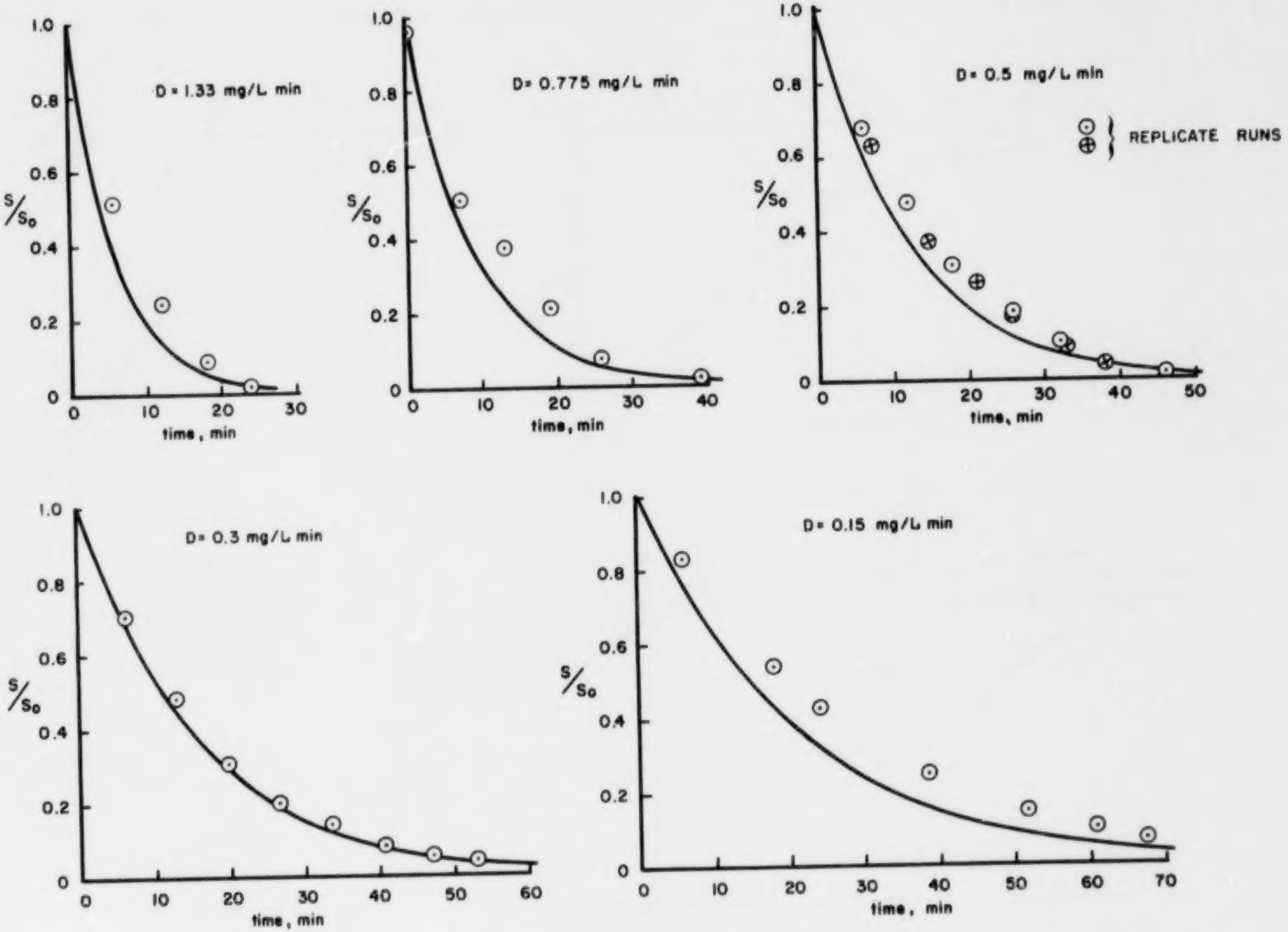

Figure A-7. Bromodichloromethane in purified water. UV intensity = 0.375 W/L.

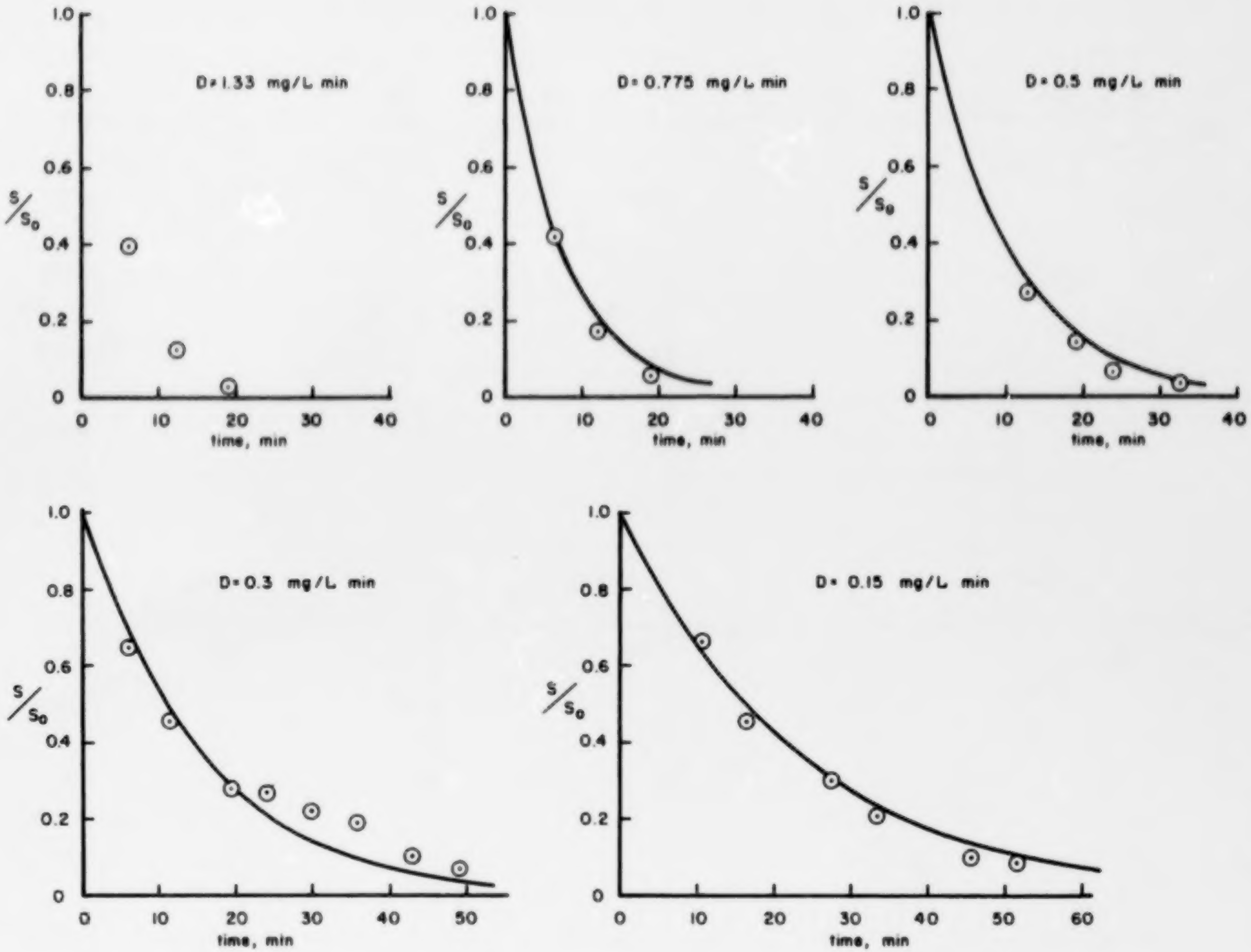

Figure A-8. Bromodichloromethane in purified water. UV intensity = 0.189 W/L.

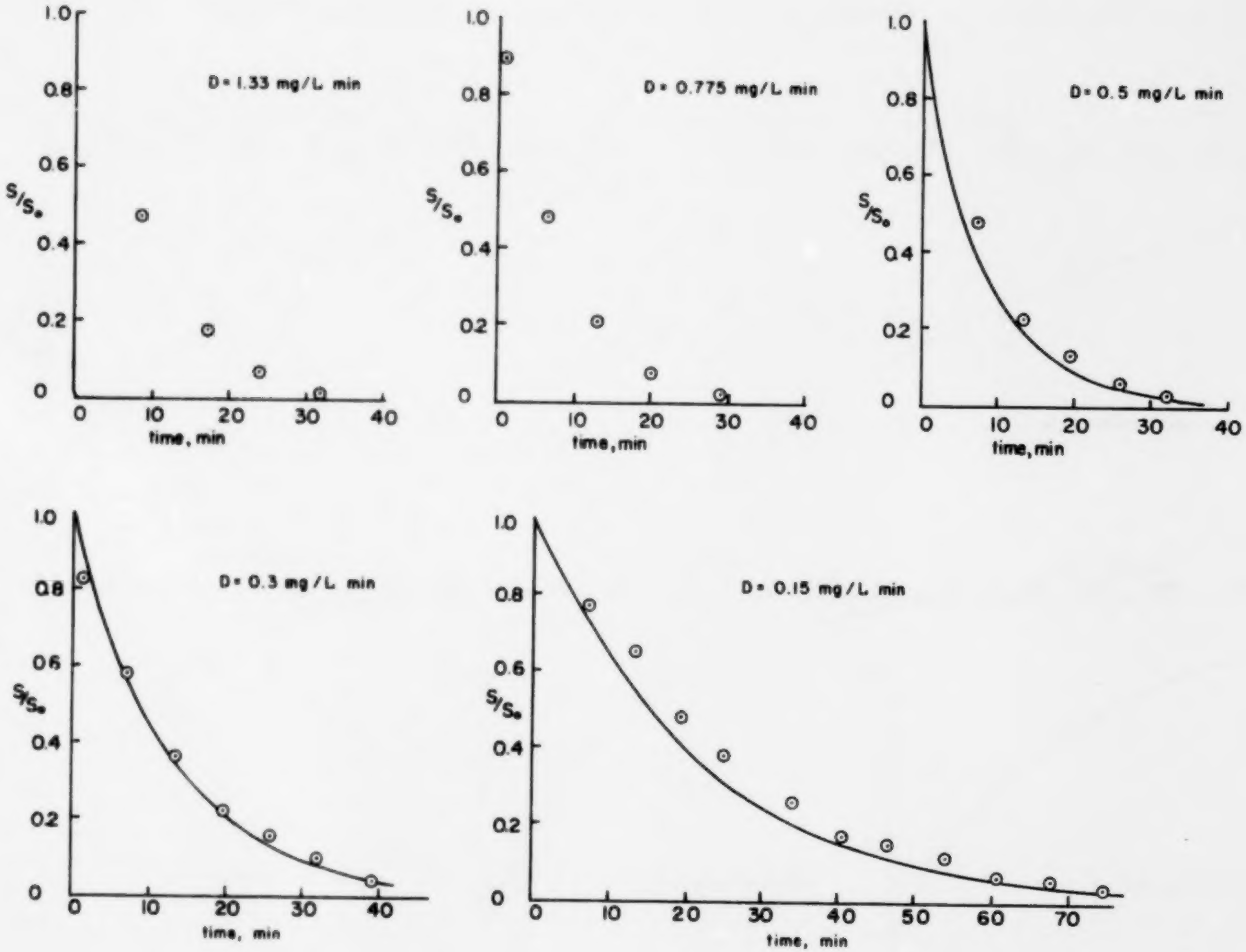

Figure A-9. Bromodichloromethane in purified water. UV intensity = 0.084 W/L.

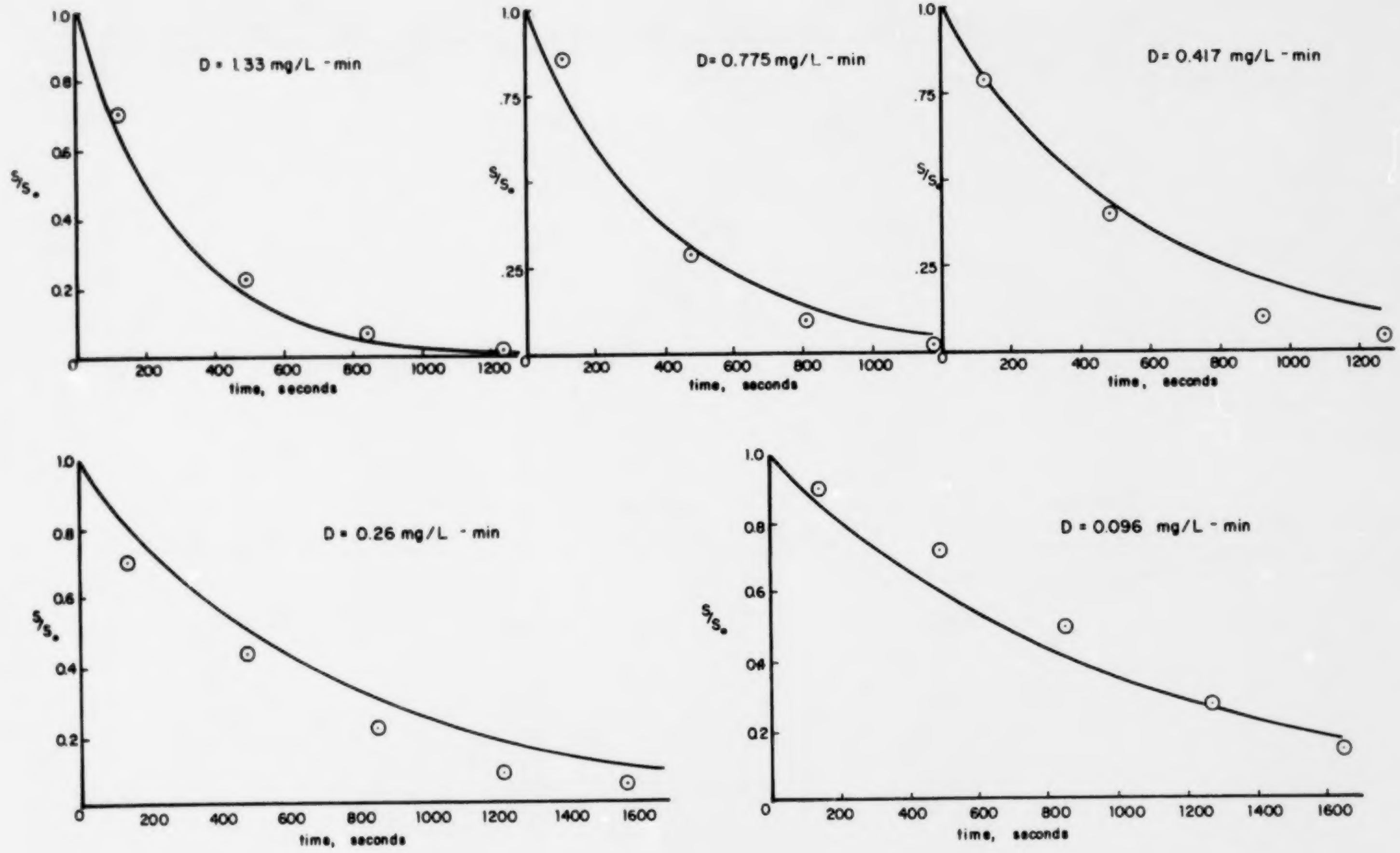

Figure A-10. Tetrachloroethylene in Lake Lewisville water. UV intensity = 0.375 W/L.

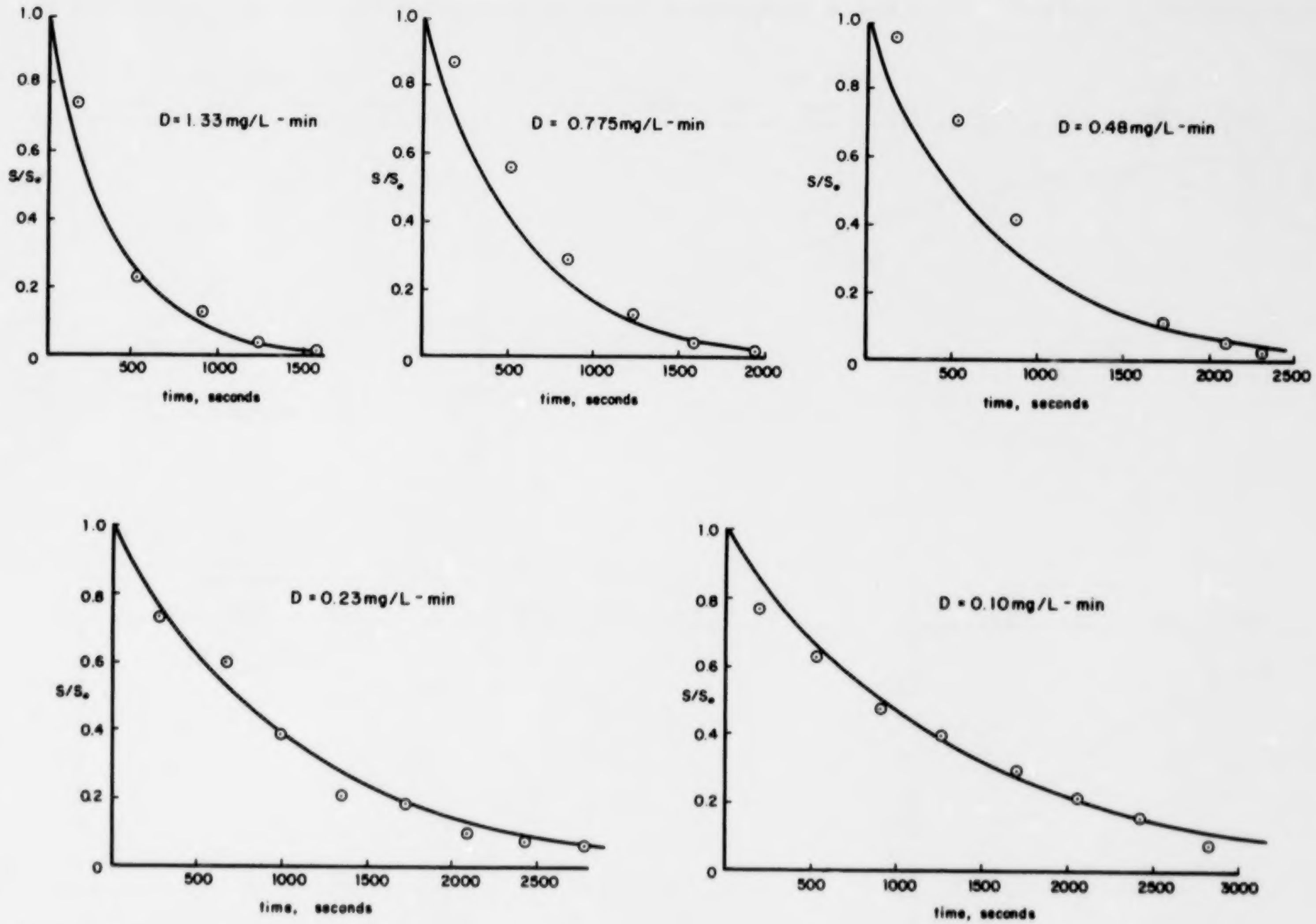

Figure A-11. Tetrachloroethylene in Lake Lewisville water. UV intensity = 0.189 W/L.

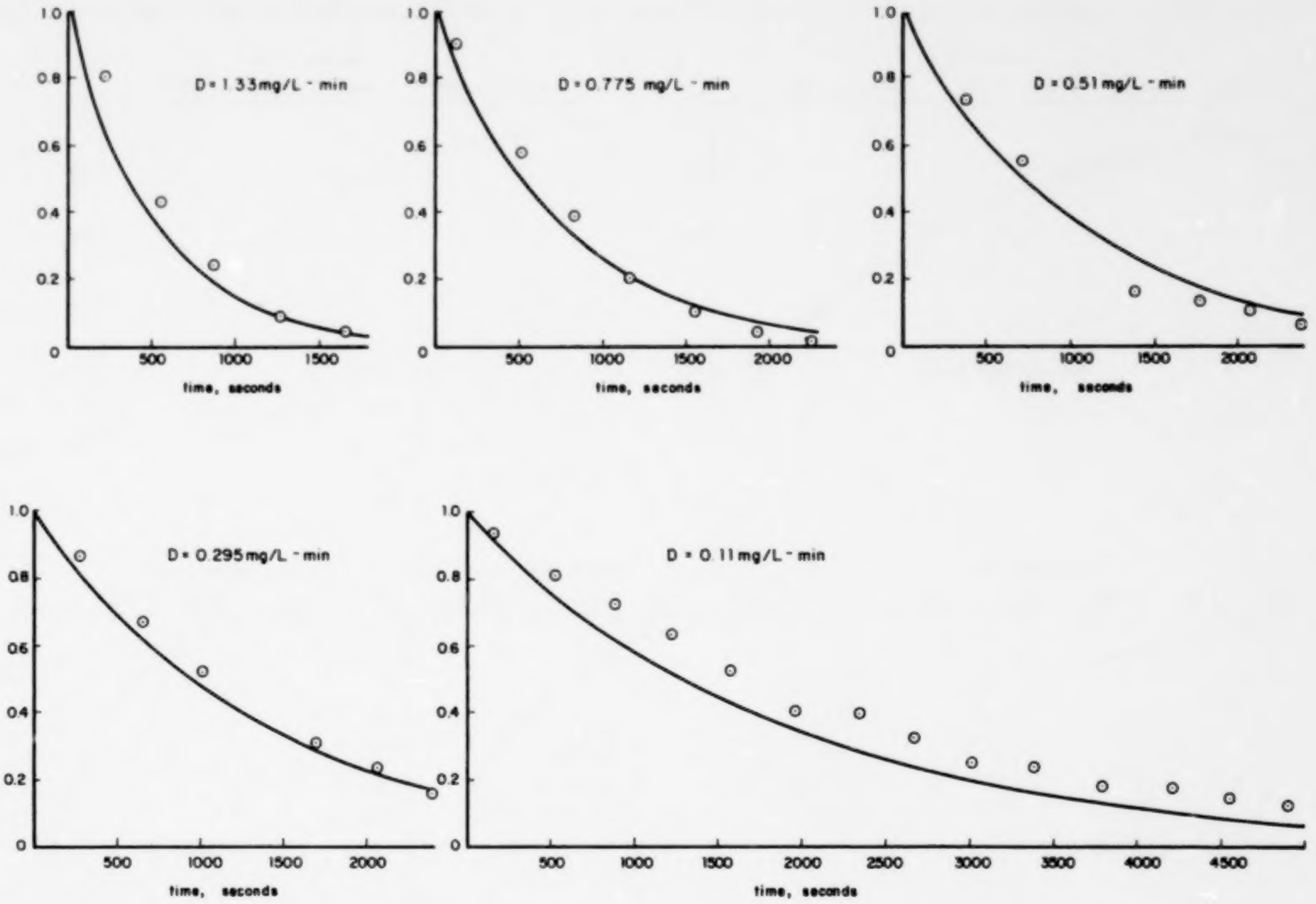

Figure A-12. Tetrachloroethylene in Lake Lewisville water. UV intensity = 0.189 W/L.

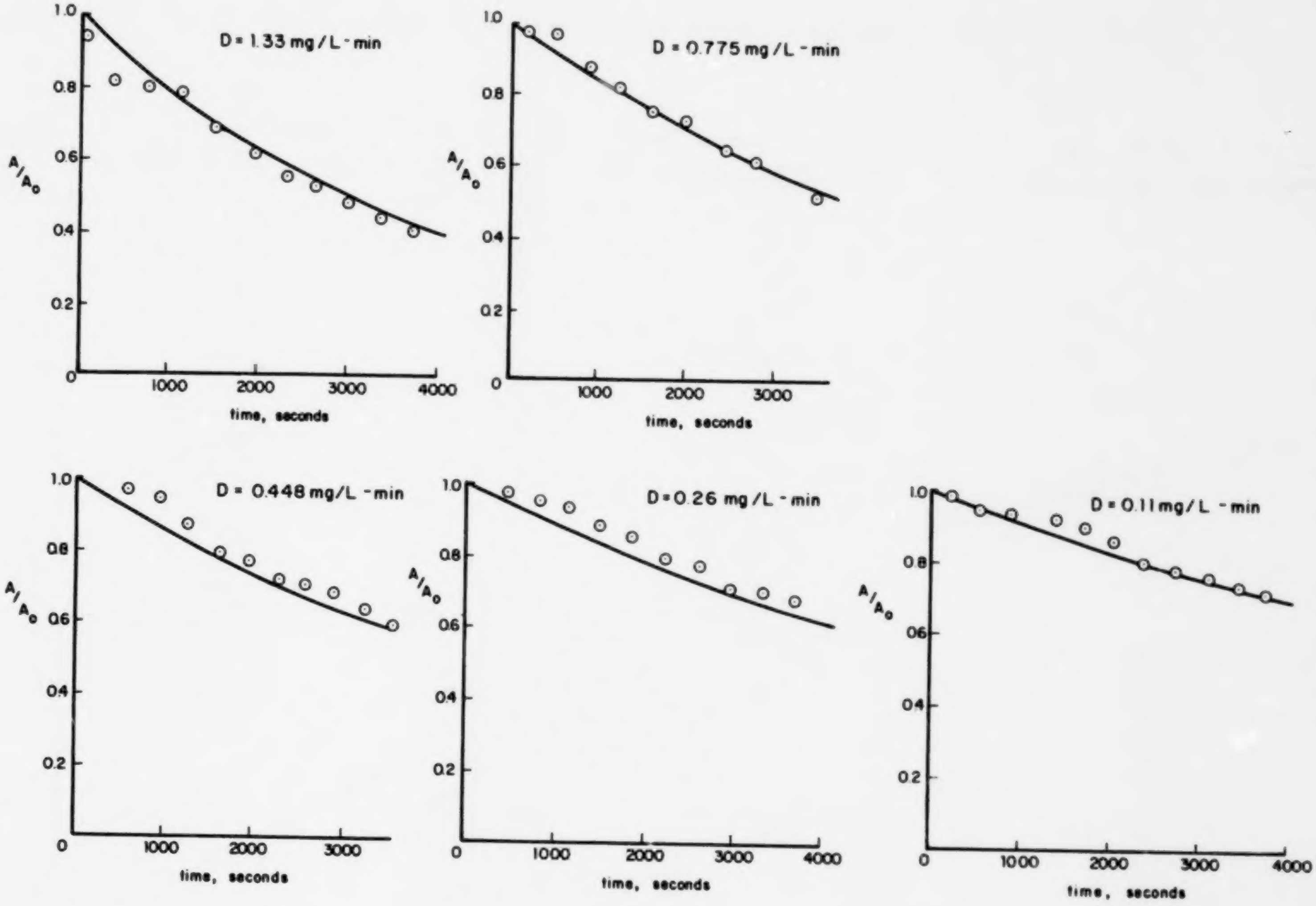

Figure A-13. Chloroform in Lake Lewisville water. UV intensity = 0.375 W/L.

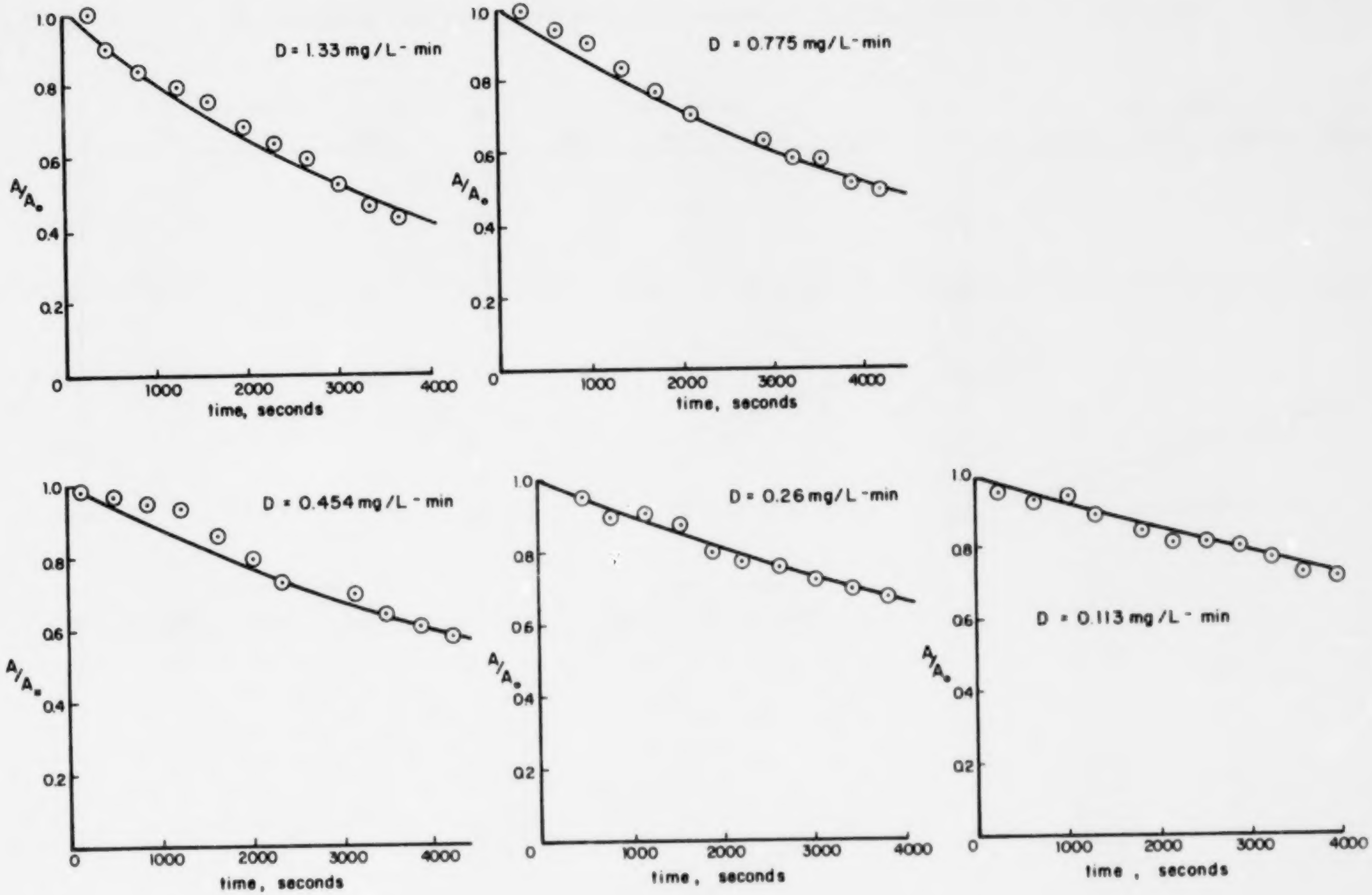

Figure A-14. Chloroform in Lake Lewisville water. UV intensity = 0.189 W/L.

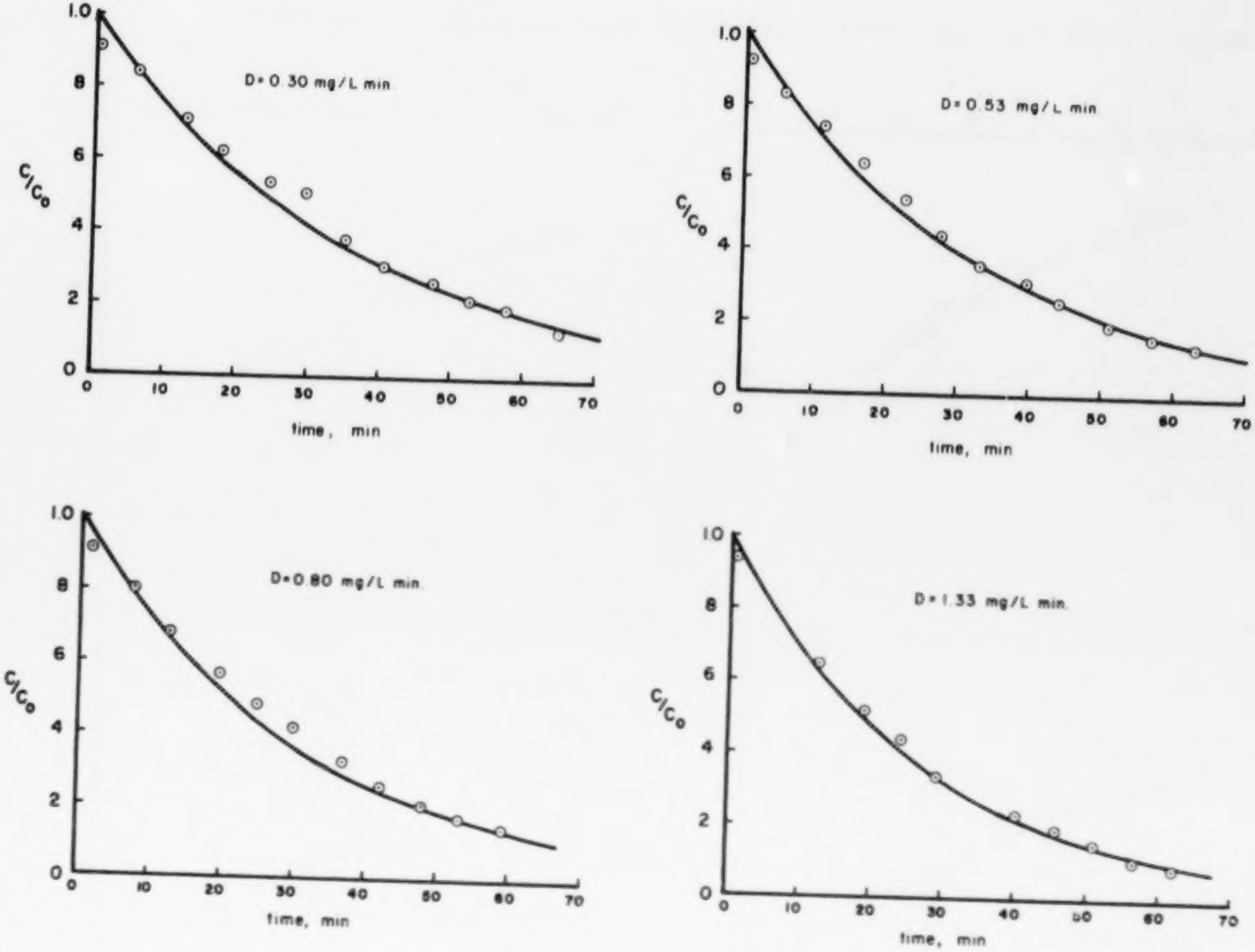

Figure A-15. Bromodichloromethane in Lake Lewisville water. UV intensity = 0.375 W/L.

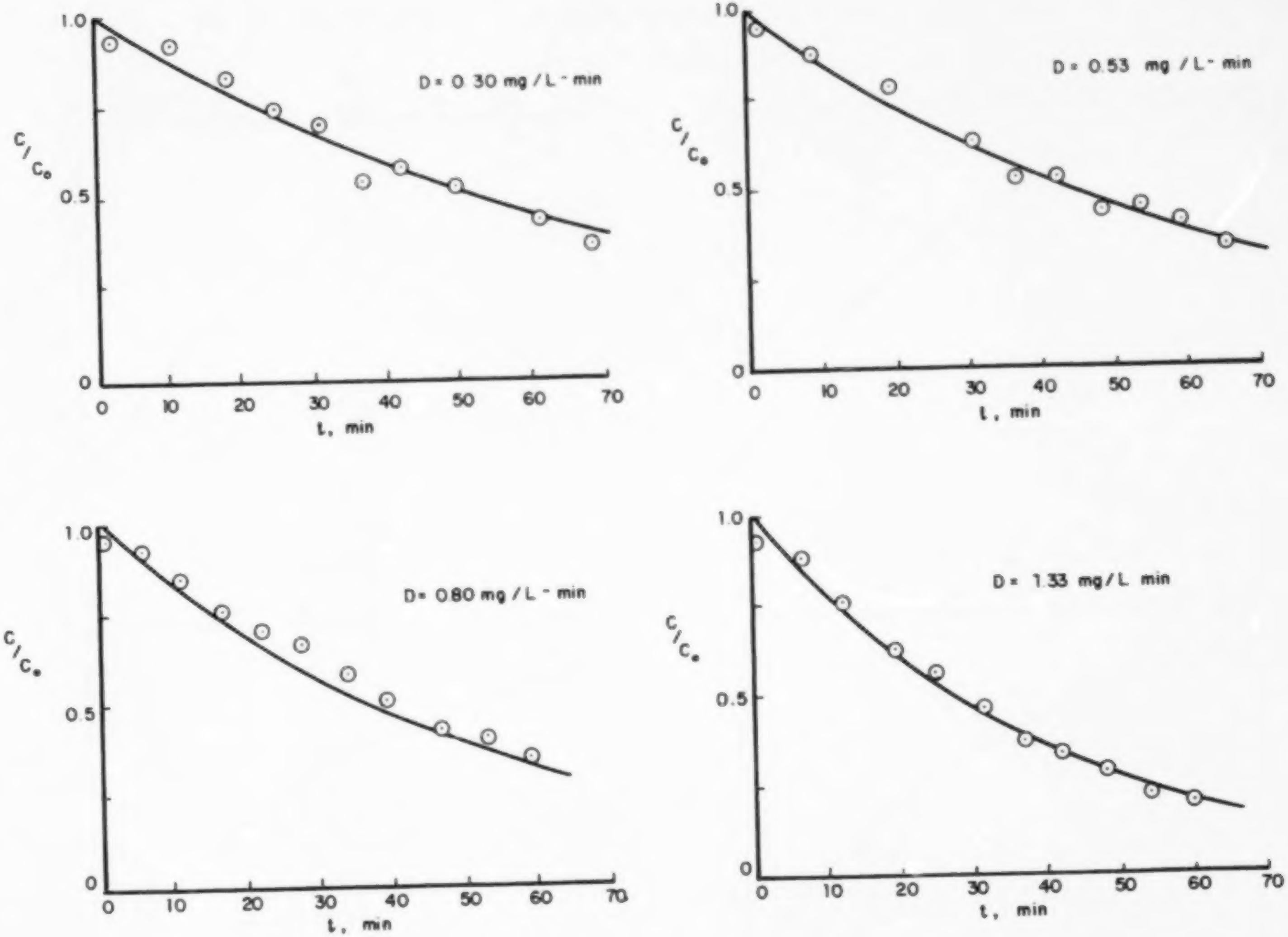

Figure A-16. Bromodichloromethane in Lake Lewisville water. UV intensity = 0.189 W/L.

APPENDIX B

CHEMICAL KINETICS OF OZONE/ULTRAVIOLET-INDUCED REACTIONS OF ORGANIC COMPOUNDS IN WATER - EXPERIMENTAL DETAILS

CONSTRUCTION OF THE REACTION SYSTEM

The ozone contacting reactor used in this work was a 6 inch O.D. by 10 inch high quartz bell jar with flat flanges, which was purchased from Quartz Scientific Inc., Fair Park Harbor, Ohio (Figure 11, main report). The cover, impeller, sparger and baffles are fabricated from Pyrex glass and fitted to the bell jar by Mr. Tom Denton, glass-blower of the Department of Chemistry, North Texas State University. The impeller is driven by an electric motor with glass shaft through a PFTE O-ring. The stirring speed is controlled by a variable transformer which is calibrated using a RMP Tachometer Model C-891, Power Instruments, Inc., Skokie, Illinois. The openings on the cover are used for inlet and outlet of ozone/oxygen gas mixture, also for introducing substances to the reactor and withdrawing samples for analysis. Stainless steel Swagelok nuts and Teflon ferrules are used for sealing the openings. The whole reactor is set and locked into an aluminum stand made by the machine shop of the Physics Department, North Texas State University. The dimensions of the entire reactor are such that it fits snugly into a Rayonet Photochemical Reactor, the Southern New England Ultraviolet Co., Middletown, Connecticut, which is equipped with low pressure mercury lamps, R.P.R. 2537 Å, concentric to the reactor axis. Up to a total of sixteen lamps may be used, each of which is rated at 14.0 watts. The spectral energy distribution of the 2437 Å lamp is shown in Figure B-1.

The geometry of the contacting reactor is designed such that when three liters of solution is contained it will be fully exposed to the radiation of the lamps.

Figure B-2 shows the schematic diagram of the photolytic ozonation system. Oxygen (O) is fed to the generator, Grace Model LG-2-L2, W. R. Grace & Co., Columbia, Maryland, via valve (A). The concentration of ozone in the gas can be varied either by variation of gas flow (B) or primarily by the generator reaction chamber pressure and voltage. Under certain conditions a portion of the gas from the generator is vented to the ozone destroyer (P) so as to give the desired flow of O_3/O_2 gas into the reaction flask.

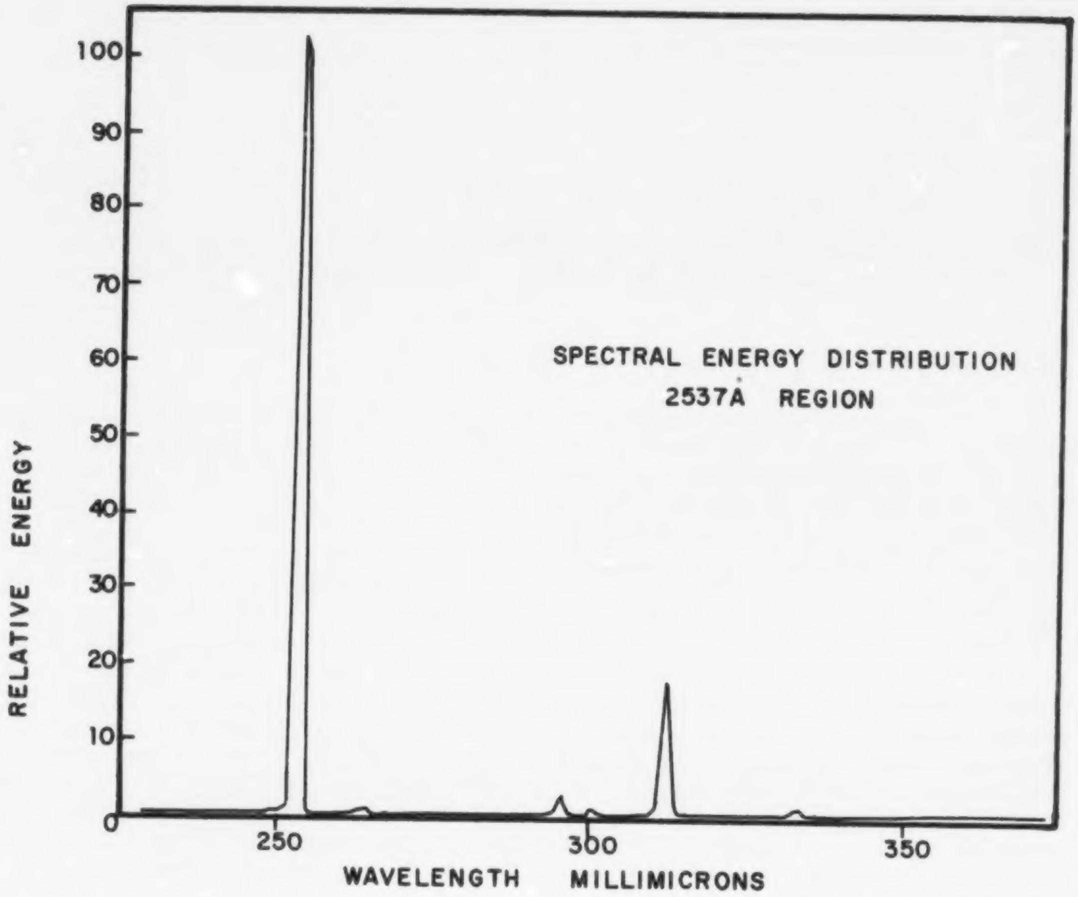

INTENSITY READINGS IN MICROWATTS/cm^2 AT:

WAVE LENGTH (A)	2 INCHES FROM LAMPS
2537	16000
2652	488
2804	16
2894	22
2967	83
3022	40
3129	313
3654	267
4047	316
4359	960
5461	523
5780	113

Figure B-1. Spectral distribution from ultraviolet lamp.

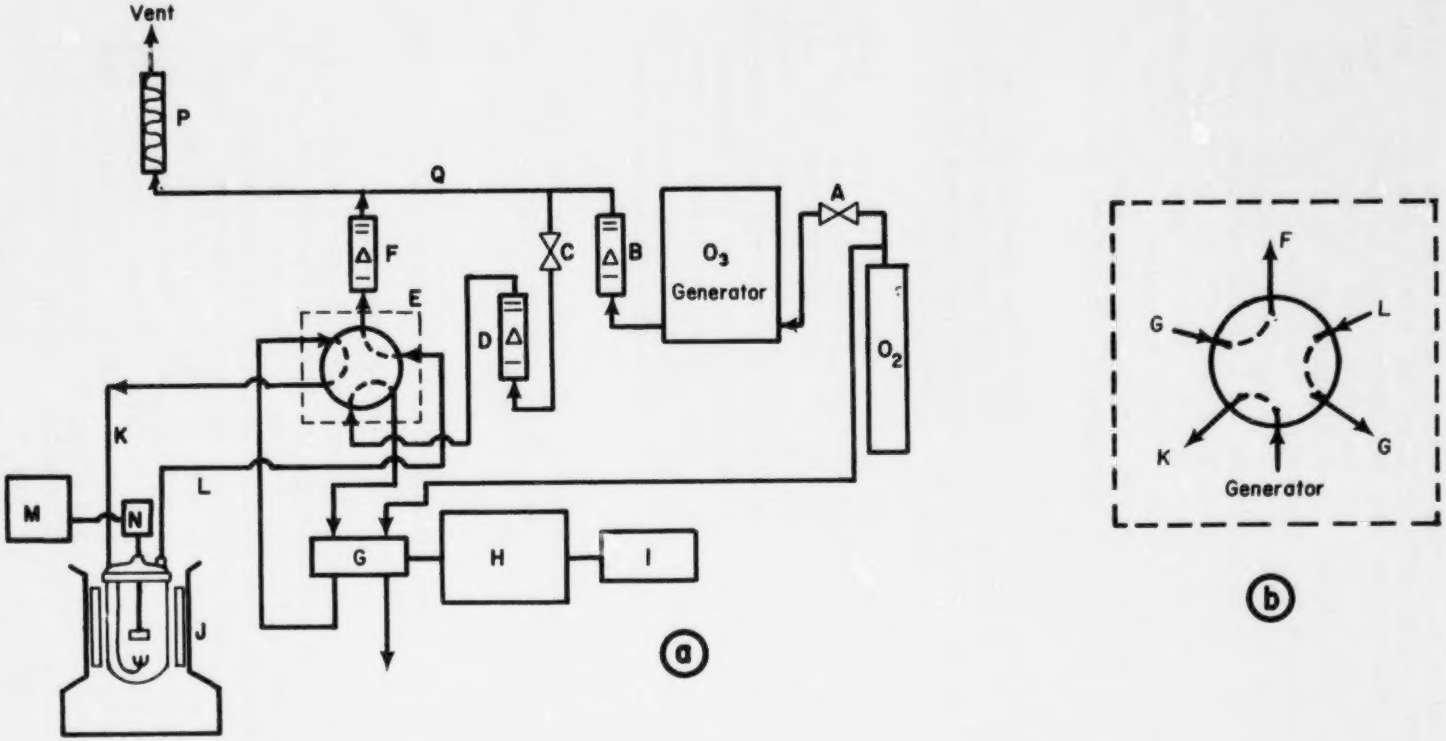
Vent
P
Q
F
E
C
B
O₃ Generator
A
O₂
D
K
L
M
N
G
H
I
J
a
F
G
L
K
G
Generator
b

(A)	VALVE	(I)	RECORDER
(B)	ROTAMETER	(J)	PHOTOCHEMICAL REACTOR
(C)	FLOW CONTROL VALVE	(K)	ENTRANCE TO REACTOR
(D)	ROTAMETER	(L)	EXIT FROM REACTOR
(E)	SIX PORT VALVE	(M,N)	STIRRER AND CONTROLLER
(F)	ROTAMETER	(P)	OZONE THERMAL DESTRUCTION UNIT
(G,H)	OZONE MONITOR	(Q)	VENT LINE

Figure B-2. (a) Schematic diagram of the photolytic ozonation system. (b) Alternative flow for ozone off gas measurement.

Flow of the gas stream in the reaction system is controlled by a six-way valve (E), made of one disc of stainless steel and one block of Teflon. The valve may be connected in such a way to direct either inlet O_3/O_2 (K) or the off-gas stream (L) to the UV cell (G) of an ISCO Model UA-5 Absorbance Monitor (H), Instrumentation Specialties Co, Lincoln, Nebraska (Figure B-2 insert). The monitor is originally designed for liquid chromatography. In this work, O_3/O_2 mixture is passed through the sample cell and oxygen from the gas cylinder (O) is used as reference. The readings of the monitor at 254 nm are calibrated to indicate the ozone concentration in the mixture. In order to monitor the changing of ozone concentration during the runs, an OmniScribe recorder (I), Houston Instrument, Houston, Texas, is connected to the UA-5.

In the normal flow configuration, the flow entering the contacting reactor is controlled by valve (C) and the flow rates entering (K) and exiting (L) from the reactor are measured by Fisher & Porter rotameters (D) and (F) respectively.

The O_3/O_2 mixture exiting from the generator is split into two streams so as to give the desired flow of O_3/O_2 gas into the reactor. One stream (Q) goes directly to the destroyer (P) and the other goes to the six-way valve (E). The destroyer is maintained at 350°C. All the O_3 in the split stream (Q) and reactor off-gas stream (L) is destroyed by passing through the heated tube and vented to an exhaust hood. The O_3/O_2 mixture in the reactor off-gas stream may be directed into the UA-5 monitor by the six-way valve for ozone concentration measurement as shown in the insert to Figure B-2.

The Rayonet Photochemical Reactor (J) has a fan on the bottom of the inside chamber to vent the heat generated from the lamps. The lamps are connected to the lamp-holders mounted on the shiny aluminum wall.

MEASUREMENT OF OZONE DOSE RATE, OZONE CONCENTRATION IN SOLUTION, AND ULTRAVIOLET RADIATION FLUX

Three liters of boric acid buffered potassium iodide solution (BKI) (150) made from deionized, carbon filtered water is placed in the reactor and stirring begun. The gas flow rate of the O_3/O_2 mixture into the contacting reactor is measured, and samples of the resulting iodine solution are withdrawn. The concentration of iodine is determined colorimetrically at $\lambda = 352$ nm on a Spectronic 20 (Bausch & Lomb, Rochester, N.Y.), which is previously calibrated by standard iodine solution (151). By knowing the time between two samples and the flow rate, the ozone dose rate in mgO_3/min-L liquid can be calculated for a fixed reading on the UA-5. A calibration curve of absorbance vs. concentration of ozone in the gas mixture is constructed for direct ozone concentration measurement with the UA-5. The stoichiometry of the ozone/iodine reaction is assumed to be

$$2H^+ + O_3 + 2I^- \longrightarrow I_2 + O_2 + H_2O$$

Measurement of dissolved ozone in solution is as follows. A portion of the solution to be analyzed (1-5 ml., depending on the concentration of ozone) is withdrawn and mixed immediately with BKI solution to make a total volume of 10 ml. The resulting iodine absorption is measured on a Spectronic 20 and compared with a calibration curve as described above. The concentration of ozone in solution is expressed as $mg/L_{liq.}$.

The effective radiation transfer rate from one or more lamps of the Rayonet Photochemical Reactor is measured by ferrioxalate actinometry. The calculation of photons being transferred into the reactor is adapted from Parker (152). The effect of gas flow and stirring rate on radiation transfer rate is also measured.

MATERIALS

The water used in this work was prepared by purifying the deionized, distilled water which was supplied by Ahlfinger's Water Corp., Dallas, Texas. The water in a five-gallon glass jar was forced by nitrogen through a four foot long by one inch O.D. glass tubing containing 22 inches of Filtrasorb 400 activated carbon (Calgon Corp.), 12 inches of XAD-4/8 (Rohm and Haas), 1 inch of Bondapak C18/Corasil (Waters Associates) and a 0.45 micron filter (Millipore Corp.). The TOC content of this water was checked periodically with a Dohrmann DC-54 Organic Carbon Analyzer and generally was below 600 μg/L. The resulting water was used for all the kinetic studies in purified water medium and for determination of by-products in this work. The purified water for ozonation and photolytic ozonation runs was further purified by applying a high ozone dose rate with UV radiation for at least twenty minutes to destroy ozone demand which might be present. Water temperature was ambient. For kinetic studies in purified water, no pH adjustment was made, so that no additional ions would be present to serve as radical scavengers. The pH of this purified water was 6.5 - 7.0. When a different pH was needed, it was adjusted using NaOH and H_2SO_4 solution for pH = 4, 6 and 8, and Borax buffer for pH = 10.

Water was collected from Lake Lewisville, Texas, and stored in five-gallon glass jars with good sealing. Before being used as a medium for photolysis, ozonation and photolytic ozonation the water was double-filtered through Whatman Quantitative 1 and 4 filter papers. The carbonate, bicarbonate, ammonia and COD contents had been checked according to Standard Methods (157) and TOC was also measured.

Model compound HCB was either obtained from Analabs, Inc., North Haven, Connecticut or synthesized in the laboratory by Ullman's method (153-156). 2,4,6-trichloroaniline was obtained from Aldrich Chemical Corporation, Inc.; sodium nitrite and copper dust (electrolytic grade) from Fisher Scientific Co.; pentane, methanol and hexane, nanograde, from Mallinckrodt, Inc.; internal standard, hexachlorobenzene, from EPA, Research Triangle Park, N.C. All other standard laboratory chemicals were of reagent grade.

PREPARATION AND ANALYSIS OF SAMPLE SOLUTIONS

Stock solutions of chloroform, bromodichloromethane, and tetrachloroethylene were prepared by stirring pure compound in contact with water until it dissolved to produce an almost saturated solution. The concentration of this solution was determined by gas chromatography from comparison with weighed standard solutions. The reaction mixture was prepared by spiking 3 L of water in the reactor with the appropriate amount of concentrate to yield a concentration of 100 µg/L. Direct aqueous injection was used on all dilute aqueous solutions after determining the blank value of the water itself, which was always low (0-2 µg/L). Direct aqueous injection gas chromatography was performed on a 2 mm i.d. X 6' chromosorb 101 (100/120) column at 160° - 200°C depending upon the compound. Detection was by Tracor or Hewlett-Packard ^{63}Ni electron capture, the signal of which was electronically integrated.

Trihalomethane precursors (TTHMFP) were analyzed by chlorination of the samples at an applied dose of 50 mg/L chlorine for three days. Previous studies had shown that for Cross Lake water, three days was sufficient time to reach the plateau in trihalomethane (THM) formation. At the end of three days, excess chlorine was quenched with sodium sulfite and THMs analyzed by liquid-liquid extraction with pentane. The samples were buffered to pH 6.5 using phosphate prior to the chlorination, and the samples were stored in the dark at 26°C for the three day reaction period. Gas chromatography of non-aqueous solutions was on a 6' X 2 mm i.d. column of 12½ % Squalane on Supelcoport (100/120) using electron capture detection.

Because of the limited solubility of hexachlorobiphenyl (HCB), a different procedure was used for preparation of HCB solutions. Model compound, HCB, was weighed to 0.1 mg and dissolved in methanol as a stock solution. An 18 µl portion of this solution was spiked into 3 liters of water to give the 60 parts-per-billion (µg/L) concentration which was used for all the kinetic runs. A portion of the solution was withdrawn from the reactor at 1, 3, 5, 10, 15, 20, 25, 30, 35, 40, 45, 50, 60, 70, and 80 minutes after the runs began. In some cases, zero time sample was also withdrawn, but this practice was of quite limited value since a finite mixing time is required to achieve homogeneity. Each sample was placed in a twenty-five mL glass vial containing 0.5 mL of ozone quenching reagent (120 mg total of Na_2SO_3). The sample solution was withdrawn from the reactor by using a glass syringe and used to fill the vial up to an engraved mark on the vial indicating a 20.5 mL volume. One mL of hexanes containing internal standard, hexachlorobenzene, was added. The vials were put on a Lab-Line Junior Orbit Shaker, Lab-Line Instruments, Inc., Melrose Park, Illinois, and shaken at the highest speed for twenty minutes. A 3 µL aliquot of the organic layer was injected into the gas chromatograph for detection of internal standard and HCB.

Gas chromatographic (GC) detection of HCB and internal standard was performed on a Model 560 isothermal gas chromatograph, Tracor, Inc., Austin, Texas, equipped with Ni-63 electron capture (EC) detector. A 1 foot by ¼ inch O.D. glass column containing 10% SP-2100 on 100/120 mesh Supelcoport, Supelco, Inc., Bellefonte, Pennsylvania, was used. Carrier gas was 10% methane and 90% Argon, Union Carbide Corp., Linde Division. The oven temperature was kept at 176°C; injection port and detector were at 200°C and 350°C respectively. A programmable computing integrator, Supergrator-3, Columbia Scientific Industries, Austin, Texas, was used to quantify and record the heights and areas of the GC peaks.

PROCEDURE FOR KINETIC RUNS

During the kinetic runs, it was desirable insofar as possible to have the ozone flow and UV light equilibrated within the reactor before substrate was added. Because of the required mixing time, this procedure did not give a true zero-time measurement of substrate concentration, but surmounted severe mathematical difficulties involved with a non-constant ozone concentration. In all cases where the reaction was first-order in substrate (all model compounds but HCB), it was the slope of the semi-log plot which was of importance, as will be explained later, so that the exact initial concentration did not have to be known. Therefore, the spiking of substrate was done in such a way as to introduce a nominal 100 µg/L (±5-8%) of substrate at time = 0 into a steady-state ozone/UV system. Furthermore, since 10-30 µmoles/L of ozone per minute were being introduced into a system to which 0.6 - 0.9 µmoles/L of substrate had been added, perturbation from that steady-state was minimized, providing a good approximation to a pseudo-first order system. This procedure avoided having to solve the simultaneous differential equations which would result if the reactor could not be assumed to be in a steady state at the beginning of the reaction.

The experimental procedure, therefore, was to place three liters of purified water into the reactor, then introduce the desired ozone flow and dose rate into the reactor with the desired intensity of UV present, until the ozone concentration stabilized. The necessary amount of aqueous solution of test compound was then added and the timer started. Samples were withdrawn periodically by syringe and directly injected into the chromatograph for analysis. During the experiments, ozone concentration in the liquid and in the gas streams into and out of the reactor was monitored. In the case of tetrachloroethylene, the higher dose rates gave a reaction which was so fast that only one data point could be collected before the substrate in the reactor was depleted below the detectable level. In these cases, substrate was respiked and the sample withdrawn after a different elapsed time. This process was repeated until a sufficient number of points had been collected to construct a disappearance curve.

Since the solubility of HCB in water is very low, it was first dissolved in methanol, as described previously. To begin a run, 18 µL of that stock solution was spiked into the water in the reactor, resulting in a substrate concentration of 60 µg/L. Sampling and analysis then proceeded as described in the previous section.

Experiments to determine the rate of destruction of substrate by ozone without UV (ozonolysis or "ozone-only") were conducted identically but with no UV radiation present. Experiments to determine the rate of destruction of substrate by UV with no ozone present (photolysis or "UV only") were conducted identically to the ozone/UV experiments but the O_3/O_2 gas stream was replaced by nitrogen at the same flow rate. Experiments with nitrogen flow and no UV were conducted to determine the rate of purging of substrate from the reactor in the case of a volatile substrate or of adsorption to the walls in the case of a hydrophobic substrate such as HCB, and these rates used to correct the experimental results of other runs.

When investigating the kinetics of destruction of the test compounds in a natural water matrix, the ozone flow and UV radiation could not be equilibrated prior to the beginning of the experiment because of the degradation of the natural organics which would occur. For these experiments the natural water was spiked with test compound and the preset ozone concentration and UV turned on at time = 0. Sampling was then conducted as described previously. As with purified water, a sample of the natural water itself was anlyzed to provide a blank to be subtracted from results obtained during the run. In almost all cases, the blank was found to be negligible.

EXPERIMENTAL DIFFICULTIES

Since ozone is so reactive and the ozone/UV process in particular is not well understood, it is worthwhile to mention a few of the experimental difficulties encountered in this investigation, in order to save other investigators from encountering the same pitfalls.

The single greatest difficulty encountered was the consistency of the water used in the experiments. When a natural matrix was used, 20-30 gallons was collected at one time since it was found that even just a couple of weeks later, the lake water might have greatly different properties. It was not practical to store the entire 20-30 gallons at 4°C so series of experiments were performed continously over a period of just a few days. Even under these conditions it could be seen that the water was changing somewhat during the period of storage. Naturally this change is to be expected in an actual treatment situation also, but in a kinetic study of this type, small changes can affect the apparent dependency of the reaction rate on, for example, UV intensity more than the actual rate of any one experiment appears to be affected. It is strongly recommended that investigators store natural water at 4°C and perform groups of experiments on the same water in the shortest possible time span. The addition of chemical preservatives is questionable without further investigation, due to the radical scavenging properties of many substances.

A source of even greater exasperation at the beginning of these studies was the difficulty of producing consistent good quality purified water. Reaction rate for indiscriminate free radical species with mixtures is shown in Section 4 of the main report to be proportional to the quantity

$$k_M[M]\,\Omega^{-1} = k_M\,[M]\,\{\sum_i k_i[S_i]\}^{-1} \quad ,$$

where $[S_i]$ is the concentration of substance i present and k_i is its reaction rate constant, and M represents the substrate of interest. Assuming for simplicity that the reaction rate constants are equal and that only one other component, S, is present

$$k_M\,[M]\,\Omega^{-1} = \frac{M}{M+S} \quad .$$

When M is large and the impurity S is small

$$M/(M+S) = 1 \quad .$$

But when M is small and S is large, as in the case of a micropollutant in natural water,

$$\frac{M}{M+S} \simeq \frac{M}{S} < < 1 \quad .$$

For the case of purified water, M ≈ 100 μg/L while S = TOC may be 100-600 μg/L. Clearly in this situation it is more important to have consistent water than extremely pure water, since compared to substrate level, the water cannot be absolutely pure. A natural consequence of this situation is that the purified water kinetics are probably not absolute rates, but are to be taken as the practical upper limit--a useful reference point--with the natural matrix studies at the other end of the scale.

As an aid in obtaining pure water, the water used in the purified water kinetic runs was "burned" with ozone/UV before introduction of the substrate. The effect of this burning is shown in Figure B-3, where two consecutive runs using the same water were performed. The data shown in the figure is from work early in the project, using water which was not as clean as that used in the kinetic runs reported below, and so the effect is exaggerated. Presumably, organic matter is present intially so that the substrate must compete with organic carbon for the active species. As the interfering matter is removed, the rate of substrate removal increases until the final rate in curve A is seen to approach that in curve B, where the same experiment has been rerun using the same water. In the later kinetic experiments, it is not known how much organic matter remained after the burn, hence the statement about these results being a practical upper limit. Other issues relative to this point will be discussed in a later section.

Another difficulty encountered at first was ozone measurement. The UV absorbance procedure described above is strongly recommended since it not only provides a continous monitor of the incoming and outgoing ozone stream, but also because is does not necessitate interruption or change in the back pressure of the gas stream in order to perform a measurement. The strip chart recorder informs the operator at a glance if an unnoticed power surge has occurred, not an uncommon occurence in these investigators' laboratory.

A third problem encountered in this investigation was the tendency of the power output of the UV bulbs to change over the weeks. It was found necessary to perform the actinometric calibration frequently to ensure a correct value for the UV intensity. It is not sufficient to merely state the manufacturers figures for power output, transmission coefficient of quartz, etc., as a 10% error can change the final kinetic expression considerably.

PROCEDURE FOR KINETIC RUNS ON DESTRUCTION OF TRIHALOMETHANE FORMATION POTENTIAL

Water Sample Sources

Ohio River water was shipped to the location of the ozone reactor (Houston Research Inc., Houston, Texas) by motor freight in epoxy-lined 55 gallon drums. Water from Caddo Lake, Texas

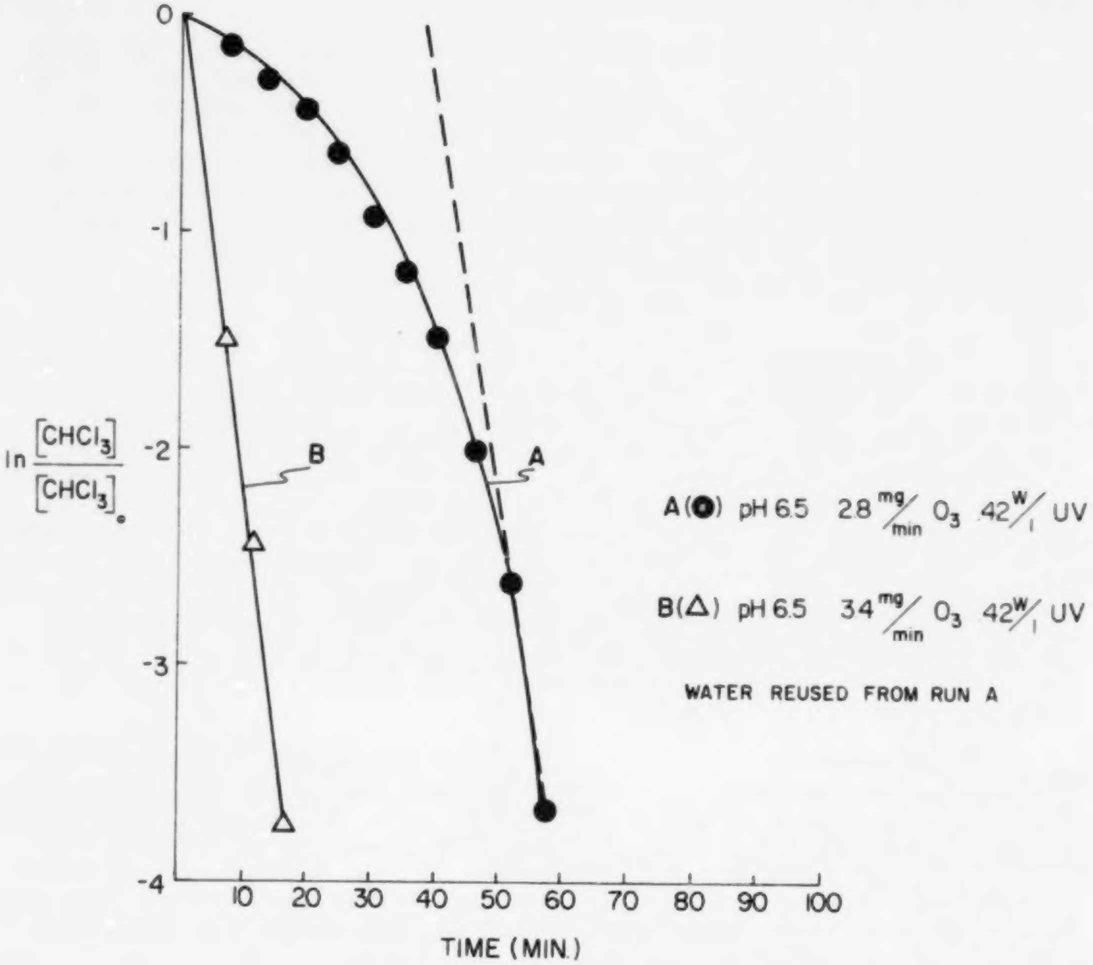

Figure B-3. Effect of water purity on photolytic ozonolysis of chloroform.

was shipped in 5 gallon glass bottles by private automobile. Ohio River water was used as received; lake water was run unfiltered and after filtration through S & S No. 588 paper. Humic acid (Aldrich Chemical) solutions were prepared in commercial distilled water which had been filtered through activated carbon (Calgon Filtrasorb 400) and an XAD-2 polisher (Rohm and Haas).

Ozonolysis and Ozone/UV Treatment

The reactor used in these studies has been described previously (103). It is a stainless steel cylindrical reactor of approximately 22 liter volume, designed so as to achieve maximum gas-liquid transfer. Ozone is generated by a W. R. Grace Model LG-2-L2 Corona generator using high purity oxygen. The transfer lines from the generator are stainless steel, and provision is made to divert the O_3/O_2 stream to an iodide trap for calibration of the ozone content entering the reactor. In later runs (on Caddo Lake water), provision was added to allow exit gases from the reactor to be trapped so that a calculation of ozone consumed could be made. Ports in the reactor allow for removal of samples during the course of a run, addition of reagents to the reactor, temperature measurement, etc. Two quartz wells extend into the reactor from the top; they house two Hanovia high-pressure mercury-vapor lamps, at 200 and 450 watts, respectively. A coil of metal tubing around the reactor may be used for cooling during photochemical runs; however, there is still some rise in temperature when lamps are used for sustained periods. Oxygen flow rates of 200 ml/min (STP) were used in all runs reported here. Ozone content of the gas stream leaving the generator was calculated by the iodide-thiosulfate procedure, and is expressed as mgO_3/l (STP) or as W/W%. Under the conditions used, 1% W/W O_3/O_2 corresponds to a dose rate of 14 mg O_3/sl of gas or 2.8 mgO_3/min.

The procedure for making an ozone or ozone/UV run was as follows: Twenty liters of river or lake water was charged into the reactor, which had been "cleaned" with deionized water plus ozone/UV for at least four hours. The reactor was capped and ozone flow introduced at a flow rate of 0.2 sl/min with a precalibrated ozone content. In the case of ozone/UV runs, either one or both of the lamps was turned on approximately five minutes prior to the introduction of the ozone.

In the case of humic acid runs, 20 l of "organic free" water was charged into the reactor and ozone flow (20 mgO_3/min) was initiated. After the ozone had stabilized at 2.2 mg/L, a concentrated solution of humic acid in 0.1 N NaOH was added so as to give a total humic acid concentration of 1 mg/L. Enough 6N sulfuric acid was immediately added to adjust the pH to 7.0. Ozone flow at 0.2 sL/min (7% W/W) was continued. In the case of

O_3/UV runs, the lamps were turned on at the moment of humic acid addition.

Sampling Procedure

Precursor levels were measured by chlorination of samples withdrawn from the reactor at time zero (before ozonation) and at intervals thereafter. Triplicate samples were withdrawn directly into 120 mL septum bottles containing excess ozone quenching agent (solid Na_2SO_3) and phosphate buffer, so as to give a final pH value of 6.5. The samples were immediately topped with PTFE-lined septa and sealed with crimped aluminum caps. These three samples were stored in ice and later shipped by air freight to Denton for analysis in the NTSU laboratory. One other sample drawn at the same time was used on-site to measure pH and residual ozone by the iodide-thiosulfate procedure.

Shipping time to Denton was approximately five hours in most cases. Upon receipt, the chilled samples were stored immediately in a standard refrigerator and processed after no longer than a sixteen hour total delay since sampling.

Chlorination of all samples was carried out by the same procedure. Chlorine water was added to each bottle with a microliter syringe through the septum. Sufficient chlorine was added so as to give the desired residual, usually 10 mg/L for Ohio River samples and 15 mg/L for Caddo Lake samples.

Samples were stored in the dark at 25±1° for seven days. On the final day, trihalomethane analysis was carried out by the pentane liquid-liquid extraction procedure developed in this laboratory (167). Generally, chlorine residual at the final day was in the 1.0-2.0 mg/L range.

APPENDIX C

CHEMICAL KINETICS OF OZONE/ULTRAVIOLET-INDUCED REACTIONS OF ORGANIC COMPOUNDS IN WATER - DETAILS OF KINETIC ANALYSIS FOR FIRST-ORDER SUBSTRATES

A MATHEMATICAL TECHNIQUE

The following is a brief explanation of a useful mathematical technique which is used extensively throughout the following sections. This explanation is intended to make the following section on kinetics more readable to those with limited mathematical background, and no attempt is made to be rigorous.

It is a property of logarithms that the log of a product is the sum of the logs:

$$\ln AB = \ln A + \ln B.$$

Another property of logrithms is that the log of a quantity to some power, b, is equal to b multiplied by the log of the quantity.

$$\ln B^b = b \ln B.$$

Combining these two properties gives the following expression:

$$\ln AB^b = \ln A + b \ln B.$$

This expression is useful in kinetic analysis since rate laws frequently have the form

$$-\frac{dS}{dt} = \text{Rate} = kS^a \;.$$

Taking the log of both sides yields

$$\ln \text{Rate} = \ln k + a \ln S, \qquad [C-1]$$

which is the equation of a straight line. Therefore, if ln Rate is plotted vs. ln S, the line will have slope a and intercept ln k. Use of this technique allows the step-by-step evaluation of the dependency of a rate expression on various parameters, as shown in several of the following sections.

KINETIC ANALYSIS OF OZONE/UV REACTIONS WHICH ARE FIRST ORDER IN SUBSTRATE

I. Purified Water as the Reaction Medium

A. Tetrachloroethylene--Since the rate of purging was found to be insignificant compared to the reaction rate of TCE, the purging term in eq. 71 of the main report was omitted and the data was modeled using a three-term equation of the following form:

$$-\dot{S} = \frac{-dS}{dt} = k_o\, S^{a}(O_3)_l^{b} + k_p\, I^{c}S^{d} + k_u I^{i}D^{m}S^{n} ,$$

$$\text{(ozonolysis)} \quad \text{(photolysis)} \quad (O_3/\text{UV})$$

Where S = substrate concentration in moles$\cdot L^{-1}$

I = UV intensity in $W\cdot L^{-1}$

$(O_3)_l$ = ozone concentration in liquid, in moles$\cdot L^{-1}$

D = ozone dose rate, in $mg\cdot L^{-1}\ min^{-1}$, where L is liters of substrate solution.

In addition, k_o, k_p, k_u = appropriate rate constants, and a, b, c, d, i, m, n = reaction orders, all to be evaluated experimentally.

The experiments using ozone alone were analyzed by first plotting $\ln S/S_o$ vs. t. Within the precision of the data, these plots were linear, indicating that reaction could be considered first order in substrate (a=1). The experiments are carried out by equilibrating ozone flow with purified water, then spiking 100µg/L of substrate (water concentrate) into the reactor at t=0, in order to have $(O_3)_l$ constant. Since there is a finite mixing time, there are temporary inhomogeneities in the reactor and the reaction has slightly different characteristics at the very beginning. Therefore, the following procedure was used to obtain rate constants.

For each experimental point, $-(\ln S/S_O)/t = k_O\ (O_3)_l^{b}$ was calculated and tabulated, as below:

t,sec:	390	730	1040	1400	1740	2160	2495	2845	3240
$10^5 \times (-\ln S/S_o)/t$:	153	121	115	107	109	109	106	105	105

Clearly, after the first couple of points, the reaction settles into first order. The procedure used was to start at the end of the table and work toward the front calculating the mean and standard deviation, then applying the 4σ rule (160) for outlying results to each successive value of $(-\ln S/S_o)/t$ until some value failed to fall within four standard deviations (σ) of the previously calculated mean. For the example given, only the first value was eliminated. The logarithm of the resultant $\overline{K}$ (average) was plotted along with error bars representing σ for the log of each ozone dose rate. This plot is shown in Figure C-1. The dotted line is a least squares fit of all five points, and is seen to miss the error bars on three of those five points. This line has a slope of 0.76. When the outlying point is eliminated, linear regression yields a line which fits all remaining points and has a slope of 0.98. This line was selected, the exponent forced to unity, and the appropriate correction made in the rate constant, yielding

$$\frac{-dS}{dt} = k_o \, (O_3)_1 S \text{ (for ozonolysis)}$$

$$\text{where } k_o = 5.87 \text{ L mole}^{-1} \text{ sec}^{-1}$$

To evaluate the photolysis term,

$$\frac{-dS}{dt} = k_p \, I^c \, S^d$$

$k_p \, I^c$ was taken as the slope of the (linear, if first order in S; i.e., d=1) $\ln S/S_o$ vs. t plot, and was calculated for 1, 2 and 4 lamps for two different dates (and therefore two different UV intensities, due to lamp deterioration). Of these data, the old 1 lamp data was found not to be first order in substrate and was eliminated. The remainder of the $k_p \, I^c$ values were divided by their experimentally determined I values to determine if they were first order in I (c=1). Again, the discarding of one outlying value (4σ rule) gave

$$\frac{-dS}{dt} = k_p \, IS \text{ (for photolysis)}$$

$$\text{where } k_p = 9.46 \pm 0.58 \times 10^{-3} \text{ L}\cdot\text{W}^{-1} \text{ sec}^{-1}.$$

In order to evaluate the ozone/UV term of the rate expression, $\ln S/S_o$ vs. t plots were made of the ozone/UV data, and were found to be linear; therefore

$$-(\ln S/S_o)/t = K = \{k_o (O_3)_1 + k_p I + k_u I^i D^m\} \; .$$

The first two terms in K were calculated from experimental data and the previously determined rate constants, and subtracted

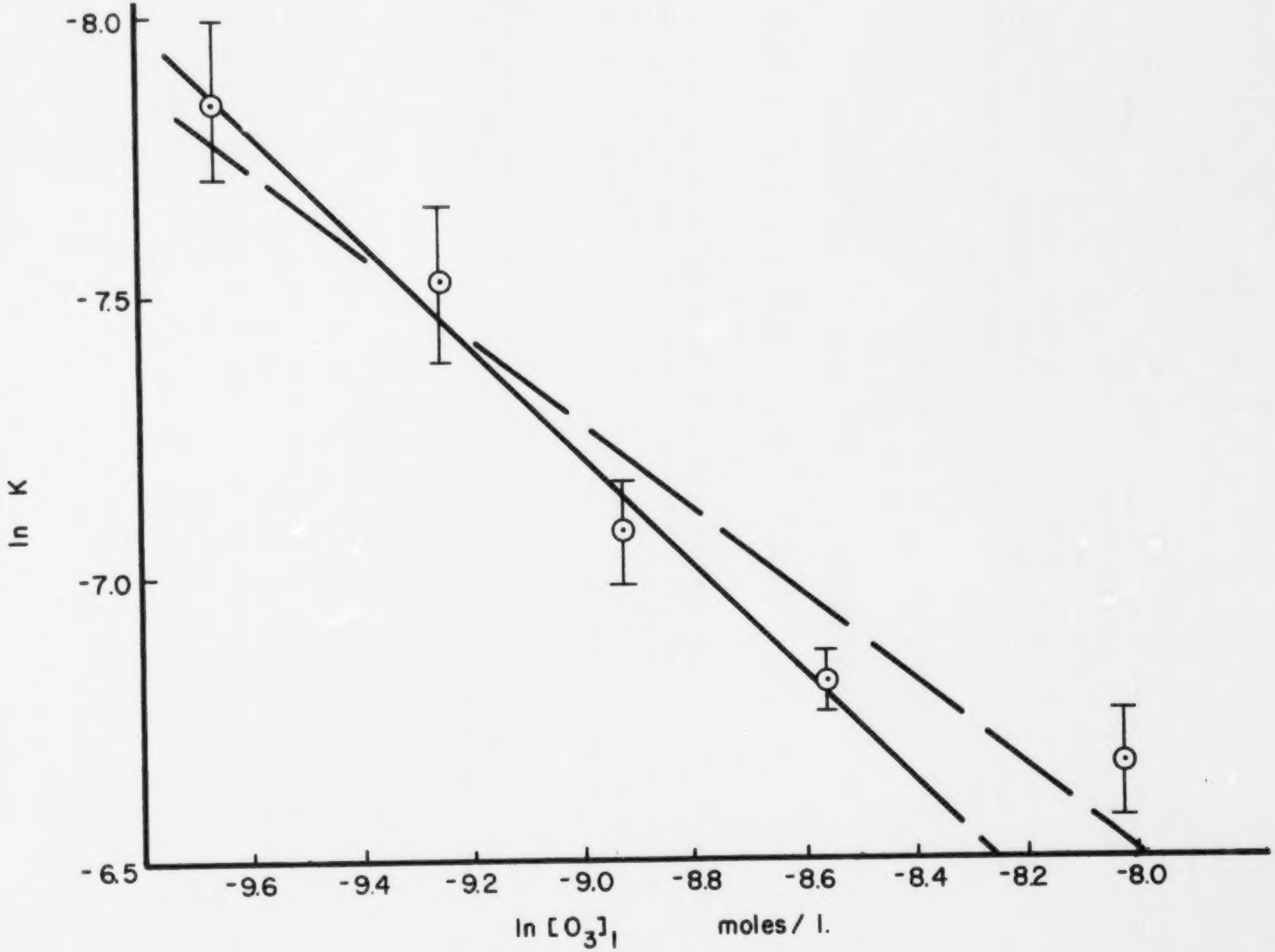

Figure C-1. Determination of order and rate constant of ozonolysis of tetrachloroethylene.

from the experimental values of $-(\ln S/S_o)/t$ for the ozone/UV experiments. The log of the resulting $\beta = k_n I^i D^m$ was plotted vs. ln D, i.e., $\ln\beta = \ln k_n I^i + m \ln D$ as before, to give Figure C-2. Linear regression gave the top two curves for 2 and 4 lamps, and the dotted line for the one lamp plot. Reconsideration of the raw data suggested elimination of the experiment which used the highest dose rate of ozone, and a least squares fit of the remaining points yielded the solid line shown drawn through the 1 lamp data. The resulting slopes are 0.96, 0.96, 0.93 for 1, 2, and 4 lamps respectively. Plotting the intercepts vs. ln I (Figure C-3) yields a slope of 1.04 and a rate constant of 0.109. Forcing both exponents to unity gives the final rate expression:

$$\begin{array}{lccccc} -\dot{S} = \frac{-dS}{dt} = & k_o(O_3)_1 S & + & k_p IS & + & k_u IDS \\ \text{mole } L^{-1}\text{sec}^{-1} & 5.87\pm0.31 & & (9.46\pm0.58)\times10^{-3} & & 0.109 \\ & L\cdot\text{sec}^{-1}\text{mole}^{-1} & & L\cdot\text{sec}^{-1}W^{-1} & & L^2\text{min sec}^{-1}\text{mg}^{-1}W^{-1} \end{array}$$

At this point destruction curves were calculated to verify the adequacy of the derived rate expression and the assumptions used. These plots are shown in Figures A-1,2,3 (Appendix A) where the equation is seen to describe the experimental results within the limits of precision of the data.

B. Chloroform--In this system, the ozone/UV reaction is so fast compared to purging, photolysis, and the ozone-only reaction that the data can be well represented by just the ozone/UV term of the rate equation,

$$\frac{-dS}{dt} = k_u I^a D^b S^c = K_u S^c = K_u' D^b S^c$$

As before, a plot of $\ln S/S_o$ vs. t was linear, indicating that the reaction was first order in substrate (c=1). For a given UV intensity, I, plots of $\ln K_u$ vs. ln D gave b = 1.5 and $\ln K_u'$ as the intercept. Plots of $\ln K_u'(I)$ vs. ln I gave a = 0.266 and $k_u = 7.97\text{X}10^{-3}$ when time is given in seconds. The final expression is

$$\frac{-dS}{dt} = k_u I^{0.266}\, D^{1.50}\, S \quad ,$$

$$\text{where } k_u = 7.97\text{X}10^{-3}\ \text{sec}^{-1}\left(\frac{W}{L}\right)^{-0.266}\left(\frac{\text{mg}}{L\,\text{min}}\right)^{-1.50}$$

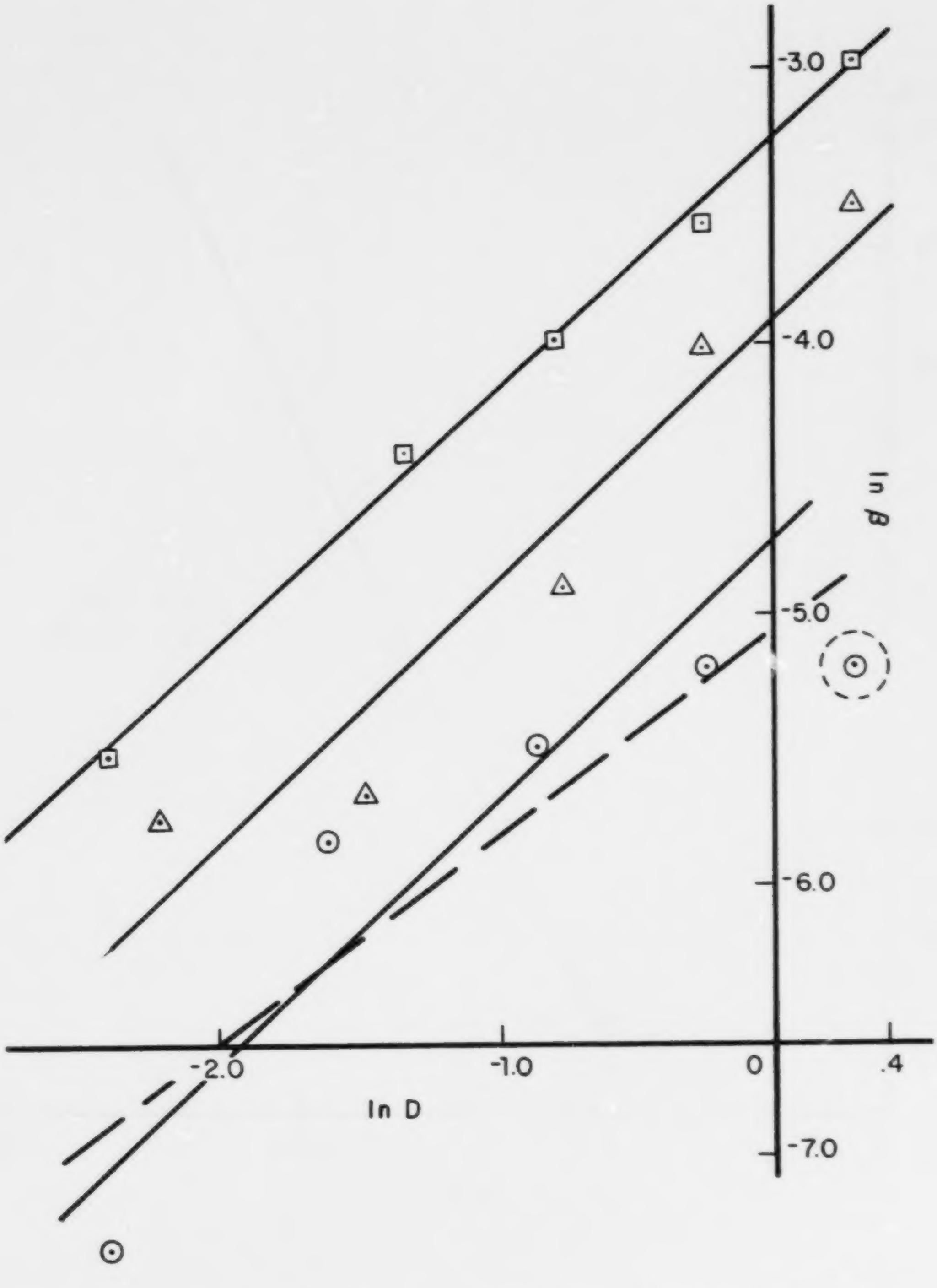

Figure C-2. Determination of substrate order in O_3/UV term (tetrachloroethylene).

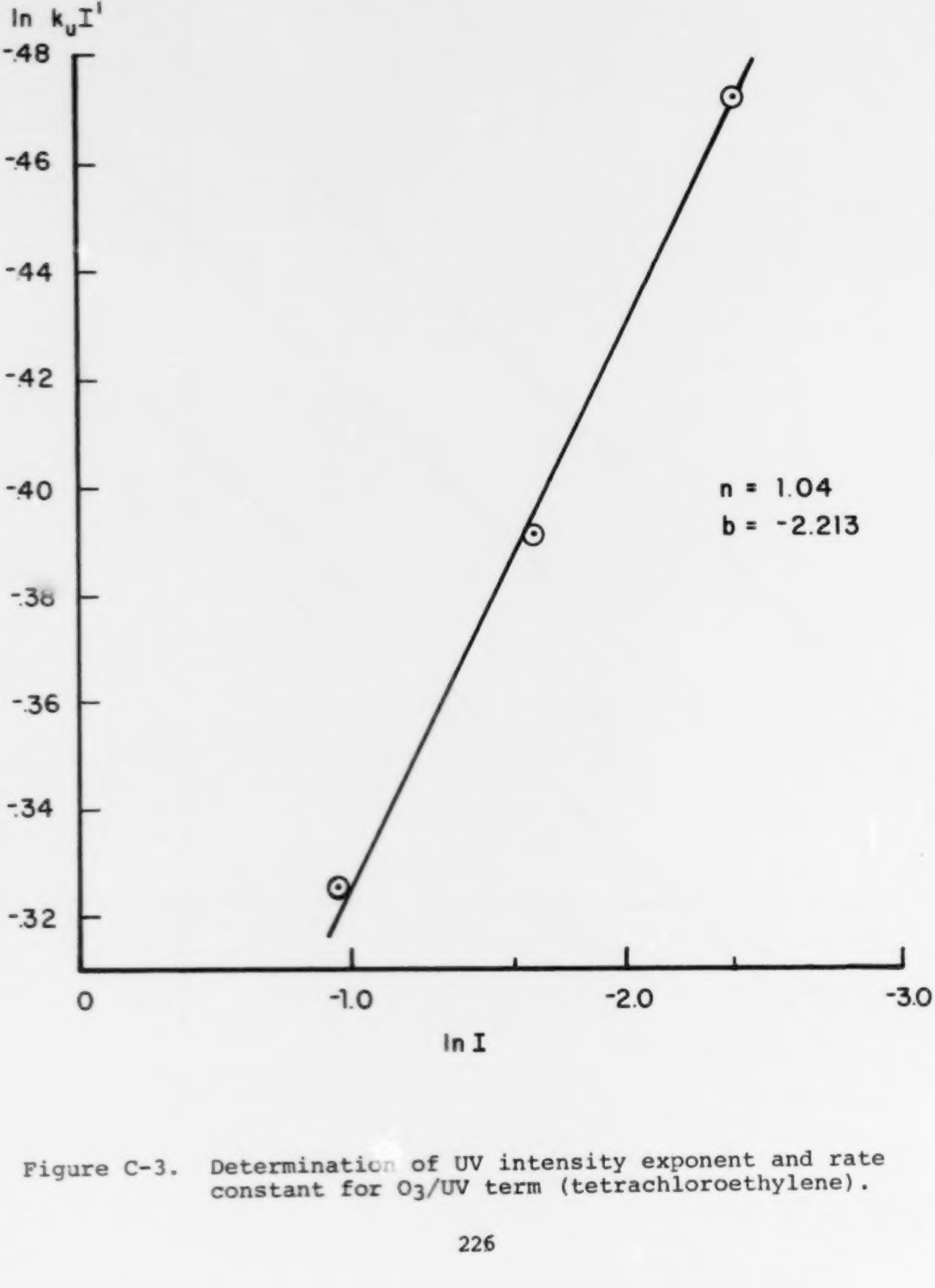

Figure C-3. Determination of UV intensity exponent and rate constant for O_3/UV term (tetrachloroethylene).

and the units of I and D are Watts/L and mg/L-minute, respectively. The experimentally determined disappearance curves, along with the curve fit calculated from the above equation are shown in figures A-4,5,6.

C. Bromodichloromethane--An anomaly was found in the results for bromodichloromethane (BDM) in purified water. Unlike the two compounds discussed previously, for a given ozone dose rate, runs using four lamps were found to be slower than those using only two lamps, which were in some cases slower than those using only one lamp. Many of the experiments which produced this unusual data were rerun and the results were found to be exactly reproducible. The photolysis results were found to be in the expected order, that is, with four lamps giving faster destruction than with two lamps, and the photolysis was found to be first order in UV intensity. Photolysis experiments run months apart by different workers gave results so close to each other that the data sets were combined to evaluate the photolysis term (Figure C-4). As before, the ozone/UV pseudo-first-order (PFO) rate constants were evaluated from the slopes of ln S/S_o vs. t plots (Figures A-7,8,9. The combined purging/photolysis rate constants were subtracted from the total ozone/UV PFO rate constants to separate out the portion due to the ozone/UV reaction(s). Since $[O_3]_\ell$ was below the detectable limit, the ozonolysis term was neglected. When these PFO rate constants, $K_u{}^*(I,D)$ were plotted against the ozone dose rate, D, the curves were found to consist of two portions, a ramp and a plateau, as seen in Figure C-5.

Inspection of these plots shows that as ozone dose rate is increased from a value of zero, the rate of the ozone/UV portion of the reaction increases linearly, until a cut-off point is reached, after which increasing the dose rate no longer increases the reaction rate. Furthermore, when the UV intensity is approximately doubled in going from 0.084 W/L to 0.189 W/L, the dose rate cut-off approximately doubles also. Apparently, the cut-off for 0.375 W/L was outside the range of experimentation and would by inference be expected to lie at slightly over D=2 mg/L min. The implication that there is a relationship between UV intensity and maximum effective ozone dose rate is of great importance from both a mechanistic and practical point of view, and will be discussed in a later section.

It is not known whether the non-coincidence of the three y-intercepts in Figure C-5 is meaningful or a result of experimental error. In this treatment it is handled as experimental error, the 0.189 W/L intercept set equal to the other two intercepts and the UV intensity dependence of the rate constant determined as follows.

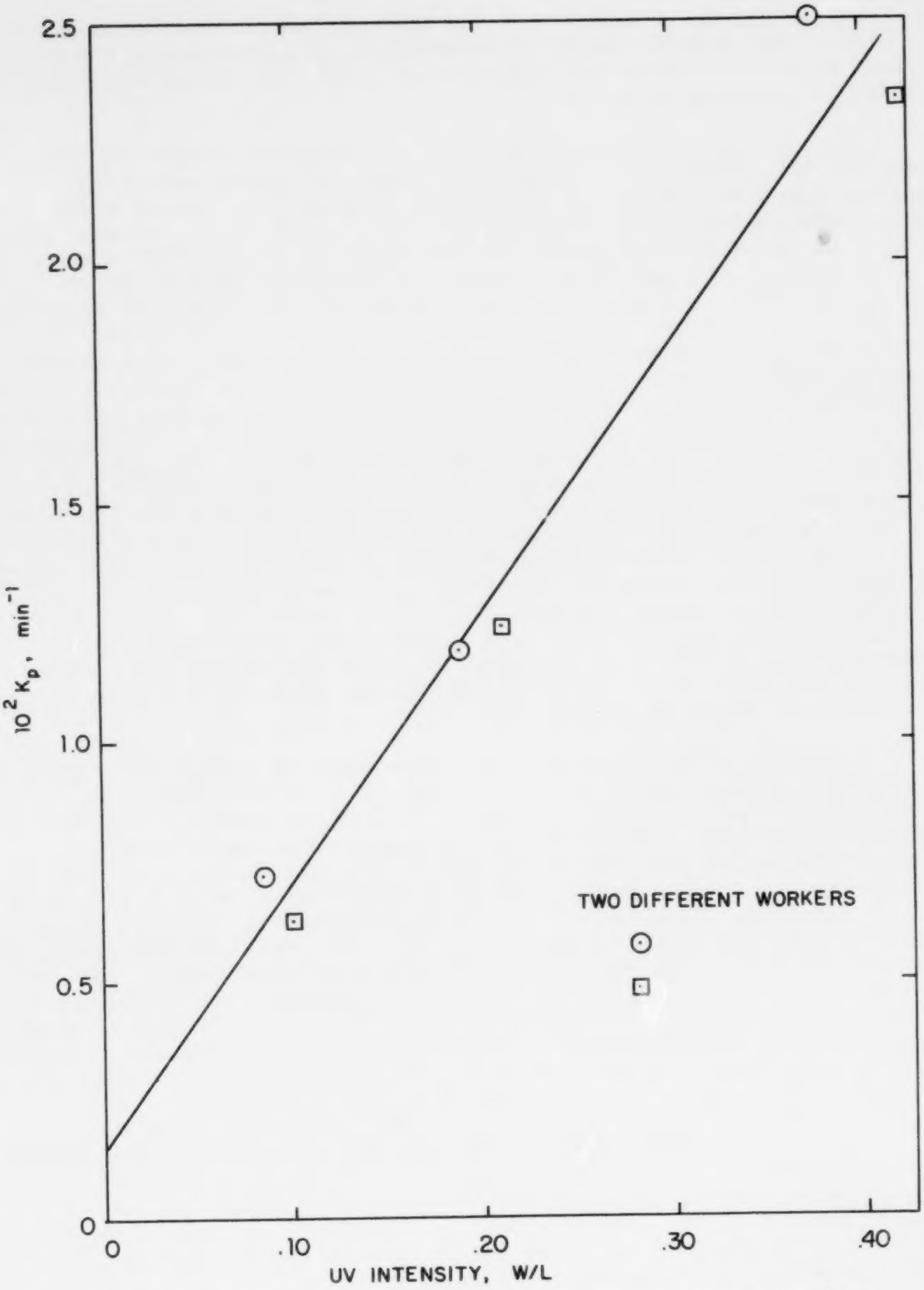

Figure C-4. Determination of photolysis rate constant for bromodichloromethane in purified water.

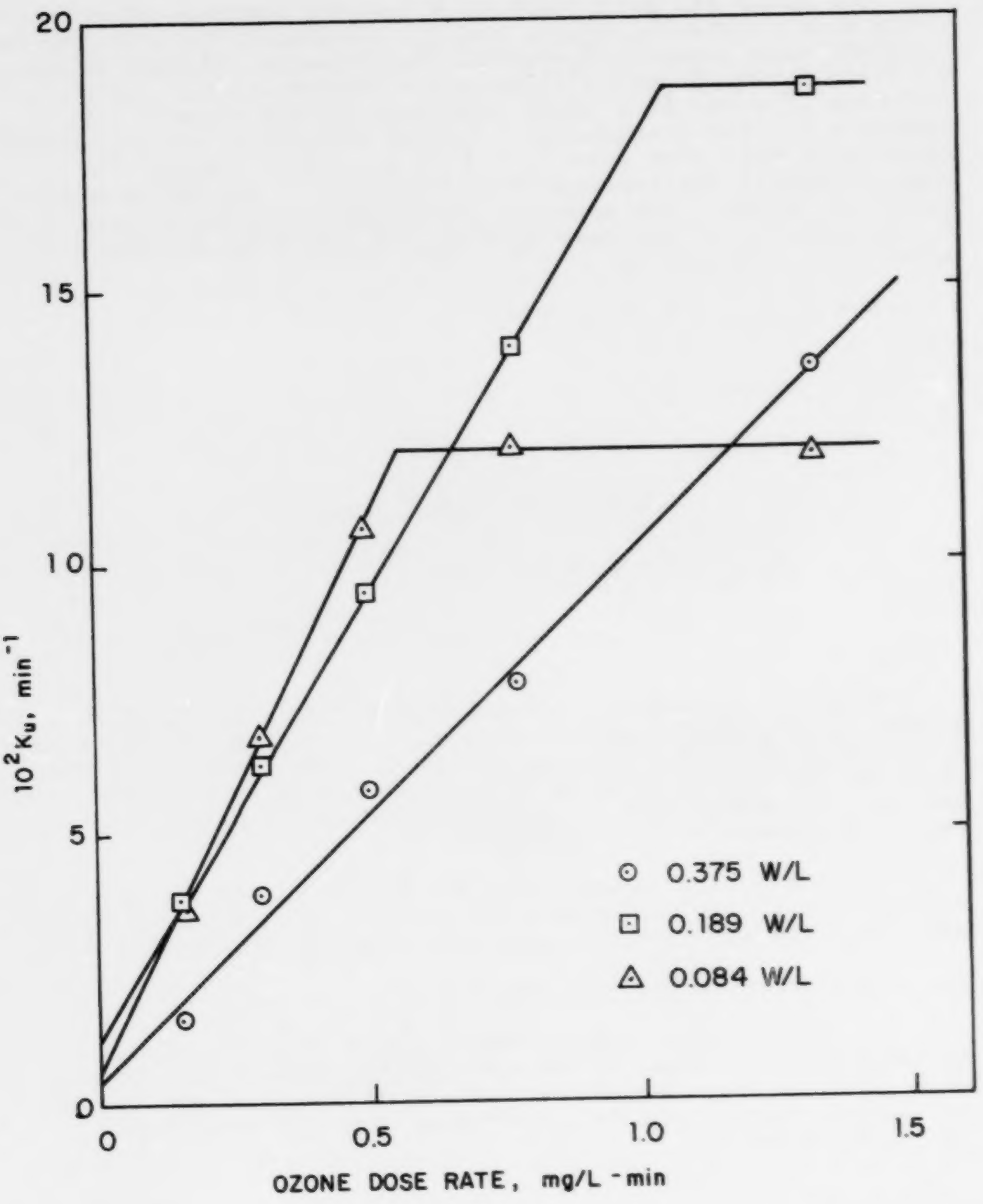

Figure C-5. Pseudo-first-order rate constants for bromodichloromethane in purified water.

The total PFO rate constant K had the purging and photolysis rate constants, k_{purge} and K_p, subtracted to give the PFO ozone/UV rate constant $K_u = k_u I^e D^f$ (see equation 71,main report). Plotting K_u vs. D gave a slope which represents $\beta = k_u I^e$. Plotting ln β vs. ln I gives intercept k_u and slope e (see equation C-1 and discussion). Linear regression of the points comprising this plot gave $k_u = 6.56 \text{ X } 10^{-2} \text{min}^{-1} (\text{W/L})^{0.466} (\text{mgO}_3/\text{L min})^{-1}$ and the reaction order, e, of the UV intensity equal to -0.466. The non-zero intercept of K_u vs. D shows that K_u is actually of the form $K_u = k_c + k_u I^{-0.466} D$, so that the total rate constant is

$$K = k_{purge} + K_p + k_c + K_u$$

$$= k_{purge} + k_p I + k_c + k_u I^{-0.466} D$$

where $k_{purge} = 1.43 \text{ X } 10^{-3} \text{ min}^{-1}$

$k_p = 5.62 \text{ X } 10^{-3} \text{ min}^{-1} \text{ (W/L)}^{-1}$

$k_c = 8.78 \text{ X } 10^{-3} \text{ min}^{-1}$

$k_u = 6.56 \text{ X } 10^{-2} \text{ min}^{-1} (\text{W/L})^{0.466} (\text{mgO}_3/\text{L min})^{-1}$

This equation should not be used for dose rates below the lowest experimental value (0.15 mg/L min) because of the term k_c which is neither a function of UV intensity nor ozone dose rate and yet is not present in the photolysis/purging experiment. The term k_c undoubtedly arises from the oversimplification of a very complicated kinetic situation.

These somewhat unusual results are discussed further in the summary section which follows the rest of the kinetic analysis details. The experimental data are shown in Figures A-7,8,9.

II. Lake Water as the Reaction Medium

A. Tetrachloroethylene--Destruction of tetrachloroethylene in lake water by ozone/UV is sufficiently slower than in pure water, that a term describing purging of TCE from the reactor by the gas stream must be included in the rate equation. The form chosen was

$$-S = -\frac{dS}{dt} = KS$$

$$= (k_{purge} + K_o + K_p + K_u)\ S$$

$$\text{(purging)} \quad \text{(ozonolysis)} \quad \text{(photolysis)} \quad (O_3/UV)$$

$$= (k_{purge} + k_o D^a + k_p I^b + k_u I^c D^d)\ S$$

The ozone/UV reaction, as well as purging, ozonolysis, and photolysis were all within experimental error of being first order in substrate. As before, I represents UV intensity and D is the ozone dose rate. Since the ozone concentration in the liquid was continually changing throughout the reaction, the rate equation was written in terms of ozone dose rate rather than ozone concentration in the liquid. During ozone/UV runs, in which ozone is destroyed by ultraviolet radiation, the concentration of ozone in the liquid was monitored and the effective dose rate (dose rate which gave the same profile) used in the kinetic analysis, since in a strictly ozone reaction, only the bulk liquid concentration is important.

Plots of ln C/C_o vs. t for the ozone (only) reaction were made and found to be linear. The corresponding rate equation is

$$\frac{-dS}{dt} = (k_{purge} + k_o D^a)\ S,$$

so that

$$-\frac{1}{S}\ \frac{dS}{dt} = \frac{d\ \ln\ S}{dt} = k_{purge} + k_o D^a$$

is the slope of the above plots. These slopes were plotted vs. D and the result was a straight line whose slope was k_o and whose intercept was k_{purge}. The fact that the plot was linear indicates that a = 1. This plot is shown in figure C-6.

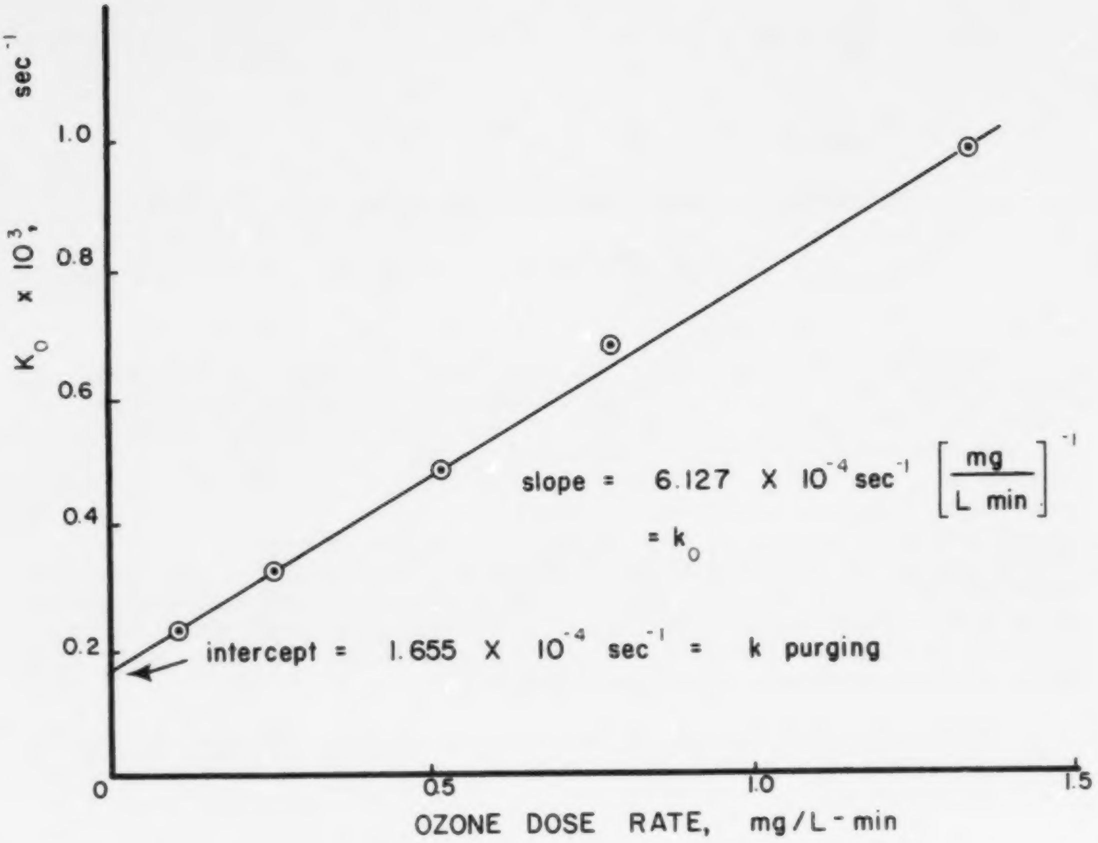

Figure C-6. Ozonolysis of tetrachloroethylene in lake water.

For photolysis experiments, the rate expression is

$$-\frac{dS}{dt} = (k_{purge} + k_p I^b)\ S = K_p' S.$$

The values previously obtained for k_{purge} were subtracted from K_p' to obtain numerical values of $k_p I^b$ for different I. Then

$$\ln(k_p I^b) = \ln k_p + b \ln I$$

yields k_p and b when $\ln(k_p I^b)$ is plotted vs. ln I.

The rate constants in the ozone/UV experiments were obtained by taking $-(\ln C/C_o)t^{-1}$ as described in the previous section on tetrachloroethylene in pure water. From these values of K were subtracted k_{purge}, K_p, and K_O (using D effective to calculate K_O). The logarithm of the value of K_u thus obtained was plotted vs. lnD to determine the order of the factor D. It was found to be 1.00±.09 for the 0.084 and 0.189 W/L experiments and 0.469 for the 0.375 W/L experiments. Since the uncertainty in the determination of K was almost twice as large for the .375 W/L experiments as in the other two sets, and because in the absence of data to the contrary a first order situation is most likely, a value of d = 1.0 was used in subsequent calculations, subject to final comparison of calculated rate data with that collected experimentally.

Intercepts of the previous plots gave values of $\ln k_u I^a$, which, when plotted vs ln I as before yielded a as the slope and $\ln k_u$ as the intercept.

The final values of the constants in the rate equation

$$-\frac{dS}{dt} = (k_{purge} + k_o D_{eff} + k_p I^{0.670} + k_u I^{0.419} D)\ S$$

are:

$k_{purge} = 1.66 \times 10^{-4}\ \mathrm{sec}^{-1}$

$k_p = 1.31 \times 10^{-3}\ \mathrm{sec}^{-1}(\mathrm{W/L})^{-0.670}$

$k_o = 6.13 \times 10^{-4}\ \mathrm{sec}^{-1}(\mathrm{mg/L\text{-}min})^{-1}$

$k_u = 2.97 \times 10^{-3}\ \mathrm{sec}^{-1}(\mathrm{mg/L\text{-}min})^{-1}(\mathrm{W/L})^{-0.419}$

For typical values of UV intensity I = 0.375 W/L and ozone dose rate D = 1.33 mg/L min, the various terms in the rate constant are:

$$-\frac{1}{S}\frac{dS}{dt} = 1.66 \times 10^{-4} + 1.31 \times 10^{-3}(.518) + 6.13 \times 10^{-4} D_{eff} + 2.97 \times 10^{-3}(1.33)\ 0.663$$

$$= 1.66 \times 10^{-4} + 6.79 \times 10^{-4} + 0 + 2.62 \times 10^{-3}$$

(purging) (photolysis) (ozonolysis) (ozone/UV)

It is seen that purging and photolysis contribute a greater proportion of the total rate expression than in the case of TCE in pure water, but that the dominant term is still the ozone/UV reaction. In the case which has the highest D_{eff} of those studied, $I = 0.084$ and $D = 1.33$, $D_{eff} = 0.13$ mg/L min, the terms are

$$-\frac{1}{S}\frac{dS}{dt} = \underset{\text{(purging)}}{1.66 \times 10^{-4}} + \underset{\text{(photolysis)}}{2.49 \times 10^{-4}} + \underset{\text{(ozonolysis)}}{7.97 \times 10^{-5}} + \underset{\text{(ozone/UV)}}{1.40 \times 10^{-3}},$$

and ozonolysis still plays a minor role.

The integrated form of the above rate equation was used to calculate disappearance curves for each of the ozone/UV experiments performed, and the results are shown in figures A-10 - A-12. Agreement with experiment is seen to be very good, considering the opportunities for error accumulation in a stepwise analysis of the type required here.

B. Chloroform--Kinetic analysis on chloroform was carried out using the methods described in previous sections. PFO rate constants were determined for photolysis at two different UV intensities and a plot of K_p vs I extrapolated to $I = 0$ to determine the purging rate constant, k_{purge}. Ozonolysis was performed at an ozone dose rate of $D = 1.33$ mg/L min, and the purging rate constant previously determined, was subtracted from the slope of a plot of S/S_o vs t for the ozonolysis. The resultant PFO rate constant for ozonolysis was divided by the ozone dose rate to give a second order rate constant, $k_o = 4.26 \times 10^{-5}$ sec^{-1}(mg/L min)$^{-1}$, where

$$\text{OZONOLYSIS RATE} = \frac{-dS}{dt} = k_o D\ S$$

The concept of dose rate was introduced because even though the presence of UV generally kept the aqueous ozone concentration below the detectable limit, a relationship to the amount of active specie generated was needed. When trying to calculate the extent of ozonolysis which occurs in the presence of UV in purified water experiments, the effective dose rate was defined as that dose rate which in a non-UV experiment resulted in the same equilibrium ozone concentration as was found in the experiment, and was thus generally zero. In the case of natural water experiments, the ozone and UV could not be equilibrated before adding substrate because of the resultant changes in the matrix and the effect of those changes on the reaction rate. Therefore, in natural matrix experiments the effective dose rate is by analogy defined as the dose rate which, in an ozonolysis (non-UV) experiment produces the same aqueous ozone concentration profile as seen in the ozone/UV experiment being analyzed. In the chloroform experiments described here, the effective dose rate was found to be 50-80 times smaller than the actual dose rate, with the result that the ozonolysis itself contributes very little to the disappearance rate of substrate.

As in previous examples, the ozonolysis and photolysis contributions were subtracted out of the total pseudo-first-order rate constants for the ozone/UV experiments to yield the PFO rate constant for the ozone/UV portion of the reaction,

$$K_u = k_u I^a D^b$$

For each set of experimental conditions, ln K_u was plotted vs ln D to yield intercept ln $k_u I^a$ and slope b = 0.562 ± 0.212. The values of the intercepts of the two lines representing the two different UV intensities were so close together that only a very slight UV dependence was seen (Figure 14, main report), resulting in the following expression.

$$K_u = k_u \; I^{-0.028} \; D^{0.562}$$

$$\approx k_u \; D^{0.562}$$

where $K_u = 1.53 \times 10^{-4}\ \mathrm{sec}^{-1}\ (\mathrm{mg/L\ min})^{-0.562}$

$= 9.18 \times 10^{-3}\ \mathrm{min}^{-1}\ (\mathrm{mg/L\ min})^{-0.562}$

The total rate expression which results is

$$-\dot{S} = -\frac{dS}{dt} = k_{purge} + k_o D_{eff} + k_p I + k_u D^{0.562}$$

$$= \text{purging} + \text{ozonolysis} + \text{photolysis} + O_3/\text{UV}$$

where $k_{purge} = 1.59 \times 10^{-5}\ \mathrm{sec}^{-1}$

$k_o = 4.26 \times 10^{-5}\ \mathrm{sec}^{-1}\ (\mathrm{mg/L\ min})^{-1}$

$k_p = 7.63 \times 10^{-5}\ \mathrm{sec}^{-1}\ (\mathrm{W/L})^{-1}$

$k_u = 1.53 \times 10^{-4}\ \mathrm{sec}^{-1}\ (\mathrm{mg/L\ min})^{-0.562}$

The experimental disappearance curves, along with the curve fit calculated from the equation 86 are shown in Figures A-13 and A-14.

C. Bromodichloromethane--As in previous data sets, the first approach taken was to analyze the ozone-only and UV-only data in order to subtract their contributions from the experimental ozone/UV rate constant. Although a few of the experimental curves have a slight "less than first order" look (the semi-log plot curves slightly downward), it is small enough that the data can be adequately represented using an expression which is first order in substrate. This was verified by comparison of the calculated disappearance curves with those obtained experimentally.

Because of time limitations, only two different ozone concentrations were run in the ozone-only experiments. Similarly only two different UV intensities were used in the UV only experiments, so that one cannot absolutely distinguish between various orders for these parameters. The procedure used was to assume that these reactions were first order with respect to ozone and UV respectively, and that substrate disappearance was due to reaction plus purging from solution. The pseudo-first-order rate constant for the overall disappearance was plotted vs. the appropriate parameter (ozone dose rate, D, or UV intensity, I) and the straight line defined by the two points extrapolated to the y-axis, where D or I is equal to zero. Since this value should represent the rate constant for disappearance of substrate in the absence of reaction, it was taken as the purging rate constant. Values were compared from the ozone-only and UV-only plots, as a check of the validity of the above assumption of first order, and the values were found to be 3.01×10^{-4} and 2.30×10^{-4} min^{-1} respectively - well within experimental error.

During the ozone/UV experiments, the ozone level in the liquid was found to be negligible. Therefore, to determine the portion of the ozone/UV rate constant which is due to the ozone/UV reaction, just the purging and UV-only terms were subtracted, that is, the rate expression was assumed to have the form

$$\frac{dS}{dt} = KS = \sum_i K_i S = (K_{purge} + K_{phot} + K_u)\, S$$

$$= (k_{purge} + k_p I + k_u I^a D^b)\, S$$

Allowing b to take on any value resulted in a dependency of b on I. Even when b was fixed at b = 1, a satisfactory fit could not be obtained, and it was concluded that, as in the case of bromodichloromethane in purified water, the situation was more complicated than strict adherence to the model allowed. The idea of identifying a particular term with a particular reaction was abandoned, and the data was empirically fit to the form

$$K = k_1 + k_2 I + k_3 I^a D$$

The resulting equation was

$$K(\text{min}^{-1}) = -7.386 \times 10^{-3} + 8.948 \times 10^{-2} I + 5.038 \times 10^{-3} I^{-0.481} D.$$

The experimentally determined rate equations for the corresponding ozone-only and UV-only reactions were

$$-\frac{dS}{dt} = \underset{\text{(purge)}}{3.01 \times 10^{-4}} + \underset{\text{(ozonolysis)}}{4.86 \times 10^{-3}\ D}$$

and

$$-\frac{dS}{dt} = \underset{\text{(purge)}}{2.30 \times 10^{-4}} + \underset{\text{(photolysis)}}{2.99 \times 10^{-2}\ I} \quad ,$$

respectively, where t is measured in minutes. For comparison, selected values of the rate constants (in min^{-1}) of the ozonolysis, photolysis, and ozone/UV reactions are shown below.

I,w/l D,mg/l min	0	.189	.375
0	2.6×10^{-4}	5.43×10^{-3}	1.10×10^{-2}
.30	1.76×10^{-3}	1.29×10^{-2}	2.86×10^{-2}
1.33	6.77×10^{-3}	2.46×10^{-2}	3.70×10^{-2}

The experimental disappearance curves, along with the curve fit, calculated from equation 88 are shown in Figures A-15 and A-16.

APPENDIX D

RESULTS OF KINETIC ANALYSIS OF OZONE AND OZONE/UV DESTRUCTION OF HEXACHLOROBIPHENYL IN WATER

The same general form for the rate expression is used for HCB as for the previously discussed substrates, except that the purging term is not applicable because of the low volatility of HCB, which is a solid at room temperature. Studies were made using the usual gas flow through the reactor but with no ozone or UV present, to determine that HCB was neither stripped from solution by the gas nor adsorbed onto the walls of the vessel. Thus, the ozonation rate expression was of the form

$$-\dot{S} = -\frac{dS}{dt} = k_o \, D^m \, S^n \qquad [D\text{-}1]$$

while the ozone/UV reaction was described by two terms,

$$-\dot{S} = -\frac{dS}{dt} = K_u \, I^a D^b S^c \; + \; k_p I^d S^e \quad . \qquad [D\text{-}2]$$

As before, the ozone concentration in solution was very low during an ozone/UV reaction (although not, in general, zero because of the higher dose rates used) and the ozonolysis term was not included, any occurring ozonolysis being lumped into the much larger ozone/UV term. The results are summarized below, by reaction medium.

I. LAKE WATER AS THE REACTION MEDIUM

The ozone concentration profile in the ozonation of HCB in water is shown in Figure D-1. It should be noted that the dose rates used here are for the most part higher than those used for the three compounds previously described. The ozone-oxygen gas flow rate was kept at 0.20 L/min and the stirring rate at 500 rpm. HCB was spiked and well-mixed before the introduction of ozone. The profile shows there was a short induction period in only one case, following which the ozone concentration increased smoothly. With UV radiation applied, a quasi-equilibrium state resulted at first as shown in Figure D-2. During this time it appears that an immediate ozone demand of the matrix is being filled, as judged by the proportionate lengths of the induction periods in Figure D-2, and by the approximate correspondence between the equilibrium levels of curves D = 1.16

and D = 3.95 in Figures D-1 and D-2 respectively and the lengths of their induction periods. This ozone demand should have little or no effect on the ozone/UV process, however, since the great difference between the ozone levels in Figures D-1 and D-2 indicate that most of the ozone accumulated in Figure D-1 is photolyzed in Figure D-2.

Based on equations in reference 145, one can obtain the η and K_La values from the ozone concentration profiles with or without UV. The quantity η is the ratio of the equilibrium ozone concentration predicted by Henry's law to that actually found. Since K_La should not be reaction dependent when most of the fast reacting organics are depleted, it was used to calculate K_D's for ozone concentration profiles at various UV radiation transfer rates. As discussed in reference 145, K_D is the first-order rate constant for the disappearance of ozone. In this work, the concept has been expanded to include photodecomposition as well as autodecomposition. This will be explained in greater detail in the section on mass transfer. The results are shown in Table D-1. The values of η and K_D were proportional to the UV radiation transfer rates as expected. The destruction of HCB by ozonation is very slow as shown in Figure D-3. As in the case of photolysis, ozonation is faster at the beginning of the reaction and slows down rapidly. A simple rate expression cannot be used to describe the whole reaction path; however, the initial rates of ozonation of HCB in natural water were obtained and are shown in Table D-2. Figure D-4 shows that the rates are first order with respect to the ozone dose rate. Ozonation rates at longer reaction times are significantly retarded as compared to initial rates and appear to be nearly independent of ozone dose rates. As shown in Figure D-1, the concentration of ozone in the liquid phase is very high in this region and has reached a steady state level dependent on the dose rate. It is clear that ozonation in this region is rate controlling, i.e. the rate is independent on the ozone dose rate.

Based on equation D-1 the initial rate expression for ozonation of HCB in lake water can be written as

$$-\dot{\alpha}_M = K_oD \cdot \alpha_M \quad ,$$

where $\alpha = C_M/C_M^o$

with $K_o = 1.38 \times 10^{-2}$ L (mg ozone)$^{-1}$ at pH 8. In the limiting region the rate is independent of ozone dose rate.

Photolytic ozonation of HCB in lake water was carried out at various ozone and UV dose rates, and at different pH values. As an example, the photolytic ozonation data of HCB under 0.25 W/L and various ozone rates are shown in Figure D-5. The destruction curves are smooth and the reaction is generally very fast compared to ozonation. The photolysis curve under the same radiation rate is also shown for comparison. At long reaction times it is significant that the reaction rate is approximately equal to that of photolysis. Under these conditions it is possible that the photolytic ozonation process is retarded by radical scavengers produced in the reaction and only the direct photolysis process remains. The reaction order with respect to HCB and dose rate in equation D-2 was determined by the following procedure. A smooth line was drawn through the data points, and the tangents to the curve at certain values of α_M were taken as the values of $-\dot{\alpha}_M$. For each Ω_M, the values were corrected for photolysis by the equation of O_3/UV rate = $r = -\dot{\alpha}_M - \Omega_{M,\lambda}$. Equation [52] of reference (161) is used for the photolysis in this system.

$$\Omega_{M,\lambda} = k_p I^{1/2} S$$

where $k_p = 1.02 \times 10^{-2}\ L^{1/2}/W^{1/2}$ min in purified water

$= 1.36 \times 10^{-2}\ L^{1/2}/W^{1/2}$ min in lake water.

This is the equation which describes the behavior over the greatest portion of the photolysis disappearance curves.

Values of r were fit to the following rate equation.

$$r = -\alpha_M - \Omega_{M,\lambda} = k_u I^i D^m \alpha_M^n \qquad [D-3]$$

From the log-log plots of r and α_M, the slope yields the reaction order n with respect to α_M. The values of $k_u I^i D^m$ then were calculated and used for obtaining m and i. The values of n, m and i estimated from various runs are

$n = 2$
$m = 1$
$i = 1$

The values of k_u's of various runs are listed in Table D-3. Thus, the empirical equation for photolytic ozonation of HCB in Lake Lewisville water is expressed as

$$-\dot{\alpha}_M = k_u \cdot I \cdot D \cdot \alpha_M^2 + k_p \cdot I^{1/2} \cdot \alpha_M$$

where $k_u = 1.31 \times 10^{-1}\ L^2/W\text{-mg}$

$k_p = 1.36 \times 10^{-2}\ L^{1/2}/W^{1/2}\text{-min.}$

This expression was solved for time, t, as function of α_M and the values of t vs. α_M in each case were calculated by using the HP 2000 computer system. As shown by the solid lines in Figures D-5 and D-6, the agreement between calculated and experimental points is satisfactory.

In order to make the comparison of ozonation and photolytic ozonation of HCB, Figure D-6 shows the runs with the same ozone dose rate at various UV radiation rates. The effect of UV radiation on ozonation is obvious.

II. PURIFIED WATER AS THE REACTION MEDIUM

In the kinetic study of ozonation and photolytic ozonation in purified water, substrate is spiked into the water which has been equilibrated with either ozone or ozone/UV. Under these conditions, the concentration of ozone in the liquid phase is constant.

Expressions for the rate of disappearance of substrate by ozonation and photolytic ozonation are similar to those used in natural water matrix (equations D-1 and D-2 respectively).

In purified water, pH effects on the ozonation and photolytic ozonation were studied in addition to effects of ozone and UV dose. In the experiments, pH was adjusted prior to the addition of substrate. The pH was not further controlled for the values of 4, 6 and 8; however, borax buffer was used for pH = 10.

Figure D-7 shows the effect of pH on the ozone degradation rate of HCB in purified water. As expected, ozonation at elevated pH is accelerated (34) presumably by the formation of hydroxyl radicals, however, the effect is not dramatic. The rate law of ozonation of HCB in purified water is determined to be

$$-\dot{\alpha}_M = k_o \cdot D^{\frac{1}{2}} \cdot \alpha_M^3 \qquad [D-4]$$

and the rate constants are listed in Table D-4. The rate expression for photolytic ozonation is

$$-\dot{\alpha}_M = k_u \, D^{1\frac{1}{2}} \cdot I \cdot \alpha_M^3 + k_p \cdot I^{\frac{1}{2}} \cdot \alpha_M \qquad [D-5]$$

where $k_p = 1.02 \times 10^{-2}$ $L^{\frac{1}{2}}/W^{\frac{1}{2}}$-min and values of k_u are listed in Table D-4. The pH effects on the O_3/UV destruction rate of HCB are also noticeable as shown in Figure D-8. Figure D-9 shows the photolytic ozonation runs conducted in purified water at pH = 8. Figures D-10 and D-7 compare kinetics in lake water and purified water at the same pH and similar UV radiation transfer rate, from which one can see that the lake water matrix does not interfere significantly with the destruction rate; however, the effect on the "ozone only" reaction is more apparent.

Summary--The ozone and ozone/UV reactions of HCB have been found to be kinetically complex and to slow down tremendously in the region beyond about $S/S_o = 0.5$. For this reason they have not been included in the process design calculations, although their kinetic analysis has been outlined above, omitting the exhaustive mathematical details. Possibly because of the methanol present, ozone/UV reaction of HCB in purified water was found to be approximately the same speed as in lake water, although the mathematical form of the empirical rate equation differed.

TABLE D-1. VALUES OF η, K_La AND K_D FOR OZONE PROFILES WITH AND WITHOUT UV IN LAKE LEWISVILLE WATER

Runs	I_a (W/L)	D (mg/ min-L)	η*	K_La (min^{-1})	K_D* (min^{-1})
NLLW-1	0	1.16	2.83 ± .87	$(1.78 \pm .32) \times 10^{-2}$	$(3.29 \pm 1.65) \times 10^{-2}$
2		2.19			
3		2.95			
4		4.04			
6	.12	1.21	8.93 ± 1.47	$(1.78 \pm .32) \times 10^{-2}$	$(1.41 \pm .26) \times 10^{-1}$
7		2.22			
8		3.04			
12	.25	2.16	17.90 ± 1.47	$(1.78 \pm .32) \times 10^{-2}$	$(3.00 \pm .26) \times 10^{-1}$
13		3.04			
14		3.95			
17	.49	2.16	34.88 ± 9.77	$(1.78 \pm .32) \times 10^{-2}$	$(6.01 \pm 1.73) \times 10^{-1}$
18		3.03			
19		3.91			

* Average value from individual runs. From reference 145 and equation 93 of the body of this report.

$\eta = 1 + \frac{kd}{K_La}$. In this work $\eta = 1 + \frac{kd + kp}{K_La} = 1 + \frac{K_d}{K_La}$

TABLE D-2. INITIAL RATE, R_o, AND INITIAL RATE CONSTANT, K_o, FOR OZONATION OF HCB IN LAKE LEWISVILLE WATER (a)

Runs	D (mg/min-L)	$R_o = -d(HCB/HCB_o)/dt$ ($\times 10^2$ min^{-1})	$K_o = R_o/D$ ($\times 10^2$ L mg^{-1})
NLLW-1	1.16	1.66	1.43
NLLW-2	2.19	2.86	1.30
NLLW-3	3.00	4.00	1.33
NLLW-4	4.04	5.88	1.45

(a) HCB_o = 0.1666mM, Flow Rate = 0.2 L/min, 500 rpm.

TABLE D-3. RATE CONSTANTS, k_u, FOR PHOTOLYTIC OZONATION OF HCB IN LAKE LEWISVILLE WATER (a)

Runs	I (W/L)	D (mg/min-L)	k_u (L^2/W-mg)
NLLW-6		1.21	
7	.12	2.22	0.132
8		3.04	
11		1.14	
12		2.16	
13	.25	3.04	0.125
14		3.95	
16		1.21	
17	.49	2.16	0.108
18		3.03	
19		3.91	

(a) $[HCB]_o$ = 0.168 mM, Flow Rate = 0.3 L/min, 500 rpm.

TABLE D-4. pH EFFECTS ON THE RATE CONSTANTS k_u, and k_o OF HCB DESTRUCTION BY OZONATION AND PHOTOLYTIC OZONATION IN PURIFIED WATER

pH	k_o*	k_u**
4	3.56×10^{-3}	0.89×10^{-1}
6	3.75×10^{-3}	1.40×10^{-1}
8	6.91×10^{-3}	2.12×10^{-1}
10	1.21×10^{-3}	---

* equation D-4
**equation D-5

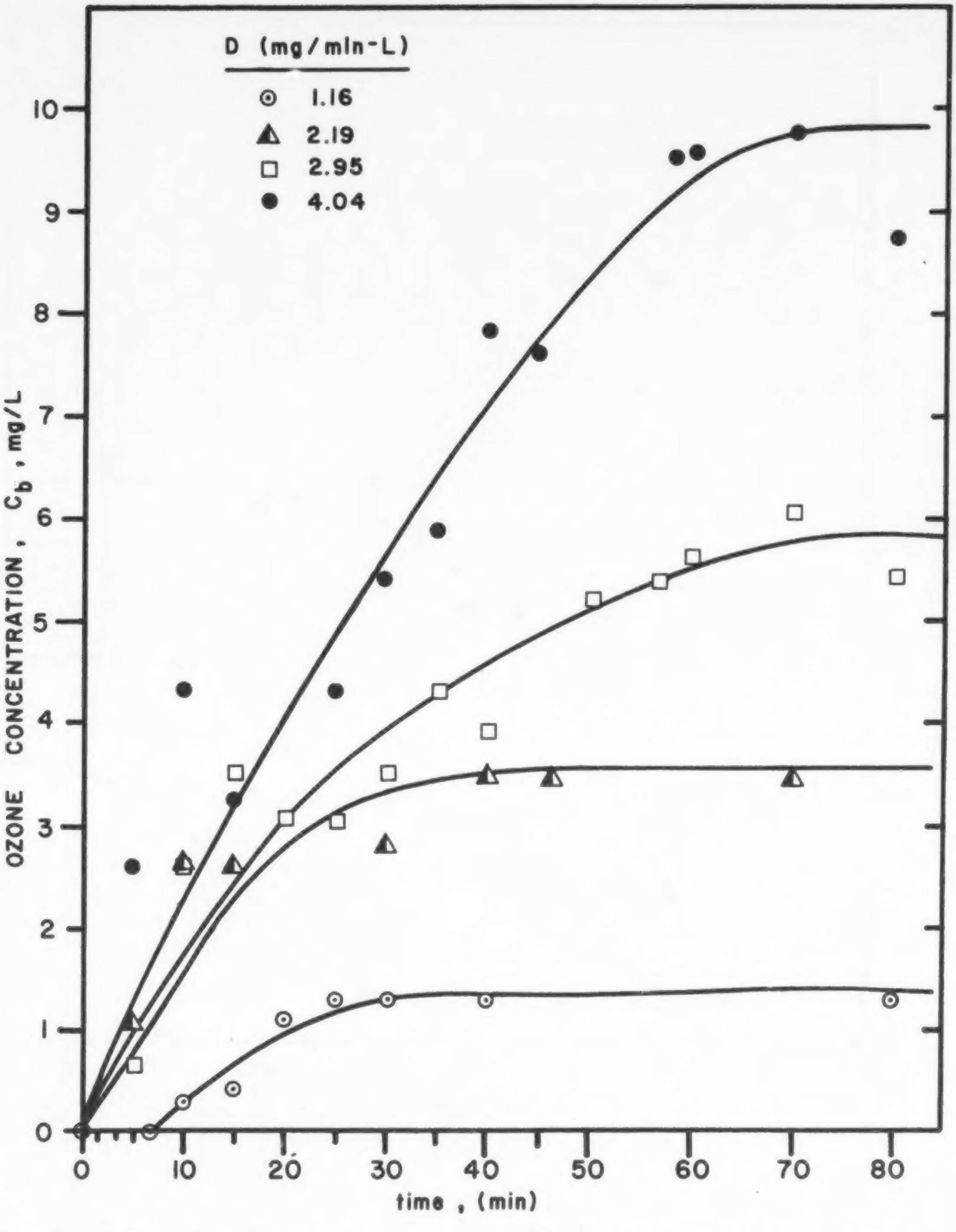

Figure D-1. Ozone concentration profile for ozonation of HCB in lake water.

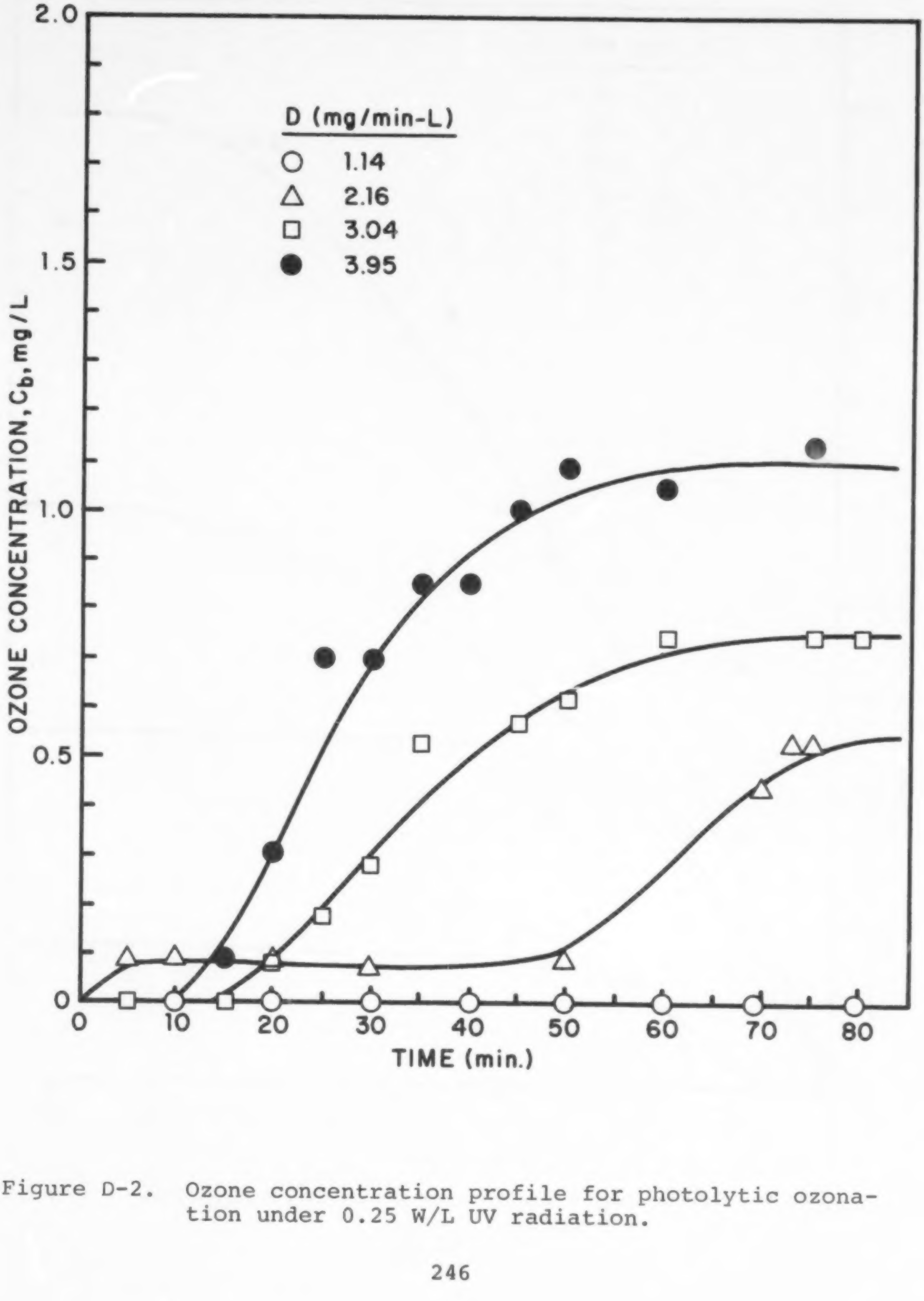

Figure D-2. Ozone concentration profile for photolytic ozonation under 0.25 W/L UV radiation.

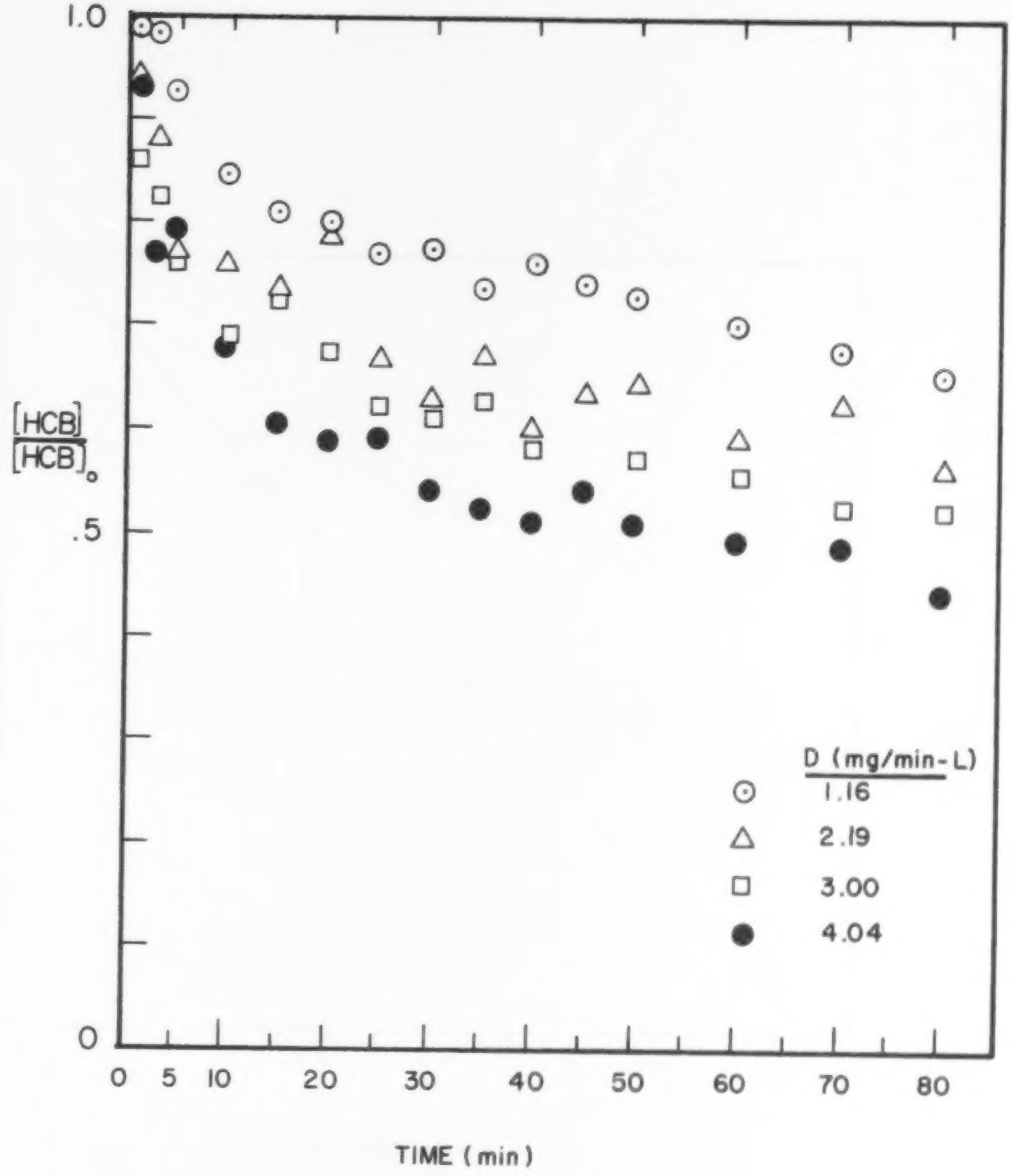

Figure D-3. Effects of dose rate on the direct ozonation of HCB in lake water.

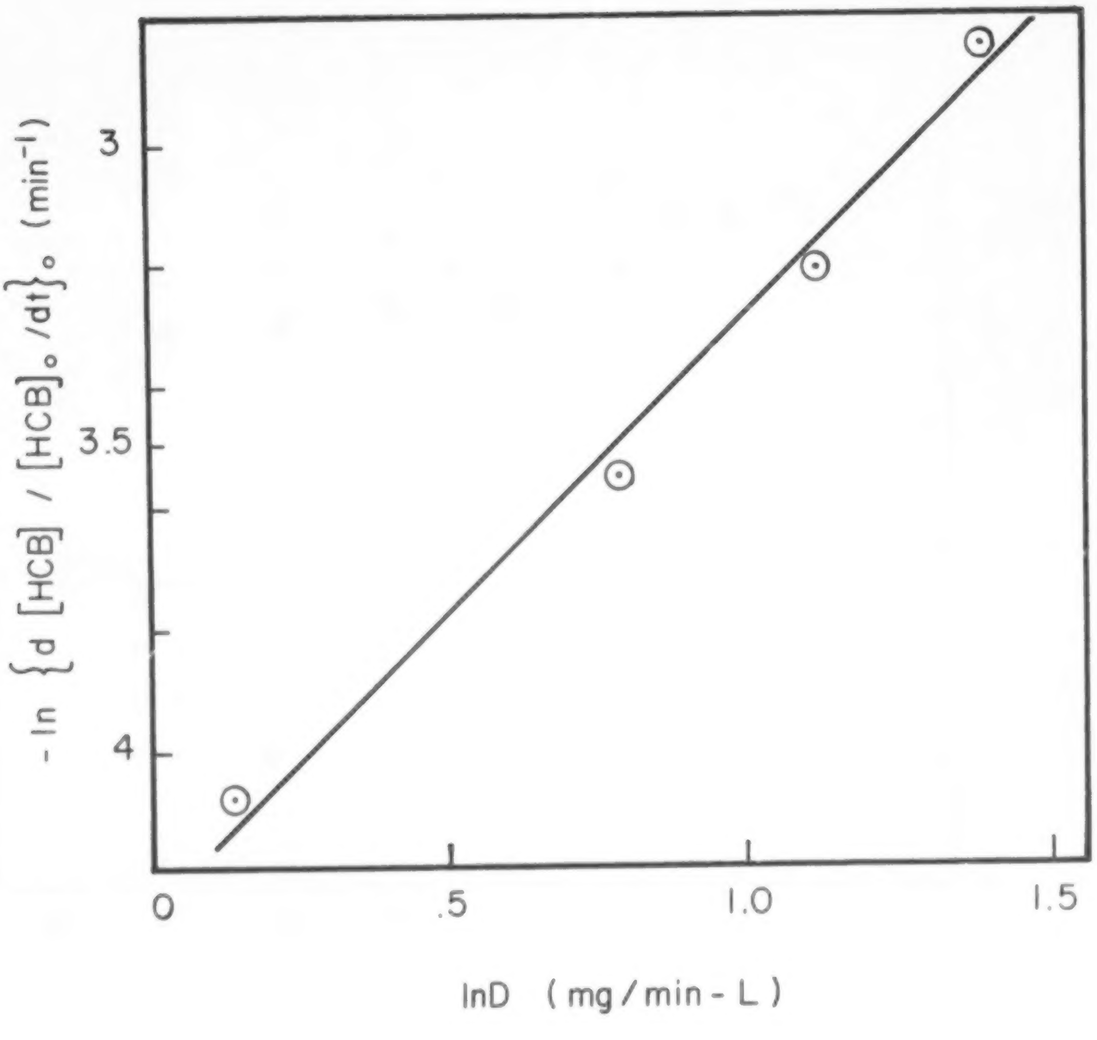

Figure D-4. Initial rates of direct ozonation of HCB in lake water at various ozone dose rates.

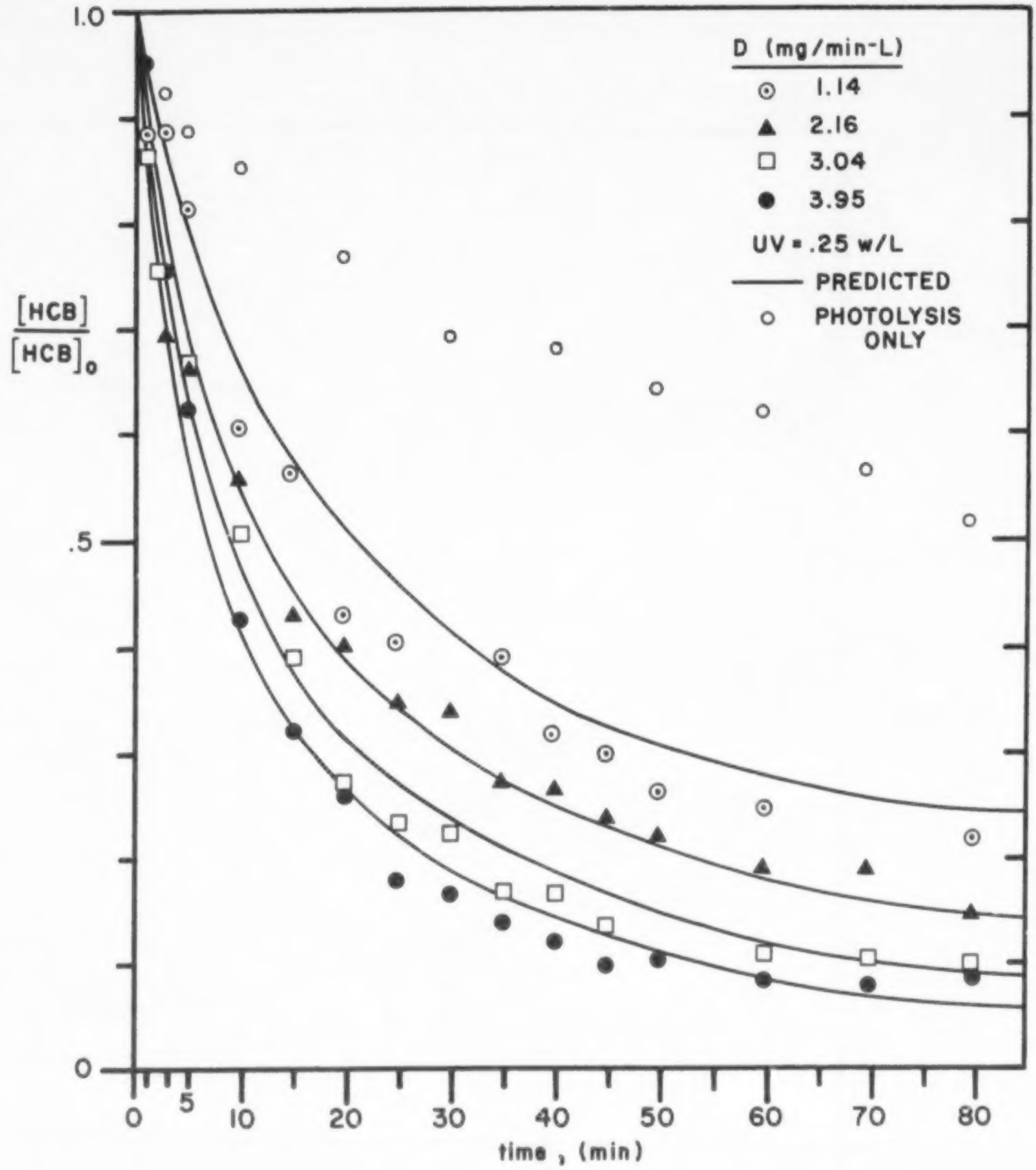

Figure D-5. Effects of dose rate on the photolytic ozonation of HCB in lake water.

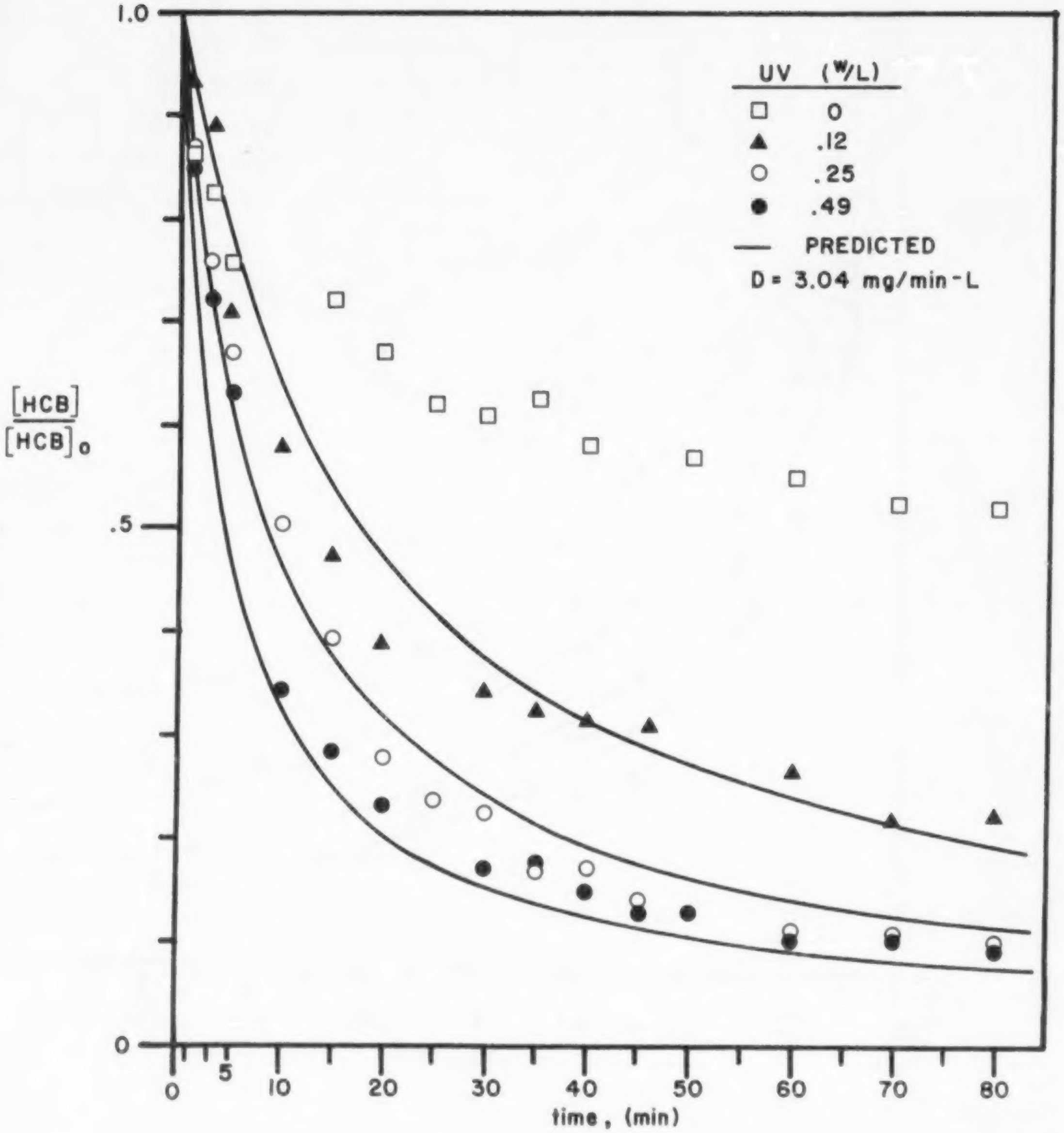

Figure D-6. Effect of UV radiation transfer rates on the photolytic ozonation of HCB in lake water.

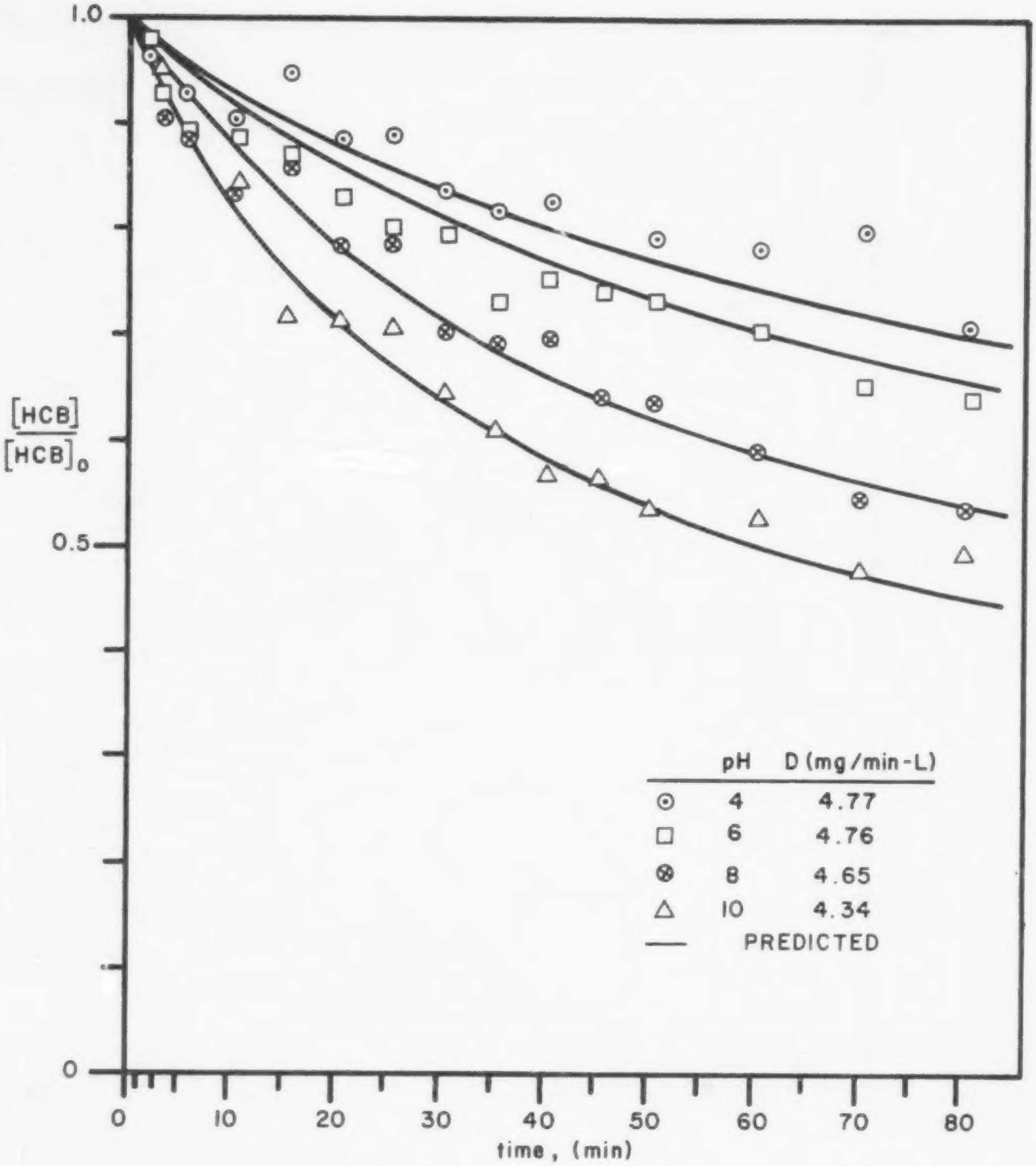

Figure D-7. pH effects on the rate of ozonation of HCB in purified water.

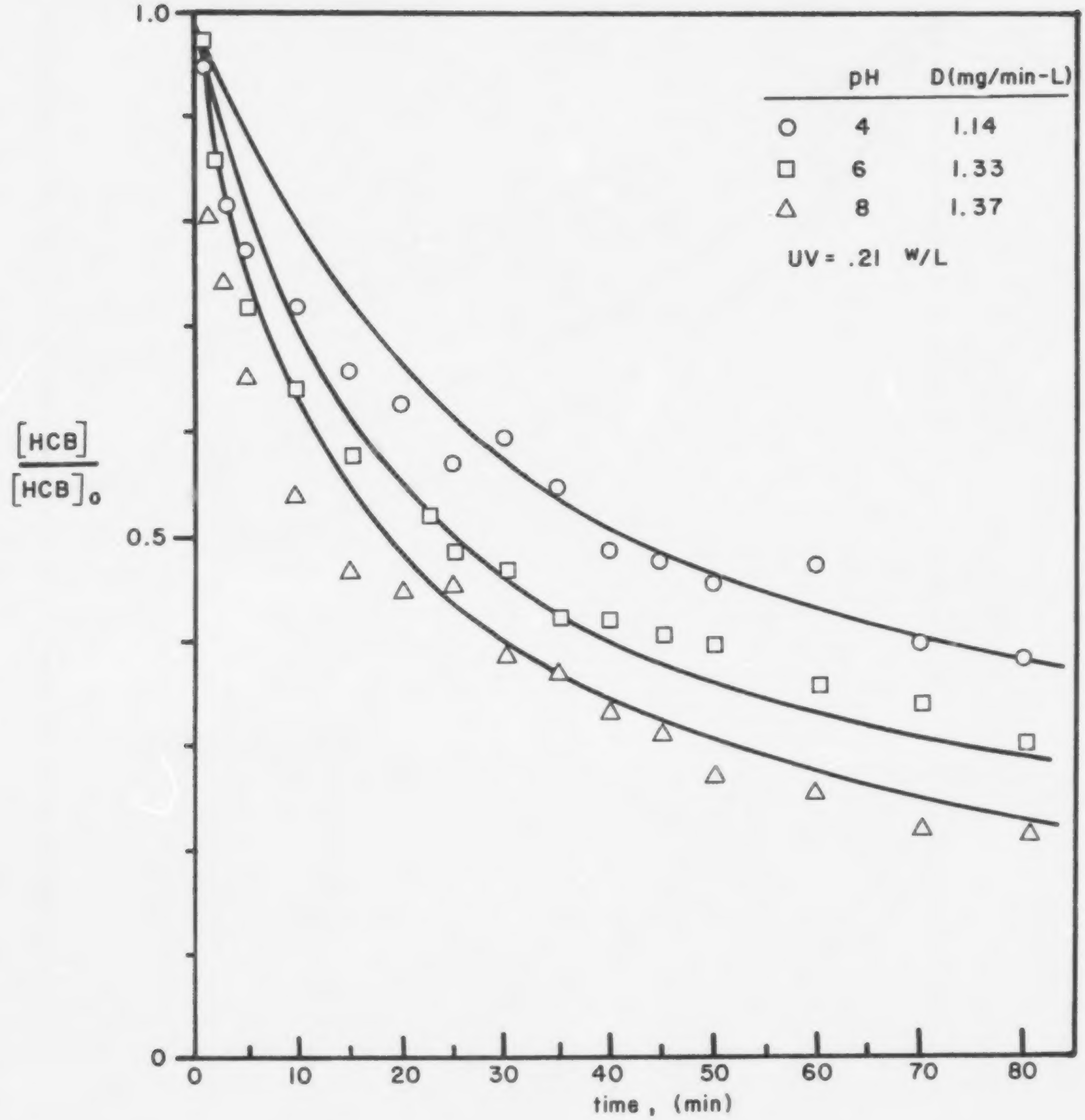

Figure D-8. Effect of pH on rates of photolytic ozonation of HCB in purified water

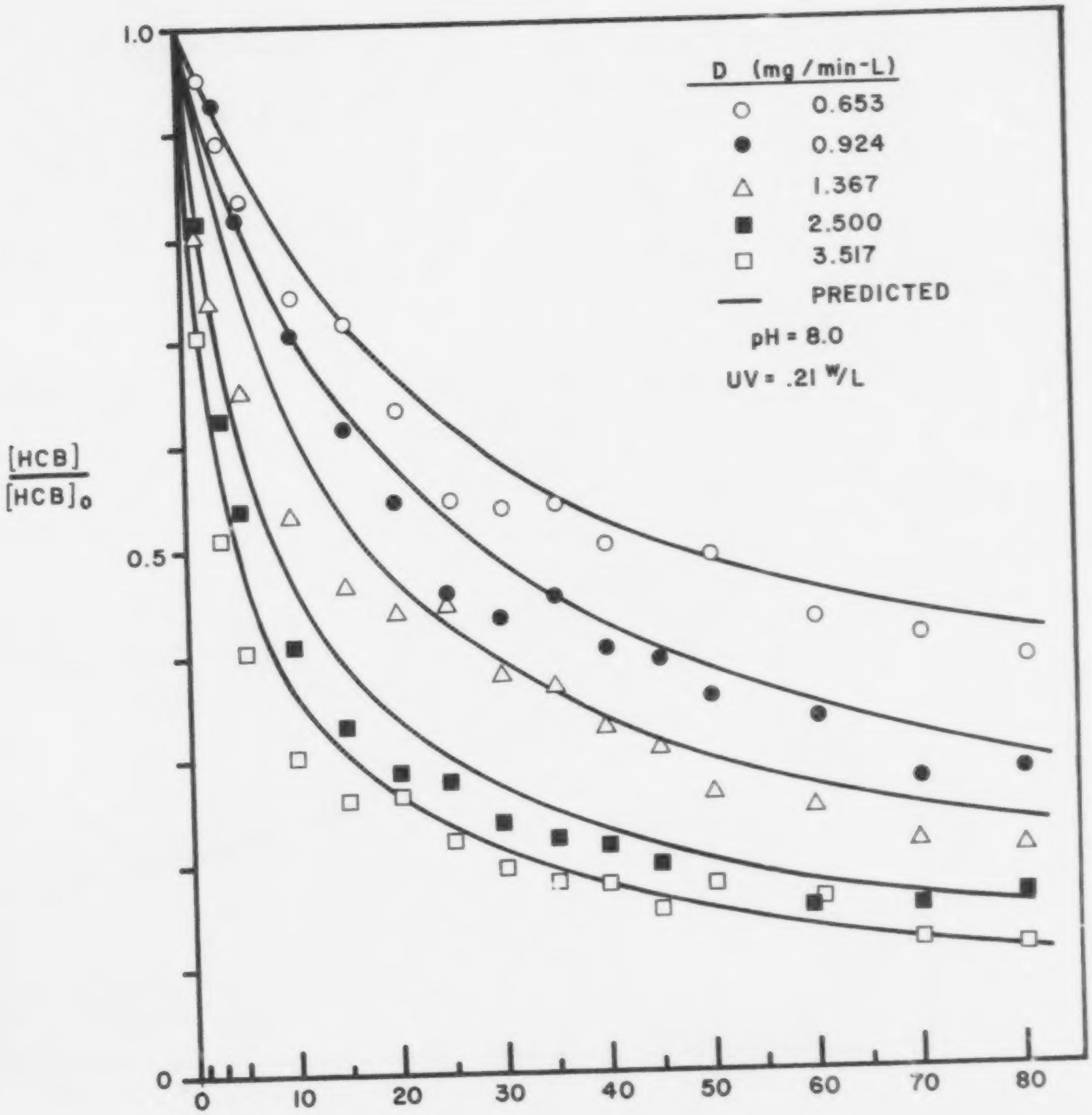

Figure D-9. Photolytic ozonation of HCB in purified water.

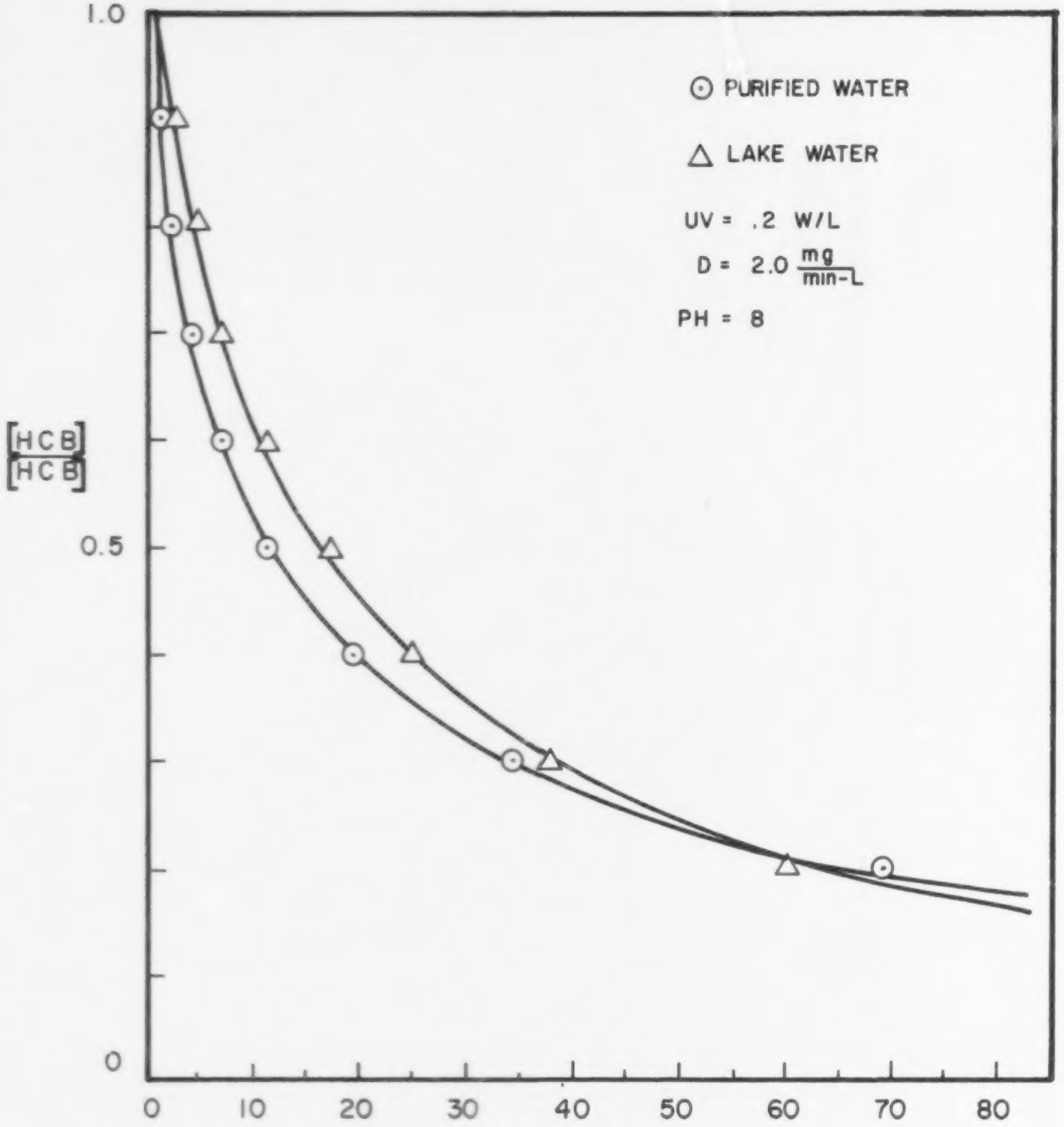

Figure D-10. Comparison of photolytic ozonation in lake water and purified water. UV intensity = 0.2 W/L.

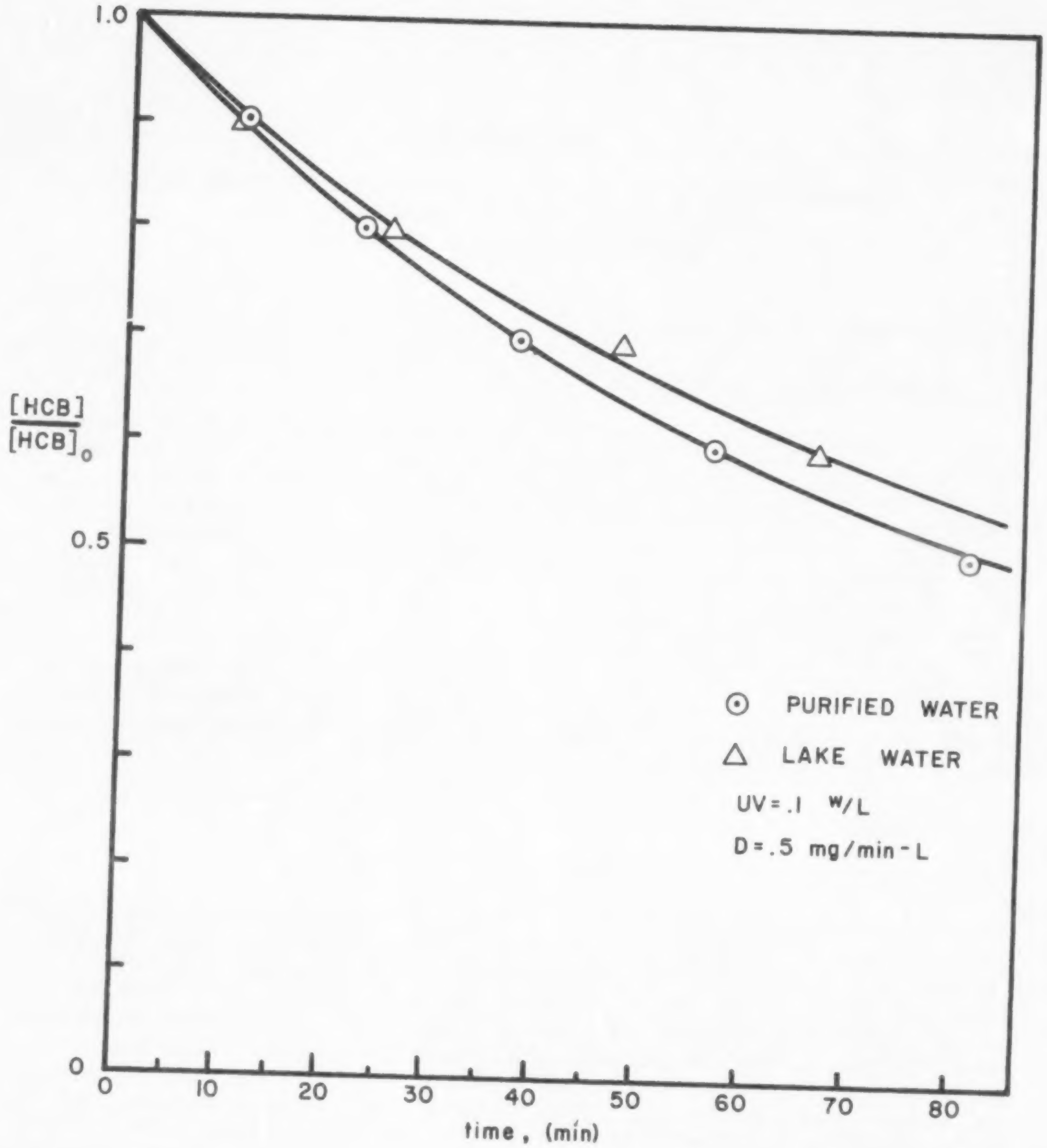

Figure D-11. Comparison of photolytic ozonation in lake water and purified water. UV intensity = 0.1 W/L.

APPENDIX E

IDENTIFICATION OF CHEMICAL BY-PRODUCTS FROM OZONE/ ULTRAVIOLET-INDUCED REACTIONS OF ORGANIC COMPOUNDS IN WATER

EXPERIMENTAL PROCEDURES

I. Experimental Apparatus

Besides the large contacting reactor described in Section 5 above, a small reactor was designed particularly for the study of oxidation by-products. Figure E-1 shows the design of the reactor. The body was made of quartz for the transfer of UV radiation, and had a reaction volume of 45 mL. Ozone was directed through the Pyrex tubing and sparged into the solution by a glass frit. The whole reactor was placed at the center of the Rayonet Photochemical Reactor. The operation of the reaction system was similar to that with the large contacting reactor, but the flow of O_3/O_2 was kept at 75 ml/min. The Swagelok nuts on the ozone inlet could be removed for taking samples from the solution; however, in so doing, the supplies of O_3 and UV were temporarily interrupted.

Analytical Instruments

Gas Chromatography/Mass Spectrometry

The Finnigan Model 3200 gas chromatograph/mass spectrometer (GC/MS) system with a Model 6100 data system was used to separate, detect and identify the components. All samples were chromatographed using a 30 meter by 0.25 mm I.D. SE-30 wall coated glass capillary column (Supelco, Inc.). A splitless technique was used in order to obtain high detectability. All the data were stored on magnetic tapes and interpreted by comparison with published mass spectra, commercially available computer data or by *a priori* interpretation based on the mass fragments. The GC/MS system was used primarily for the identification of the structure of products. Some packed columns were also used to assist in the identification of peaks found using the Model 5710A GC/FID.

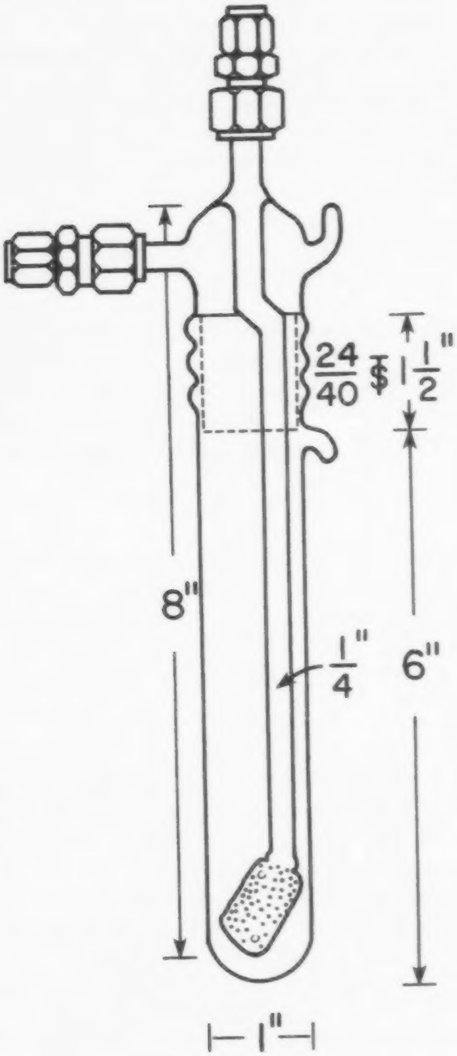
24/40 $
1 1/2"
8"
1/4"
6"
1"

Figure E-1. Reactor for ozone and ozone/UV treatment of HCB.

High Pressure Liquid Chromatography (HPLC)

The Waters Associates Model ALC-201 liquid chromatograph and solvent programmable Micromeritics Model 7000B liquid chromatograph were used to separate large amounts of product samples and to perform fractional collection for GC/MS identification. A Tracor 974A variable wavelength detector was connected to either liquid chromatograph. A wavelength of 255 nm was used for all separations. Organic solvents used were filtered and degassed. Purified water described previously was pumped through a C-18 reverse phase column for further purification. Three types of HPLC columns were used, one containing Partisil 10 ODS (permanently bonded C-18) (Whatman), another containing Bondapak C-18/Corasil, 35-50 microns (Waters Associate, Inc.), and the third containing Lichrosorb RP-18, 10 microns (EM Laboratories, Inc.). All were slurry packed into 15 cm by 4.6 mm I.D. stainless steel columns in the laboratory.

An electrochemical detector (ECD), Model LC-4 (Bioanalytical Systems Inc., West Lafayette, Ind.), was also used for detection of easily oxidized or reduced components in freeze-drying samples from the reaction mixture. In most cases, ECD and UV detectors were used and compared simultaneously.

Microcoulometry

A Dohrmann Envirotech Microcoulometric Titration System (MCTS-20) was used to measure the amount of chloride in the reaction mixture. The sample was injected directly into the T-300-S titration cell. The amount of chloride in nanograms was shown digitally on the display on the front panel.

Analytical Procedures

HCB in methanol was spiked into 45 mL of purified water as a suspension; usually 2-5 mg was applied. It was found necessary to make product runs at a much higher concentration than that used in the kinetic runs and, since the solubility limit of these relatively insoluble compounds was greatly exceeded, a cloudy suspension of substrate was the starting material for these studies. After ozone/UV treatment for a brief period, the cloudiness disappeared indicating that the substrate had reacted, and the treatment was stopped. The suspension was subjected to photolysis, ozonation and photolytic ozonation. Ozone dose rate was 6.14 mg/min. At the end of a run, the whole solution was extracted with anhydrous ether according to the scheme shown in Figure E-2. The acidic extraction fraction was methylated using diazomethane by the procedure and apparatus of Keith (158). Both neutral and acidic fractions were concentrated to a final volume of 200 μL and internal standard, hexamethyl benzene, was added for quantitative determination of the yields of products.

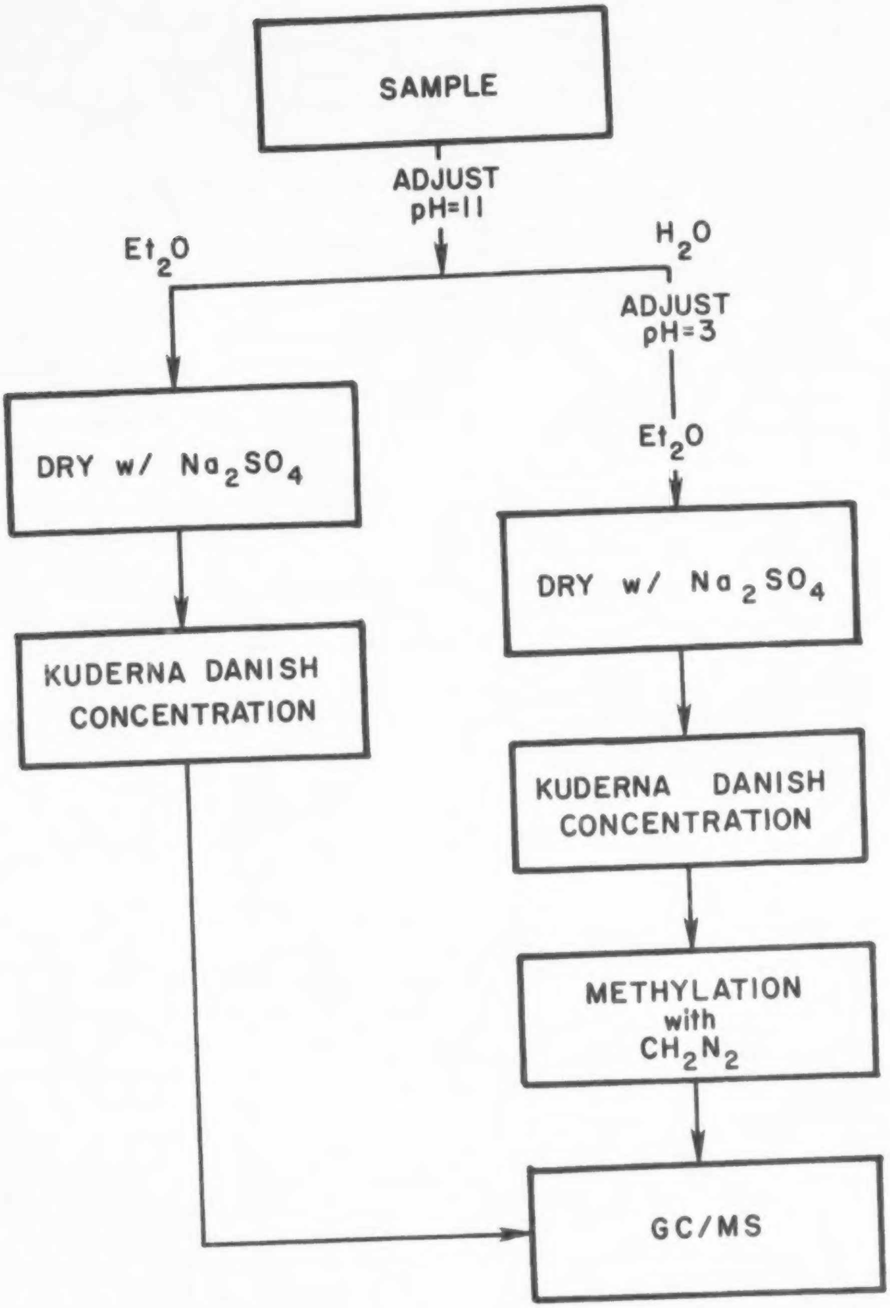
SAMPLE
ADJUST pH=11
Et₂O
H₂O
ADJUST pH=3
DRY w/ Na₂SO₄
Et₂O
DRY w/ Na₂SO₄
KUDERNA DANISH CONCENTRATION
KUDERNA DANISH CONCENTRATION
METHYLATION with CH₂N₂
GC/MS

Figure E-2. Extraction scheme.

The products were chromatographed on the Hewlett Packard Model 5710A GC/FID or Finnigan Model 3200 GC/MS. Structures were assigned by rationalization of the mass spectra. These were confirmed by comparison with known spectra from the literature (164-166) or from analysis of an authentic sample in this laboratory.

Nonextracted small acids and oxalic acid were determined by the modified methods of Bethge and Lindstrom (159). A portion of aqueous solution resulting from photolytic ozonation was made basic by adding tetrabutylammonium hydroxide and dried at 40°C in a heated vacuum desiccator, Precision Scientific Co., Chicago, Illinois. The residues were dissolved in acetone and either benzyl bromide or an alkyl iodide was added. Small acids were converted to benzyl derivatives and GC/FID chromatographed on the butanediol succinate column. Oxalic acid was converted to its ethyl derivative and chromatographed on the SP-1000/H_3PO_4 column.

The relationship of the formation of several major products to the photolytic ozonation time were studied. Several runs were carried out, each having different reaction time, and the products in each sample were chromatographed by GC-FID and GC/MS using the SP-2100 column and SE-30 capillary column.

The large contacting reactor was also used for study of products. Three liters of reaction solution were extracted according to the scheme in Figure E-2. The products were identified by GC/MS and the concentrated samples were chromatographed using HPLC. Collections of HPLC fractions was carried out by collecting the components in 5 mL vials immediately after the UV detection cell.

In the case of the volatile chlorinated compounds chloroform, bromodichloromethane, and tetrachloroethylene, the chromatograms obtained from the kinetic work were searched for the appearance of new peaks during a run, which would probably indicate that a halogen was being formed. In only one case was such a peak found during ozone/UV or ozone-only experiments, and those results will be described in the later section which covers results.

In addition to chromatographic monitoring of the reaction mixture, product runs were made for chloroform and tetrachloroethylene in which the off-gas was bubbled through basic solution in order to trap expelled carbon dioxide. The off-gas was next directed to another trap containing pentane or isooctane, in order to trap volatile nonpolar compounds. When gas chromatographic analysis showed that most of the substrate had been destroyed in a particular run, additional gas was sparged through the headspace to ensure the removal of CO_2 to the trap, then the reaction mixture was analyzed by microcoulometry to determine the chloride content and by titration to determine the amount of hydrogen ion formed. Ozone consumption was calculated from the dose rate and treatment time. The final reaction mixture was extracted by a modification of the method of Henderson, Peyton and Glaze (167) and that extract checked for the presence of products by gas chromatography and GC/MS.

Ozonation and Photolytic Ozonation Products of Natural Water

Caddo Lake water was ozonated without UV irradiation in order to identify products of the oxidation/photolysis reactions which occur. Three liters of filtered Caddo Lake water was treated for 25 minutes with 500 ml/min of 2.4% by weight of ozone in oxygen, corresponding to a dose rate of 28.4 mg/min. The reactor was stirred at a rate of 365 rpm, and in the UV run, 8 low-pressure, 75 W bulbs were used. One liter of the treated water was adjusted to pH 11 and extracted with 150 ml, 75 ml, and 50 ml portions of ether. The extracts were passed through a drying column of sodium sulfate and then concentrated to 200 µl. The extracted water was adjusted to pH 3, extracted and dried as above, and concentrated to 2 ml. This was split into two portions, one being derivatized with Methelute and one with diazomethane. Controls (no ozone) and ether and diazomethane blanks were run, and these, as well as the samples, were diluted with an equal volume of hexane prior to splitless capillary chromatography/mass spectrometry using a 30 meter SP-2100 WCOT column in a Finnigan 3200 GC/MS system. The samples derivitized with methelute had many spurious and interfering peaks which were present in the control, and those samples were discarded.

I. Results of Product Studies on Chloroform

These results are given in the body of the report.

II. Results of Product Studies on 2,2',4,4',6,6'-Hexachlorobiphenyl

This section of Appendix E contains reconstructed gas chromatograms and mass spectra from which products of the ozone/UV treatment of hexachlorobiphenyl were identified. Figures E-3 -E-7 show the reconstructed gas chromatograms and mass spectra from product studies on HCB photolysis. Table E-1 contains the major acidic products identified and their location in Figures E-8, E-9, and E-10. Figures E-11 through E-17 give mass spectra and major fragmentation patterns for products identified in the reconstructed gas chromatogram shown in Figure E-8. Results are discussed in Section 6 of the main report.

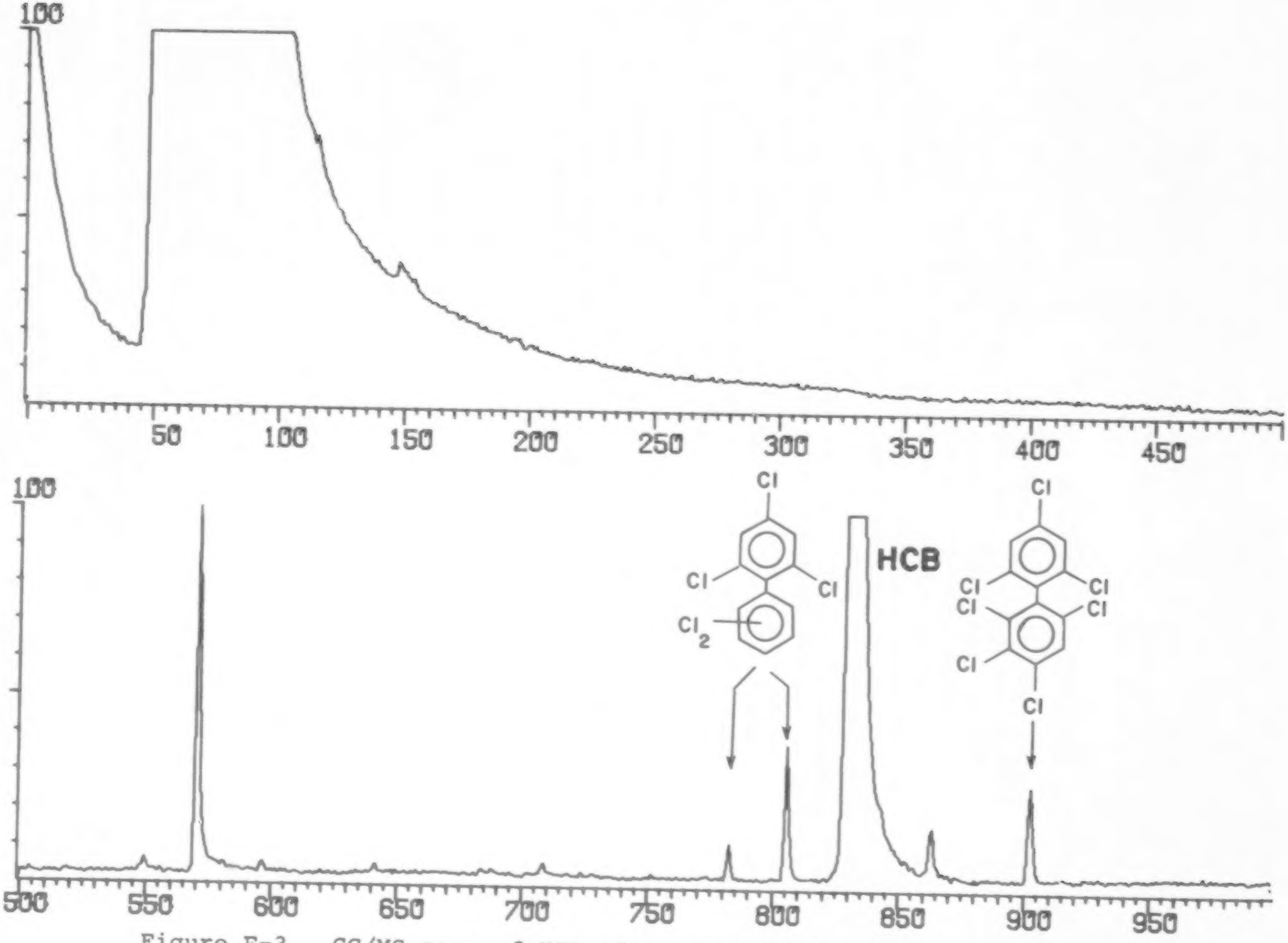

Figure E-3. GC/MS scan of HCB after photolysis under nitrogen.

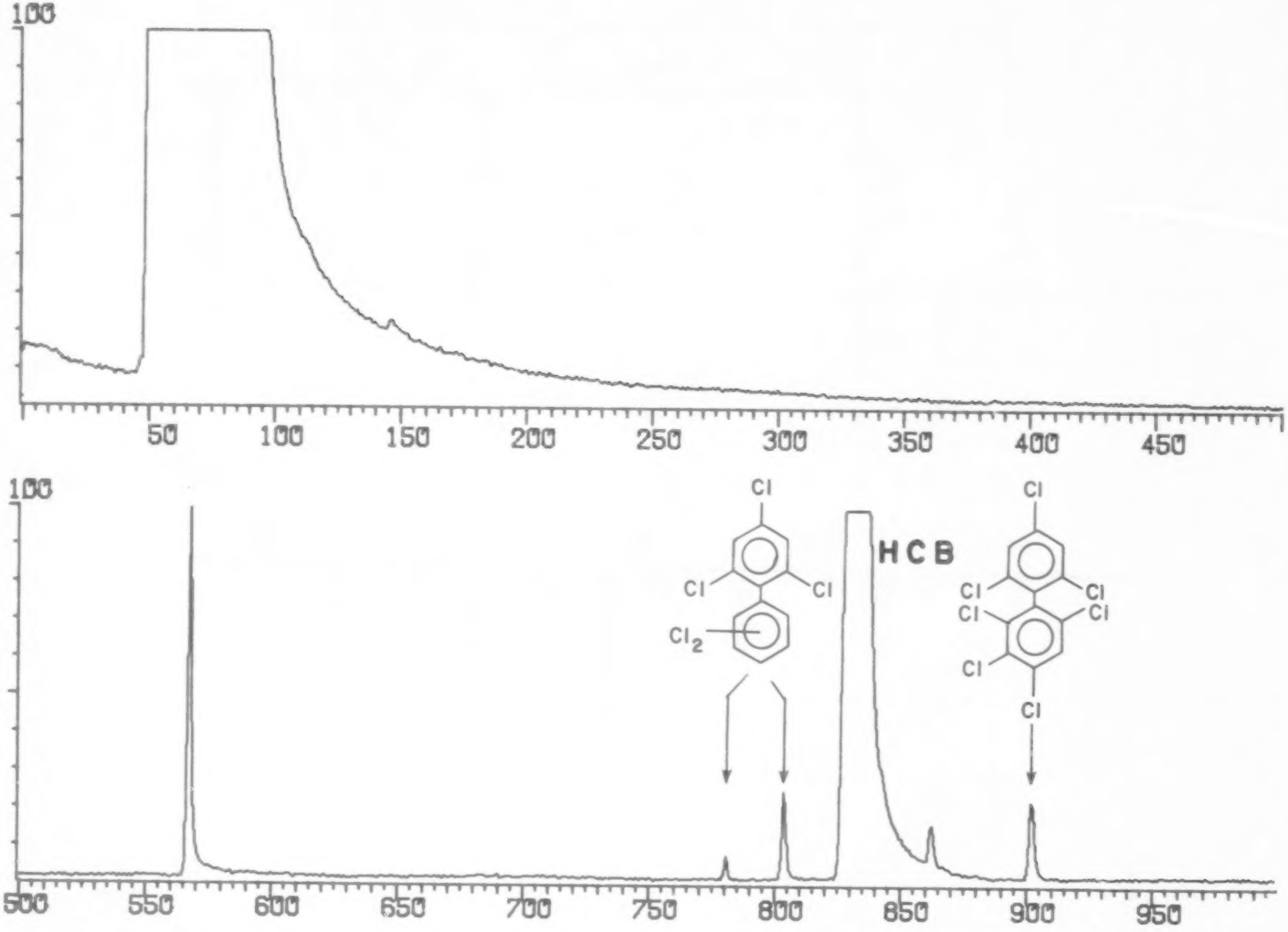

Figure E-4. GC/MS scan of HCB after photolysis under oxygen.

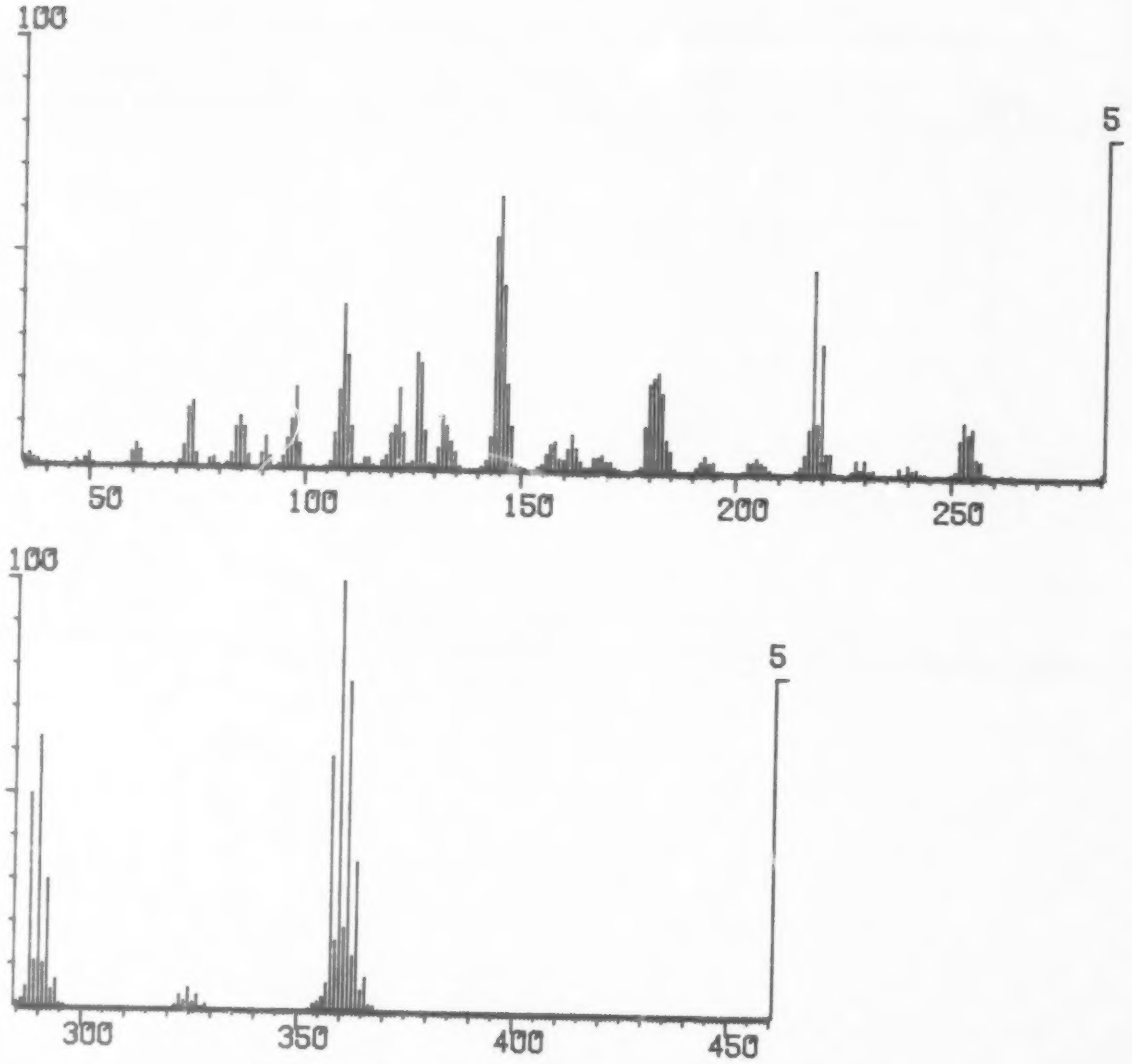

Figure E-5. Mass spectrum of spectrum no. 834.

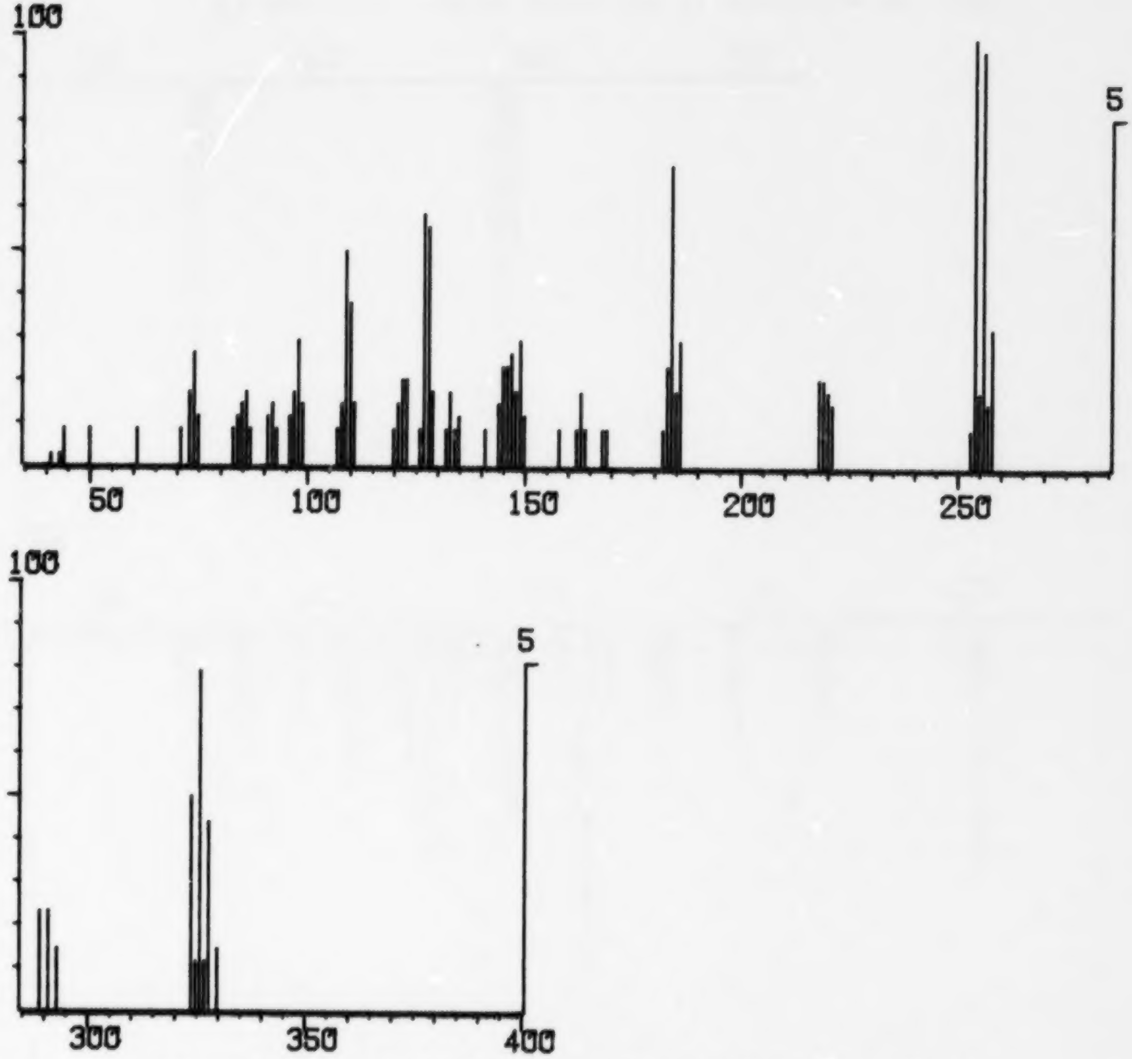

Figure E-6. Mass spectrum of spectrum no. 806.

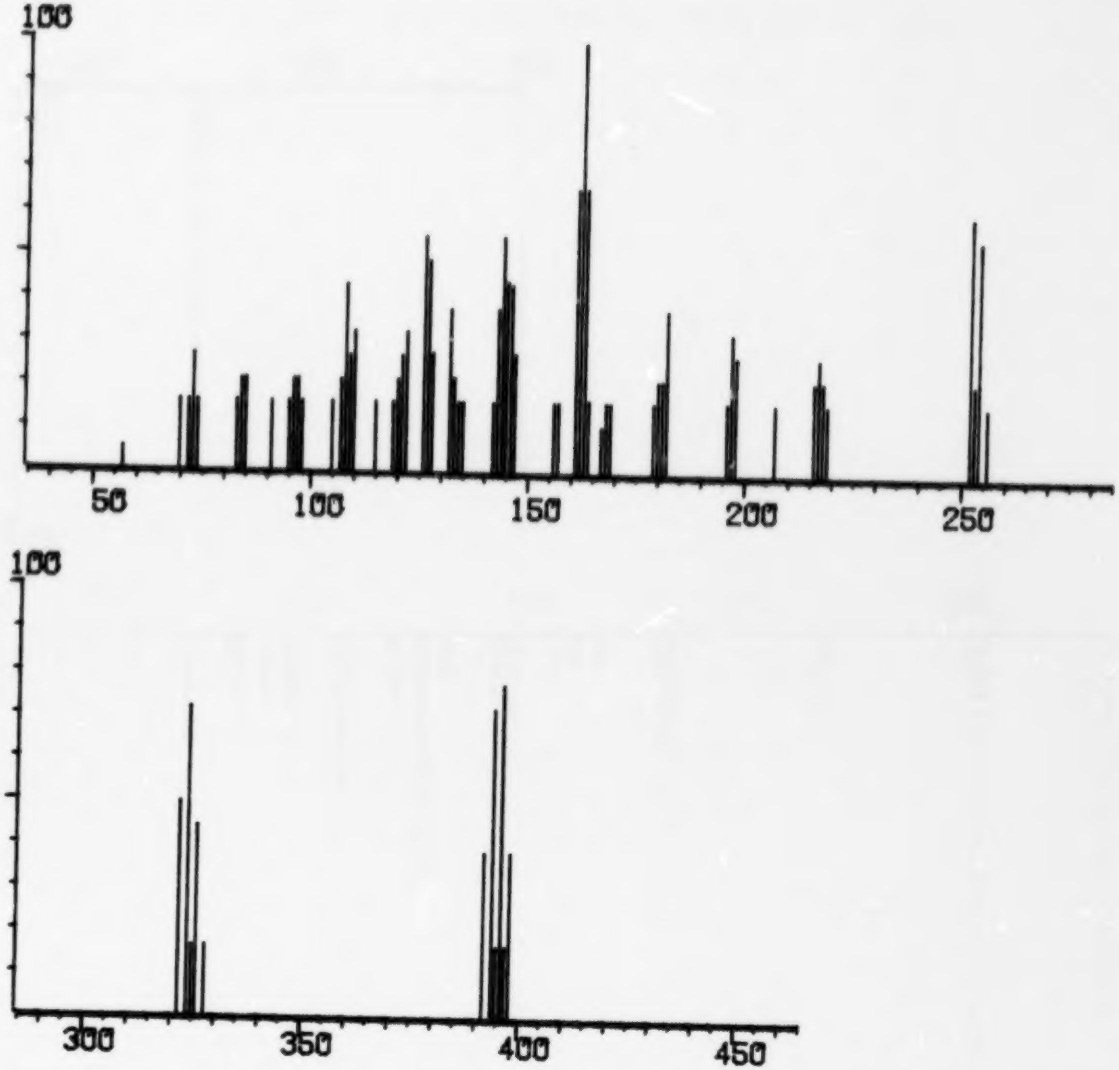

Figure E-7. Mass spectrum of spectrum no. 903.

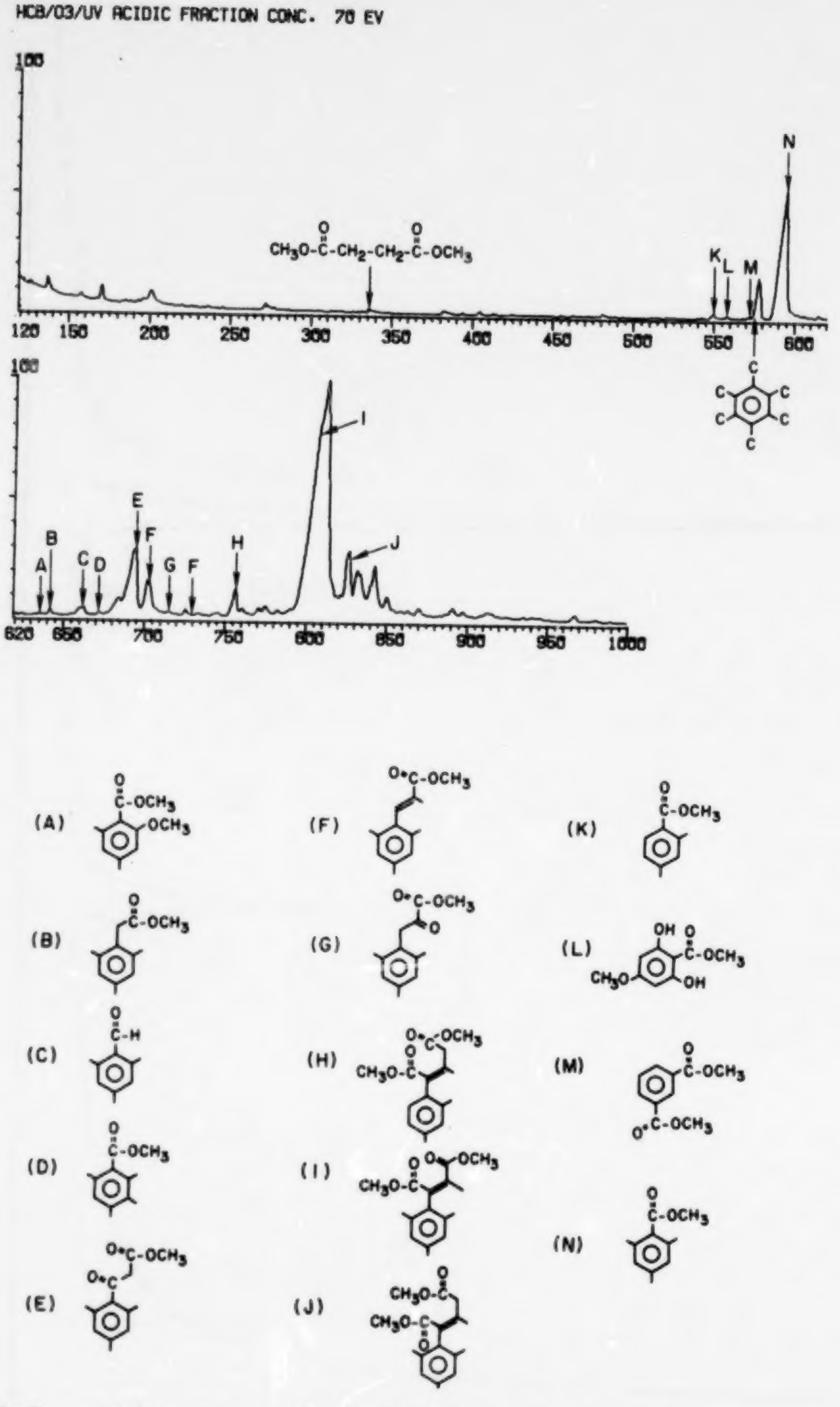

Figure E-8. GC/MS scan of acid fraction from the photolytic ozonation of HCB.

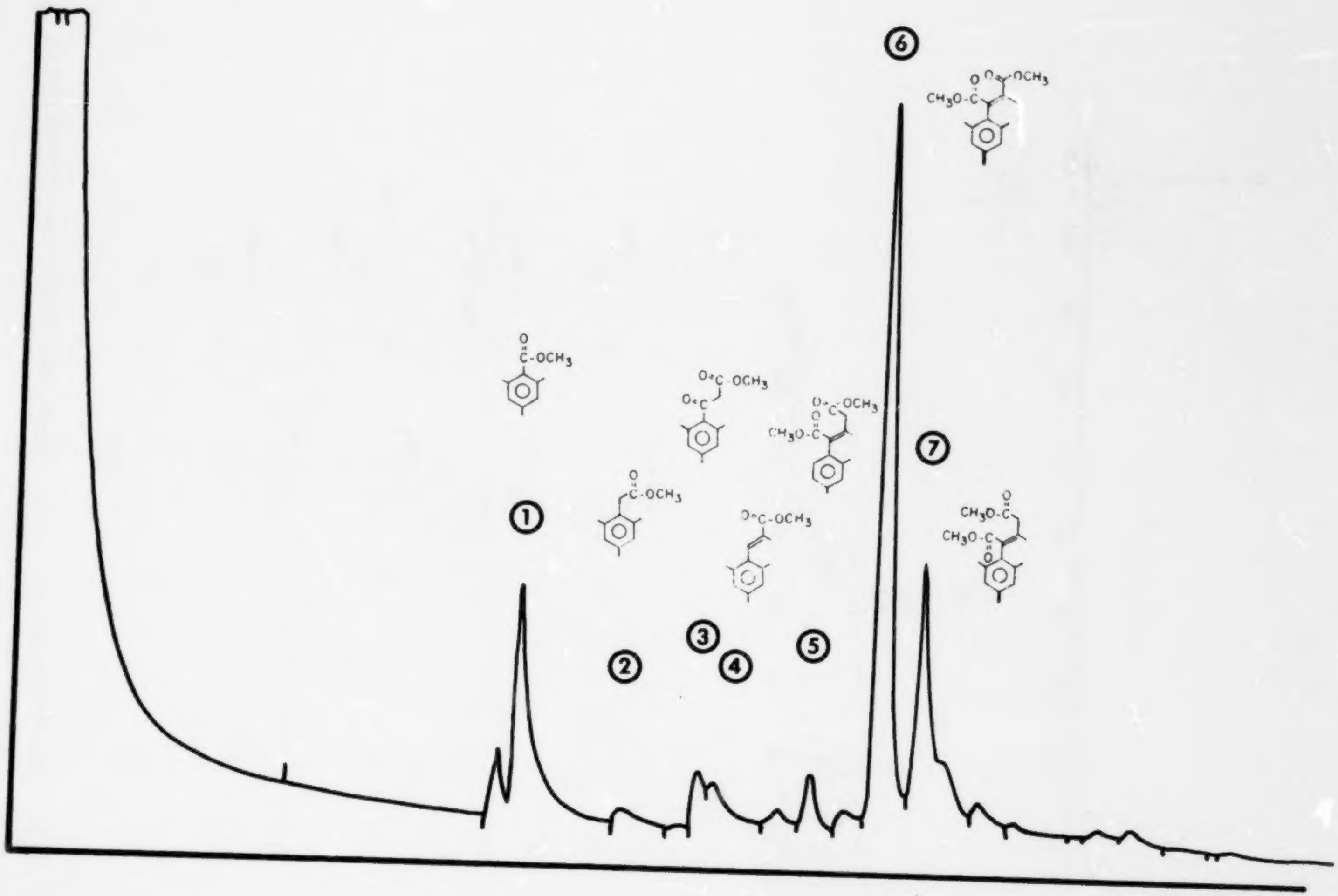

Figure E-9. FID chromatogram of HCB/O_3/UV reaction mixture.

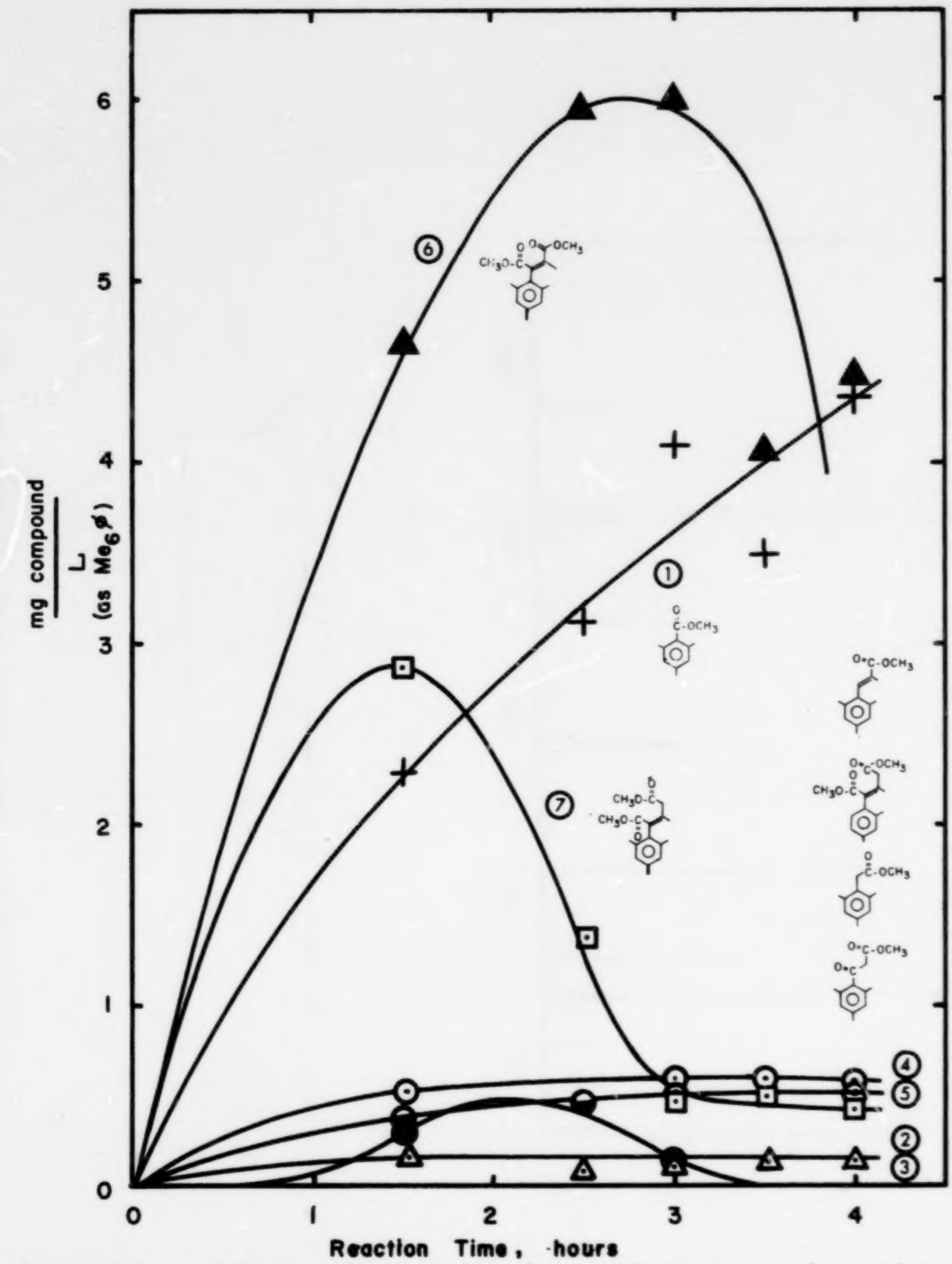

Figure E-10. HCB photolytic ozonation products at various time intervals.

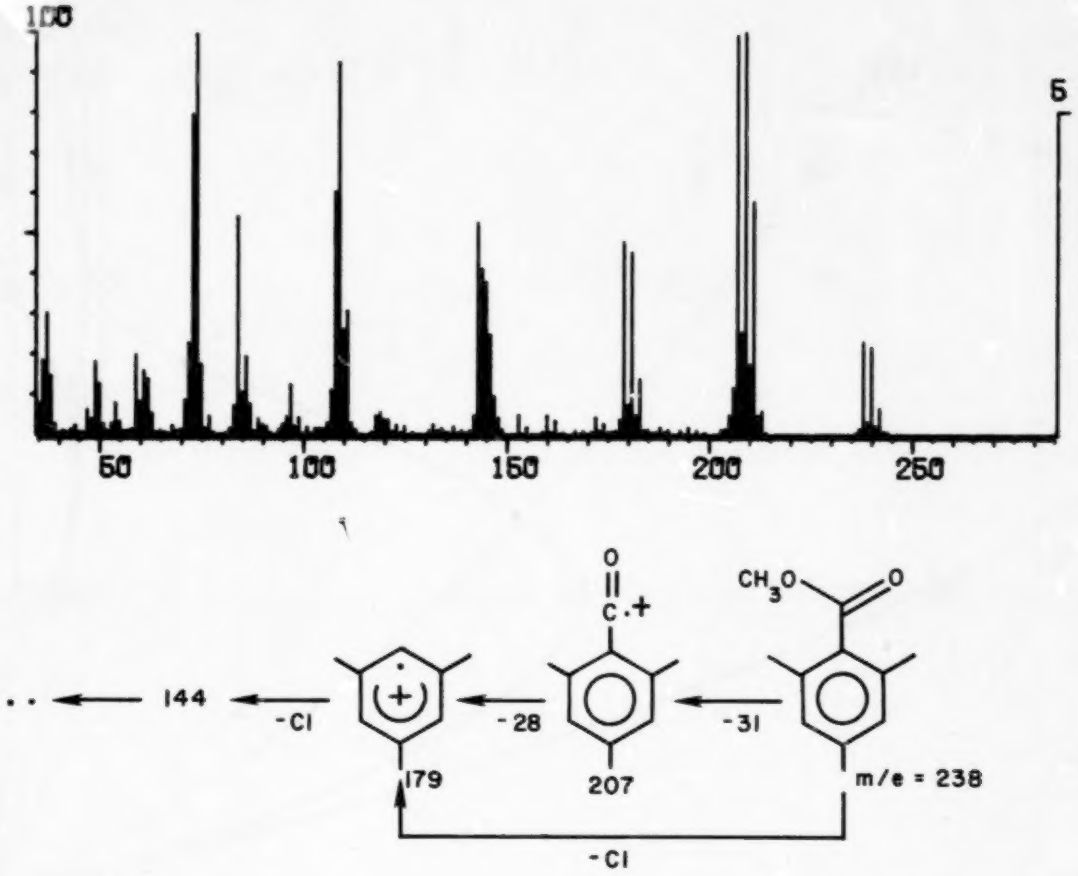

Figure E-11. Mass spectrum of spectrum no. 590.

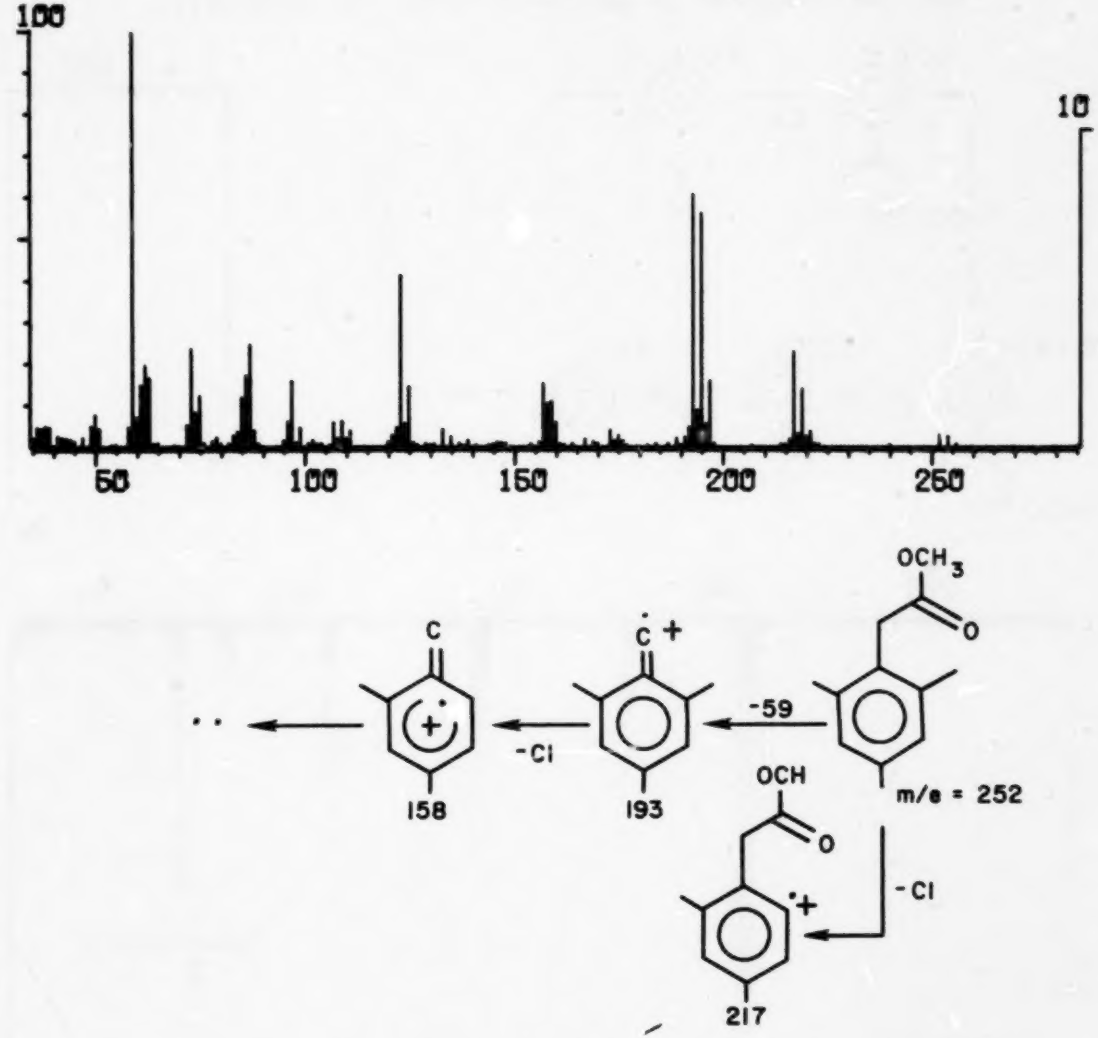

Figure E-12. Mass spectrum of spectrum no. 640.

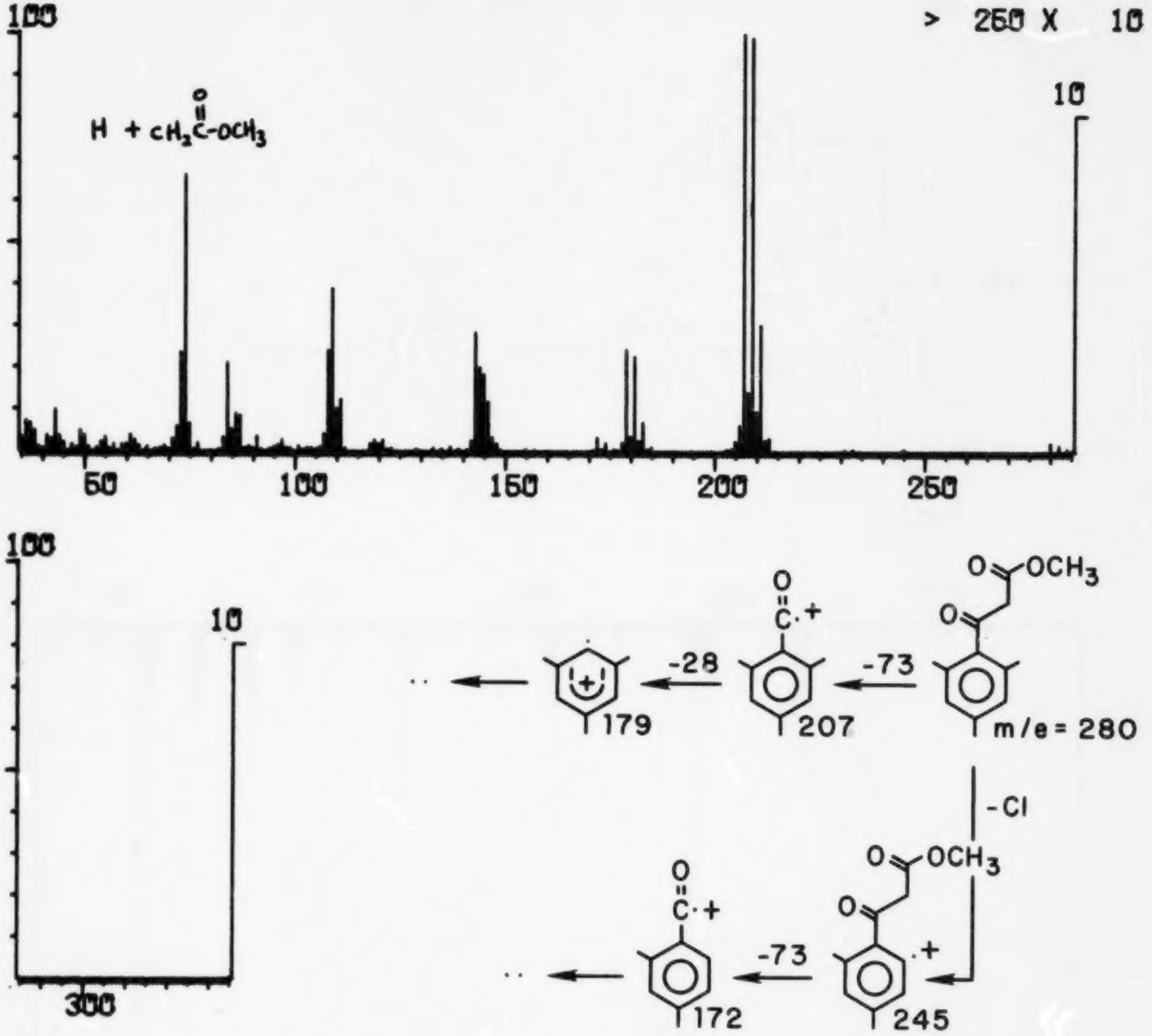

Figure E-13. Mass spectrum of spectrum no. 690.

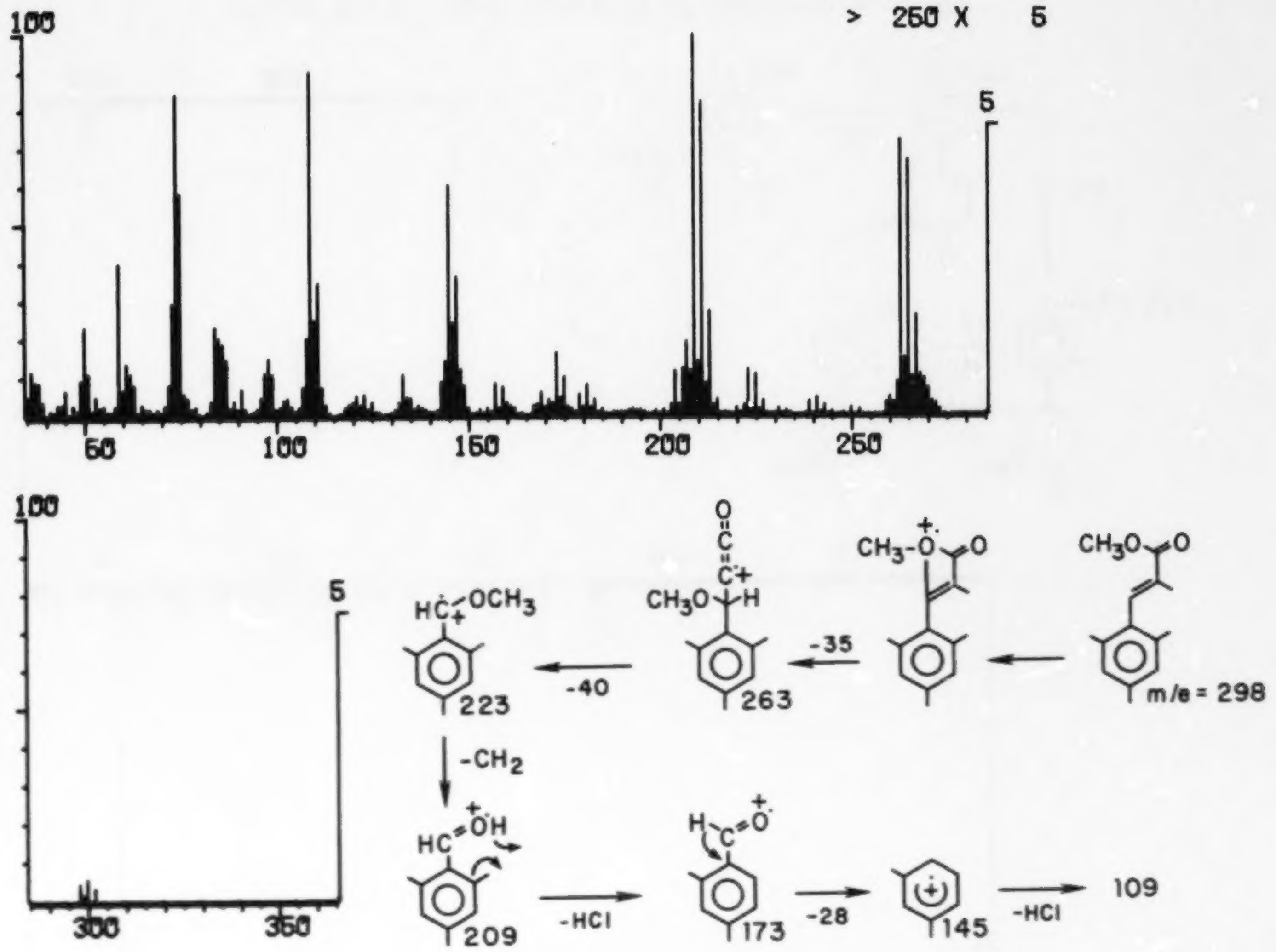

Figure E-14. Mass spectrum of spectrum no. 700.

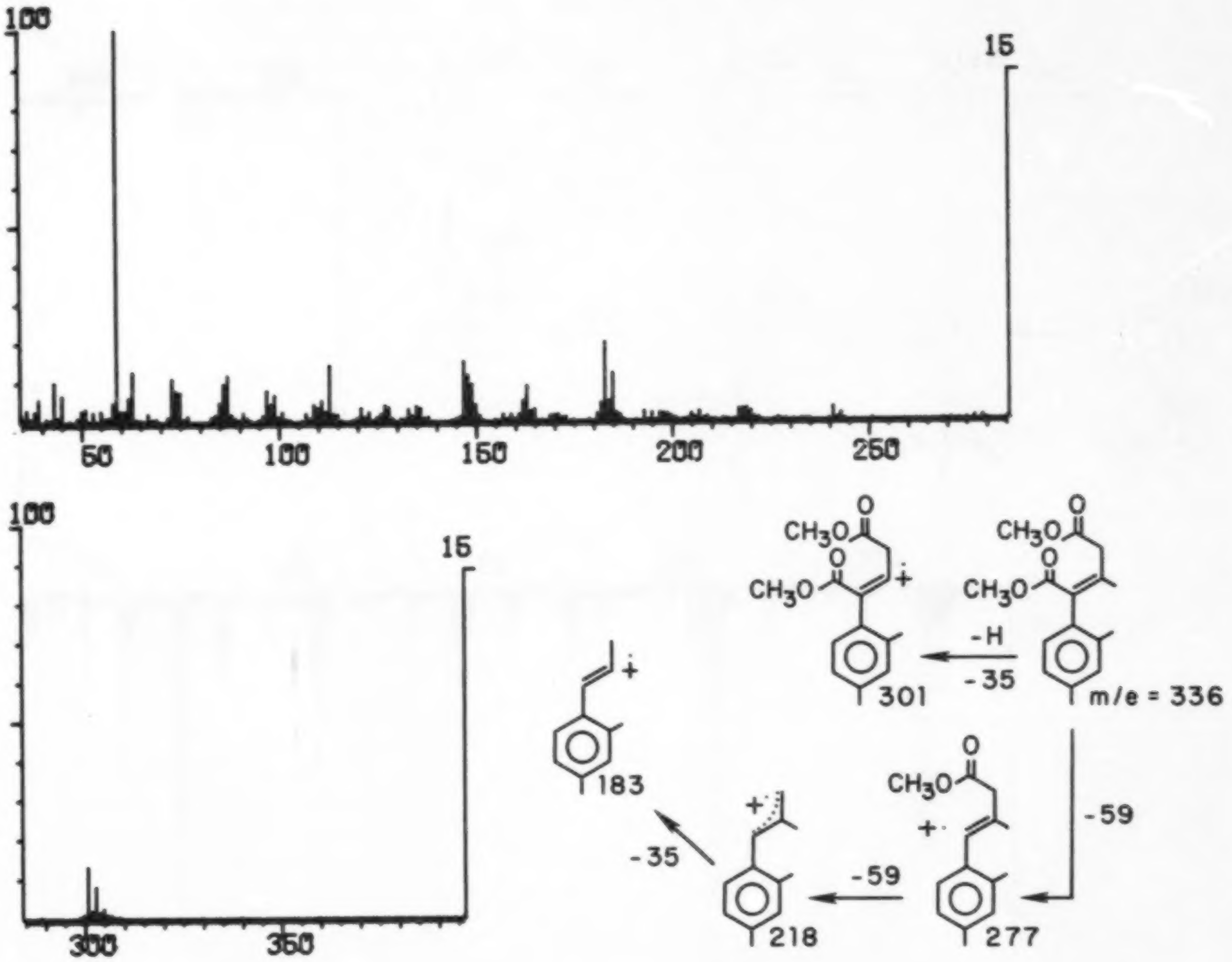

Figure E-15. Mass spectrum of spectrum no. 755.

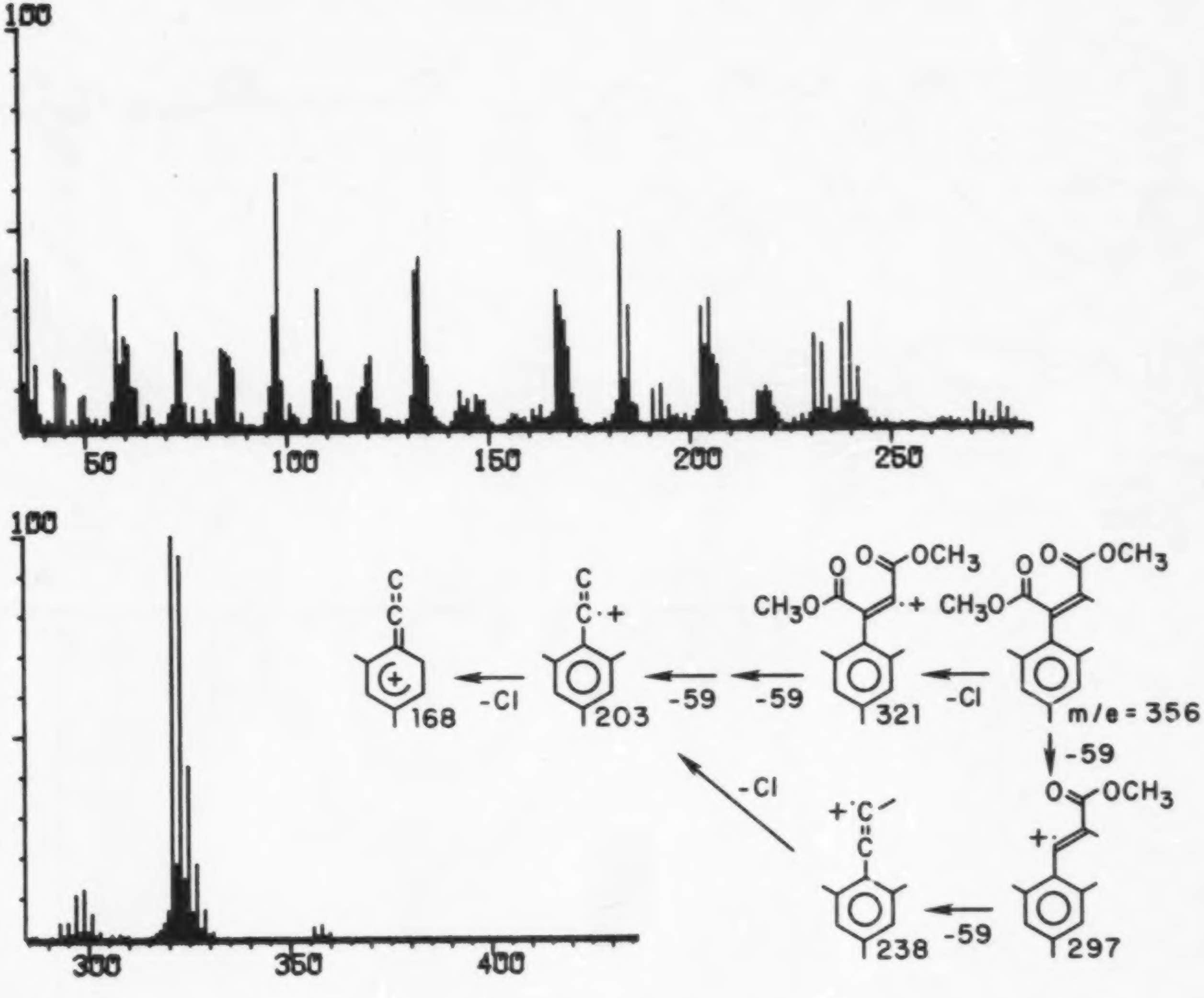

Figure E-16. Mass spectrum of spectrum no. 807.

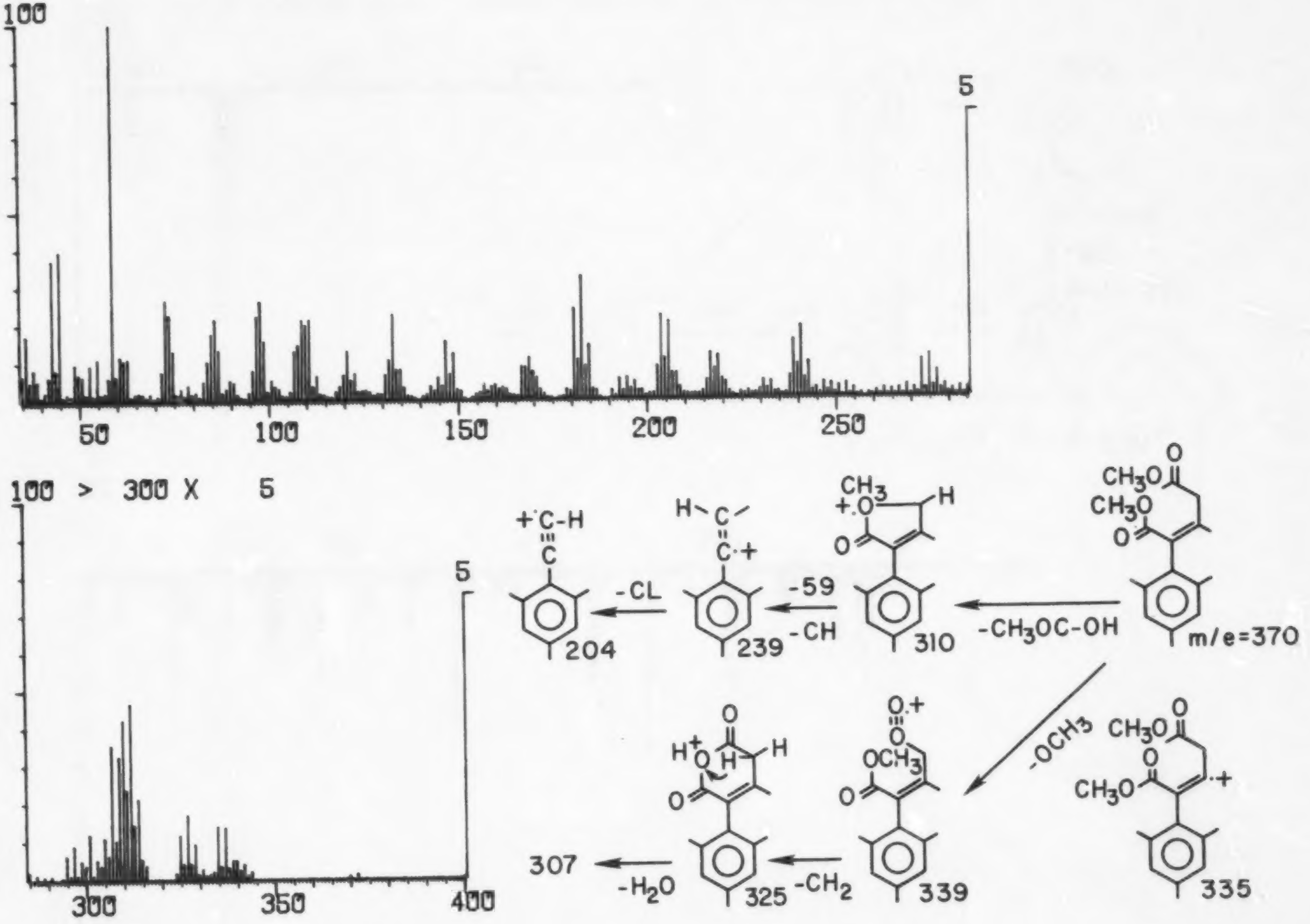

Figure E-17. Mass spectrum of spectrum no. 820.

TABLE E-1. MAJOR ACIDIC PRODUCTS IDENTIFIED IN PHOTOLYTIC OZONATION OF HCB IN WATER

Peak No.#	Compound ( )*	Structure
1.	2,4,6-trichlorobenzoic acid (590)	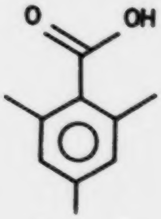
2.	2-(2,4,6-trichlorophenyl) acetic acid (640)	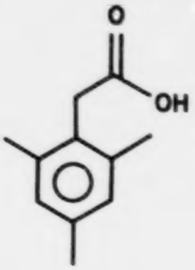
3.	3-keto-3-(2,4,6-trichlorophenyl)-propanoic acid (690)	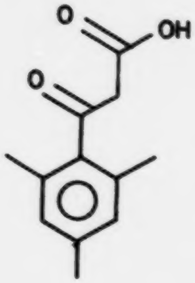
4.	2-chloro-3-(2,4,6-trichlorophenyl)-2-propenoic acid (700)	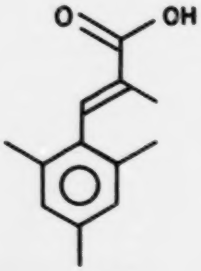

# Peak number from Figure E-9

( )* Spectrum number of compound from Figure E-8

TABLE E-1 (Continued)

Peak No.#	Compound ( )*	Structure
5.	2-(2,4-dichlorophenyl)-3-chloro-2-pentenedioic acid (755)	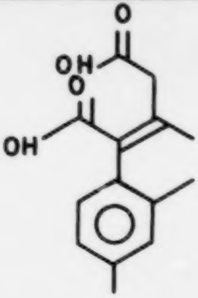
6.	2-chloro-3-(2,4,6-trichlorophenyl) maleic acid (804)	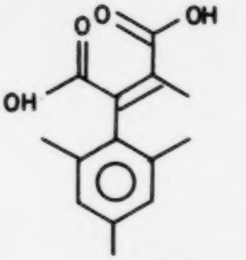
7.	2-(2,4,6-trichlorophenyl)-3-chloro-2-pentenedioic acid (820)	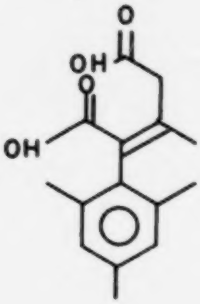

* Peak number from Figure E-9

( )* Spectrum number of compound from Figure E-8

III. Results of Product Studies on Caddo Lake Water

Following, in Figures E-18 through E-23 and Table E-2 are the reconstructed gas chromatograms and corresponding list of compounds determined in extracts from controls, ozonated Caddo Lake water and the same water treated with ozone/UV. Results are discussed in Section 6 of the main report.

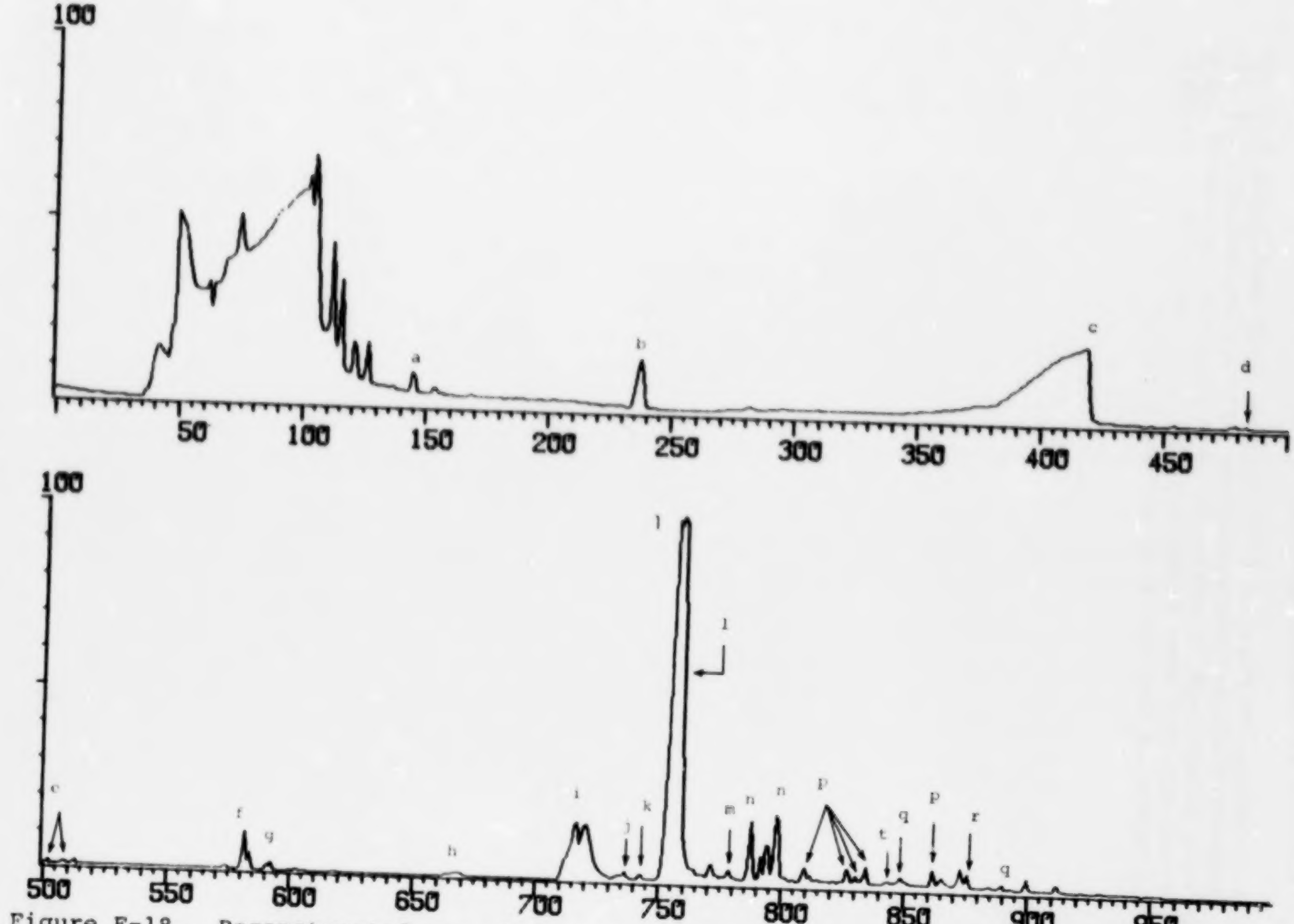

Figure E-18. Reconstructed gas chromatogram; Caddo Lake water, ozonated. netural fraction.

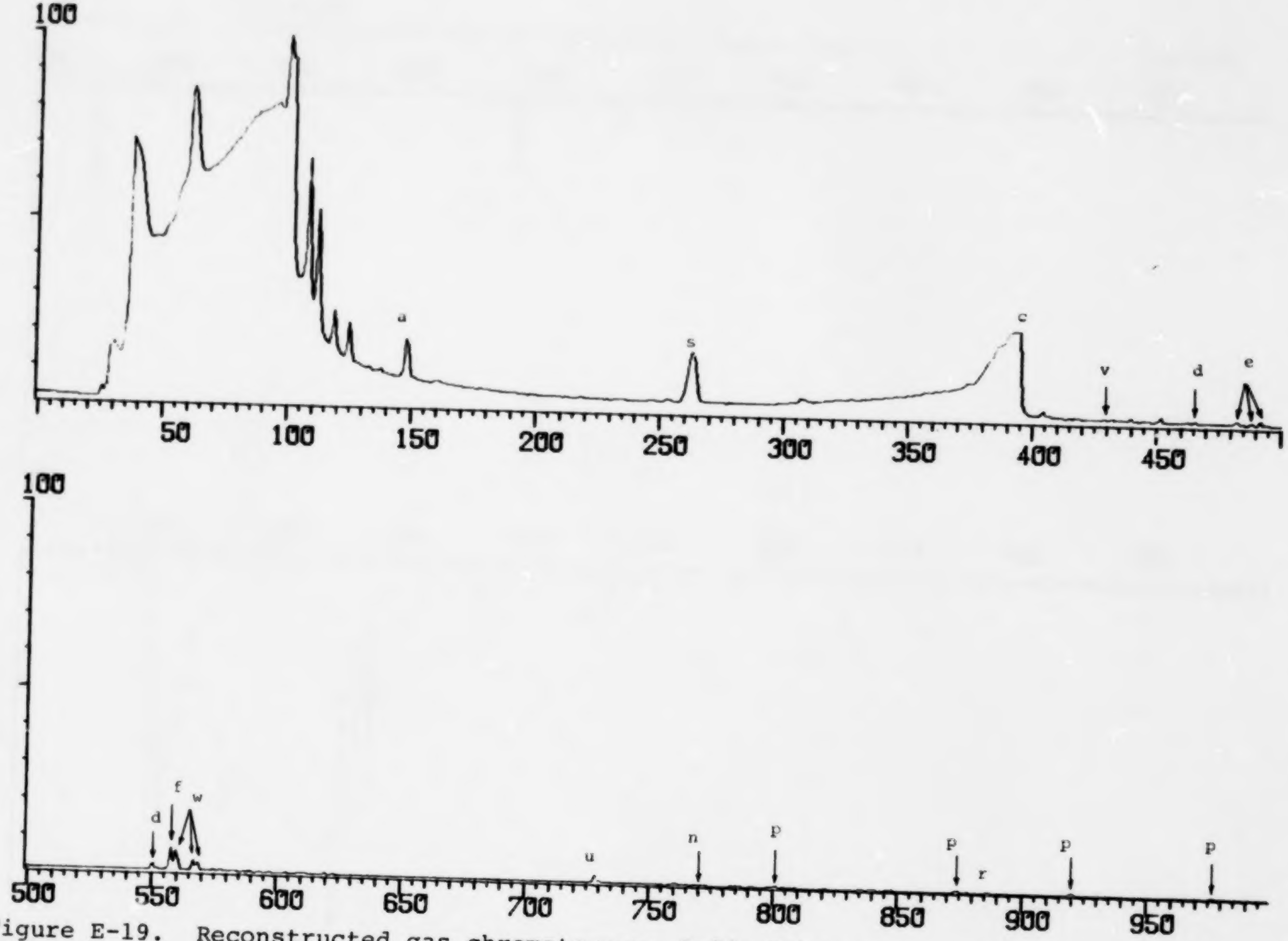

Figure E-19. Reconstructed gas chromatogram; Caddo Lake water, ozone/UV. neutral fraction.

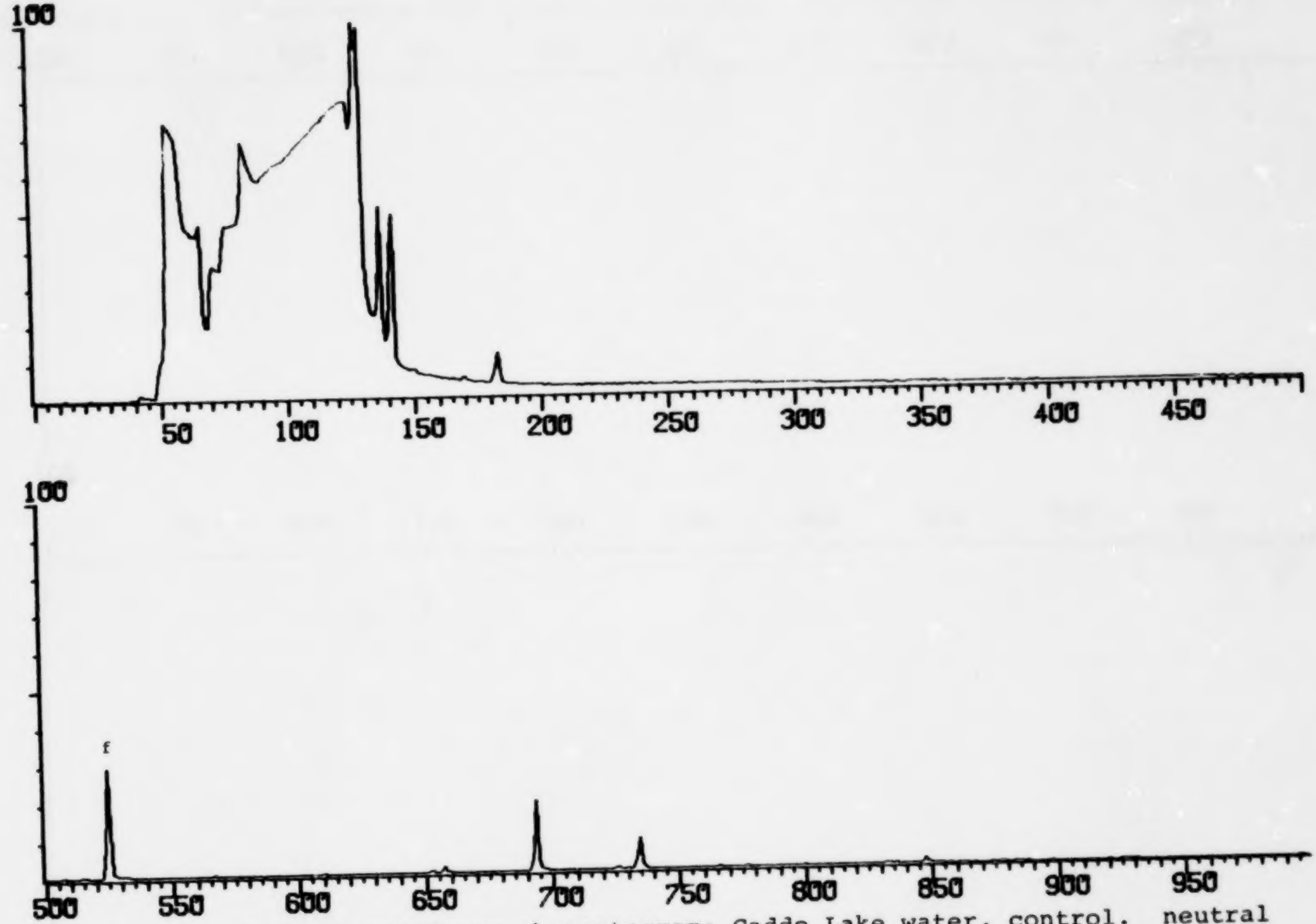

Figure E-20. Reconstructed gas chromatogram; Caddo Lake water, control. neutral fraction.

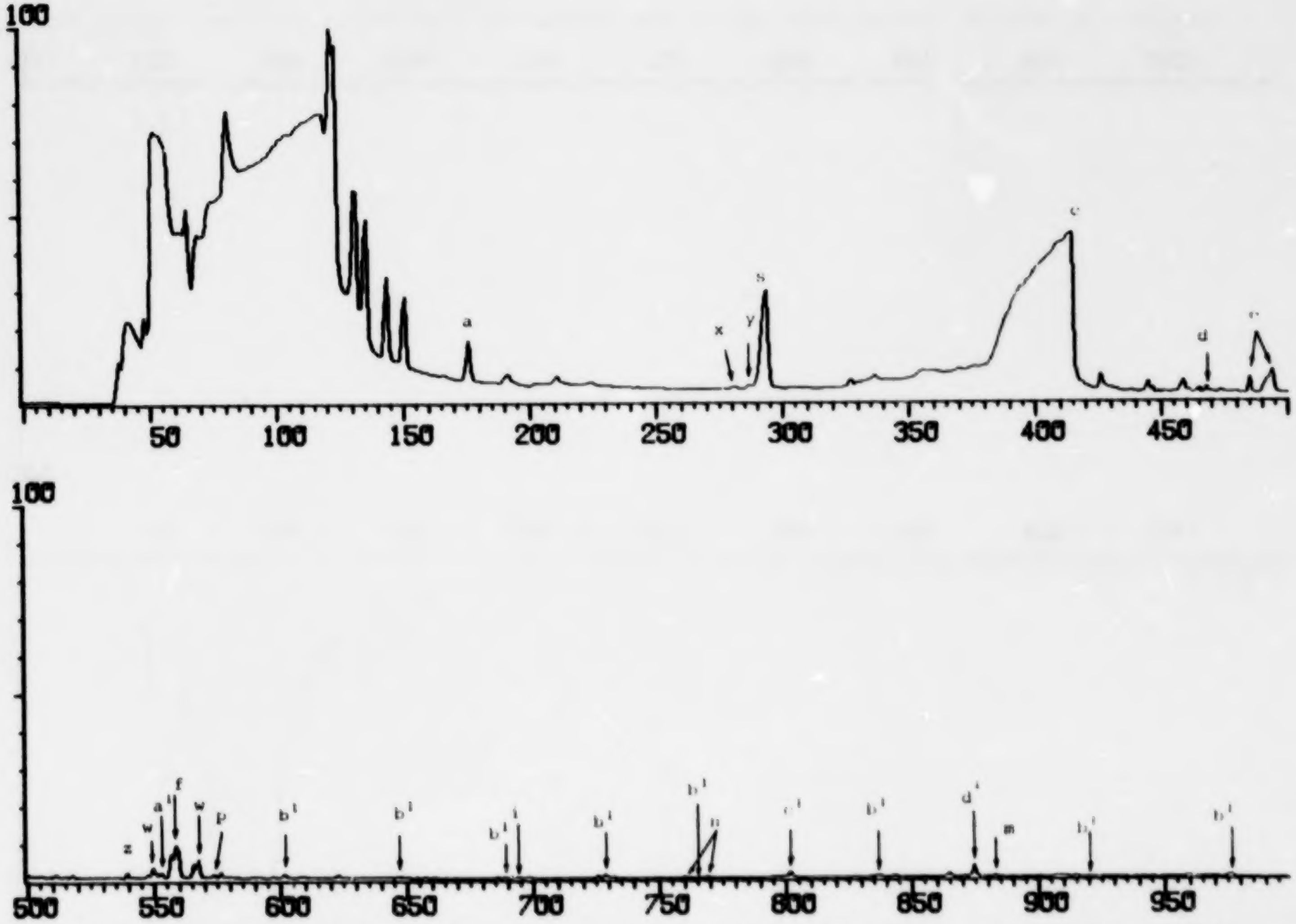

Figure E-21. Reconstructed gas chromatogram; Caddo Lake water, ozonated. acidic fraction. (diazomethane)

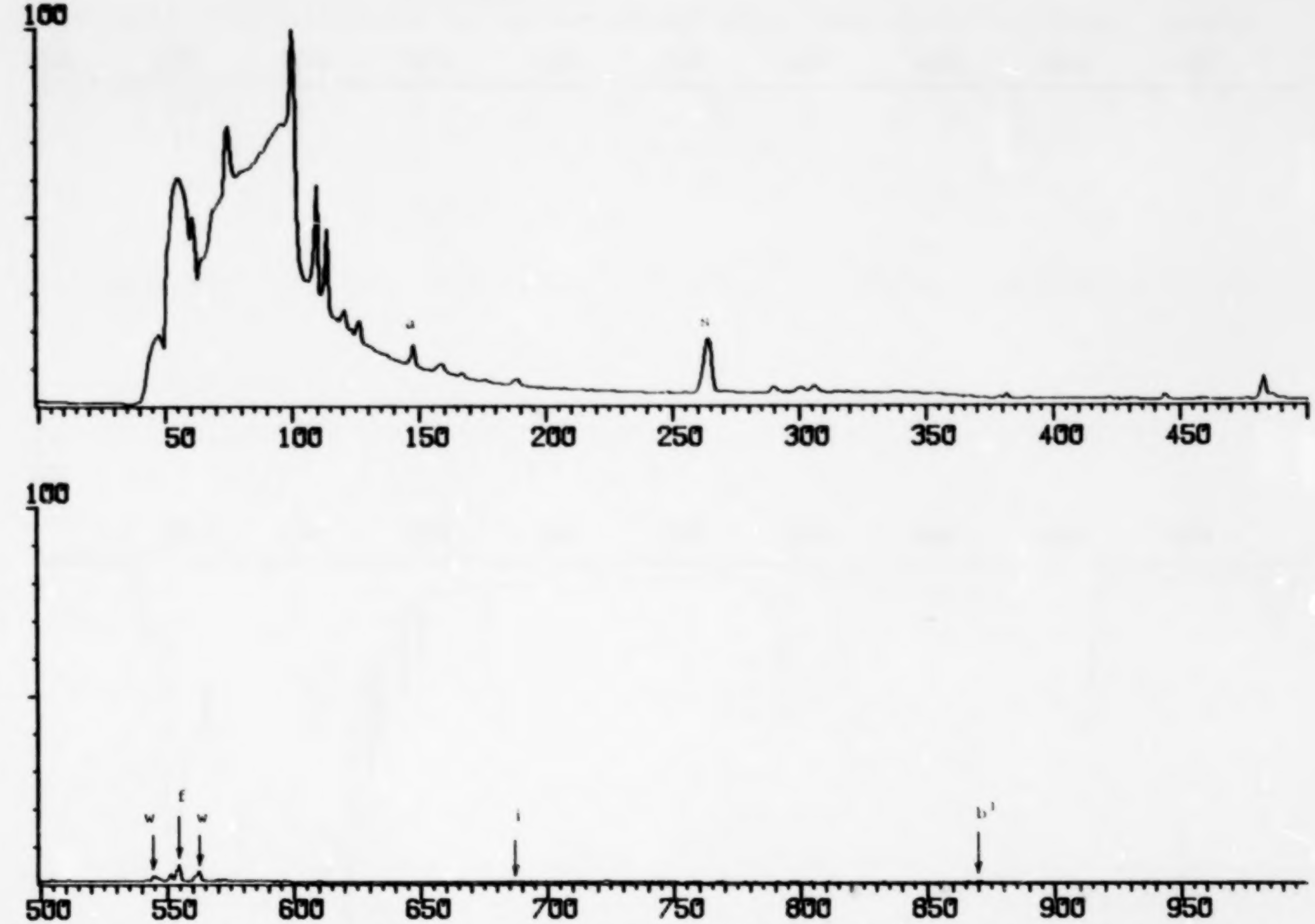

Figure E-22. Reconstructed gas chromatogram; Caddo Lake water, ozone/UV. acidic fraction (diazomethane).

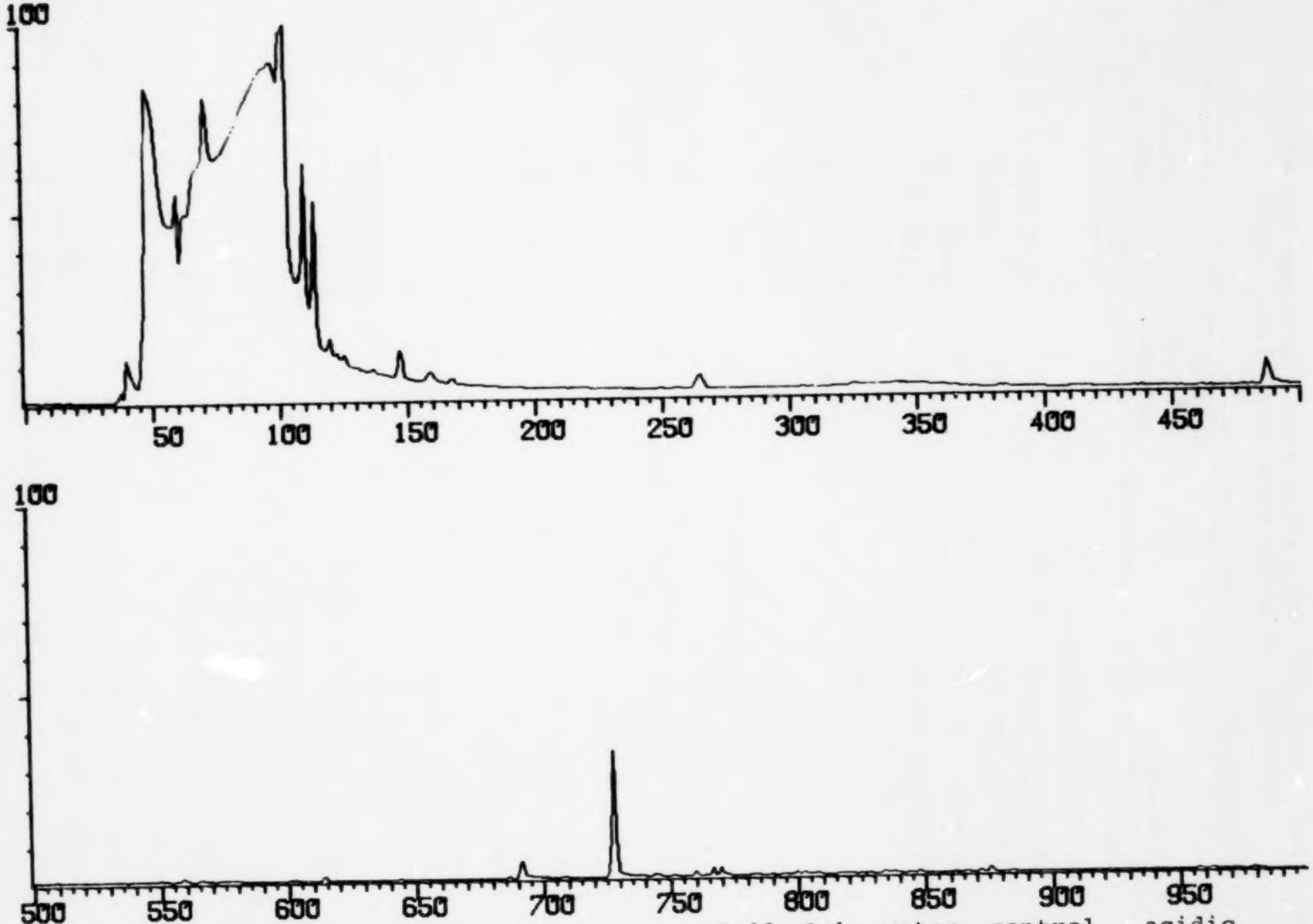

Figure E-23. Reconstructed gas chromatogram; Caddo Lake water, control. acidic fraction (diazomethane).

TABLE E-2. PRODUCTS IDENTIFIED FROM THE OZONE AND OZONE/UV TREATMENT OF WATER FROM CADDO LAKE, TEXAS

	Product	Method of Identification	Occurs in Chromatogram
a	n-Heptane	1	I,II,III,IV(Note 5)
b	2,4-Dimethylhexane	1	I
c	Note 4a, below	2	I,II,III
d	Note 4b, below	-	I,II,III
e	Note 4c, below	-	I,II,III
f	Trichlorobenzene, internal standard	1	I,II,III
g	2,3-Dimethylheptane	1	I
h	n-Decane	1	I
i	Dicyclohexyl Amine	1	I,III,IV
j	2,6-Di-t-Butylbenzoquinone	1	I
k	Note 4d, below	-	I
l	M=195, similar to substituted pyridones	2	I
m	Diethyl Phthalate	1	I.III
n	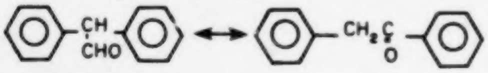	3	I,II,III
p	Hydrocarbon	2	I,II,III
q	Bleed	2	I
r	Phthalate	2	I
s	3-Methylheptane	1	II,III,IV
t	2,6-Di-t-Butyl-4-Ethyl Phenol	1	I
u	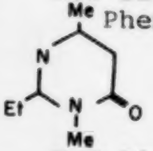	1	II
v	N,N-Diethylformamide	1	II
w	Note 4e, below	-	II,III,IV
x	Propyl Ethyl Ketone	1	III
y	Methyl Butyl Ketone	1	III
z	see Note 4f, below	-	III

(Continued)

TABLE E-2 (Continued).

	Product	Method of Identification	Occurs in Chromatogram
a[1]	RCO_2Me	2	III
b[1]	RCO_2Me, $R > C_6$	2	III
c[1]	$CH_3(CH_2)_{12}CO_2Me$	1	III
d[1]	$CH_3(CH_2)_{14}CO_2Me$	1	III

1) Registry of Mass spectral Data, Stenhagen, E.; Abrahammson, S.; McLafferty, F.W.: John Wiley, New York, 1974.

2) Suggested by fragmentation pattern.

3) Fetizon, M. and Audier, H.: Organic Mass Spectrometry, 8 (1974) 201.

4) No positive identification. Distinctive ions along with suggested compounds and source are given below:

a) 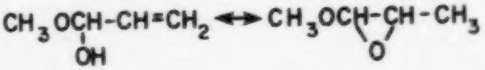

$CH_3O\underset{OH}{C}H\text{-}CH{=}CH_2 \leftrightarrow CH_3OC\underbrace{H\text{-}C}_{O}H\text{-}CH_3$

Acrolein Methyl Hemiacetal M/e=88,73,70,61,45,44,42

b) 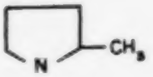

M/e=85 > 84, 57, 43

c) $CH_3CH_2CN{=}N\text{-}OH$ or $CH_3CH_2CH_2NO$ M/e=73, 55, 45

d) Almost matches Registry spectrum for Delta-10-Tetrahydroconstunolide,

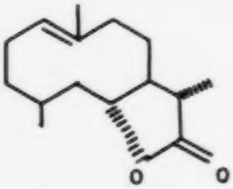

but not quite. Difference could be the instrument, but spectrum is similar in fragmentation pattern to

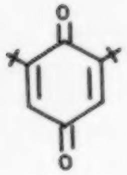

+16. Possibly

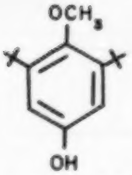

or

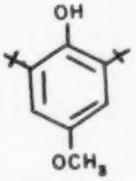

The latter are often used as antioxidants in ether.

e) Long chain N-Methyl Amine or possibly Hydrocarbon.
M/e = 85 < 84, 57, 55, 43

f) M/e = 111, 89, 75 < 73, 47 < 45 > 43

5) I = ozone only: neutral and basic compounds; II = ozone/UV: neutral and basic; III = ozone only: acidic compounds (Diazomethane derivatized); IV = ozone/UV: acidic compounds (Diazomethane derivatized).

APPENDIX F

QUALITY CONTROL DURING THE KINETIC RUNS

The purpose of this appendix is to outline sources of experimental error which were unique to this project, present experimentally determined limits to these errors, and evaluate the importance of these errors on the desired outcome. There are several difficulties which combine to produce the unique experimental environment in which an analytical method must be chosen for this project. The first is the low concentration level at which these experiments were run in order to realistically simulate an actual water supply. This is, of course, more of a problem in some cases than others but more importantly, combines synergetically with the following. The ozone/UV system is highly complex, highly reactive, and not well understood. The effects the complexity can have on the analytical method are unknown, and after consideration of all known effects, one can only hope that the data are real, as is the case with any experimental endeavor. The simpler and faster the analytical method, however, the less opportunity there is for artifacts to occur. The greatest problem in this particular project is the quantity of data which must be collected to achieve the desired result. Fifteen to twenty gas-chromatographic analyses may go into determining one disappearance curve. Multiplying by the number of kinetic runs performed during this project gives a very large number of analyses. Doubling or tripling the number of analyses by replication doubles or triples the length of the project without significantly increasing the amount of information which is gained. The result of this trade-off is that it is desirable to use analyses which only require one injection. This choice also satisfies the simplicity and speed requirements mentioned earlier. Next to direct monitoring (such as spectroscopic) inside the reactor, the natural choice for the analytical method would be direct aqueous injection gas chromatography, where allowed by detection limits, since sample handling is minimized and the analysis is performed immediately upon sampling (within 30 seconds). Analyses were performed in this manner for chloroform, bromodichloromethane, and tetrachloroethylene, but not for hexachlorobiphenyl. Hexachlorobiphenyl requires a concentration step and is therefore extracted from ozone-quenched aliquot of reaction mixture, using hexane to which an internal standard has been previously added. Data for specific substrates will now be considered by individual compound

The concept of standard deviation (N-1 weighted) will be employed as a measure of precision, even though a statistically valid number of data points has not been collected.

CHLOROFORM

Standard solutions spanning the concentration range 0-400 μg/L were made up by spiking known concentrations of an ethanol concentrate into water. The most concentrated solution was used to calibrate the computerized Hewlett-Packard 5840 gas chromatograph, then the remaining solutions were analyzed on the basis of that calibration. Only one injection was made per solution to simulate the analysis of an actual kinetic run. The results are shown in Figure F-1 and in the following table.

Prepared concentration,μg/L	160	80.0	40.0	20.0	4
Analyzed concentration,μg/L	162	73.8	36.8	19.5	n.d.

The purified water was checked for chloroform by the same method, and it was found to be negligible. The peak corresponding to 4 μg/L was visible but was not integrated by the electronic integrator. Another linearity study was performed similarly over a narrower range, and duplicate injections were made. The integrator was calibrated on the highest concentration. The data is shown in Figure F-2 and this table:

Prepared concentration,μg/L	37.1	23.2	18.5	13.9	9.3
Analyzed concentration,μg/L	37.1	24.6±.05	17±2	13.2±.9	9.5±5

In another experiment, three separate solutions of aqueous chloroform were prepared from the same concentrate, to determine the variance of Co (substrate concentration at t=0) from one run to the next. Each solution was analyzed in triplicate and the averages averaged in order to calculate a standard deviation among the solutions. The data is shown below:

	Peak Areas, μV Seconds ÷ 3.2†			Average ± Std. Dev.
Solution A	162,300	163,500	161,400	162,400±1053 (0.6%)
Solution B	154,800	154,500	152,700	154,000±1136 (0.7%)
Solution C	153,100	155,600	157,100	155,266±2021 (1.3%)
Average of Averages				157,222±4528 (2.9%)

† The Hewlett-Packard integrator uses units of 3.2 μV Seconds

Solution B was then diluted by a factor of ten and that solution analyzed in triplicate:

1/10B 14,210 15,950 12,700 Avg=14,286 ± 1626 (11.4%)

These figures indicate that at either Co = 100 µg/L or 1/10 Co = 10 µg/L, the precision of the measurement is about 1 µg/L.

BROMODICHLOROMETHANE

Solutions of five different concentrations in the range of 3-300 µg/L were prepared by spiking an ethanol concentrate into water, and each resulting solution analyzed by a single direct aqueous injection. This time the integrator was calibrated on the lowest concentration:

Prepared concentration, µg/L	2.93	14.6	29.3	147	293
Analyzed concentration, µg/L	2.93	12.4	28.9	149	286

The data are plotted in Figure F-3. As with chloroform, three aqueous solutions were made up identically to be 100 µg/L in bromodichloromethane. A portion of one of the solutions was diluted by a factor of ten, and a portion of the resulting solution again diluted by a factor of ten. The resulting solutions were analyzed in triplicate. The data are given below and plotted in Figure 4.

	Peak Area, µV Seconds ÷ 3.2			Average ± Std. Dev.
Solution A	719,800	716,600	724,000	720,133±3711 (0.5%)
Solution B	686,200	693,400	695,800	691,800±4995 (0.7%)
Solution C	675,600	662,400	675,400	671,133±7564 (1.1%)
			Average of Averages-	694,355±24,599 (3.5%)
1/10 B	54,570	55,040	55,020	54,877±266 (0.5%)
1/100 B	4,717	4,758	4,680	4,718±39 (0.8%)

Comparison of the precision of analysis to the reproducibility of solution preparation for solutions A, B, and C, seems to indicate that the standards can not be prepared as accurately as they could be analyzed. This factor is probably the major contributor to the deviation on the 10 µg/L point from the line in Figure F-4. This deviation corresponds to about 2 µg/L.

HEXACHLOROBIPHENYL

Three solutions of HCB were identically prepared by spiking from an ethanolic concentrate. The solutions which were made up to contain 60 µg/L of HCB, were analyzed in triplicate by extraction into nanograde hexanes (mixture of isomers) to which had been added hexachlorobenzene as an internal standard. Because of the instrumental work load, a gas chromatograph which did not have a functioning integrator was used for the work.

The integrator available was able, however, to measure peak heights electronically, and the results reported here are based on those heights. One of the solutions was diluted by a factor of six and a portion of that solution diluted by another factor of six. These two solutions were also analyzed in triplicate as above. The data are given in the following table and are shown in Figure F-5.

Solution	Peak Height HCB/Peak Height Internal Standard			
	#1	#2	#3	Average ± Std. Dev.
A(60 μg/L)	1.312	1.483	1.498	1.43 ± 0.10 (7.0%)
B	1.507	1.557	1.378	1.48 ± 0.09 (6.1%)
C	1.526	1.436	1.435	1.47 ± 0.05 (3.4%)
	Average of Averages			1.46 ± .03 (1.8%)
1/6 A(10 μg/L)	0.256	0.246	0.237	0.249 ± 0.009 (3.6%)
1/36 A(1.65 μg/L)	0.0571	0.0559	0.0563	0.0564 ±0.0006 (1.1%)

In contrast to the case of bromodichloromethane, these data seem to indicate that the solutions (Co) can be prepared with reasonable accuracy (±1.8%), but that the analytical method is not as precise as for the two compounds described previously. This is to be expected since there are three measurement steps (sample, quench, and extraction solvent), and one extraction, rather than just one measurement as in direct aqueous injection. Measurement of the injection volume into the syringe is not counted for the HCB analysis since this is an internal standard technique.

EFFECT OF ANALYTICAL PRECISION ON END RESULTS

At the present time only the effect on τ will be discussed. It will, further, be discussed only for the case of a reaction which is first order in substrate, in the interest of simplicity.

When integrated, the rate expression gives

$$\ln S/S_o = -kt.$$

Let $\tau(\ell)$ be the time at which $S/S_o = e^{-\ell}$.

If the standard deviation is expressed as a fraction, ε, of the measured value, then the limits set by the above equation on t correspond to the case in which the errors are in opposite directions.

$$t_{\pm} = -\frac{1}{k}\ln\frac{S\,(1\pm\varepsilon)}{S_o(1\mp\varepsilon_o)} = -\frac{1}{k}\left[\ln\frac{S}{S_o} + \ln\frac{(1\pm\varepsilon)}{(1\mp\varepsilon_o)}\right], \quad \text{or}$$

$$\delta \pm = t - t \pm = \frac{1}{k} \ln \frac{1 \pm \varepsilon}{1 \mp \varepsilon_o} .$$

The fraction by which this measurement should deviate from the true value of τ is then

$$f \pm (1) = \delta \pm / \tau\ (1) = \ln \frac{1 \pm \varepsilon}{1 \mp \varepsilon_o} / \ln (S/So), \text{ but}$$

$\ln S/So = \ln e^{-1} = -1$, or $f \pm (1) = \delta \pm / \tau\ (1) = \frac{1}{1} \ln \frac{1 \pm \varepsilon}{1 \mp \varepsilon_o}$.

For example, the analysis of solution A of HCB gave $\varepsilon_o = 0.07$. Using the percent deviation of solution $\frac{1}{6}$ A(17% remaining) as an approximation to $\tau(3)$ (5% remaining), then $\varepsilon = 0.036$, and

$f+(1) = -\frac{1}{1} \ln \frac{1.036}{0.93} = -0.108$, $\qquad f-(1) = 0.104$

$f+(3) = 0.036$, $\qquad f-(3) = 0.035$.

In other words, the lack of precision encountered in the analysis of solution A of HCB could contribute about 10% error to $\tau(1)$ and about 3½% to $\tau(3)$. If, on the other hand, the error from 1/36 A had been used, the effect on τ would be

$f+(1) = 0.084$ $\qquad f-(1) = 0.079$

$f+(3) = 0.028$ $\qquad f-(3) = 0.026$.

It can be seen from the sample calculations given above and below that $f \pm (1) \sim \varepsilon + \varepsilon_o$ and $f(1) = \frac{1}{I} f(1)$. This is easily proven using the series expansion of $\ln (1 + x)$.

Four important points should be made about the above effect

1) $f \pm (1)$ represents the worst possible case, that is, maximum errors in opposite directions.

2) Some of the worst data obtained in the precision studies was used in the above tables; calculations with $\varepsilon = \varepsilon_o = 0.036$ yield $f \pm (1) = 0.072$ and $f \pm (3) = 0.024$.

3) The importance of the effect is less as more substrate is destroyed.

4) The fact that the standard deviations for the individual solutions in the HCB experiment are much higher than that for the average of the averages, implies that if one fits a destruction curve to the data, and then extracts τ from that curve, the actual error in τ will be smaller than that predicted by the above analysis.

As can be seen in Appendix B, the scatter in the kinetically determined rate constants has been calculated as a standard deviation and reported in the summary tables in Section 5.

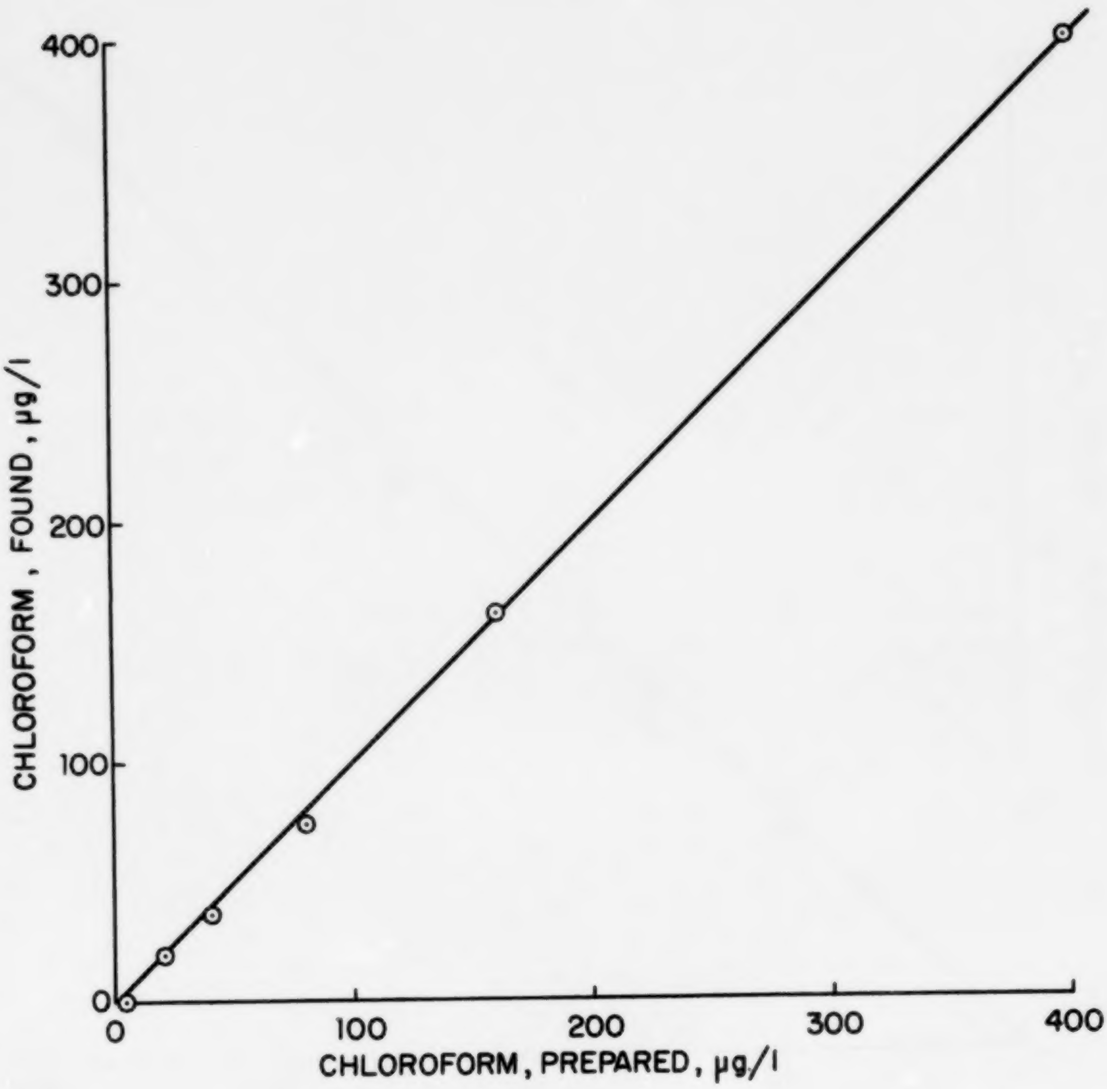

Figure F-1. Linearity of chloroform analysis. Broad Range (0-400 µg/L).

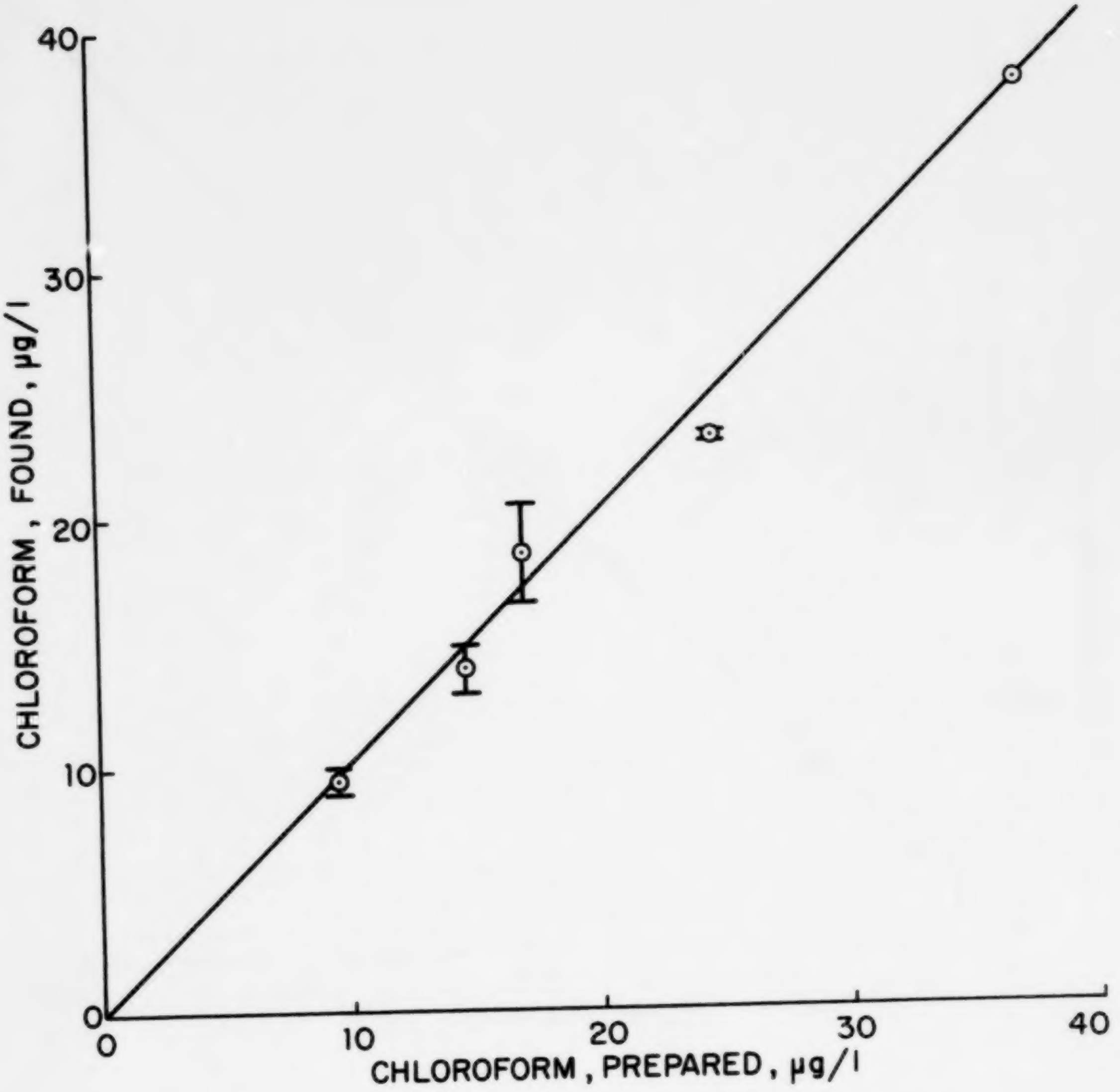

Figure F-2. Linearity of chloroform analysis. Narrow Range (o-40 µg/L).

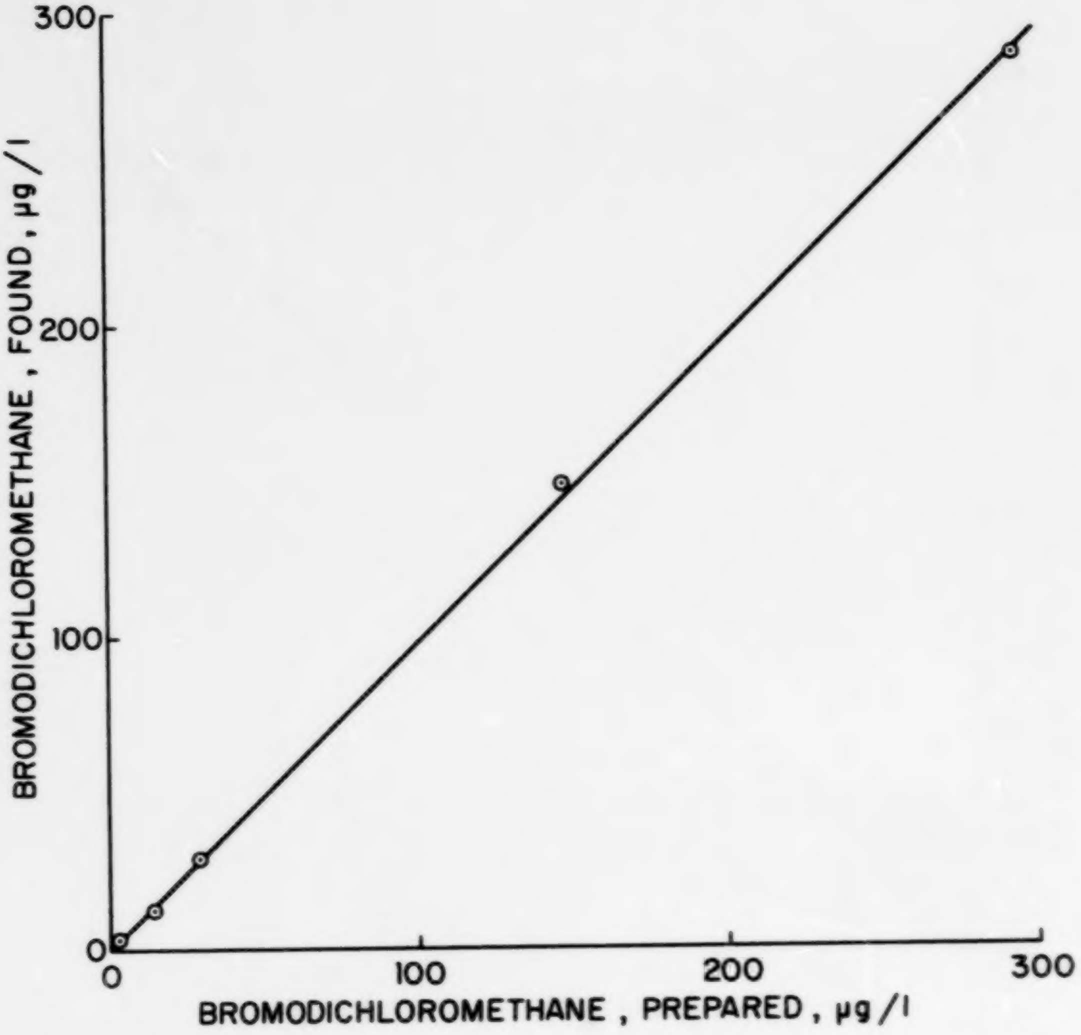

Figure F-3. Linearity of bromodichloromethane analysis.

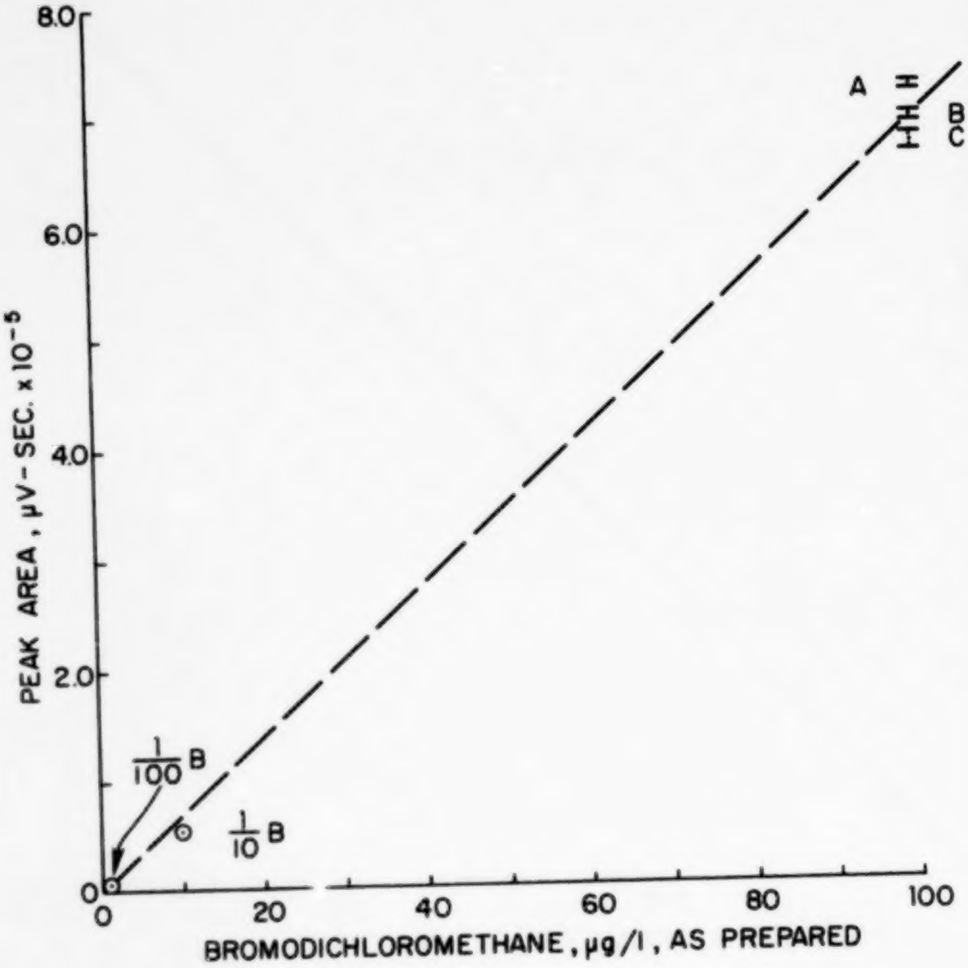

Figure F-4. Linearity of bromodichloromethane analysis upon serial dilution in water.

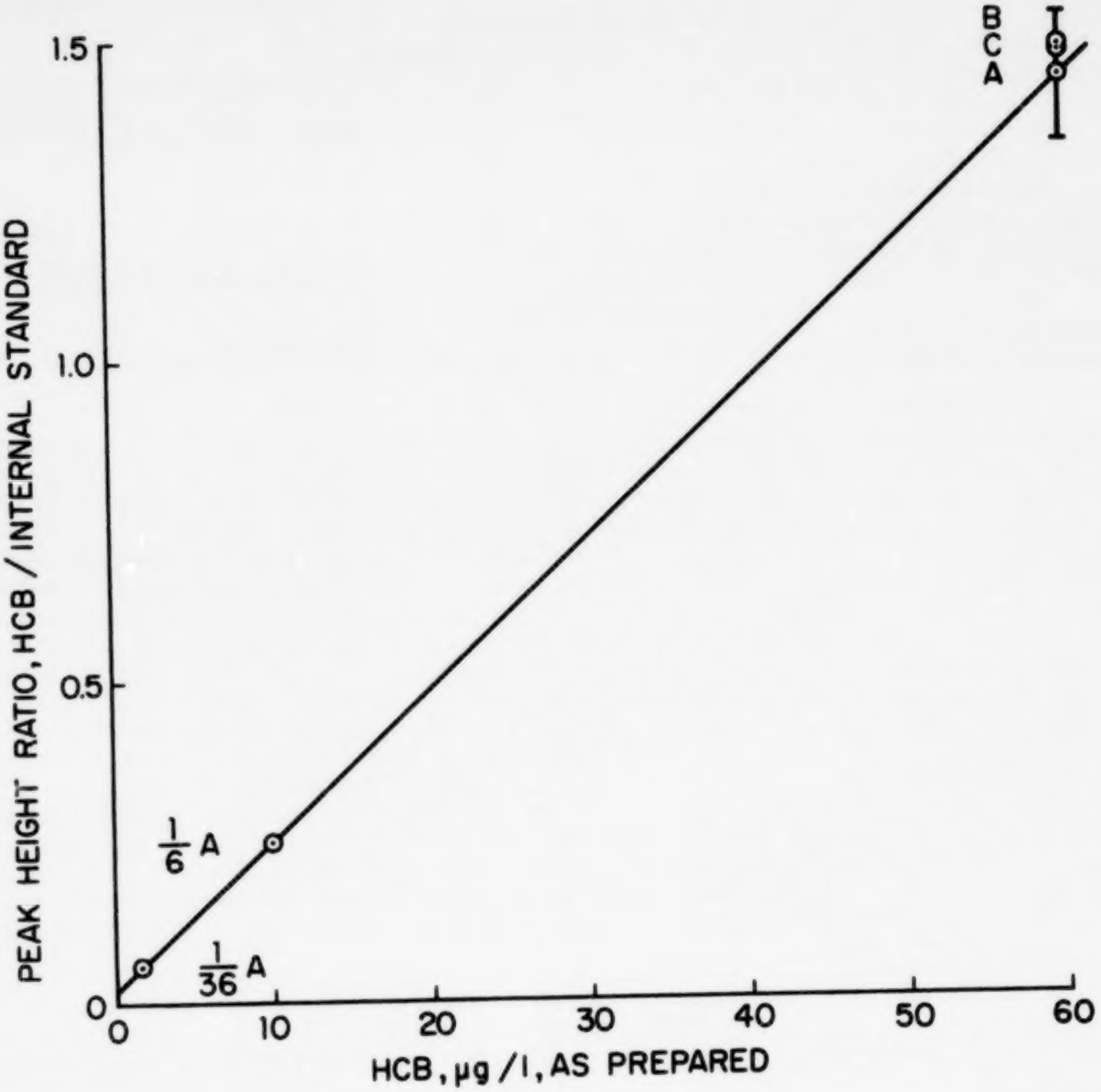

Figure F-5. Linearity of hexachlorobiphenyl analysis upon serial dilution in water. (error bars shown for solution A only).